UNIL | Université de Lausanne

Unicentre
CH-1015 Lausanne
http://serval.unil.ch

Year : 2020

Oxygen and the Brain Natriuretic Peptide are both factors modulating cardiomyocyte cell fate in vitro and in vivo

Bon-Mathier Anne-Charlotte

Bon-Mathier Anne-Charlotte, 2020, Oxygen and the Brain Natriuretic Peptide are both factors modulating cardiomyocyte cell fate in vitro and in vivo

Originally published at : Thesis, University of Lausanne

Posted at the University of Lausanne Open Archive http://serval.unil.ch
Document URN : urn:nbn:ch:serval-BIB_BE72A429636D6

Droits d'auteur
L'Université de Lausanne attire expressément l'attention des utilisateurs sur le fait que tous les documents publiés dans l'Archive SERVAL sont protégés par le droit d'auteur, conformément à la loi fédérale sur le droit d'auteur et les droits voisins (LDA). A ce titre, il est indispensable d'obtenir le consentement préalable de l'auteur et/ou de l'éditeur avant toute utilisation d'une oeuvre ou d'une partie d'une oeuvre ne relevant pas d'une utilisation à des fins personnelles au sens de la LDA (art. 19, al. 1 lettre a). A défaut, tout contrevenant s'expose aux sanctions prévues par cette loi. Nous déclinons toute responsabilité en la matière.

Copyright
The University of Lausanne expressly draws the attention of users to the fact that all documents published in the SERVAL Archive are protected by copyright in accordance with federal law on copyright and similar rights (LDA). Accordingly it is indispensable to obtain prior consent from the author and/or publisher before any use of a work or part of a work for purposes other than personal use within the meaning of LDA (art. 19, para. 1 letter a). Failure to do so will expose offenders to the sanctions laid down by this law. We accept no liability in this respect.

UNIL | Université de Lausanne
Faculté de biologie et de médecine

Centre Hospitalier Universitaire Vaudois CHUV
Division d'Angiologie, Département Cœur-Vaisseaux

Oxygen and the Brain Natriuretic Peptide are both factors modulating cardiomyocyte cell fate *in vitro* and *in vivo*

Thèse de doctorat ès sciences de la vie (PhD)

présentée à la

Faculté de biologie et de médecine
de l'Université de Lausanne

par

Anne-Charlotte BON-MATHIER

Master en Biologie, Développement et Biologie Cellulaire, Université de Fribourg

Jury

Prof. Thorsten Krueger, Président
Dre MER Nathalie Rosenblatt-Velin, Directrice de thèse
Dre Francesca Rochais, Experte
Dre Marie-Noëlle Giraud, Experte

Lausanne
(2020)

UNIL | Université de Lausanne
Faculté de biologie et de médecine

Centre Hospitalier Universitaire Vaudois CHUV
Division d'Angiologie, Département Cœur-Vaisseaux

Oxygen and the Brain Natriuretic Peptide are both factors modulating cardiomyocyte cell fate *in vitro* and *in vivo*

Thèse de doctorat ès sciences de la vie (PhD)

présentée à la

Faculté de biologie et de médecine
de l'Université de Lausanne

par

Anne-Charlotte BON-MATHIER

Master en Biologie, Développement et Biologie Cellulaire, Université de Fribourg

Jury

Prof. Thorsten Krueger, Président
Dre MER Nathalie Rosenblatt-Velin, Directrice de thèse
Dre Francesca Rochais, Experte
Dre Marie-Noëlle Giraud, Experte

Lausanne
(2020)

UNIL | Université de Lausanne
Faculté de biologie et de médecine

Ecole Doctorale
Doctorat ès sciences de la vie

Imprimatur

Vu le rapport présenté par le jury d'examen, composé de

Président·e	Monsieur	Prof.	Thorsten	**Krueger**
Directeur·trice de thèse	Madame	Dre	Nathalie	**Rosenblatt-Velin**
Expert·e·s	Madame	Dre	Francesca	**Rochais**
	Madame	Dre	Marie-Noëlle	**Giraud**

le Conseil de Faculté autorise l'impression de la thèse de

Madame Anne-Charlotte Mathier-Bon

Master of science in biology, Université de Fribourg, Suisse

intitulée

Oxygen and the Brain Natriuretic Peptide are both factors modulating cardiomyocyte cell fate *in vitro* and *in vivo*

Lausanne, le 30 juin 2020

pour le Doyen
de la Faculté de biologie et de médecine

Prof. Niko GELDNER
Directeur de l'Ecole Doctorale

I. Acknowledgements

I would like to gratefully acknowledge the members of the jury, for accepting to evaluate my PhD thesis: Prof. Thorsten Krueger, president of this jury, Dre MER Nathalie Rosenblatt-Velin, Director of this thesis, Dre Francesca Rochais and Dre Marie-Noëlle Giraud, experts.

II. Remerciements

Je tiens tout d'abord à remercier ma directrice de thèse, Dre MER Nathalie Rosenblatt-Velin sans qui l'aboutissement de ces travaux ne se serait réalisé. Qu'elle trouve ici le témoignage de ma reconnaissance. Merci d'avoir investi du temps pour me guider dans la maîtrise de mes connaissances. Merci de m'avoir enseigné son sens de la rigueur scientifique. Merci pour son sens critique qui m'a été très utile. Merci pour sa grande disponibilité et ses précieux conseils dans la rédaction de ma thèse et sa relecture efficace et attentive. Merci de m'avoir permis de me surpasser.

Je tiens également à exprimer toute ma gratitude à Stéphanie, Christelle, Tamara et Na pour l'aide inestimable qu'elles m'ont apportée tout au long de ces quatre années de thèse. En effet, la réalisation de cette thèse n'aurait pas été possible sans leur participation, leur contribution et leur bonne humeur. De plus, je tiens également à les remercier ainsi que Nathalie pour le climat de travail au laboratoire qui nous a permis de travailler dans d'excellentes conditions. Les discussions avec Nathalie sur la famille, les voyages et la Bretagne ;-) avec Steph sur les enfants et la thèse :-) avec Christelle sur les voyages, le ski et les bons produits du terroir fribourgeois ;-), avec Na sur notre avenir dans la recherche ;-), et avec Tamara sur nos hommes et sur nos nombreux comptages cellulaires ;-) vont me manquer. Un grand merci encore les filles !!! Je compterai encore sur vous ces prochaines années pour m'apporter tous les bons conseils pour élever des enfants sans le moindre cri ;-). Je n'oublie pas les stagiaires de l'école de la santé qui nous ont secondés : Marion, Jeremy, Malorie, Marjorie, Matthieu.

Je tiens également à remercier mes collègues et amis que j'ai eu la chance de rencontrer lors de ces quatre années de thèse, qui ont toujours été présents et m'ont permis de vivre ces années avec l'optimisme requis pour ne pas flancher. Un grand merci à Tania, Loïc, Marie-Laure, Laurianne, Charlotte, Dario, Corinne, Alexia, Martine, Manon, Diane, Jessica, Mergim, Thomas et Florent.

Je remercie sincèrement le département d'Angiologie et plus particulièrement, le Prof. Lucia Mazzolai, pour son soutien lors de ma dernière année de thèse.

Je remercie toutes les personnes avec qui j'ai collaboré au cours de ma thèse : Alexia Carboni notre étudiante de master qui a généré les résultats du LCZ696, Dre Corinne Bertonneche et Anne-Catherine Clerc pour avoir effectué les chirurgies sur les souris.

J'adresse enfin ma plus profonde reconnaissance à ma famille et à mes amies qui m'ont longuement entendue parler de cellules régénératrices et l'ont supporté ;-) qui n'ont pas perdu patience pendant toutes ces années et lors des innombrables conversations sur les cellules cardiaques.

A mes parents pour leur présence, leur disponibilité, leur aide, leur abnégation sans limite pour me permettre d'atteindre mes objectifs. Pour m'avoir encouragée pendant toutes ces années d'études et ce travail de thèse.

A mes beaux-parents ainsi qu'à Pascal, Tamara et Stefan pour leur écoute et leur soutien.

A mon frère, bien plus disponible pour les autres que moi. A lui, qui m'a toujours soutenue et encouragée alors que je ne lui rendais pas forcément. Merci Gregory d'être là pour moi, je ferais de mon mieux pour te rendre au moins autant que tu m'as donné.

A mes deux amies d'enfance Kira et Zenia qui ont su m'écouter et me soutenir avec de nombreux cafés et apéros tout au long de cette thèse.

A Damian, sans qui rien ne serait. Merci de sa patience, de son aide, d'être resté présent même aux heures sombres. Merci pour toutes les tâches qu'il a assumées à ma place. Merci de m'avoir motivée dans les moments de doute. D'autres découvertes et bouleversements nous attendent prochainement dans cette nouvelle vie à trois qui va commencer. La parentalité sera une magnifique aventure et une belle suite à la thèse.

III. Abstract

Cardiovascular diseases are associated with high mortality rate due to a massive loss of cardiac cells in injured hearts. Therefore, cardiac research focuses on the discovery of new treatments able to replace dysfunctional cardiac cells, and more precisely the contractile cardiomyocytes (CMs). Adult mammalian CMs have the ability to proliferate. However, this capacity is not sufficient to restore the heart after injury. That is why the aims of my thesis were to determine whether modulation of oxygen and brain natriuretic peptide (BNP) concentrations could improve the adult heart regeneration capacity.

Oxygen is a key regulator of CM cell fate. Low oxygen level during development stimulates CM proliferation, whereas high oxygen level after birth inhibits CM proliferation. After myocardial infarction (MI), reduction of oxygen level increases CM proliferations. Thus, **the first aim** of my study was to determine the effect of different oxygen concentration on neonatal CM cell fate *in vitro*. Oxygen level inside the adult heart in physiological conditions is estimated close to 3% O_2 (physiological/normoxic environment). However, all CM cell cultures are performed *in vitro* at 20% O_2, which is thus an hyperoxic environment. Therefore, we compared CM cell fate in neonatal CM cell cultures performed at 20% O_2 to those performed at 3% O_2. We demonstrated that 3% O_2 favors CM dedifferentiation and proliferation *in vitro* (see results, section 4.1). Thus, the cultures of neonatal CMs in 3% oxygen highlight cellular physiological mechanisms occurring in CMs which can be blind in the cultures performed in an hyperoxic environment (i.e. at 20% O_2).

BNP is a cardiac hormone. BNP supplementation after MI in adult hearts improves the cardiac function and decreases heart remodeling. CMs express BNP receptors and are thus susceptible to respond to BNP stimulation. **The second aim** of my PhD thesis was therefore to investigate if a part of the cardioprotective effect of BNP is triggered by a modulation of CM cell fate. For this purpose, injections of BNP were performed in: 1) injured adult mice (i.e. after MI), 2) unmanipulated adult mice, which exhibit a low potential of CM proliferation and 3) unmanipulated neonatal mice, which exhibit a high potential of CM proliferation. We demonstrated that BNP treatment in all these mice resulted in an increased number of CMs. After MI, BNP increased CM number by protecting them against cell death and likely also by stimulating their proliferation. Indeed, it is clear that BNP stimulates the re-entry of CMs into the cell cycle. In healthy neonatal and adult mice we established that BNP stimulates CM proliferation. Interestingly, BNP treatment led also to activation of the MAP/ERK signaling pathway in CMs isolated from these three animal models, suggesting that BNP could trigger CM proliferation via the activation of MAP/ERK signaling (see results, section 4.2).

An alternative treatment able to increase BNP level after MI in a clinical setting is the use of LCZ696 (Entresto®) Novartis), which associates an angiotensin receptor blocker (valsartan) with an inhibitor of neprylisin (sacubitril), an enzyme responsible for the natriuretic peptide degradations. LCZ696 treatment improved heart functions and attenuated cardiac remodeling 10 days after MI in adult mice. Preliminary results demonstrated that LCZ696 increased the number of CMs and stimulated CM re-entry into the cell cycle (see supplementary data, chapter 8).

Altogether, our results demonstrate that BNP treatment is a valuable therapeutic strategy aimed to improve CM survival and renewal.

IV. Résumé

Les maladies cardiovasculaires sont associées à un taux de mortalité élevé en raison d'une mort massive des cellules cardiaques. C'est pourquoi la recherche en cardiologie se concentre sur la découverte de nouveaux traitements capables de remplacer les cellules cardiaques dysfonctionnelles, et plus précisément les cardiomyocytes (CMs). Les CMs des mammifères adultes ont la capacité de proliférer. Cependant, cette capacité n'est pas suffisante pour restaurer le cœur après un infarctus. Mon travail de thèse avait pour but de déterminer si la concentration d'oxygène et du peptide natriurétique de type B (BNP ; une hormone cardiaque) pouvaient stimuler dans le cœur adulte les mécanismes de régénération cardiaque.

La concentration d'oxygène (O_2) est un facteur modulant le devenir des CMs. Un faible taux d'oxygène pendant le développement stimule la prolifération des CMs, alors qu'une augmentation de ce taux après la naissance inhibe la prolifération des CMs. Après un infarctus du myocarde (IDM), la diminution de la concentration en oxygène augmente la prolifération des CMs. **Le premier objectif** de ma thèse était de définir l'effet de différentes concentrations d'oxygène sur les CMs en culture. La concentration d'oxygène à l'intérieur du cœur adulte, dans des conditions physiologiques, est estimée à 3% O_2 (normoxique). Cependant, toutes les cultures de CMs sont réalisées à 20% O_2, ce qui représente un environnement hyperoxique pour les CMs. Nous avons donc comparé des cultures de CMs isolées de cœurs nouveau-nés faites à 3% O_2 et à 20% O_2. 3% O_2 favorise la dédifférenciation et la prolifération des CMs (résultats, section 4.1). Ainsi, les cultures de CMs nouveau-nés à 3% O_2 mettent en évidence des mécanismes physiologiques des CMs pouvant être masqués dans des cultures en milieu hyperoxique (20% O_2).

En ce qui concerne le BNP, celui-ci est sécrété par toutes les cellules cardiaques, dont les CMs. L'injection de BNP après un IDM chez les souris adultes améliore la fonction cardiaque et diminue le remodelage du cœur. Les CMs expriment les récepteurs du BNP et sont donc susceptibles de répondre à une stimulation du BNP. **Le deuxième objectif** de ma thèse avait pour but d'étudier si l'effet cardioprotecteur du BNP est dû en partie à un effet sur les CMs. Des injections de BNP ont été effectuées chez : 1) des souris adultes après IDM, 2) des souris adultes non-manipulées, présentant un faible potentiel de prolifération des CMs et 3) des souris nouveau-nées non-manipulées, dotées d'un fort potentiel de prolifération des CMs. L'ajout de BNP a entraîné chez toutes ces souris une augmentation du nombre de CMs. Après un IDM, le BNP a augmenté le nombre de CMs en diminuant leur mort et probablement aussi en stimulant leur prolifération. En effet, au sein des cœurs infarcis, nous avons clairement démontré que le BNP stimule la réentrée des CMs dans le cycle cellulaire. Chez des souris nouveau-nées et adultes, le BNP stimule la prolifération des CMs. Nous avons aussi démontré que le BNP activait la voie de signalisation MAPK/ERK chez des CMs isolés des trois modèles de souris, suggérant que le BNP pouvait stimuler la prolifération des CMs par cette voie de signalisation (résultats, section 4.2). Un autre traitement pouvant augmenter le taux de BNP est le LCZ696 (Entresto®), qui associe un antagoniste des récepteurs de l'angiotensine à un inhibiteur de la néprilysine (enzyme responsable de la dégradation des peptides natriurétiques). Nous avons montré que le LCZ696 améliorait les fonctions cardiaques et atténuait le remodelage cardiaque après un IDM chez des souris adultes. Les résultats préliminaires ont démontré que le LCZ696 augmentait le nombre de CMs et stimulait la réentrée des CMs dans le cycle cellulaire (suppléments, section 8). Nos résultats démontrent que l'injection de BNP pouvait être considérée comme est une stratégie thérapeutique visant à améliorer la survie et le renouvellement des CMs après un IDM.

V. List of Abbreviations

aa	amino acid
ACE	angiotensin-converting enzyme
α-SKA	alpha-skeletal actin
ANP	atrial natriuretic peptide
AraC	cytosine-beta-D-arabinofuranoside
ATP	adenosine triphosphate
Aurkb	aurora kinase B
BFP	blue fluorescent protein
BNP	brain natriuretic peptide
BrdU	bromodeoxyuridine / 5-bromo-2'-deoxyuridine
BZ	border zone
cAMP	cyclic adenosine monophosphate
CDC	cardiosphere-derived cell
CDK 1, 4, 14	cyclin dependent kinase 1, 4, 14
cGMP	cyclic guanosine monophosphate
c-kit	tyrosine kinase receptor
CM	cardiomyocyte
CNP	c-type natriuretic peptide
CPC	cardiac precursor cell
cTNI	cardiac troponin I
cTNT	cardiac troponin T
CVD	cardiovascular disease
Dab2	disabled homolog 2
DAMP	damage associated molecular pattern molecule
DAPI	4’,6-diamidino-2-phenylindole
DPP-4	dipeptidyl peptidase-4
DR5	death receptor 5
Dsred2	red fluorescent protein
ECM	extracellular matrix
EF	ejection fraction
eGFP	enhanced green fluorescent protein
ErbB 2, 4	erythroblastic leukemia viral oncogene homolog 2,4
ESC	embryonic stem cell
FACS	fluorescence-activated cell sorting
FasR	Fas receptor
FCS	fetal calf serum
FGF-1, 10	fibroblast growth factor 1, 10
Fosl1	fos-like antigen 1
FOXO3	forkhead box O3
FUCCI	fluorescence ubiquitination-based cell cycle indicator
GC	guanylyl cyclase
GFP	green fluorescent protein
GTP	guanosine triphosphate
HF	heart failure
HIF-1α, β	hypoxia inducible factor 1 subunit alpha, beta
i.p.	intraperitoneal
I/R	ischemia/reperfusion
iCM	induced cardiomyocyte
IDE	insulin-degraded enzyme
IHC	intermittent hypoxia conditioning
IHF	immunohistofluorescence
IHT	intermittent hypoxia therapy
IL-1β, 6	interleukin 1beta, 6
iPSC	induced pluripotent stem cell
IQGAP3	IQ motif containing GTPase activating protein 3
Isl-1	islet-1
Klf4	kruppel-like factor 4
KO	knockout
LAD	left anterior descending coronary artery
Lats1	large tumor suppressor 1

lncRNA	long non-coding RNA
LV	left ventricle
LVDD	left ventricle diameter in diastole
LVDS	left ventricle diameter in systole
LVVol	left ventricle volume
LVWTD	left ventricle wall thickness in diastole
LVWTS	left ventricle wall thickness in systole
MADM	mosaic analysis with double markers
MAPK	mitogen-activated protein kinase
MAPK/ERK	mitogen-activated protein kinase / extracellular signal-regulated kinase
Mef2c	myocyte-specific enhancer factor 2C
Meis-1	myeloid ecotropic viral integration site 1
MEK 1, 2	dual specificity mitogen-activated protein kinase kinase 1, 2
MerCreMer	tamoxifen inducible Cre recombinase
MI	myocardial infarction
MPTP	mitochondrial permeability transition pore
MRP 4, 5	multidrug resistance-associated protein 4, 5
Myh6	alpha-myosin heavy chain
Myh7	beta-myosin heavy chain
NEP	neprilysin
NMC	non myocyte cell
NO	nitric oxide
NOS	nitric oxide synthase
NP	natriuretic peptide
NPR-A, B, C	natriuretic peptide receptor A, B, C
NRG-1	neuregulin-1
O_2	oxygen
Oct-3, 4	octamer-binding transcription factor 3, 4
PBS	phosphate-buffered saline
PDE 2, 3, 4, 5	phosphodiesterase 2, 3, 4, 5
pGC	particulate guanylyl cyclase
pH3	phospho-histone H3
PI3K	phosphoinositide 3-kinase
PKG	protein kinase G
PLB	phospholamban
pPLB	phophorylated phospholamban
RhoA	Ras homolog family member A
RIPK 1, 3	receptor-interacting protein kinase 1, 3
ROS	reactive oxygen species
RT-qPCR	real-time quantitative polymerase chain reaction
Runx1	runt-related transcription factor 1
RZ	remote zone
Sca-1	stem cells antigen 1
SERCA	sarco/endoplasmic reticulum Ca^{2+}-ATPase
sGC	soluble guanylyl cyclase
Sox 2, 4	SRY (sex determining region Y)-box transcription factor 2, 4
TAZ	tafazzin
Tbx 5, 20	T-Box transcription factor 5, 20
TEAD1	TEA domain family member 1
Thr17	threonine 17
Tmsb10	thymosin beta 10
TNFR1	tumor necrosis factor receptor 1
TRAIL	tumor necrosis factor related apoptosis inducing ligand
VEGF	vascular endothelial growth factor
YAP	yes-associated protein 1
ZI	infarction zone

VI. Table of Contents

VII. List of Figures

VIII. List of Tables

1. Introduction

Cardiovascular diseases (CVDs) are defined by the world health organization (WHO) as "a group of disorders of the heart and blood vessels". CVDs are the major cause of mortality worldwide involving myocardial infarction (MI) and strokes (www.who.int).

Each year, 17.9 million people die from CVDs which corresponds to 31% of all deaths worldwide. Due to the sedentary lifestyle of the population, the prevalence of CVDs will increase dramatically. In fact, 23.3 million people will suffer from CVDs in 2030. It thus becomes urgent to find an effective treatment to reduce the mortality rate due to CVDs.

Ischemia affects the functional activity of the heart because of a massive death of cardiac cells (i.e cardiomyocytes, endothelial cells, fibroblasts, cardiac precursor cells, smooth muscle cells and immune cells), via necrosis and/or apoptosis. This initiates a multicellular process, involving the rapid infiltration of inflammatory cells into the area of injury to remove the necrotic cells and to initiate reparation and the development of a fibrotic scar. The surviving cardiomyocytes (CMs) become hypertrophic in order to compensate the CM cell loss and the decrease of cardiac contractile activity. Afterwards, in 25% of the cases, MI leads to heart failure (HF) and death in the first five years following MI (1).

Over the past 30 years, many therapies have emerged to treat CVDs. They focus on three approaches: 1) decrease the blood volume, such as aldosterone antagonist or diuretics; 2) decrease pressure overload by using β-adrenergic blockers, ACE inhibitors; 3) increase cardiac input/contractility, such as digoxin (2). Although these therapies decrease mortality rate, they are not able to restore heart contractility. Indeed, the damaged cardiac cells, especially the necrotic and/or apoptotic CMs, are not replaced by new ones. Thus, curative treatment for patients with end stage heart failure remains cardiac transplantation. Nevertheless, the lack of available donors and the long waiting time for patients do not allow to avoid death. For this reason, the key challenge for cardiac research is to rapidly find alternative treatment(s) in order either 1) to protect cardiac cells from cell death and/or 2) to stimulate cardiac regeneration.

1.1. Cardiomyocyte death after ischemia

Ischemia induces, within the first 24 hours, the extensive loss of cardiac cells, mainly CMs. Several cell death mechanisms are stimulated in the ischemic hearts, such as necrosis, apoptosis, autophagy and necroptosis (Fig. 1) (3). Few hours after MI, the activation of necrosis leads to an extensive loss of CMs.

Necrosis is characterized by cell swelling, cell membrane disruption and cell lysis associated with an acute inflammatory response (Fig. 1) (4). Ischemic conditions induce necrosis through an excessive influx of water into the cells, resulting in the opening of the mitochondrial permeability transition pore (MPTP) and the rupture of the membrane of mitochondria (5). This rupture leads to the release of cellular components able to induce also apoptosis that peaks around 4.5 hours post-MI (Fig. 1) (6).

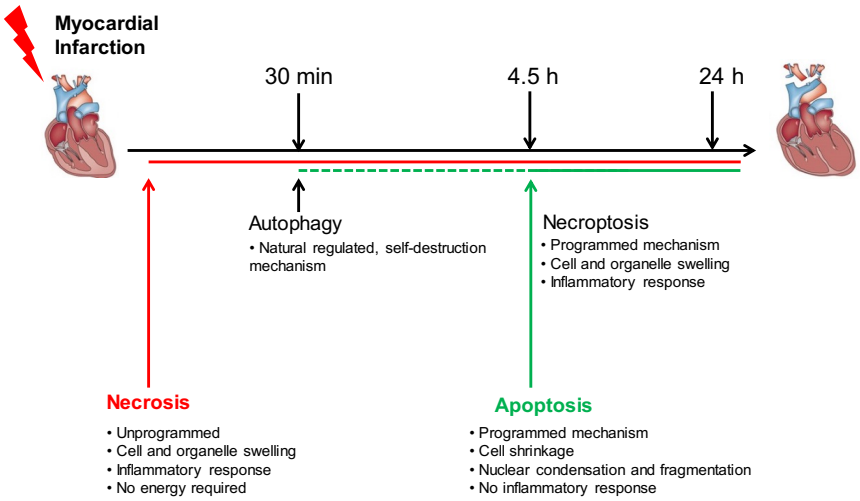

Figure 1: *Signaling pathways involved in CM cell death after MI.*

The mechanism of necroptosis is a hybrid mechanism between apoptosis and necrosis. This mechanism combines the morphological features of necrosis and the characteristics of the programmed cell death apoptosis (5). Necroptosis is characterized by the loss of membrane integrity and the release of damage-associated molecular pattern molecules (DAMPs), which results in an inflammatory response (7). Necroptosis is triggered via the stimulation of the death receptors (i.e. TNFR1, FasR), which are linked to key mediators of necroptosis, the receptor-interacting protein kinase 1 and 3 (RIPK1 and RIPK3). The presence of the caspase 8 is crucial in the decision between apoptosis and necroptosis. Indeed, the absence of the active form of caspase-8 prevents RIPK1 cleavage and then promotes its association with RIPK3 at the mitochondria membrane. This association leads to

MPTP opening and ROS production (3, 5). By contrast, the presence of the active form of caspase 8 cleaves RIPK1 kinase leading to inhibition of the necroptosis signaling and activation of apoptosis (5).

Autophagy is a programmed cell death, which occurs 30 min after ischemia (Fig. 1) (8). During this process, a double-membrane vesicle (autophagosome) envelops cytoplasmic components, including organelles (i.e. mitochondria) and protein aggregates. The formation of autophagosome is divided in 3 steps: nucleation, elongation and maturation. Finally, autophagosome fuses with lysosomes for degradation and recycling of their contents (3, 9, 10). Autophagy is considered to be a physiological mechanism essential to cell survival, where damaged organelles and misfolded proteins are degraded and recycled for ATP production during cellular stress (6, 11, 12). Indeed, starvation, growth factor depletion and hypoxia are well known factors that activate autophagy in order to increase cell survival (13). In physiological conditions, autophagy appears to play a protective role on CMs by preventing activation of apoptosis (14). However, in pathological conditions, the level of autophagic activity determines whether autophagy is protective or detrimental. This level of activity depends on the activated upstream signaling mechanism, which differs depending on the heart diseases (i.e. ischemia or I/R injury). Indeed, it was shown that autophagy could be protective during permanent ischemia, whereas it could be detrimental during I/R injury (14, 15). Currently, it is difficult to know if inhibiting or activating key factors related to autophagy at a specific time and for a specific cardiac disease will protect cardiac cells or trigger cardiac cell death (9).

During my PhD thesis, I focused on apoptosis after MI because it plays an important role in the process of cell death, in the process of LV remodeling and development of heart failure (3, 16). Apoptosis is a programmed cell death, resulting in cell shrinkage, membrane blebbing, DNA fragmentation and degradation of the structural proteins of CMs, such as the cardiac Troponin and α-actin. However, contrary to necrosis, apoptosis does not initiate inflammatory response (17). Two distinct signaling pathways are involved in apoptosis: The intrinsic pathway and the extrinsic pathway (Fig. 2). The intrinsic pathway is triggered by oxidative stress, hypoxia and Ca^{2+} overload and induces the permeabilization of the outer membrane of mitochondria through the oligomerization of Bax/Bak. The cytochrome C is released from the mitochondria into the cytosol and the procaspase 9 is recruited. The procaspase 9 is the mediator

of the intrinsic pathway responsible for the activation of the caspase 3. Bax and Bak proteins belong to the Bcl-2 family and are related to pro-apoptotic molecules. By contrast, Bcl-2 is related to anti-apoptotic members that inhibit cell death pathway in heart injury by preventing pore formation and the release of cytochrome C (17).

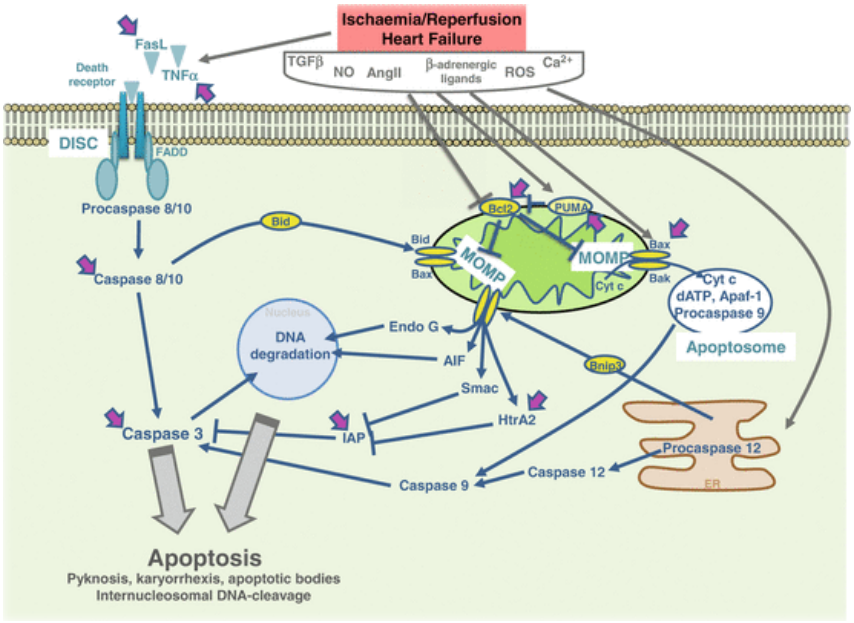

Figure 2: *Apoptotic signaling pathways.* Two distinct signaling pathways drive apoptosis: The intrinsic pathway driven by mitochondria and the extrinsic pathway driven by specific receptors (5).

The extrinsic pathway is triggered by death receptors (i.e. DR5) and their ligand (i.e. TRAIL). This process recruits FADD and procaspase 8 or 10. The auto-proteolytic cleavage of the procaspase 8 or 10 results in the release of caspase 8 or 10, which are responsible for the cleavage of other downstream effector caspases. Both pathways activate the effective caspase 3, which induces cell death.

1.2. Cardiac regeneration

The regeneration is the natural ability of living organisms to repair and restore structural and functional integrity of the lost or damaged organ. This process involves the replacement of one damaged cell type by cells of the same nature. Regeneration implies the recovery of the original cell number and organ function after a damage.

Heart regeneration occurs naturally during the life of organisms such as urodeles, newts and zebrafish. Indeed, zebrafish hearts regenerate completely after 20% of ventricular amputation, through the proliferation of pre-existing CMs (18). In

contrast to the heart of lower vertebrates, the heart of mammals was for a long time considered as a post-mitotic organ with no capacity to regenerate. However, in the past decade, some results highlight the fascinating possibility that mammalian heart has an endogenous regenerative capacity. Indeed, study based on the interpretation of carbon-14 birth dating demonstrated in humans, that the mammalian heart has a low physiological regenerative capacity (19). However, this process occurs at low rate (0.5-1% of the CMs are renewed per year) (19, 20). On this basis, two distinct mechanisms, able to replace CMs after ischemia, have been described: 1) the differentiation of endogenous (i.e. cardiac cells) or exogenous (i.e. bone marrow cells) precursor cells 2) the proliferation of pre-existing CMs.

1.2.1. The differentiation of precursor cells as source of new cardiomyocytes

The two last decades, numerous researches were aimed to determine whether the use of precursor cells is beneficial in order to regenerate hearts after injury. Thus, many clinical trials have been performed on patients suffering from CVDs.

The first-generation of cell-based therapy consisted to inject non-cardiac precursor cells such as unselected bone marrow derived mononuclear cells, purified mesenchymal stem cells, endothelial progenitor cells or skeletal myoblasts (21). These cells are available from autologous sources, they can be expanded in high number *ex vivo* and then injected at an adequate quantity into the heart. Numerous clinical trials have been performed, but controversial results were obtained with regard to cardiac recovery on patients suffering from acute myocardial infarction and chronic heart failure (23). Indeed, the *in vitro* cell selection and expansion as well as the delay in cell injection after hypoxia limit the cell potential to regenerate hearts. Therefore, low survival and low engraftment of these cells were reported (21, 24, 25).

Due to the disappointing results obtained with the first-generation strategy, cardiac research shifted toward the second-generation of cell-based therapy, which includes the use of multipotent cardiac precursor cells (CPCs), pluripotent stem cells (i.e. embryonic stem cells (ESCs) and induced pluripotent stem cells (iPSCs). CPCs are derived from the heart, they are multipotent, self-renewal and they can differentiate into three different lineages: CMs, endothelial cells and vascular smooth muscle cells. They can be isolated from the Hoechst-extruding side population, from the epicardium, the atria or the ventricles (26, 27). Different CPC populations are described in humans and/or mice such as c-kit positive cells (c-

kit$^+$), Sca-1 positive cells (Sca-1$^+$) (not in humans), Isl-1 positive cells (Isl-1$^+$) and cardiosphere-derived cells (CDCs) (28-30).

Two main clinical studies were performed on human injured hearts (SCIPIO with c-kit$^+$ cells and CADUCEUS with CDCs). These therapies consisted to isolate CPCs and CDCs from the donor hearts, to expand the cells *ex vivo* and then to re-inject the cells into the donor heart (31, 32). These clinical trials reported controversial results regarding improvement of the cardiac function, but it was shown in CADUCEUS study that the scar mass was significantly reduced and that the viable heart mass and the regional contractility increased on one-year follow-up (32). In animal models, CPCs (c-kit$^+$, Sca-1$^+$, Isl-1$^+$ cells) have been shown to participate in heart regeneration by differentiating into CMs during physiological growth, but also in pathological conditions (26, 33-35). However, after several years of controversy, several groups have used new mouse models allowing to trace the lineage of CPCs and they demonstrated that precursor cells are able to differentiate into CMs during embryogenesis, but not in adult hearts during physiological ageing or in pathological conditions (36-40).

ESC and iPSC were also studied for their high potential of differentiation and proliferation (41). One clinical trial on patients with ischemia-induced heart failure demonstrated that transplanted ESCs improve cardiac function (42). Several studies in animal models confirm the beneficial use of ESCs (43-46). However, these studies also demonstrated the crucial limitations of these cells. Indeed, ESC injections induce teratomas and cause serious safety and ethical issues (i.e. immunogenic properties, proarrhythmic effects), complicating the potential use of these cells in clinics (47).

iPSCs were also developed by reprogramming dermal fibroblasts using retroviral expression of the fourth transcription factors Oct-3/4, Sox2, Klf4 and c-Myc. This strategy, aimed to obtain cells with the same characteristics as ES cells, gives rise to functional CMs *in vitro* after differentiation obtained by culture in presence of different factors (26). Few pre-clinical trials were achieved on large animal models (i.e. porcine and non-human primates), which showed encouraging results by increasing the cardiac function (48, 49). However, these cells have a low engraftment rate and their use could increase the risk of tumorigenesis and arrhythmias. To overcome some of these limitations, another approach proposes to target directly resident cardiac fibroblasts without isolating them. By direct reprogramming strategy, Ieda and his group demonstrated the ability to

transdifferentiate mouse dermal fibroblasts into functional beating CMs (iCMs) by using three transcription factors, Gata4, Mef2c and Tbx5 (50). In injured murine hearts, the direct reprogramming of cardiac fibroblasts by using retroviral delivery of reprogramming cocktails improves cardiac function and reduces fibrosis (51-53).

Although promising progress has been made in the field of cardiac stem-cell based therapy, the low engraftment and low survival rate of the injected cells suggest, that the improvement of cardiac function observed is rather the consequence of a paracrine stimulation of endogenous repair mechanism.

1.2.2. The proliferation of pre-existing cardiomyocytes as source of new cardiomyocytes

Numerous researches demonstrated that the renewal of CMs during ageing and in pathological conditions occurs mainly by the proliferation of "pre-existing" CMs (54-56). This capacity is clearly dependent on signals coming from the environment.

During embryogenesis, depletion of 60% of the heart has no consequence on cardiac function into adulthood thanks to complete replacement of the CM pool by intensive proliferation of the surviving CMs (57). However, numerous studies demonstrated that the CM proliferation capacity declines during the first week of postnatal life. In the mouse hearts, 5% to 10% of the CMs proliferate up to day 4 after birth, while only 1% of CMs proliferate 5 days after birth (58, 59). Consequently, surgical resection of the hearts performed few days after birth in mice leads to a complete heart regeneration thanks to intensive CM proliferation and no fibrosis development (60). In neonatal pig hearts, acute MI until 2 days after birth leads to a complete cardiac regeneration by CM proliferation, which leads to restoration of cardiac function. However, 2 days after birth, CMs exit from the cell cycle and systolic function is impaired (61). In humans, several clinical reports suggest that similarly to neonatal mice, neonatal human hearts have the capacity to regenerate and to completely restore the cardiac function after MI (62-64). They suggest that this process is triggered by CM proliferation since an increased number of CMs expressing the proliferative marker Ki67 was detected (62).

In adult mouse hearts, in physiological conditions, CM proliferation rate declines drastically. The formation of new CMs occurs at a frequency of 0.015% in the

hearts of young adult mice over a period of 8 weeks (65). In injured adult hearts, first evidences of CM proliferation came from the group of Senyo who demonstrated, thanks to multi isotope mass spectrometry analysis, that pre-existing CMs are the main source of newly formed CMs during ageing, but also after MI. The rate of CM proliferation increases 5-fold after MI (54).

Even if CM proliferation exists in adult mammalian hearts, this process is so limited that it is not sufficient to restore the impaired cardiac function after heart injury. Therefore, cardiac research concentrates its efforts to better understand why the proliferation capacity of CM declines during physiological ageing in mammals. The aim is thus to determine, how factors, regulating the transition from neonatal to adult stage (i.e. the oxygen concentration, CM metabolism, CM nucleation and CM structural organization), can modulate CM proliferation arrest (Fig. 3).

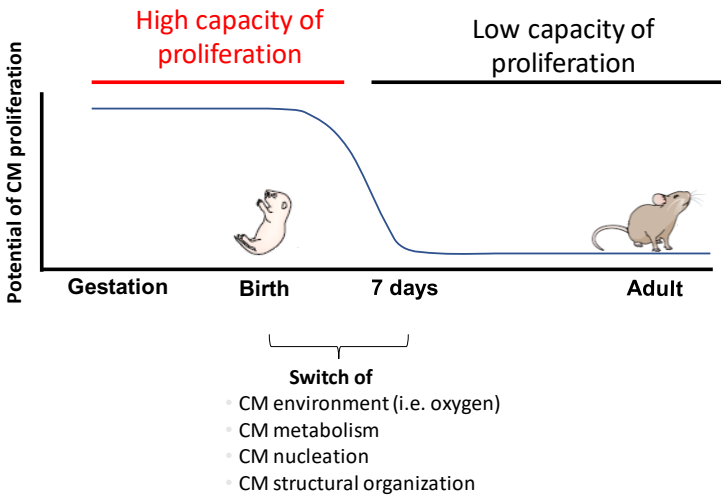

Figure 3: *CM proliferation capacity in mammals declines with age.* The proliferation capacity of CMs is high during gestation and during the first few days after birth, but decreases rapidly. Different factors are involved in this decrease such as environmental factors, metabolism, CM nucleation and CM structural organization.

1.2.2.1. Oxygen concentration

Both zebrafish and mammals, during intra-uterine life, are living in low oxygen environment (can reach up to 15-30mm Hg). While zebrafish remains in the same environment for its entire life, mammals at birth increase rapidly their level of oxygen (as the atmospheric environment corresponds to 160mm Hg) (66, 67). This rapid increase of oxygen concentration leads to the expansion of the pulmonary alveoli, which in turn induces an increased blood volume into the two ventricles. Thus, CMs have to resist to the increased workload. In order to respond to this new environment, several structural modifications are taking place in CMs

which refer, for example, to mitochondria. Indeed, mitochondria adapt their metabolism to high oxygen level. However, this adaptation induces also the release of reactive oxygen species (ROS). High levels of ROS can induce cellular toxicity by promoting protein and nucleic acid damages, which could result in cell cycle arrest and apoptosis (68-71). Thus, the switch of oxygen concentration is considered as the main cause of CM cell cycle arrest between neonatal and adult mammalian hearts. Therefore, several recent studies examined the effect of the oxygen concentration on CM cell fate.

During ischemia, decreased oxygen supply in adult hearts induces 1) a switch from a fatty acid to a "fetal–like" metabolism based on glycolysis, 2) cell death, 3) CM hypertrophy, 4) fibrosis, and 5) a decrease of heart contractility (72). Thus, hypoxia modulates gene expression coding for proteins involved in metabolism, cell death, proliferation and/or differentiation. These transcriptional responses are in part mediated by the transcription factor HIF-1 (hypoxia inducible factor 1).
HIF-1 is a heterodimer protein composed of an α- and a β-subunit. The α-subunit is regulated in an oxygen-sensitive manner, and is localized in normoxic conditions (i.e. 20% of oxygen supply) in the CM cytoplasm, while the constitutive β-subunit is localized in the nucleus. In normoxic conditions, HIF-1α is rapidly degraded. By contrast, in presence of low oxygen concentrations, HIF-1α escapes from proteasomal degradation, accumulates in the cytoplasm and translocates into the nucleus, where it dimerizes with HIF-1β. The heterodimer modulates the transcription of several genes, such as the gene coding for the glucose transporter GLUT1, involved in the metabolism switch after hypoxia, or the gene coding for the vascular endothelial growth factor (VEGF) involved in angiogenesis (73).
Interestingly, HIF-1 seems to modulate gene and protein expressions involved in CM proliferation, including cyclin D1, VEGF, p38 MAPK and YAP (74-76). Kimura and his group demonstrated that the pool of CM, proliferating in ischemic adult hearts, expresses HIF-1α (77). Thus, 2 weeks after MI induction, mice were submitted to a reduction in inspired oxygen concentration (7% O_2 instead of 20%). These mice displayed increased cardiac function and reduced cardiac fibrosis when compared to mice living at 20% oxygen. Furthermore, an increased proliferation of CMs expressing HIF-1α was detected in the infarcted mice surviving at 7% oxygen (78). In addition, Vujic and his group demonstrated that exercise stimulates CM proliferation in mice, which may be attributed to a hypoxic environment due to the upregulation of HIF-1α (79). However, the expression of

HIF-1α can not only stimulate CM proliferation. Indeed, 1% oxygen induces HIF-1α expression on neonatal CMs *in vitro*, but inhibits their proliferation and induces cell apoptosis (80). Furthermore, a chronic maternal hypoxia (10.5% O_2) reveals a fetal CMs exit from the cell cycle (81).

Altogether, these results suggest that the level of hypoxia as well as the maturity of the CMs undergoing hypoxia are critical factors to modulate CM proliferation.

1.2.2.2. CM metabolism

During embryonic development and its low oxygen environment, anaerobic glycolysis and lactate oxidation are the main sources of cardiac energy (82). Immediately after birth, although under high oxygen supply, the heart relies predominantly on glycolysis and lactate oxidation. During the first week of life, metabolism switches from glycolysis to fatty acid oxidation as a main source of ATP production (83). With this new substrate, adult heart increases its metabolism efficiency and the contractility essential for the body growth. This switch of metabolism is followed by CM growth. In addition, CM mitochondria mass increases and its internal structure is reorganized such as the shape of the cristae. All mitochondria modifications induce ROS production (84). Interestingly, low concentration of ROS is non-toxic for the cells. Indeed, antioxidants such as N-acetylcysteine, α-tocopherol (vitamin E), ascorbate (vitamin C) or the activation of endogenous antioxidant signaling pathways have the capacity of scavenging ROS (85). However, when the antioxidant capacity of the cells is not sufficient to neutralize ROS, they accumulate and generate oxidative stress, which contributes to cardiac dysfunction, cardiac remodeling and cell death after I/R injury (86, 87).

After ischemia, the decreased oxygen supply induces a switch from a fatty acid to a "fetal–like" metabolism based on glycolysis (88). This metabolism switch should be favorable to regeneration (i.e. fetal life). Indeed, in some reports, it was shown that a "fetal-like" metabolism based on glycolysis and/or fatty acid inhibition after MI stimulates CM proliferation (89-91). By contrast, other works demonstrated the beneficial role of fatty acid oxidation to stimulate CM proliferation within the first 5 days after birth (92, 93). Indeed, between 2-4 days after birth, fatty acid β-oxidation activation increases CM proliferation and CM maturation (hypertrophy and binucleation). Thus, fatty acid β-oxidation activation could stimulate both CM proliferation and CM maturation few days after birth and induces 7 days after birth cell cycle activity arrest.

1.2.2.3. CM nucleation

Another important characteristic of CMs is their state of nucleation and ploidy. In zebrafish and in mammals, during heart development and shortly after birth, CMs are mononucleated (one nuclei) and diploid (2n). In mammals during the first week after birth, CMs become multinucleated and/or polyploid (more than two sets of chromosomes) as a consequence of the adaptation of CMs to their new environment. Interestingly, this is correlated with the arrest of CM proliferation (71, 94). Thus, mononucleated and diploid CMs are associated to a normal productive cell cycle progression, whereas polyploidy and binucleation are related to an arrest of cell cycle progression (95-97). Mononucleated and diploid CMs undergo G1 phase, S phase, G2 phase and finally mitosis, including karyokinesis (nuclear division) and cytokinesis (cell division) (Fig. 4). Thus, a real CM proliferation will produce two mononucleated and diploid daughter cells (Fig. 4 on the right).

Polyploidy occurs when cell cycle is abrogated after the S phase (process of endocycling) (Fig. 4 on the left). Multinucleation occurs when cell cycle is abrogated during cytokinesis (Fig. 4 on the left). Several cytokinesis failures lead to multinucleation (i.e. tri- or quadri-nucleated), whereas several karyokinesis failures lead to polyploidy (i.e. 4, 8, 16n) (98).

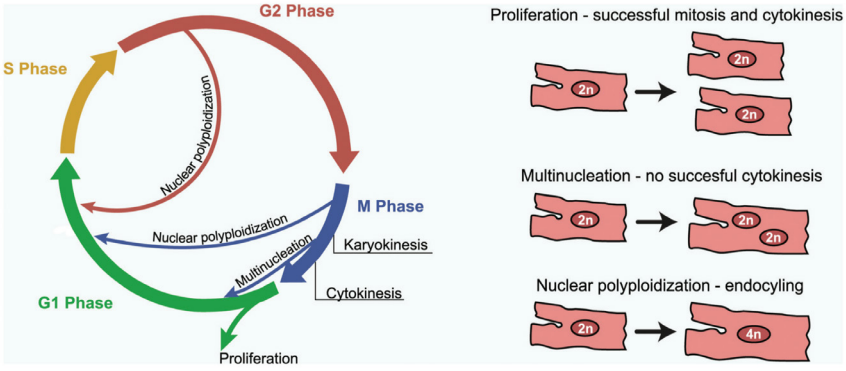

Figure 4: *Schematic representation of mitosis failure.* **On the left:** Different phases of the cell cycle, including mitotic failures, are represented. Between S phase and M phase, nuclear polyploidization occurs, whereas binucleation or multinucleation occurs only during M phase. **On the right:** Consequences of mitotic failures (99).

The state of nucleation and/or polyploidy in CMs is highly dependent on the organisms, the development stage, the genetic background and the regulation of the body temperature (endotherm or ectotherm). For example, ectotherm species, such as zebrafish and newts display mononucleated/diploid CMs, which are able to proliferate (100). By contrast, CMs from endotherm species, such as birds, mice

and humans are mainly multinucleated and polyploid (101). Among these endotherm species, the ratio of multinucleated/polyploid CMs is highly dependent on the species (98, 102). Indeed, human adult CMs are mainly mononucleated and polyploid whereas mice, rabbits and rats are predominantly binucleated and pigs multinucleated (>8 nuclei) (103). The genetic background in adult mammalian CMs is also a factor modulating the frequency of adult mononuclear CMs (104).

It is well admitted that CM proliferation is linked to mononucleated and diploid CMs. However, new findings highlight the benefit of multinucleation and polyploidy. In fact, it seems that binucleated and/or polyploid CMs could also proliferate in neonatal mouse hearts 7 days after birth (65, 105, 106). Furthermore, in zebrafish, polyploid CMs support heart regeneration (107). Indeed, the regeneration of the epicardium in zebrafish is performed due to the collaboration of two distinct CM cell types: the leader cells and the follower cells. The leader cells are localized at the front of the regenerating tissue and arise during heart injury and high mechanical tension. This environment induces a process of endoreplication as a result of failed cytokinesis, leading to "leader polyploid/multinucleated cells". The follower CM cells are localized behind the leader cells, they are small, mononucleated and proliferate rapidly (108). Interestingly, leader cells display greater migration velocities, mechanical tension and have a greater surface coverage compared to the follower cells (107). Thus, leader cells were shown to support the process of regeneration in zebrafish due to their properties (polyploid/binucleated) (107).

Another advantage of polyploid/multinucleated CMs is the ability to increase their size and their metabolic activity. Thus, these cells are more resistant to stress and have the ability to maintain heart contractility after injury compared to mononucleated diploid CMs. Furthermore, it was shown that hypoxia on mice triggers an increased number of polyploid and multinucleated CMs. Interestingly, these cells display a better adaptation to stress by decreasing apoptosis and ROS production compared to mononucleated/diploid CMs (76).

To conclude, the level of DNA content present in CMs is a key factor determining cell cycle progression, cell death and metabolic activity. While, mononucleated diploid CMs are related to cell cycle activity, binucleated polyploid CMs are beneficial for heart function and for CM survival after cardiac damage. Thus, currently it is not clear, if binucleated polyploid CMs can also be useful for the heart after injury (99).

1.2.2.4. CM structure

Quickly after birth, CMs undergo a first phase of proliferation (until 5 days) and then a second phase of hypertrophy. This process transforms CM architecture (109). The architecture becomes more complex with an increase of intracellular structures, such as sarcoplasmic reticulum, myofilaments and mitochondria (110, 111). The CMs switch from a polygonal to an elongated form. The complexity of the adult CM cell structure could also limit their proliferation. That is why several studies, performed on zebrafish, on mice (*in vitro* and *in vivo* after MI) and on humans suggested that CMs have to go through a step of dedifferentiation before proliferation (18, 106, 112, 113). This process was described *in vitro*, with a partial or total loss of the highly organized sarcomere structures (106, 114). The cells become smaller and re-express some fetal genes such as Nkx2.5, Gata-4, Runx1, Dab2, α-SKA, Fosl1, Sox4 and Tmsb10 (Fig. 5) (18, 115-117). Simultaneously, CMs down-regulate the expression of mature CM proteins such as alpha myosin heavy chain (α-MHC) and cardiac Troponin, and re-express the fetal isoform of the MHC (β-MHC) (Fig. 5). This new structure should facilitate their re-entry into the cell cycle in order to undergo karyokinesis and cytokinesis.

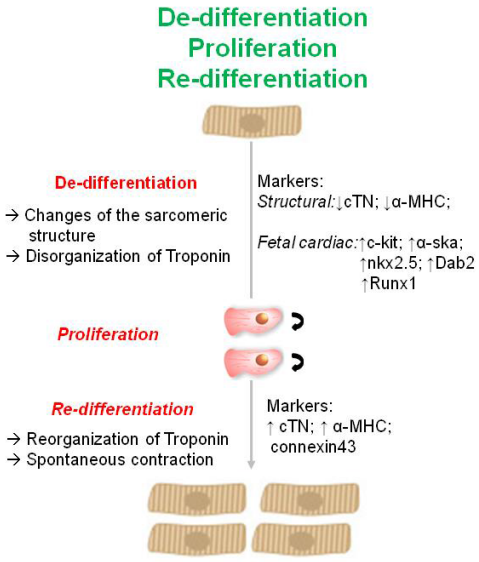

Figure 5: *Process of CM dedifferentiation.*

This process was described in human hearts and in hearts of animal models suffering from heart diseases (113, 116, 118). CM treatment with Oncostatin M or components of the extracellular matrix (ECM) (i.e. agrin) are able to induce CM dedifferentiation (115, 119) . In adult infarcted mouse hearts, CM dedifferentiation occurs mainly in the infarct border zone and leads to a partial loss of Troponin I expression in CMs ($cTnI^{+/-}$ cells). In this zone, dedifferentiated CMs proliferate and

build new connections with the remaining tissue via the connexin 43 (106). The advantage of CM dedifferentiation in hearts depends on the nature of the cardiac diseases: CM dedifferentiation induces CM remodeling and improvement of cardiac function after MI, whereas in dilated cardiomyopathy this process deteriorates cardiac performances (115, 120).

Although dedifferentiation was highlighted in hearts of animal models and in humans, the direct link between dedifferentiation and proliferation has not yet been established. Indeed, it remains difficult to demonstrate *in vivo* that dividing cells go through a dedifferentiation step prior to divide. Recently, a new tri-transgenic cardiac nucleus-specific reporter mouse based on Cre/LoxP system was used to characterize CM cell cycle activity associated with CM dedifferentiation *in vivo* (117). This mouse model combines the reporter green fluorescent protein (GFP) with a blue fluorescent protein (BFP), fused with the histone H2B reporter gene. Both are under the control of a specific promoter for mature CMs (α-myosin heavy chain). Thanks to this mouse, the origin of new CMs could be determined by evaluating GFP protein expression into the cytoplasm and also CM dedifferentiation via BFP protein expression in nuclei. GFP protein is expressed only in CMs after Tamoxifen injection and Cre recombinase expression, whereas BFP is constitutively expressed in CMs and linked to nuclei. Thus, to study dedifferentiated CMs, they focused on GFP^{+} $BFP^{+/-}$ CMs. Dedifferentiated CMs from post-infarct hearts were separated by fluorescence-activated cell sorting and a transcriptome analysis was performed to determine the expression of the cell cycle markers (117). GFP^{+} $BFP^{+/-}$ CMs are associated with an upregulation of genes, related to adult CM dedifferentiation (i.e. Runx1 and Dab2) and cell cycle activity (i.e. cyclin D3 and Cdk14). Thus, they concluded that the majority of CMs undergoing cell cycle progression after MI are dedifferentiated, which in turn is a prerequisite for CM proliferation. However, the direct link between dedifferentiation and a real proliferation leading to increased number of CMs after heart injury remains elusive and based only on transcriptomic analysis. To conclude, the direct link between CM dedifferentiation and CM proliferation is not yet elucidated.

1.2.2.5. Signaling pathways in neonatal and adult cardiomyocytes during proliferation

CM proliferation occurs during embryonic, fetal and post-natal life and is driven by several factors and signaling pathways. CM proliferation arrest early after birth is conducted either by the silencing or by the activation of endogenous signaling pathways. The key question of adult cardiac regenerative medicine is to determine whether these endogenous signaling pathways could be re-activated or inactivated in adult hearts during physiological ageing and/or after injuries, in order to induce CM cell cycle re-entry. Also, the presence of adult specific signaling pathway(s) (i.e. not present during fetal or post-natal life) able to control CM proliferation cannot be excluded, but will be more difficult to identify, as most research focuses on the "already known" signaling pathways involved in heart development (109). In this section, four of these signaling pathway will be described:

a) phosphoinositide 3-kinase (PI3K)/AKT

PI3K/AKT regulates as well CM proliferation as CM apoptosis and plays a cardioprotective role after heart injury (121). PI3K/AKT is activated by different stimuli, such as YAP/TEAD1, FGF-1 and neuregulin-1 (NRG-1). NRG-1 and both co-receptors ErbB2 and ErbB4 are highly expressed in fetal CMs and regulate cardiac development (122). Through the heterodimerization of ErbB2 and ErbB4, NRG-1 triggers the activation of signaling pathways such as PI3K/AKT and the MAPK/ERK in order to stimulate CM proliferation (Fig. 6A) (123, 124). However, at birth and at juvenile stage, ErbB2 expression diminished and then CM proliferation decreases. Growth factors, such as FGF-1 and FGF-10, have also been shown to stimulate CM proliferation trough the activation of PI3K/AKT pathway (125, 126). In fetal and adult mice, FGF-10 stimulates CM proliferation through FOXO3/p27(kip1) pathway (125). The FOXO family transcriptional factors are regulated by AKT phosphorylation.

Activation of PI3K/AKT pathway leads to the progression of G1 to S phase, which is determined by the cyclin dependent kinase (CDK). Therefore, constitutive expression of AKT prolongs the half-life of cyclin D and stimulates cell cycle activity (Fig. 6A) (127). Furthermore, PI3K/AKT also regulates the G2/M phase progression that leads to increased proliferation in neonatal CMs (Fig. 6A) (128).

b) Ras-Raf-MEK-ERK (MAPK/ERK)

The activation of MAPK/ERK pathway stimulates CM proliferation, CM hypertrophy and protects CMs against cell death (129). In CMs, ERK signaling cascade is initiated by activation of the small G protein Ras, leading to the recruitment and activation of MAP3K and c-RAF. Then, they activate MEK1/2 and ERK1/2 leading to the translocation of ERK1/2 into the nucleus and the modulation of the transcription of several genes, such as GATA-4, cyclin D1 and D2 (Fig. 6A) (130-132). NRG-1 and its heterodimers receptors ErbB2 as well as the extracellular matrix protein agrin are factors stimulating CM proliferation via MAPK/ERK signaling pathway activation (95, 133). In neonatal and adult CMs, NRG-1 activates MAPK/ERK signaling to stimulate CM proliferation and also activates PI3K/AKT signaling to induce CM dedifferentiation and hypertrophy (95).

c) p38 MAPK

The p38 MAPK pathway activation during the development blocks CM proliferation and induces CM hypertrophy (134). Furthermore, in neonatal and adult mice, inhibition of the p38 phosphorylation triggers CM proliferation by stimulating genes related to G2/M phase, such as cyclin A2 and cyclin B (Fig. 6A) (135, 136). In adult infarcted hearts, p38 inhibition associated with FGF-1 stimulation increases cardiac regeneration through the stimulation of CM proliferation and inhibition of apoptosis (137).

d) Hippo Pathway

Hippo signaling pathway plays an evolutionarily conserved role during development in the control of the organ size. Two key components of this pathway are the transcriptional co-activators YAP and TAZ (138). Activation of the Hippo pathway induces the phosphorylation of the complex YAP/TAZ and its proteolytic degradation into the cytoplasm. By contrast, Hippo pathway inhibition induces the translocation into the nucleus of the non-phosphorylated YAP/TAZ complex and thus activates the transcription of many genes related to cell proliferation, differentiation, survival and migration (138). Inactivation of this pathway leads to an increase of the heart size during the development due to the stimulation of CM proliferation. After MI, Hippo pathway inhibition stimulates heart regeneration by increasing CM proliferation, CM dedifferentiation, survival and reduction of scar size (139-141).

Hippo signaling is linked to PI3K/AKT pathway (Fig. 6A). In the nucleus, YAP interacts with the transcription factor TEAD1 to upregulate the transcription of several genes such as Pi3kcb, which activates downstream mitogenic pathways, including the PI3K/AKT pathway (Fig. 6A) (142). Furthermore, Hippo signaling is associated with glycolytic metabolism to induce CM proliferation. Indeed, in neonatal infarcted heart, the activation of Toll-like receptors-3 stimulates glycolysis, which in turn inhibits Lats1 (large tumor suppressor 1 phosphorylating YAP) and then activates CM proliferation (143).

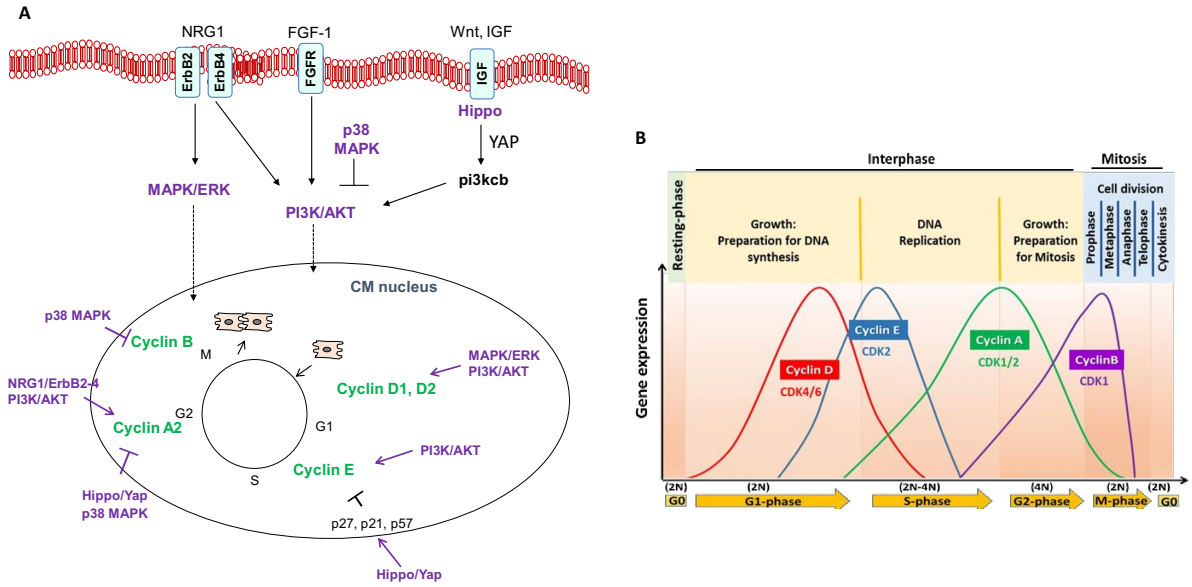

Figure 6: *Cellular signaling pathways in CM proliferation.* **A:** Four main signaling pathways are involved in CM proliferation, such as p38 MAPK, MAPK/ERK, Hippo and PI3K/AKT. All of them converge into the nucleus to regulate key regulators of the cell cycle progression, including cyclin D1, D2, E, A2 and B. Purple: Signaling pathways; green: Cell cycle regulators. **B:** Cyclin expressions across cell cycle (144).

All these signaling pathways act on the transcriptional regulation of cell cycle regulators, including cyclins, cyclin-dependent kinases (CDKs) and CDKs inhibitors (i.e. p21, p27, p57) (Fig. 6B). Depending on the regulation of signaling pathways, the expression of cyclins, CDKs and CDKs inhibitors will be modulated in order to trigger CM re-entry into cell cycle and cell division.

Overexpression of cyclin D2 was shown to promote CM proliferation and improve cardiac function after MI in mammals (145). Repression of cyclin D1 was related to cell cycle arrest at the G2 checkpoint in adult CMs (146). However, the upregulation of cyclin D1 only pushes the cell to re-enter the cell cycle, but without proliferation, leading to the formation of binucleated CMs (127). Thus, both cyclins D1 and D2 push CMs to re-enter the cell cycle; however, only the cyclin D2 triggers

CM proliferation. In addition, overexpression of cyclin A2, a key regulator mediating G1/S and G2/M transition, leads to CM proliferation and increased cardiac function after MI in mice and pigs (147-149). Furthermore, it was found that overexpression of cyclins and CDKs (i.e. CDK1, CDK4, cyclin B1 and cyclin D1) induces CM proliferation and improves cardiac function after heart injury (97).

Finally, transcription factors can also regulate the expression of these cell cycle regulators. Some of them were already described as main factors which stimulate CM proliferation via the cell cycle regulators such as E2F, GATA-4, TBx20, Meis-1 and HIF-1α (150-153).

1.2.3. Methods to identify cardiomyocyte proliferation

The determination of CM proliferation is one major indicator of heart regeneration after injury. This last decade, several technics have been used to estimate the level of CM proliferation. These technics include labeling assays such as stainings against 5'-bromo-2'-deoxyuridine (BrdU), Ki67 and pH3. These methods detect CM proliferation by measuring the DNA replication (karyokinesis). BrdU is integrated during the synthesis of cDNA and thus indicates cell cycle progression through the S phase. Ki67 is expressed in all phases of the cell cycle (except G0) and pH3 is a histone phosphorylation expressed during the G2/M phase.

One main characteristic of CMs is their capacity to replicate DNA without cell division, leading to the formation of binucleated and/or polyploid CMs (see section 1.2.2.3). The already described technics (labeling assay) do not allow to discriminate between binucleation and cell division, a process that occurs at the end of the mitosis.

To overcome this limitation, staining against Aurora B (Aurkb) is widely used. Aurkb is localized in the nucleus during the G2/M phase and on the midbody during cytokinesis (Fig. 7). This marker helps to discriminate between a real cell division from a binucleation by highlighting the localization of the midbody. During cell division, Aurkb is expressed symmetrically between the two nuclei of the dividing cell, whereas during binucleation Aurkb is localized at the extremity of the two daughter cells (Fig. 7) (154). However, a report suggested that Aurkb staining alone is not sufficient to discriminate between binucleation and cell division, (155). Therefore, new technics have emerged recently in order to visualize real CM cell division. Some of these technics will be described in the next part.

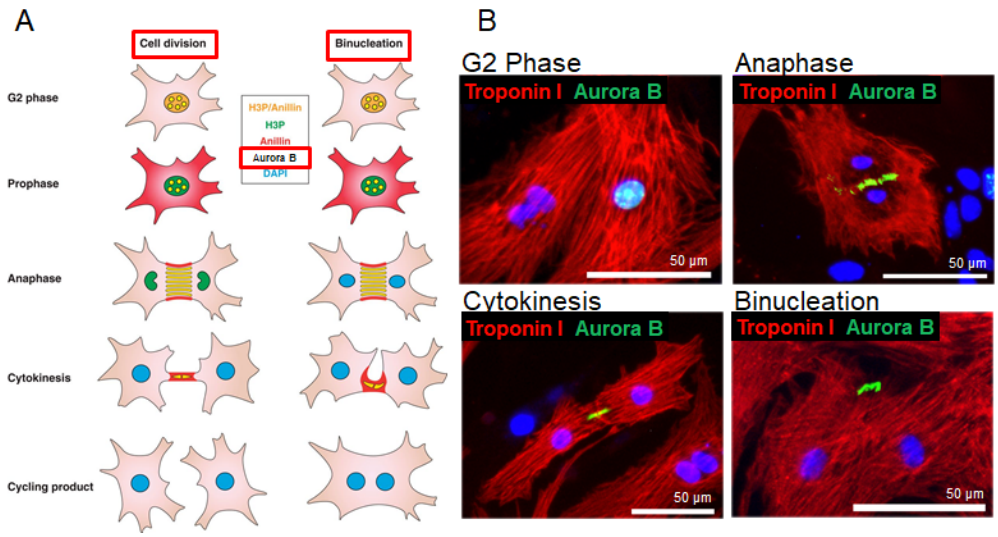

Figure 7: *Aurora B (Aurkb) localization during CM proliferation.* **A:** Schema adapted from Engel and his group *(154)*. **B:** Personal pictures representative of Aurora B (green) Troponin I (red) staining on neonatal CMs after 14 days of culture.

The first method to discriminate CM cell division from binucleation is reported by Hesse and his group and is based on the distance and position between two nuclei of dividing CMs. Cells were stained with the two mitotic markers, Aurkb and Ki67, and a marker allowing to identify CMs. With this method, dividing cells show positive labelling for Ki67 and AurkB, localized symmetrically between the two nuclei of the dividing cell with a distance of ≤5µm between both nuclei (see section 4.2 Fig 28). By contrast, binucleated cells show a distance ≥5µm between both nuclei (155).

Other methods combine the use of key markers of the mitotic spindle, such as IQGAP3, RhoA and anillin (156). The late mitotic phase is characterized by the assembly of the contractile ring (localized with actomyosin) and the midbody (Fig. 8). Leone and his group focused on the mitotic spindle orientation and expression of several proteins involved in the central spindle microtubules alignment. Three proteins, IQGAP3, RhoA and anillin have been shown to be disturbed during binucleation, since these proteins are delocalized during an inefficient anchorage of the actomyosin ring to the plasma cell membrane. (Fig. 8) (156). As shown in Figure 8, the use of IQAP3 and/or RhoA helps to discriminate cell division from multinucleation.

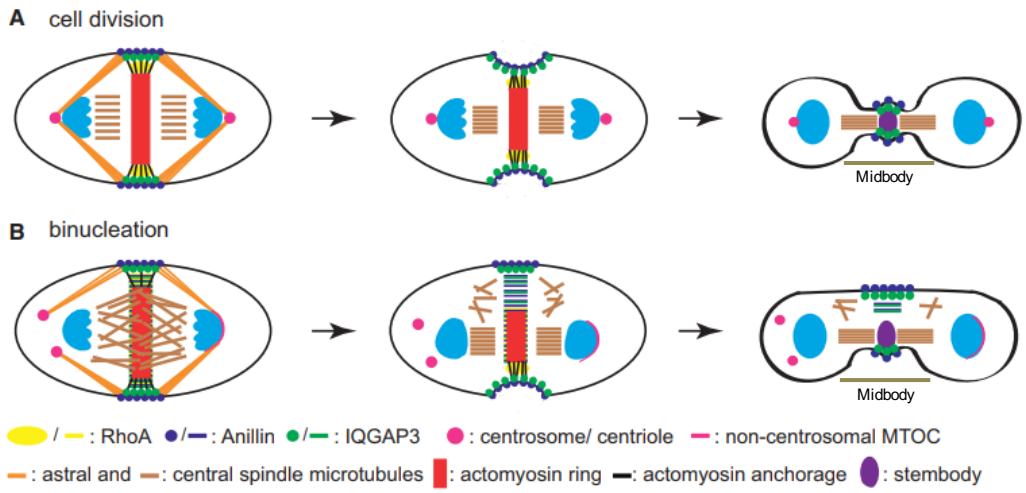

Figure 8: *Localization of mitotic spindle markers in cell division and binucleation (156).* **A:** CM cell division with the localization of specific mitotic spindle markers, such as IQGAP3, anillin and RhoA. **B:** CM binucleation associated with a failure in the localization of mitotic spindle markers due to an improper furrow ingression.

Genetic fate mapping in mice was also developed to discriminate between binucleation and cytokinesis.

MADM (mosaic analysis with double markers) mice are used for lineage tracing and are based on the Cre-loxP-dependent interchromosomal mitotic recombination (157). Two chimeric genes code either for a part of the coding sequence of Green Fluorescent Protein (GFP) or for the Red Fluorescent Protein (Dsred2). During the G2 phase, Cre-loxP-mediated homologous recombination. Thanks to this recombination, the dividing cells will be labeled with a single color, either in green (GFP) or in red (Dsred2). By contrast, the non-dividing cells (binucleation) remain colorless (as mother cells) or appear yellow due to the double-labeled (red and green) (97, 158).

Furthermore, Raulf and his group generated Myh6 MerCreMer mice combined with the human histone 2B-mCherry (H2B) and eGFP-anillin. With the localization of the H2B and anillin, the visualization of cell cycle progression and division could be performed (Fig. 8) (155, 159).

One major advantage of both lineage tracing systems (MADM and Myh6 MerCreMer transgenic mice) is the use of a specific cardiac promoter (i.e. α-MHC), which makes it possible to distinguish CMs from others cardiac cells. Thus, CM fate can be easily analyzed by immunohistochemistry or also by using time lapse imaging.

The Fluorescence Ubiquitination-based Cell Cycle Indicator (FUCCI) transgenic mice is also a valuable tool to follow cell cycle progression and proliferation of CMs (160, 161). Two main proteins (Geminin and DNA replication factor 1 (Cdt1))

regulate the cell replication by ensuring one round of replication per cell cycle. These proteins oscillate inversely during the cell cycle: Cdt1 level is high during G1, whereas Geminin level is high during the S, G2 and M phases (162). Two transgenic mice were generated, one with the protein Cdt1, fused with red emitting fluorescent protein, and the other with Geminin, fused with green emitting fluorescent protein. Both of these mouse strains were crossed in order to generate heterozygous mice, and as a result the following fluorescence labelling could be observed depending on the phases of the cell cycle: cells in G1 phase are labelled in red, cells in the transition from G1/S are labelled in yellow and cells in the S/G2 and M phases are labelled in green. These mice can be used to determine the phase of the cell cycle for each CM in the heart.

1.3. The Brain Natriuretic Peptide is involved in the regulation of cardiac cell fate

Over the past decade, cardiac research has focused on the discovery of new factors able to stimulate CM proliferation. During my thesis, I focused on the oxygen (see section 1.2.2.1) and the Brain Natriuretic Peptide (BNP).

Brain natriuretic peptide (BNP), which belongs to the natriuretic peptide family (NP), is a hormone mainly secreted in the ventricle. Two other members of NPs exist, the atrial natriuretic peptide (ANP), secreted in the cardiac atria, and the C-type natriuretic peptide (CNP), secreted in the brain, bone and vascular endothelial cells. BNP was first discovered in the bovine brain, but it is now well established that the main source of BNP in the body is the heart and especially the ventricle (163). BNP displays an endocrine effect (by acting on remote organs) and/or acts directly on the heart itself (164). In fact, it has several functions on organs, such as on kidneys by increasing the natriuresis and diuresis, on vessels by increasing vasodilatation, on the autonomic nervous system by reducing blood volume and on the adipose tissue by promoting mitochondrial biogenesis (165). In the heart, BNP has a cardioprotective effect after MI by increasing the cardiac function and decreasing heart remodeling (166).

1.3.1. BNP biosynthesis

BNP is a polypeptide of 32 amino acids (aa) in humans and pigs and 45 aa in mice and rats (167). The transcript of the gene encoding BNP is first translated to a 134-aa preprohormone named preproBNP (Fig. 9). Then, preproBNP is processed by cleavage of the N-terminal fragment (via corin and/or furin) to produce the

proBNP (108-aa). Finally, proBNP is enzymatically cleaved by corin and/or furin, resulting in an inactive secreted 76-residue amino-terminal fragment (NT-proBNP) and in an active 32-aa C-terminal fragment (BNP) (Fig. 9). ProBNP, NT-proBNP and BNP are present in the circulation (168). However, only the biological active form of BNP (1-32aa) is able to trigger biological responses by binding on natriuretic peptide (NP) receptors. This process is rapid due to the short half-life of BNP, which is 9-20min (169).

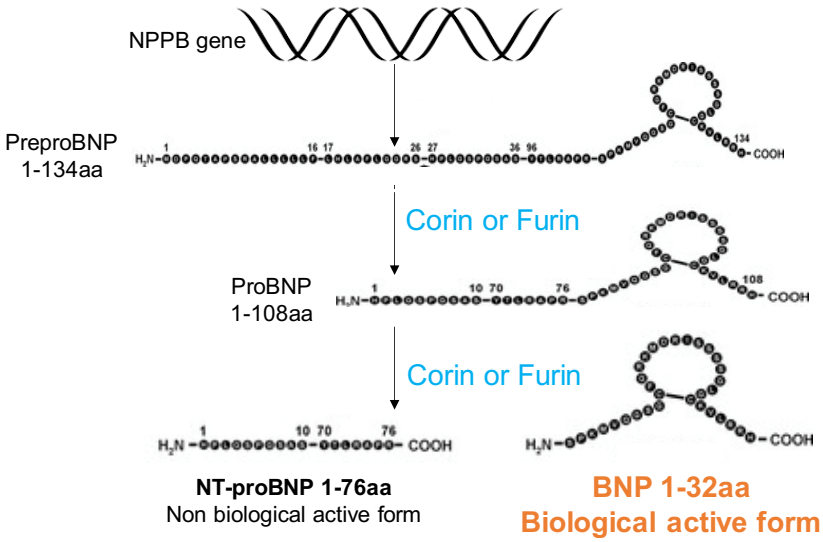

Figure 9: *BNP synthesis pathway.* After NPPB transcription, preproBNP and proBNP are cleaved by corin or furin to produce the inactive form, NT-proBNP and the active form BNP. Schema adapted from Ichiki T et al *(170)*.

1.3.2. Natriuretic Peptide Receptors

Three types of NP receptors exist, namely natriuretic peptide receptors A (NPR-A), NPR-B and NPR-C. ANP, BNP and CNP have different affinities to NP receptors. Indeed, ANP binds preferentially to NPR-A, BNP binds preferentially to NPR-A and NPR-B and CNP binds preferentially to NPR-B (165). All three natriuretic peptides bind to NPR-C receptor, which was shown to be involved in their clearance. Thus, binding of the biological active form of BNP (32-aa) to NPR-A or NPR-B generates increased intracellular cGMP. This is not the case when BNP binds to NPR-C, which lacks guanylyl cyclase (GC) activity (Fig. 10A) (171).

cGMP regulates a broad array of physiologic processes in the cardiovascular system, including vascular tone, excitation-contraction coupling, cardiac and vascular remodeling (172). cGMP is produced from the conversion of GTP to cGMP after NPR-A and NPR-B activation. The accumulation of cGMP into the cytoplasm activates the phosphodiesterases (PDEs) and protein kinase G (PKG), which in turn

phosphorylates phospholamban (PPL) on the Serine 16 (Fig. 10A) (173). This signaling mediates a variety of downstream signaling cascades associated with the cardioprotective effect of NPs (171, 174, 175). Furthermore, cGMP can be export into the extracellular space via multidrug resistance proteins (i.e. MRP4 or MRP5) (Fig. 10A) (176, 177).

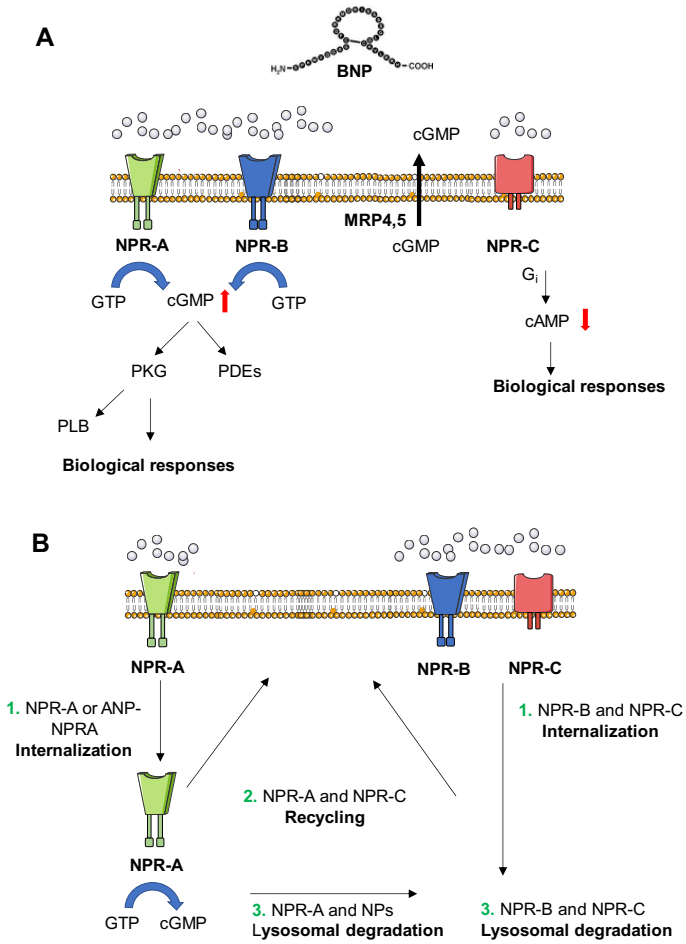

Figure 10: *Schematic representation of natriuretic peptide receptors: NPR-A, NPR-B and NPR-C coupled with cellular signaling of BNP.* **A:** BNP can bind on NPR-A, NPR-B or NPR-C. NPR-A and NPR-B increase intracellular cGMP, whereas NPR-C lacks of guanylyl cyclase activity. cGMP triggers the activation of PKG and/or phosphodiesterases (PDEs) leading to biological responses. cGMP can be exported into the extracellular domain via MRP4 and MRP5. NPR-C activation decreases cAMP concentration and induces cellular responses. **B:** Once NP receptors are activated, they may be internalized (1) and either recycled into the plasma membrane (2) or degraded in lysosomes (3). The complex ANP-NPRA (1) can be also internalized and continues to produce cGMP during intracellular trafficking.

NPR-C is coupled to an inhibitory G protein (G_i). Activation of G_i subunit leads to the inhibition of the adenylyl cyclase activity. Afterwards, the intracellular cAMP level decreases and biological responses are triggered (Fig. 10A) (178).

NPR-C was considered for a long time as the clearance receptor of cardiac NPs by mediating their internalization and degradation by lysosomal hydrolysis (179).

However, it was shown that NPR-C can also trigger cellular responses but at lower extend compared to NPR-A and NPR-B (165). Indeed, NPR-C decreases CM hypertrophy, collagen synthesis and fibrosis, but it can also increase coronary vasodilation (180, 181).

A particularity of NP receptors is that once activated, they can move from the cell surface to the intracellular space by endocytosis (internalization) in order to be either degraded or recycled into the plasma membrane (for NPR-A and NPR-C) (Fig. 10B) (182-185). Furthermore, the complex ligand-receptor ANP-NPRA can be also delivered into the intracellular compartments. In this case, cGMP continues to be produced during cell trafficking (Fig. 10B). Thus, the production of intracellular cGMP can be delayed over time thanks to the internalization of NP-NP receptor (i.e. ANP-NPR-A) (186).

1.3.3. cGMP compartmentation

The cGMP compartmentation is the segregation of the cGMP signaling pathways by spatial and temporal regulation. Two forms of guanylyl cyclase are produced after NP or β-adrenergic receptors activation: a particulate guanylyl cyclase form (pGC), produced by NPs, and a soluble guanylyl cyclase form (sGC), produced by the nitric oxide (NO) linked to β-adrenergic receptor (Fig. 11) (187). Both forms of cGMP activate PKG protein and phosphodiesterases (PDEs) (187). In some cases, cGMP also inhibits PDEs, such as cGMP derived from pGC pool, which suppress PDE3 activation (Fig. 11).

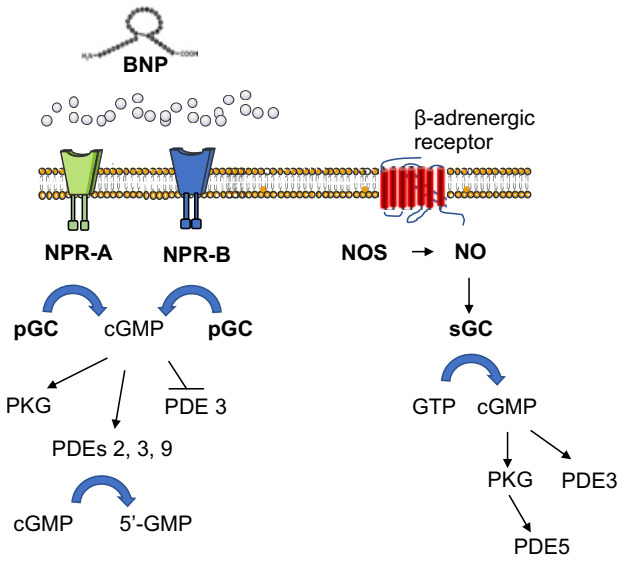

Figure 11: *cGMP compartmentation in CMs.* Two different cGMP pools exist: NP/pGC/cGMP generated by NPs (i.e. BNP) and NO/sGC/cGMP generated by the ß-adrenergic receptor and NO. Both cGMP pools are regulated by PDEs, which are restricted to different subcellular locations.

PDEs are hydrolyzing enzymes which degrade cGMP into its inactive form (5'-GMP). The PDE family includes 11 members, and 7 of them are expressed in CMs (PDE1-5, 8, 9) (165, 187). Thus, PDEs regulate the cGMP intracellular level, and their activity depends on their association with CM cellular components.

For example, PDE2 is associated with the sarcomere and T-Tubular membrane (188). PDE3 is associated with T-Tubule microdomains and forms a scaffold with SERCA and PLB at the sarcoplasmic reticulum. PDE4 is localized within the sarcolemma, while PDE5 is associated to the cytosol and also is anchored to the Z-lines (189). Therefore, as a result of the intracellular localization of the PDEs, cGMP level will be regulated differently from one area to another inside CMs. Additionally, PDEs activity are also dependent on the localization of NP receptors (190). Indeed, NPR-A is linked with T-Tubular membrane and then with PDE2, whereas NPR-B is linked with sarcolemma membrane in CMs and then not under the control of PDE2 (190). Finally, pGC and sGC pools synthesize cGMP in different cell compartments and are controlled by different PDEs. Indeed, pGC pool is under the exclusive control of PDE 2,3 and 9, whereas sGC pool is under the control of PDE 3, 5 (Fig. 11) (187). Thus, cGMP level is also compartmentalized depending on the GC pool.

To conclude, the activity of BNP on CMs will depend on the cGMP compartmentation, which modulates the intracellular level of cGMP.

1.3.4. Role of BNP in the heart

The systemic effects of BNP (i.e. natriuresis, diuresis and vasodilatation) have been well documented. However, the role of BNP in the heart itself is not fully elucidated, although all cardiac cells express the NP receptors and thus are susceptible to respond to BNP stimulation (191).

During embryogenesis, ANP and BNP are highly secreted and their level strongly decreased at adult stage (192, 193). ANP and BNP are crucial during embryogenesis and postnatal cardiac growth. Indeed, majority of NPR-A KO mice die during embryonic development due to cardiac defect, while NPR-B KO mice start to die 3 days after birth (191). Furthermore, Abdelalim and his group demonstrated that NPR-A participates in the maintenance and self-renewal of pluripotency of embryonic stem cells, whereas NPR-B is involved in their proliferation, suggesting that BNP effects could be dependent on the receptor on which it binds (194). ANP is also able to stimulate neonatal and embryonic CM

proliferation *in vitro* (195, 196). Becker and al showed that CM proliferation can be modulated during development in zebrafish by ANP or BNP and also on neonatal CMs *in vitro* by ANP (195). In neonatal CMs in culture, CM proliferation is regulated by the ANP-NPRC complex and is dependent on ANP concentration. Indeed, low dose of ANP triggers neonatal CM proliferation, whereas high dose of ANP inhibits CM proliferation. Thus, CM proliferation depends on the NP concentration and on the NP target receptors.

All these findings suggest that NPs during the development and postnatal life do not only contribute to the homeostasis of salt, water and blood pressure, but also control the proliferation of embryonic cells, including fetal and neonatal CMs.

The role of NPs in adult hearts is less known. In adult physiological mouse hearts, our group demonstrated that BNP treatment stimulates CPC differentiation ($Nkx2.5^+$ cells) into CMs but also stimulates CPC proliferation (i.e. $Nkx2.5^+$ and $Sca\text{-}1^+$ cells) (166, 197). Furthermore, BNP KO mice in physiological conditions develop fibrotic lesions in the ventricle and NPR-A KO mice develop hypertrophy and chamber dilatation (191, 198, 199). Thus, BNP can modulate fibroblast cell fate and CM hypertrophy.

In adult infarcted hearts in animal models, BNP treatment promotes the recovery of cardiac function and the preservation of cardiac tissue, demonstrating a cardioprotective role (166, 200, 201). In addition, BNP treatment inhibits fibrosis, reduces CM apoptosis, CM hypertrophy and modulates the immune response after MI (174). Indeed, it acts on immune cell mobility (by increasing neutrophil infiltration and by reducing monocyte, B and NK cell infiltration) and on the secretion of some inflammatory mediators (i.e. leukotriene B4, Prostaglandin E(2), the cardiac matrix metalloproteinase-9 and the IL-10 cytokine) (202, 203).

Finally, our group demonstrated that BNP after MI stimulates the proliferation of $Nkx2.5^+$ cells, but also stimulates the proliferation of endogenous pre-existing endothelial cells leading to accelerated and increased revascularization (166); Li Na et al., 2020; article under submission). Thus, all these findings participate to the cardioprotective effect of BNP after MI.

1.3.5. Decreased concentration of the biologically active form of BNP in injured hearts

Under mechanical stretch induced by volume or pressure overload, cardiac cells secrete high levels of BNP. However, the secretion of BNP is to a large extent biologically inactive, suggesting that heart failure progression could be the consequence of a deficit of the biological active form of BNP (204). Several reasons could explain why BNP is biologically inactive after CVDs, such as an impairment during BNP bioprocessing or a direct degradation of the active form of BNP.

In chronic HF patients, the balance between BNP active form and proBNP form is impaired. Indeed, more proBNP than BNP active form is detected in the plasma of patients (205). This observation is the result of: 1) proBNP O-glycosylation, 2) decreased levels of enzymes (corin and furin) or 3) increased activity of neprilysin (NEP) (Fig. 12). In the injured hearts, proBNP is highly glycosylated, a process which will avoid the cleavage of proBNP into BNP active form (Fig. 12A). Indeed, in chronic HF patients, O-glycosylation at the Thr17 occurs where the cleavage of corin and furin takes place (206). Furthermore, the reduction of the biological form of BNP could also be a consequence of the degradation of corin and furin (Fig. 12B). In HF patients, it was shown that the concentration of corin decreases due to its degradation by the metalloprotease 10 (207). In this case, the concentration of proBNP increases rather than the biological form of BNP. Finally, biological BNP activity can also be blocked either by downregulation of NP receptors or by a direct degradation by proteases. Indeed, neprilysin (NEP), dipeptidyl peptidase-4 (DPP-4) and insulin-degraded enzyme (IDE) cleave NPs, leading to the formation of small NPs, 5-32aa and 3-32aa (Fig. 12C) (208, 209).

All these processes are involved in the regulation of the biological form of BNP. Thus, as the active form of BNP is decreased after CVDs, we are interested to compensate this decrease by exogenous BNP. Therefore, our lab focuses on the determination of the role of BNP in cardiac cells by increasing its level in physiological and pathological conditions.

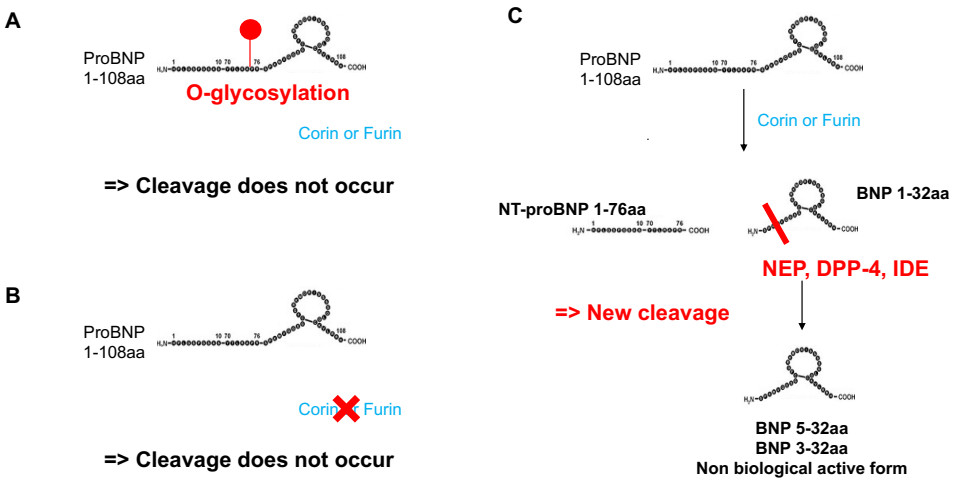

Figure 12: *Three mechanisms decreasing the level of BNP active form in injured heart.* **A:** proBNP O-glycosylation on the Thr17. **B:** the degradation of corin and furin. **C:** the direct degradation of the biological form of BNP by NEP (neprilysin), DPP-4 (dipeptidyl peptidase-4) and (IDE insulin-degraded enzyme). Schema adapted from Ichiki T et al *(170)*.

1.3.6. BNP use in clinic

Patients suffering from heart diseases present a deficit of functional active BNP (204). Thus, the development of therapeutic strategies aimed to increase the concentration of "bioactive" BNP in the hearts of these patients are relevant. There are two ways to increase the level of the biological active BNP after MI: either by an exogenous administration or by inhibiting its degradation.

The first clinical trials were conducted with Nesiritide (recombinant human BNP). Treatment based on Nesiritide led to positive hemodynamic and clinical effects in patients with acute heart failure, but induced also severe adverse effects, such as hypotension, renal failure and a higher mortality rate in the group of treated patients (210). Later, other clinical studies, based on lower doses of Nesiritide administered subcutaneously to patients with acute heart failure, reported increased cardiac function without hypotension, nephrotoxicity or increased rate of death or rehospitalization. These results reopen the debate about the usefulness of BNP therapy for patients with heart failure (210-214). Furthermore, meta-analysis suggests a protective role of ANP/BNP infusion in patients with acute myocardial infarction (215). Taken together, these results prompted a new randomized, double-blind, placebo-controlled clinical trial (BELIEVE II, in progress) to evaluate the cardioprotective effect of BNP at low doses in patients with acute myocardial infarction (216).

Interestingly, a new product, LCZ696 or Entresto (Novartis), was developed during the last 6 years, associating an angiotensin receptor blocker (valsartan) with an

inhibitor of neprilysin (NEP, sacubitril). Sacubitril inhibits the endopeptidase neprilysin (NEP), an enzyme able to degrade natriuretic peptides, angiotensin II, bradykinin and endothelin-1 (217). Thus, the use of sacubitril increases angiotensin II level (218). That is why NEP inhibitors are associated with inhibitors of the angiotensin II receptor, such as the valsartan. In the large, randomized, double-blind PARADIGM-HF trial, LCZ696 treatment promoted significant benefits in patients with chronic heart failure, when compared to angiotensin-converting enzyme inhibition (enalapril). In fact, LCZ696 reduced mortality and rehospitalization by 20% and limited the progression of heart failure (219). In patients, the cardioprotective mechanism of LCZ696 leading to reduced death and rehospitalization is not fully elucidated.

Therefore, studies were performed in animal models in order to explain the beneficial effect of LCZ696. Interestingly, it was shown that LCZ696 treatment decreases the levels of pro-inflammatory cytokine interleukins (i.e. IL-1β and IL-6), the extracellular matrix degradation due to the reduction of the metalloprotease 9 activity and also apoptosis by preserving mitochondrial function (198, 220). In infarcted rats, LCZ696 treatment decreases myocardial fibrosis, CM hypertrophy, increases the survival and the ejection fraction of treated rats compared to untreated ones (221, 222). Thus, one consequence of these beneficial effects observed in mice could be partially explained by the increased level of NPs (i.e. BNP), which was already shown to be increased after LCZ696 treatment in patient with heart failure and also in infarcted heart of rats (223-225).

2. Aims and Approaches

Cardiomyocyte (CM) proliferation is a well-known mechanism depending on its environment. Indeed, CM proliferation capacity is high during development and decreases drastically in mammals during the first week after birth. Therefore, cardiac research focuses on identifying new factors able to stimulate CM proliferation after heart injury. Thanks to a robust CM proliferation after heart injury, cardiac function could be increased and the mortality of patients suffering from heart disease decreased. That is why the aims of my thesis are to determine the role of the oxygen and the brain natriuretic peptide (BNP) concentrations on CM cell fate.

The first aim focuses on oxygen. Oxygen was shown to be a key regulator of CM cell fate. Indeed, several results suggest that low oxygen environment during development stimulates CM proliferation, whereas high oxygen level inhibits CM proliferation (59, 71). In pathological conditions (i.e. after myocardial infarction (MI)) in adult mice, reduction of oxygen concentration could provide a good environment to stimulate mechanisms of cardiac regeneration such as CM proliferation (78). Thus, one aim of my thesis was to determine the effect of different oxygen concentrations, 3% O_2 (physiological) and 20% O_2 (hyperoxic) on CM cell fate *in vitro*. Regarding oxygen concentration inside the adult heart, in physiological conditions, it is estimated close to 3% O_2 (226). However, all CM cell cultures are performed *in vitro* at 20% oxygen concentration, which is thus an hyperoxic environment. Therefore, we compared CM cell fate in neonatal CM cell cultures performed at 20% O_2 and 3% O_2 up to 14 days **(section 4.1).**

The second aim focused on the role of BNP on CM cell fate in pathological and physiological conditions. BNP is a cardiac hormone secreted by all cardiac cells (174). In humans, after MI, it was shown that the biological active form of BNP is present at a reduced concentration when compared to "healthy" hearts (227). This suggests that the resulting deficit of the biological form of BNP could be one reason of heart failure progression. On mice, supplementation of BNP after MI increased the cardiac function and decreased heart remodelling, highlighting BNP cardioprotective role (166). Interestingly, all cardiac cells express the BNP receptors: NPR-A, NPR-B and NPR-C, suggesting that they can directly respond to BNP stimulation. Thus, the second aim of my thesis was to determine, whether CMs respond to BNP stimulation in infarcted and unmanipulated hearts. For this

purpose, MI was induced in mice by permanent ligation of the left anterior descending coronary artery. Intraventricular as well as intraperitoneal injections of BNP were performed and mice were sacrificed 1, 3 or 10 days after MI. CM cell death (apoptosis) and CM proliferation were studied in BNP-treated mice and compared to saline-treated mice. Furthermore, we were interested to define the direct role of BNP on CM proliferation (*in vivo* and in neonatal CM cell culture) by studying newborn mice, which exhibit a full potential of regeneration and high capacity of CM proliferation. Finally, BNP effect on CM proliferation was also examined in adult hearts in physiological conditions. Adult CMs have a very low proliferative capacity when compared to neonatal CMs. **(section 4.2)**

3. Materials and Methods

3.1. Mice strains

All animal procedures were approved in accordance with the recommendation of the U.S. National Institutes of Health Guide for the Care and Use of Laboratory Animals (National Institutes of Health publication 86-23, 2011). All experiments were approved by the Swiss animal welfare authorities (authorisations VD3096 and VD3211) and were conform to the guidelines from Directive 2010/63/EU of the European Parliament on the protection of animals used for research. C57BL/6 mice (Wild Type mice, WT) were purchased from Janvier (Le Genest-Saint-Isle, France). Myh6-MerCreMer mice (JAK-5657) and Tomato-EGFP mice (JAK-7576) were purchased from the Jackson Laboratory (Bar Harbor, Main, US). Heterozygous Myh6-MerCreMer/Tomato-EGFP adult mice were bred in our animal facility.

3.2. *In vivo* experimental procedures

Neonatal C57BL/6 mice (3 days after birth) were injected intraperitoneally (i.p.) with NaCl or BNP every two days (1µg/2g; Bachem; synthetic mouse BNP (1-45) peptide (catalog number H-7558)) (166). BrdU was also injected by i.p. (40µl/mice, 10mg/ml; Sigma B5002) on days 5 and 9 after birth. Mice were sacrificed 11 days after birth (Fig. 13A).

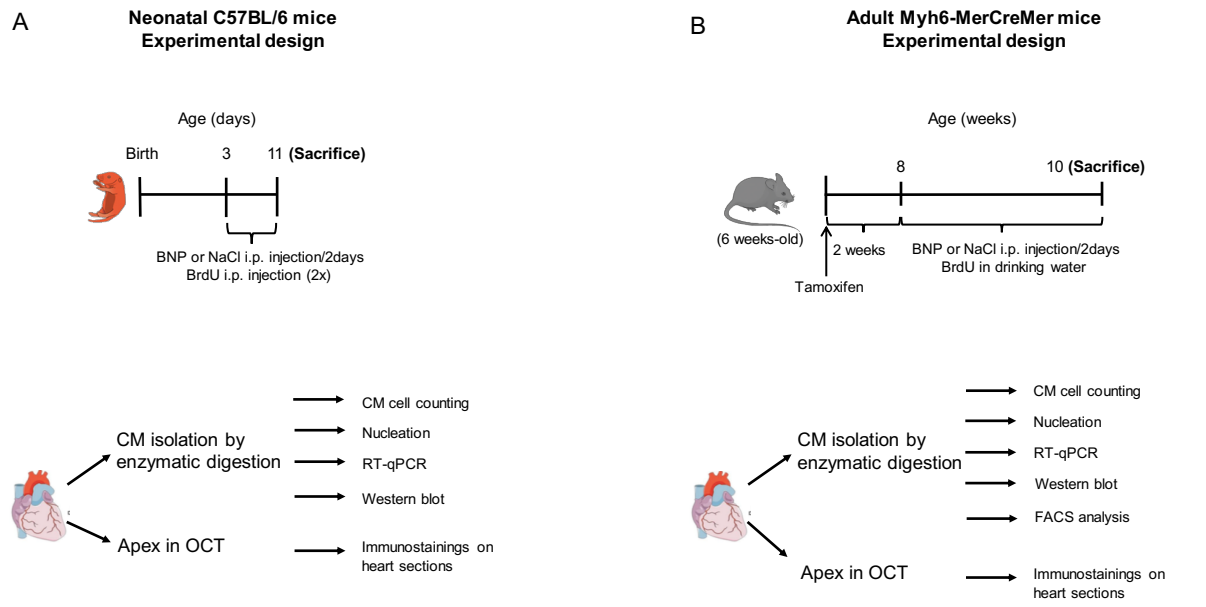

Figure 13: *Experimental procedures in neonatal **(A)** and adult unmanipulated **(B)** mice with BNP or NaCl treatment.*

Adult Myh6-MerCreMer mice (6-weeks-old) were injected with Tamoxifen (Sigma, T5648) at 40mg/kg to activate the Cre recombinase (Fig. 13B). Tamoxifen was dissolved in ethanol to a concentration of 50mg/ml and emulsified in peanut oil to a final concentration of 10mg/ml. 1mg Tamoxifen/25g body weight was injected one time by i.p. to adult mice. Two weeks after Tamoxifen injection, 80-90% of pre-existing CMs expressed the GFP protein, whereas non-myocyte cells expressed the Tomato protein (Fig. 14) (166). Then, 8-weeks-old mice were injected with BNP (2µg/20g mice) or NaCl by i.p. injection every two days (Fig. 13B) (166). BrdU was added into the drinking water (1mg/ml) and changed every 2 days during all experiment. Two weeks after the first injection, mice were sacrificed.

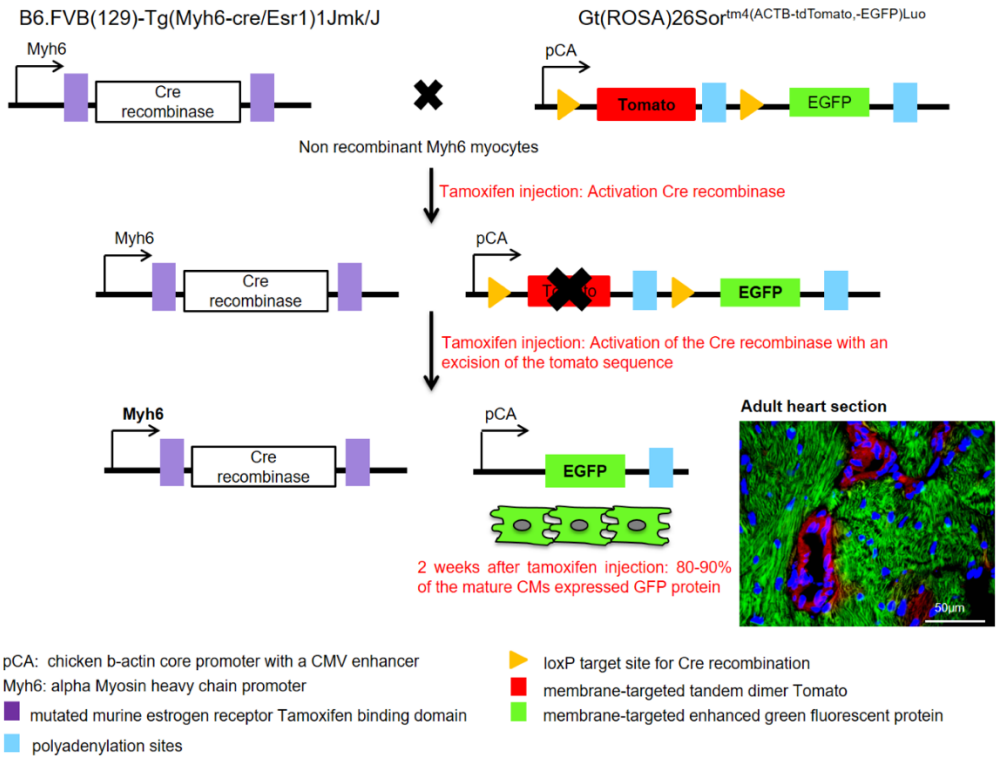

Figure 14: *Myh6-MerCreMer mouse model used for lineage tracing of mature CMs.* Picture represents heart section 2 weeks after Tamoxifen injection. GFP$^+$ cells correspond to CMs, and Tomato$^+$ cells correspond to non-myocyte cells. Two weeks after Tamoxifen injection, 80-90% of the mature CMs expressed the GFP protein (166).

Adult C57BL/6 and Myh6-MerCreMer mice (8-weeks-old) were submitted to myocardial infarction (MI) (Fig. 15). Myh6-MerCreMer mice 6-weeks-old were injected with Tamoxifen (Sigma, T5648) at 40mg/kg to activate the Cre recombinase as previously described. To generate a permanent infarction, a ligation of the left anterior descending coronary artery (LAD) was performed in C57BL/6 and Myh6-MerCreMer mice. Sham-operated animals were used as surgical controls and were subjected to the same procedures as experimental

animals, but in this case, the LAD was not ligated. Mice were anesthetized with ketamine/xylazine and acepromazine (65mg/kg, 15mg/kg, 2mg/kg respectively). Then, mice were intubated and ventilated during all the period of surgery. At the third intercostal space, the chest cavity was opened and, at the left upper sternal border, the LAD was ligated with a 7-0 nylon suture at about 1-2mm from the atria. All the surgeries were performed by the Cardiovascular Assessment Facility (CAF) of the University of Lausanne.

Directly after surgery, NaCl or BNP (1µg/20g in 20µl) was injected into the left ventricle cavity. Then, mice were injected by i.p. injection with BNP (2µg/20g mice) or NaCl, 24 hours after MI and every 2 days (166). BrdU (1mg/ml) was added into the drinking water during all the period of experiment (Fig. 15). The concentration of BNP used in this study was already shown to have no impact on blood pressure (166). C57BL/6 mice were sacrificed 1, 3 and 10 days post-MI and Myh6-MerCreMer mice were sacrificed 10 days post-MI. One day post-MI, CM cell death was assessed, while 3 and 10 days post-MI, CM number and proliferation were assessed.

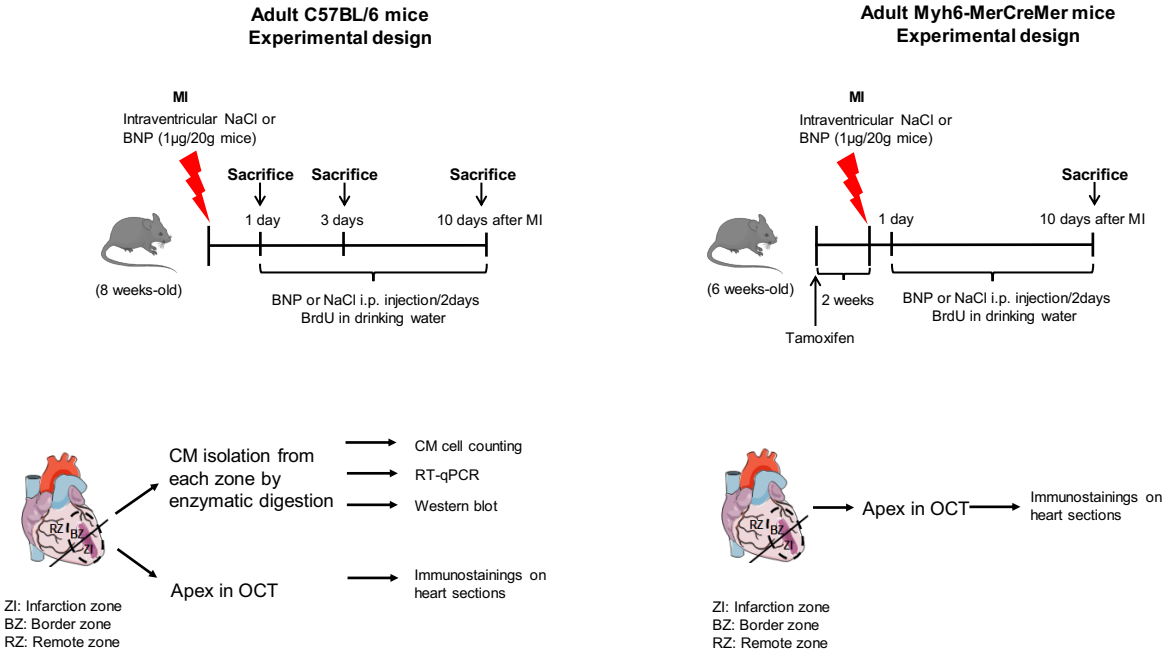

Figure 15: *Experimental procedures in adult infarcted mice with BNP or NaCl treatment.*

For C57BL/6 mice treated with LCZ696 (Entresto®, Novartis), surgeries were performed in 8 weeks-old adult mice (Fig. 16). Animals were randomly assigned into 3 different groups for treatment: H_2O, LCZ696 (6mg/kg), or LCZ696 (60mg/kg). LCZ696 (6mg/kg) corresponds to the dose used in clinic in patients

and LCZ696 (60mg/kg) has already been used on animal models and was shown to increase plasmatic ANP and BNP levels (228). LCZ696 drug was mixed, formulated in water and sonicated for 1 hour before administration. Drug was administered 24 hours after MI and once daily for 10 days by oral gavage. BrdU (1mg/ml) was added into the drinking water during all the period of experiment.

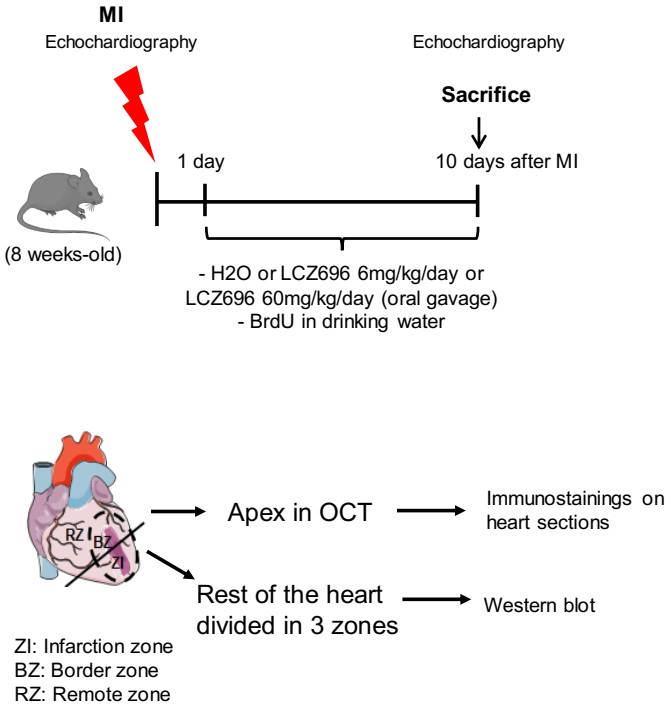

Figure 16: *Experimental procedure in adult infarcted mice with LCZ696 or H_2O treatment.*

In all experiments, for immunostainings, the apex was embedded into OCT and slowly frozen. For RT-qPCR and/or western blot analysis, the rest of the heart was frozen. Hearts from MI animals were separated into 3 zones for molecular analysis and cellular analysis: 1) the infarction zone (ZI), 2) the border zone (BZ) and 3) the remote zone (RZ).

For adult CM isolation, CMs are dissociated by enzymatic digestion according to the Langendorff-Free method (see section 3.4.1) (229). For neonatal CM isolation, CMs are dissociated by enzymatic digestion according to the method described in section 3.4.2 (166). After CM isolation, mRNA expression (RT-qPCR), protein expression (western blot), quantification of CM number, determination of CM nucleation, and FACS analysis (for unmanipulated adult mice) were performed.

3.3. Echocardiography and measurements

Echocardiographies were performed by the Cardiovascular Assessment Facility (CAF) of the University of Lausanne. Transthoracic echocardiographies were performed on adult mice using a 30 M-Hz probe and the Vevo 770 Ultrasound machine (VisualSonics, Toronto, Ontario, Canada). Mice were lightly anesthetized with 1-1.5% isoflurane, maintaining heart rate at 400-500 beats/min, and placed on a 37°C heated platform. Hair was removed with a depilatory agent. The heart was imaged in the 2D mode in the parasternal long-axis view. From this view, a cursor was positioned perpendicularly to the interventricular septum and the posterior wall of the left ventricle (LV). LV diameter in diastole (LVDD) and in systole (LVDS) as well as LV wall thickness in diastole (LVWTD) and in systole (LVWTS) were measured. Ejection fraction (EF) was calculated using the formula %EF = [(LVVD − LVVS)/LVVD] × 100, where LVVD and LVVS are LV volume in diastole and systole, respectively. Considering that changes in left ventricle volume can be considered as an index of remodeling, we calculated the percentage of increase of the left ventricle volume 10 days weeks after surgery, which is the ratio between (LVVol;d 10 days - LVVol;d before surgery) and LVVol;d before surgery x 100.

3.4. Cell culture

3.4.1. Adult CM isolation

Isolations of adult CMs were performed with the Langendorff-Free method (229). This method consists to perfuse the heart directly into the ventricle (Fig. 17). Rapidly after the sacrifice, the chest was opened, descending aorta and inferior vena cava were cut, the aorta was clamped and EDTA buffer was perfused into the right ventricle. Aortic clamping forces the passage of buffers through the coronary circulation (Fig. 17B in blue). Then, the heart was removed from the chest and the left ventricle was perfused with enzymatic solution containing collagenase II (Worthington USA, LS004176 (0.5mg/ml), collagenase IV (Worthington USA, LS004188 (0.5mg/ml) and protease (Sigma-Aldrich Singapore, P5147 (0.05mg/ml)). After digestion, clamp was removed and the heart was weighed. Afterwards, by using forceps, the heart was separated gently and was dissociated by gentle pipetting. Stop buffer solution containing 2% fetal calf serum (FCS) was added to cell suspension in order to arrest the digestion and cells were passed through 100 µm-filter. For each experiment, a full digestion of the heart was

obtained. Then, CMs were collected after 30 min of sedimentation process. During sedimentation the heavier cells (CMs) move down into the tube, while non-myocyte cells (NMCs) stay at the surface. Thanks to this sedimentation, NMCs contamination in the CM fraction corresponds to ≤5% of the total cells (personal communication) and 90% of rod-shaped CMs were collected at the end of experiment (Fig. 17C). For CMs isolated from injured heart, after digestion, the heart was divided into three zones (ZI, BZ and RZ) prior the separation with forceps and the filtration step. Each zones were weighted separately.

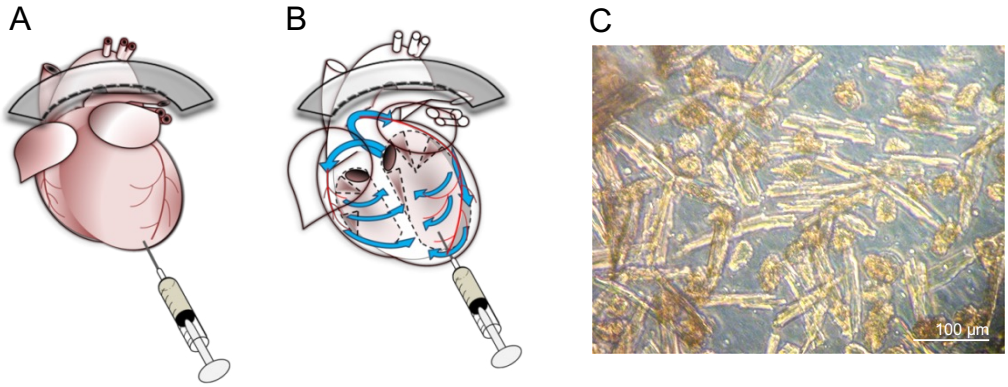

Figure 17: *Adult CM isolation method based on the Langendorff free method (229).* **A-B:** Schematic diagrams illustrating the method based on a direct perfusion into the left ventricle. Aorta is clamped. **B:** Aorta clamping forces the passage of buffer (blue) across the coronary circulation (red) assuring a good perfusion into the heart. **C:** Rod-shaped CMs obtained after cell isolation and performed by the laboratory.

3.4.2. Neonatal CM isolation and culture

Neonatal (1-2 days) C57BL/6 pups were decapitated by sterile scissors. The chest was opened and the heart was removed. After separation of the atria from the rest of the heart, the ventricles were minced and digested with 0.45mg/ml collagenase (Worthington, Biochemical Corporation, USA) and 1mg/ml pancreatin (Sigma). After 3 rounds of digestion, cells were plated 2 times for 45 min in order to separate CMs (no adherent cells) from the NMCs. Thereafter, CMs were plated on gelatine (0.1%) or laminin (10µg/ml) coated plates and cultured in 3:1 mixture of DMEM and Medium 199 (Invitrogen Corp, San Diego, CA, USA), supplemented with 10% horse serum (Oxoid), 5% fetal bovine serum (Invitrogen), 10mM Hepes and, 100U/ml penicillin G. To homogenize the experiment, ≙70000 cells were plated per well.

BNP treatments were performed on neonatal CM cultures for 14 days. Cells were exposed 7 days to cytosine-β-D-arabinofuranoside (AraC, C1768, Sigma) to inhibit the proliferation of NMCs and thus to achieve a pure CM cell culture. After 7 days

of culture, AraC was removed until 14 days of culture. CMs were cultured at 3% O_2 in a hypoxia chamber (Stem Cell Technologies, ref: 29829), flushed with 3% O_2/5% CO_2/92% N_2 (Carbagas, Lausanne, Switzerland). The oxygen concentration was controlled with an oxymeter (Stem Cell Technologies, Basel, Switzerland). Medium was replaced 3 times with fresh medium during all the period of experiment.

CMs were treated during 14 days of culture with 3 different BNP concentrations: 10nM, 100nM and 1000nM and compared to untreated CMs. Quantitative RT-qPCR as well as immunohistochemistry studies were performed after 14 days of culture to compare the gene expression and structure of CMs, cultured in BNP and untreated CMs.

3.5. Cellular analysis

3.5.1. Flow cytometry analysis

After isolation, neonatal CMs were stained during 20 min at room temperature (RT) with antibodies, listed in supplementary Table 1, chapter 8 (i.e. NPR-A and NPR-B). CMs were washed with PBS, supplemented with FCS (3%) and EDTA (2nM) (FACS buffer), were collected in FACS buffer and analyzed with Gallios Flow Cytometer (Beckman Coulter). Data analysis were generated by using FLowJo 10 software.

Adult CMs isolated from Myh6-MerCreMer hearts (Fig. 13B) were fixed with 5.5% formaldehyde and permeabilized with 0.5% saponin. CMs were stained during 20 min at RT with antibodies listed in supplementary Table 1, chapter 8 (i.e cTnI). CMs were washed one time and collected in FACS buffer. CMs were analyzed with CytoFLEX (Beckmann Coulter) cytometer and data were generated by using FLowJo 10 software.

3.5.2. Assessment of CM size

The area of CMs *in vitro* was assessed by cTnI stainings and image J software for processing. The area of CMs *in vivo* was assessed by laminin stainings and Image J software processing using CIF outliner cell Plugin. Only CMs with circularity >0.5 were considered for *in vivo* analysis.

3.5.3. Immunohistochemistry

Cells or OCT heart sections (5µm-thick cryosections) were washed in PBS 1X and fixed in paraformaldehyde (2%) or formol (4%) for 10 min at RT. After 10 min of permeabilization (0.3% Triton x-100 in PBS) and one hour of blocking with normal serum, sections were probed with primary antibodies overnight at 4°C (see supplementary Table 1, chapter 8). The second day, after washing, secondary antibody was added on cells or heart sections (see supplementary Table 1, chapter 8). Slides were mounted with Dabco (Sigma) and pictures were captured with Nikon Eclipse TS100 or 90i microscope. Images were processed with Adobe Photoshop CC2015.

For detecting BrdU incorporation, heart slides were fixed 10 min in 2% PFA, DNA was denatured 1h at RT in HCl 2N before neutralisation in Na Borate 0.1M pH=8.5 during 2x5 min. Then, sections were probed with primary antibodies overnight at 4°C (see supplementary Table 1, chapter 8).

3.5.4. Determination of CM nucleation

Isolated CMs from neonatal and adult unmanipulated hearts were fixed with 2.5% paraformaldehyde (PFA) during 15 min at RT. DAPI was added directly on cells and pictures were taken with Nikon Eclipse TS100 in order to quantify the mono and binucleated CMs.

3.5.5. cGMP quantification in plasma

BNP or NaCl was injected in unmanipulated or infarcted mice. Blood was collected 1 hour after injection. Plasma (EDTA) was centrifugated for 20 min at 1000 x g. cGMP level was quantified, using a competitive cGMP enzyme Immunoassay Kit (CG200, Sigma). cGMP was determined following the recommendation of the kit.

3.5.6. Troponin quantification in plasma

BNP or NaCl was injected directly after LAD surgery into the ventricles of infarcted hearts. Mice were sacrificed 1 days after MI and blood was collected to measure Troponin plasma levels. Plasma (heparin) was centrifugated for 20 min at 1000 x g. Troponin plasma levels were quantified, using an electrochemiluminescence immunoassay analyzer "ECLIA" (cobas e 801 immunoanalysis system, Roche) in the hematology laboratory of the Centre Hospitalier Universitaire Vaudois (CHUV).

3.6. Molecular analysis

3.6.1. Western blot analysis

Total proteins were extracted from CMs which were isolated from unmanipulated neonatal and adult hearts and also from infarcted hearts. Proteins were transferred to nitrocellulose membranes (Biorad) before incubation with primary antibodies overnight at 4°C. Secondary antibodies were added 1h at RT in the dark (see supplemental Table 1, chapter 8). The signal was detected and quantified with the Odyssey infrared imaging system (LI-COR. Biosciences, Bad Homburg, Germany). All results were related for their Tubulin expression.

3.6.2. quantitative RT-PCR

Total RNA was isolated from heart tissue, CM cell cultures and isolated CMs, using the Trizol reagent (Invitrogen Corp, San Diego, CA, USA). cDNA was synthesized from RNA, using PrimeScript RT reagent kit (Takara Bio Inc). Polymerase chain reactions (PCR) were performed using the SYBR Premix Ex Taq polymerase (Takara Bio Inc) with the ViiA^{TM}7 Instrument (Applied Biosystems). Results were obtained after 40 cycles of a thermal step protocol consisting in an initial denaturation 95°C (1s) and followed by 60°C (20s) of elongation (α-skeletal actin has an elongation time of 30s at 60°C). The sequences of primers were reported in supplementary Table 2, chapter 8. All results were normalized with the 18S housekeeping gene (Δ CT values). Means of ΔΔ CT (Δ CT_{BNP} - Δ $CT_{control}$) values (versus untreated cells or NaCl-treated mice) were calculated and results were represented as $2^{-\Delta\Delta CT}$. Statistics were performed on ΔΔ CT individual values. SEM fold increase was calculated using $2^{-\Delta\Delta\ CT\ (SEM\text{-}mean)}$- $2^{-\ means\ of\ \Delta\Delta\ CT}$ (230).

3.7. Statistical analysis

All results were presented as means ± SEM. Statistical analyses were performed using the unpaired Student T test or Wilcoxon-Mann-Whitney. The alpha level of all tests was 0.05.

4. Results

4.1. Oxygen

This work has been published in 2019 in Biochimica et Biophysica Acta (BBA) - Molecular Cell Research

Summary

It is well-established that low oxygen concentration could stimulate CM proliferation in adult infarcted hearts of mice (78). In this study, we demonstrated that oxygen concentration modulates also CM cell fate in *in vitro* experiments. Previously, physiological study estimated that the pO_2 in adult heart *in situ* is less than <21mmHg, corresponding approximatively to 3% O_2 (226). Thus, a physiological oxygen environment for CMs is close to 3% O_2. However, all *in vitro* experiments with CMs are performed at 20% O_2, which is clearly a hyperoxic environment for CMs. Therefore, in this study, neonatal CMs were cultivated up to 14 days at 3% O_2 (physiologic/normoxic conditions) and 20% O_2 (hyperoxic conditions) in order to determine the effect of both oxygen concentrations on their fate.

We determined that cultivated neonatal CMs in low oxygen concentration stimulated physiological mechanisms such as CM dedifferentiation and proliferation. Furthermore, several studies demonstrated that CM proliferation is preceded by a step of dedifferentiation (see section 1.2.2.4). Here, we showed that differentiated CMs can proliferate like dedifferentiated CMs, suggesting that CM dedifferentiation is not always required for CM proliferation.

Altogether, these results are crucial because they demonstrate that the oxygen concentration is a primordial factor modulating also CM cell fate *in vitro*. Because CM cell cultures are a powerful tool to study the morphological, biochemical, molecular and electrophysiological characteristics of CMs, it is important to use in the future the more appropriate oxygen concentration in order to extrapolate the *in vitro* results to the *in vivo* situation.

BBA - Molecular Cell Research 1867 (2020) 118460

Contents lists available at ScienceDirect

BBA - Molecular Cell Research

journal homepage: www.elsevier.com/locate/bbamcr

Oxygen as a key regulator of cardiomyocyte proliferation: New results about cell culture conditions!☆

Anne-Charlotte Bon-Mathier, Stéphanie Rignault-Clerc, Christelle Bielmann, Nathalie Rosenblatt-Velin*

Division of Angiology, Heart and Vessel department, Centre Hospitalier Universitaire Vaudois and University of Lausanne, Switzerland

ARTICLE INFO

Keywords:
Cardiomyocyte
Proliferation
Heart
Regeneration
Oxygen
Metabolism

ABSTRACT

The goal of the new therapeutically strategies aimed to treat cardiovascular diseases (CVDs) is to enhance the natural ability of the heart to regenerate. This represents a great challenge for the coming years as all the mechanisms underlying the replacement of dying cells by functional cells of the same type are not completely elucidated. Among these, stimulating cardiomyocyte proliferation seems to be crucial for the restoration of normal cardiac function after CVDs.

In this review, we summarized the recent advances about the modulation of cardiomyocyte proliferation in physiological (during ageing) and pathological conditions. We highlighted the role of oxygen and we presented new results demonstrating that performing neonatal cardiomyocyte cell cultures in "normoxic" oxygen conditions (i.e. 3% oxygen) increases their proliferation rate, when compared to "hyperoxic" conventional conditions (i.e. 20% oxygen). Thus, oxygen concentration seems to be a key factor in the control of cardiomyocyte proliferation.

Cardiac vascular diseases (**CVDs**) are defined by the world health organization as "a group of disorders of the heart and blood vessels" accounting for 30% of deaths worldwide. Ischaemic heart diseases and stroke are the "world's biggest killers", by killing 15.2 million people in 2016 (*www.who.int*). The number of patients dying from CVDs will increase to reach 23.3 million by 2030 and CVDs will remain the first cause of mortality in the world. It thus becomes urgent to find an effective treatment to stem this epidemic. Why are heart diseases not efficiently treated yet?

The major reason is that CVDs affect to a certain extent the functional activity of the heart and then of course the viability of the other organs. The current therapies based on the role of hemodynamics and neurohormones allow transforming heart failure into a chronic disease. Furthermore, they delay the onset of heart failure. None of the treatments developed until now could truly "heal" the heart, i.e. replace the **BILLION** myocytes lost after myocardial infarction (**MI**) by functional cells of the same nature in order to preserve the cardiac contractility [1]. That is why, these last 10 years new strategies were developed based on heart plasticity and on the fact that injured cardiac cells, including cardiomyocytes (**CMs**), can be replaced by functional cells of the same nature during physiological growth or ageing as well as after heart injury [2,3]. This was first done by injecting "cardiac precursor cells" (**CPCs**; undifferentiated cells which have the capacity to differentiate in vitro into mature cardiomyocytes, endothelial or smooth muscle cells) into the injured hearts [4]. CPCs were isolated from the heart itself or from different organs (blood, bone marrow, fat, skeletal muscles) [5]. This approach has resulted in only modest improvement of cardiac function, due to the low survival rate of the injected cells (<1%, 1 day after injection).

The second alternative consists to stimulate the "endogenous" cardiac regenerative capacities of the heart by injecting molecules or factors able to improve the proliferation of the mature cells or the differentiation of the "endogenous" CPCs.

In this review, we focus on the replacement of the cardiac contractile units (i.e. the cardiomyocytes) in the mammal hearts. The different factors limiting or stimulating their renewal are reviewed. Among these, the role of oxygen is highlighted and new results concerning oxygen concentration during neonatal cardiomyocyte cell cultures are added.

☆ This article is part of a Special Issue entitled: Cardiomyocyte biology: new pathways of differentiation and regeneration edited by Marijke Brink, Marcus C. Schaub, and Christian Zuppinger.

* Corresponding author at: CHUV, Division of Angiology, Institut de Physiologie, Bugnon 7a, 1005 Lausanne, Switzerland.
E-mail address: nathalie.rosenblatt@chuv.ch (N. Rosenblatt-Velin).

https://doi.org/10.1016/j.bbamcr.2019.03.007
Received 5 December 2018; Received in revised form 21 February 2019; Accepted 13 March 2019
Available online 15 March 2019
0167-4889/ © 2019 Published by Elsevier B.V.

1. Cardiac regeneration is a physiological mechanism triggered mainly by cardiomyocyte proliferation

Plasticity of the heart is a relatively novel concept. In contrast to lower vertebrates (zebrafish, urodeles) which have a high cardiac regeneration rate, the heart of mammals was for a long time considered as a post-mitotic organ with no capacity to regenerate and/or healing. This point of view was challenged, when studies based on the integration of carbon-14 birth dating demonstrated in humans, that mammalian heart has a low physiological regenerative capacity [3]. The estimation of CM turnover rate is around 0.5–1% per year; however this number is continuously subject to debate [3,6]. The newly formed cardiomyocytes originate either from the differentiation of "endogenous" precursor cells or from the proliferation of pre-existing mature cardiomyocytes [7].

The contribution of precursor cells to the cardiomyocyte renewal was first evaluated. Indeed, cells with the capacity to differentiate into mature functional cardiomyocytes exist in the heart itself and can be isolated from the Hoechst-extruding side population, or from the epicardium cells [8]. Furthermore, cells isolated from percutaneous endomyocardial biopsy from adult hearts, expressing CD90, CD105, c-kit and not CD45, are able to form cardiospheres in culture and to differentiate into cardiomyocytes [9]. The characterization of these cells remains however confusing as they share no cardiac specific marker. The c-kit protein [10] and/or the stem cell antigen-1 (Sca-1) protein [11] and/or the nuclear transcription factor islet-1 (Isl-1) [12–14] have been proposed to be CPC markers. However, cells expressing Sca-1 and c-kit, Sca-1 and Isl-1 or c-kit and Isl-1 have been isolated [14,15], demonstrating that all these markers identify the same subset of cells which are at different stages of maturation. Thus, endogenous CPCs might originate from a common precursor expressing Flk-1, Isl-1 and c-kit in an immature stage, and one step further in the cell differentiation, Sca-1 [13].

In the past, all these endogenous CPCs have been shown to participate in heart regeneration by differentiating into mature cardiomyocytes in vitro but also in vivo during physiological growth and in pathological conditions [8,16–18]. Furthermore, injections of c-kit$^+$ cells, Sca-1$^+$ cells or Isl-1$^+$ cells into infarcted hearts were considered as being beneficial for heart recovery [5,10,19,20]. Recently, the development of new mouse models allowing to trace the lineage of the cells expressing c-kit, or Sca-1 or more interestingly the cells derived from c-kit$^+$ or Sca-1$^+$ cells, clarified the role of these cells in cardiac regeneration.

Van Berlo was the first demonstrating that c-kit expressing precursor cells do not massively participate to heart formation during embryogenesis and that adult c-kit$^+$ cells differentiate only rarely into cardiomyocytes in infarcted hearts [21]. In contrast, c-kit$^+$ cells differentiate clearly into endothelial cells. These results were confirmed by other groups [22,23], and it is now well admitted that c-kit expressing precursor cells are able to differentiate into smooth muscle and endothelial cells but to lower extend into CMs in the hearts after injury [24].

Another strategy was adopted by Li and his group. They developed a genetic lineage tracing system in order to label all non-myocyte cells, which could contain precursor cells. The strategy here is to avoid specific stem cell markers. They demonstrated that precursor cells into non-myocyte cells are able to differentiate into cardiomyocytes during embryogenesis but not in adult hearts during physiological ageing or in pathological conditions [25].

Finally, very recently in the 2018 vol 138 issue of *Circulation*, five different groups using different genetically modified mouse strains, all aimed to follow the Sca-1$^+$ cell fate, reached the same conclusion: very few cardiomyocytes in neonatal and adult "unmanipulated" or "injured" hearts originate from Sca-1$^+$ cells. In other words, Sca-1$^+$ cells differentiate very rarely into cardiomyocytes in vivo during embryogenesis, physiological ageing and pathological conditions. However, like c-kit$^+$ cells, Sca-1$^+$ cells differentiate massively into endothelial cells in vivo, which could explain the benefice of cell therapies based on Sca-1$^+$ cell injections [11,19,26–32].

Isl-1$^+$ cells are involved in differentiation during embryogenesis but their role in adult hearts is reduced [33,34].

Altogether, these new results obtained thanks to new technology, demonstrate that the renewal of cardiomyocytes during ageing and in pathological conditions is mainly performed by the proliferation of "pre-existing" cardiomyocytes.

1.1. Cardiomyocyte proliferation capacity declines with age

The cardiomyocyte capacity to proliferate is clearly dependent on their maturity, on their environment and on subtle unknown mechanisms. In adult non-mammalian animals (zebrafish, axolotl, newt), numerous cycling cardiomyocytes can completely regenerate the heart during adult life, even after the resection of 20% of the ventricle [7,35].

During fetal development of mammalian hearts, cardiomyocytes display a high capacity to proliferate, essential for the expansion of the ventricular chambers [36]. Depletion of 60% of the cardiomyocytes during embryogenesis has no effect on cardiac function into adulthood, thanks to complete replacement of the cardiomyocyte pool by intensive proliferation of the surviving CMs [37]. Numerous studies demonstrated that the cardiomyocyte proliferation capacity declines during the first week of postnatal life. 5% to 10% of the cardiomyocytes proliferate up to day 3 and 4 after birth. 5 days after birth, only 1% of the cardiomyocytes proliferate and few proliferation is detected 7 days after birth [7]. Consequently, complete heart regeneration was observed in mice after surgical resection of the hearts at birth [38] thanks to intensive cardiomyocyte proliferation leading to replacement of the resected tissue without fibrosis development. The cardiac function is thus completely restored. However, this is not the case when apical resection was performed 7 days after birth. Very few cardiomyocytes proliferate and no regeneration occurs anymore. Recently, acute myocardial infarction was induced in neonatal pigs at different days after birth. Until 2 days after birth, heart is able to regenerate thanks to cardiomyocyte proliferation which leads to restoration of cardiac function. However, 2 days after birth, cardiomyocytes exit from the cell cycle and systolic function is impaired [39]. In humans, several clinical reports suggest that similarly to neonatal mice, neonatal human hearts have the capacity to regenerate and to completely restore the cardiac function after MI [40]. Furthermore, cardiomyocyte proliferation is highlighted in human neonatal hearts suffering from CVDs [41,42].

In adult "healthy" mouse hearts, the rate of cardiomyocyte proliferation declines drastically. The consensus is that myocyte proliferation exists in adult mammalian hearts but is so limited that it cannot restore the impaired cardiac function after CVDs. First evidences of cardiomyocyte proliferation came from the group of Senyo who demonstrated that pre-existing cardiomyocytes are the main source of newly formed cardiomyocytes during ageing but also after MI [43]. They estimated the formation of new cardiomyocytes at a frequency of 0.015% in the hearts of young adult mice over a period of 8 weeks. After MI, the CM proliferation rate increases by 5 fold. CM proliferation occurs mainly in the border zone of the infarct [43]. By using a mouse model, which allows discriminating myocytes originating from complete cytokinesis versus binucleation, the adult myocyte renewal rate is estimated at about 0.01–0.02% [44]. In adult human hearts, evidences for myocyte cell renewal came from the study of Bergman, in which ^{14}C incorporation in post-mortem heart samples was measured [3]. However, by this method it is not possible to determine the origin of the newly formed cardiomyocytes (i.e. from the proliferation of pre-existing cardiomyocytes or from CPC differentiation).

1.2. Adult cardiomyocyte cell structure limits their proliferation

The mechanism(s) reducing CM ability to proliferate several days

after birth was (were) not identified yet. Numerous cardiac research focus on this point and compare the factors secreted and the signaling pathways activated or inhibited between neonatal (with full potential of CM proliferation) and adult hearts (with reduced capacity of proliferation). Thus, several differences were highlighted and could participate to the reduced capacity of adult CMs to proliferate.

1.2.1. Cardiomyocyte cell structure

At birth, cardiomyocytes adapt to the new environment in order to increase heart contractility during the rapid growth of the body and to resist to increased workload. The expansion of the pulmonary alveoli at birth leads to changes in oxygen concentration, pressure charge and blood volume inside the two ventricles. Heart adapts by a first phase of hyperplasia (intensive cell proliferation) and then by a second phase where cardiomyocytes undergo hypertrophy. Rapidly, the cardiomyocyte cell structure changes [36]. Cardiomyocyte architecture becomes more complex with an increase of intracellular structures, such as myofilaments, sarcoplasmic reticulum and mitochondria [45,46]. The cardiomyocytes passes from a polygonal to an elongated form.

The complexity of the adult CM cell structure could be a brake for their proliferation. That is why several studies performed in zebrafish, in mice (in vitro and in vivo after MI) and in humans, suggested that CMs have to go through a step of de-differentiation before be able to proliferate [47–50]. In vitro, this process was described with a partial or total loss of the highly organized sarcomere structure. The cells become smaller and round and re-express some proteins such as the alpha skeletal actin (α-SKA), Nkx2.5, Gata-4, c-kit, runt-related transcription factor 1 (Runx1) and Dab2 [50–52]. They down-regulate the expression of mature cardiomyocyte proteins, Troponin I and alpha myosin heavy chain (α-MHC) and re-express the fetal isoform of the myosin heavy chain (β-MHC). Their new structure facilitates their re-entry into the cell cycle in order to undergo karyokinesis and cytokinesis.

This process was described in pathological conditions in humans and animal models of heart diseases [49,52,53] and can be mediated by Oncostatin M [51,54]. In adult infarcted mouse hearts, de-differentiation is localized mainly at the border zone with a partial loss of Troponin I expression (Troponin $I^{+/-}$ cells). In this area, de-differentiated CMs have the potential to proliferate and to build new connections with the remaining tissue via the connexin 43 [48]. The advantage of cardiomyocyte de-differentiation in the hearts depends on the nature of the cardiac disease: Cardiomyocyte de-differentiation induces cardiomyocyte remodeling and improvement of cardiac performance after MI, whereas in dilated cardiomyopathy this process deteriorates cardiac performances [51,55].

Despite the identification of this process in the hearts of several animal models and in humans, the direct link between de-differentiation and CM proliferation has not yet been established.

1.2.2. Ploidy

During the first week after birth, cardiomyocytes undergo a final round of karyokinesis without cytokinesis. That is why 80–90% of adult cardiac myocytes in rodent hearts are binucleated or polypoid. In contrast, the hearts of neonatal mice and zebrafishes, which display high capacity to regenerate, contain mainly mononucleated diploid CMs. This change of ploidy corresponds to the arrest of the cell cycle progression quickly after birth. Thus, mononucleated cardiomyocytes, which are also smaller in size, are considered as being the only CMs able to proliferate [56–60]. Interestingly, the proportion of mononucleated CMs in adult hearts is dependent on the genetic background. Furthermore, the mouse strains with the highest proportion of mononuclear diploid CMs display also the highest capacity to heart recovery after coronary artery ligation, correlating the fact that mononucleated CMs are able to proliferate and to regenerate diseased hearts [60]. This assumption is, however, subject to contreversy, since others demonstrated that mono-or binucleated adult CMs can equally proliferate [48].

1.3. Signaling pathways involved in neonatal and adult cardiomyocyte proliferation

CM proliferation exists during embryonic, fetal and post-natal life and is driven by several signaling pathways. CM proliferation arrest is controlled by the silencing or the activation of endogenous signaling pathways. The key question of adult cardiac regenerative medicine is to determine whether these endogenous signaling pathways could be re-activated or inactivated in adult hearts, during physiological ageing and/or after injuries. The presence also of adult specific signaling pathway(s) (i.e. not present during fetal or post-natal life) able to control CM proliferation cannot be excluded but will be more difficult to highlight as most research focuses on the “already known” signaling pathways involved in heart development [36].

The Hippo/Yap pathway plays an evolutionarily conserved role in the size control of the organs during development. The core of this pathway includes mammalian STE20-like protein kinase 1 and 2 (MST1/2), the scaffold protein Salvador homologue 1 (SAV1), the large tumour suppressor homologues 1 and 2 (LATS1/2) and the transcriptional co-activators Yap and TAZ [61]. Hippo pathway activation induces the phosphorylation of the complex Yap/TAZ and its proteolytic degradation. By contrast, Hippo pathway inhibition (via i.e. miRNAs, deleting *Lats, Mst1* or *sav1*) induces the translocation into the nucleus of the non-phosphorylated Yap/TAZ complex and thus the transcription of many genes related to cell proliferation, differentiation, survival and migration [61]. Thus, inactivation of this pathway leads to an increase of the heart size during the development due to the stimulation of CM proliferation. After MI, Hippo pathway inhibition stimulates heart regeneration by increasing CM proliferation. CM proliferation can also be increased by overexpressing Yap during embryonic, neonatal and adult stages in “healthy” or “injured” hearts. In the nucleus, YAP interacts with the transcription factor TEAD1, which activates downstream mitogenic pathways, such as the PI3K-Akt pathway [62].

The PI3K-Akt pathway regulates CM proliferation after activation by different protein complex, such as YAP/TEAD1 and neuregulin-1 and its receptor ErbB2 (NRG-1/ErbB2). This pathway is also activated in neonatal and adult CMs by the T-box family transcription factor (Tbx20) via the bone morphogenetic protein receptor (BMP2) and phosphorylation of Smad1/5/8 [63]. Activation of this pathway in the cells is linked to the progression in the cell cycle: Akt activation induces CDK2 phosphorylation in the nucleus, phosphorylated CDK2 translocates to the cytoplasm, where it stabilizes the CDK2-cyclin A-complex. This cytoplasmic localisation is essential for cell progression from S to G2-M phase [64].

The p38 MAPK pathway activation during the development blocks CM proliferation and induces CM hypertrophy [65]. By contrast, inhibition of the phosphorylation of p38 stimulates CM proliferation by stimulating the cyclin A2 and cyclin B in neonatal mouse hearts and adult CMs [66,67]. Furthermore, p38 inhibition associated with FGF-1 stimulation increases cardiac regeneration in infarcted rat hearts through the stimulation of CM proliferation and inhibition of apoptosis [68].

All these signaling pathways act on the transcriptional regulation of cell cycle regulators, such as cyclins, cyclin-dependent kinases (CDKs), CDK inhibitors (p21, p27, p57) or Gata-4. Depending on the activation or the repression of the different signaling pathways, the expressions of these factors are modulated. For example, overexpression of cyclin D1 and A2, positive regulators of the G1/S and G2/M transitions, promotes CM proliferation in mammals and improves cardiac function after MI in mice [69]. The overexpression of the four cell cycle regulators (i.e. CDK1, CDK4, cyclin B1 and cyclin D1) induces CM proliferation and improves cardiac function after heart injury [70].

1.4. Factors able to modulate the signaling pathways involved in cardiomyocyte proliferation

Several factors, molecules, particles can increase the CM proliferation rate in adult mouse or human hearts in pathological conditions. Some were identified and are currently tested in clinic.

1.4.1. Proteins

Neuregulin 1 [57,71], Periostin [72], growth factors (FGF-1 and FGF-10) [66,73] or carbacyclin [74] were shown to stimulate cardiomyocyte proliferation.

Neuregulin-1 (NRG-1) and its tyrosine kinase receptors (ErbB2-ErbB4) are highly expressed in fetal CMs and promote CM proliferation during development (i.e. during trabeculation) [75]. ErbB2 expression diminishes in the heart after birth and at juvenile stage. Activation of ErbB2, in mouse juvenile and adult hearts in physiological and pathological conditions (after MI), promotes CM proliferation through a de-differentiation process and improves cardiac performance [76]. In vitro, NRG-1 stimulates the proliferation of neonatal or adult murine cardiomyocytes as well as the proliferation of human cardiomyocytes (isolated from the hearts of pediatric patients) [57,77]. Through the heterodimerization of ErbB2 and ErbB4, NRG-1 triggers the activation of signaling pathways such as PI3K/AKT and the Ras/Extracellular signal-regulated kinases ERK [78].

Interestingly, NRG-1 stimulates CM proliferation and increases in clinical phase II the cardiac function of patients suffering from chronic heart failure [79].

1.4.2. Exosomes

Exosomes are the smallest vesicles released from the cells (30–100 nm of diameter). They contain proteins (structural, receptors, heat shock proteins), miRNAs (i.e. miR-146a), peptides and also cytokines (i.e. TGF-β) [80]. Cardiac cells, such as cardiomyocytes, fibroblasts, endothelial as well as cardiac progenitor cells, secrete exosomes via exocytose. Once secreted, exosomes can transfer their content from one cell to another and thus are key actors in intercellular communications.

In clinical trials, such as CADUCEUS, cardiosphere derived stem cells (CDCs) are isolated and re-injected into the injured human artery. They decrease heart scar size and increase viable myocardium by stimulating cardiac regeneration [81]. Interestingly, the benefit of these CDCs seems to be due to their secretome and more specifically to their secreted exosomes. Indeed, exosomes isolated from CDCs and injected in rodent or pig ischemic hearts, protect cardiomyocytes from apoptosis, decrease the fibrotic scar tissue and increase cardiomyocyte proliferation [82]. This is also confirmed in vitro, where exosomes secreted from CDCs decrease cardiomyocyte apoptosis and stimulate their proliferation [83]. Interestingly, these exosome protective effects are mainly explained by miRNA transfers into the host cells [84].

1.4.3. miRNAs

miRNAs are small non coding RNAs involved in the post-transcriptional gene regulations. In summary, modulations of miRNA expression promote (i.e. miR-499, miR590-3p and miR-199a) or repress (i.e. miR-15 family, miR-128) neonatal and adult cardiomyocyte proliferation in physiological stages [85] [86]. In pathological conditions, inhibition of miR-34a, or miR-128, for example, increases the cardiac function [85]. Interestingly, injection of the two miRNAs, miR-590-3p and miR-199a, into the peri-infarcted area of mouse hearts, was shown to increase cardiac regeneration, function and stimulate the proliferation of cardiomyocytes. In the case of exercise (i.e ramp swimming and/or voluntary wheel), the upregulation of some miRNAs stimulates cardiomyocyte proliferation in mouse hearts in physiological (miR-222) and pathological conditions after MI (miR-222 and miR-17-3p) [87].

1.4.4. Non long coding RNAs (LncRNAs)

LncRNAs are important factors involved in cardiac recovery after injuries [88]. By comparison with miRNAs, these RNA molecules are longer than 200 nucleotides and are highly tissue-specific, despite low level of expression. LncRNAs can act at a transcriptional and/or post-transcriptional level to regulate gene expression either by cis or trans-acting pathway.

Some LncRNAs (i.e. Braveheart or Fendrr) control the genes involved in cell differentiation during heart formation [89]. However, only few lncRNAs modulate directly cardiomyocyte proliferation. Indeed, after birth, in physiological and pathological conditions, lncRNAs were described to regulate rather the expression of miRNAs and thus indirectly cardiomyocyte proliferation. For example, CRRL (cardiomyocyte regeneration-related lncRNA) increases cardiac function in neonatal mice after MI by regulating the activity of miR-199a-3p and miR-150-5 [90]. Recently, the inhibition of AZIN2, another LncRNA, was shown to increase cardiomyocyte proliferation after MI in adult rat hearts by inhibiting miR-214 [30]. The inhibition of the LncRNA CAREL stimulates also adult cardiomyocyte proliferation via miR-296 regulation in mouse infarcted hearts [91].

2. Modulation of oxygen concentration influences cardiomyocyte proliferation

One of the factors differing between fetal, neonatal and adult life is the oxygen supply.

2.1. Increased oxygen supply at birth leads to metabolic cell adaptation and cardiomyocyte proliferation arrest

During heart formation, the main source of energy comes from anaerobic glycolysis and lactate oxidation because of low oxygen environment (between 2 and 5% oxygen in utero) [92]. Immediately after birth, despite higher oxygen supply (20% oxygen in air), glycolysis and lactate oxidation remain the major metabolic pathways to provide energy. During the first week after birth, glucose oxidation remains low, whereas fatty acid oxidation increases progressively. Therefore, during this period, cardiomyocyte metabolism switches from anaerobic glycolysis (which produces $<10\%$ of total ATP in post-natal hearts) to fatty acid oxidation as a main source of ATP production [93]. Thus, 60–80% of ATP consumed in human adult healthy heart comes from the fatty acid oxidation. This change of substrat allows the heart to increase its metabolism efficiency and its contractility, which is essential to respond to body growth. For comparison, 1 mol of palmitate oxidation produces 105 ATP moles, whereas aerobic glycolysis produces only 31 mol of ATP [94].

To respond to the increase of energy requirement, the switch of an anaerobic to an aerobic metabolism has the consequences for the cardiomyocytes to reorganize the mitochondria and to increase the production of reactive oxygen species.

Compared to the fetal life where the cells contain rare fragmented mitochondria (poorly defined with unorganized cristae), the number of mitochondria in the cells after birth increases. In addition, mitochondria undergo maturation to become elongated and branched with highly organized cristae. Thus, their DNA content as well as their size (representing 30–50% of the cell) increases [95].

At physiological conditions (i.e. 20% oxygen), oxidative metabolism produces reactive oxygen species (ROS) via the mitochondria respiratory chain. ROS are generated by electron leakage leading to the secretion of the superoxide anion ($O_2\cdot^-$) which can easily be converted to hydrogen peroxide and then to hydroxyl radical. In physiological conditions, a low concentration of ROS is non-toxic for the cells. Indeed, antioxidants such as *N*-acetylcysteine, α-tocopherol (vitamin E), ascorbate (vitamin C) or the activation of endogenous antioxidant signaling pathways have the capacity of scavenging ROS [96]. However, when the antioxidant capacity of the cells is not sufficient to neutralize

ROS, they accumulate and generate oxidative stress, which contributes to cardiac dysfunction [97]. In this case, ROS production induces protein and nucleic acid damages, leading to the modulation of the transcription of some genes, encoding proteins involved in cell death, proliferation or differentiation pathways [56].

Interestingly, the progressive heart adaptation to higher oxygen supply after birth, matches with cardiomyocyte proliferation arrest. That is why, the increase of oxygen concentration at birth leading to the increase of ROS production between neonatal and adult life, is considered by some researchers as the cause of CM cell cycle arrest [56]. Accordingly, the full heart regenerative organisms, such as zebrafishes, live in an “oxygen poor” environment.

Thus, some antioxidants, such as *N*-acetylcysteine, Pitx2 or TT-10 (multifaceted fluorinated compound) were shown to increase neonatal cardiomyocyte proliferation in vitro and in vivo, by activating the YAP pathway (for Pitx2 and TT-10) [56,98,99]. Others demonstrated that neonatal cardiomyocyte proliferation requires high oxidative metabolism. In this case, the inhibition of the respiratory chain by rotenone, leads to decreased neonatal cardiomyocyte proliferation [100].

2.2. Hypoxia stimulates HIF-1 activity

Decreased oxygen supply in adult hearts induces 1) increased cell death, 2) the switch from a fatty acid to a “fetal–like” metabolism based on glycolysis, 3) cardiomyocyte hypertrophy, 4) fibrosis, 5) decreased heart contractility. Thus, hypoxia modulates the expression of genes coding for proteins involved in cell death, metabolic, proliferation and/or differentiation pathways. These transcriptional responses are in part mediated by the transcription factor HIF-1 (hypoxia inducible factor 1).

HIF-1 is an heterodimer protein composed of a α-subunit regulated in an oxygen-sensitive manner, and localized, in normoxic conditions (i.e. 20% of oxygen supply) in the cardiomyocyte cytoplasm, and of the constitutive β-subunit, localized in the nucleus. In normoxic conditions, HIF-1α is rapidly degraded. By contrast, in presence of low oxygen concentrations, HIF-1α escapes from proteasomal degradation, accumulates in the cytoplasm and translocates into the nucleus, where it dimerizes with HIF-1β. The heterodimer modulates the transcription of several genes such as the gene coding for the glucose transporter GLUT1, involved in the metabolism switch after hypoxia, or the gene coding for the vascular endothelial growth factor (VEGF) involved in angiogenesis [101].

Interestingly, HIF-1 seems also to modulate genes involved in cardiomyocyte proliferation. Kimura and his group demonstrated that the pool of adult cardiomyocytes proliferating in ischemic adult hearts expresses HIF-1α [102]. Thus, 2 weeks after MI induction, mice were submitted to a reduction in inspired oxygen concentration (7% O2 instead of 20%). These mice displayed increased cardiac function and reduced cardiac fibrosis when compared to mice living at 20% oxygen. Furthermore, an increased proliferation of CMs expressing HIF-1α was detected in the infarcted mice surviving at 7% oxygen [103]. The expression of HIF-1α cannot alone stimulate CM proliferation. Indeed, 1% oxygen induces HIF-1α expression on neonatal cardiomyocytes in vitro, but inhibits their proliferation and induces cell apoptosis [104]. Furthermore, a chronic maternal hypoxia (10.5% O_2) leads the fetal cardiomyocytes to exit from the cell cycle [105].

Altogether these results suggest that the level of hypoxia as well as the stage of the cardiomyocytes undergoing hypoxia are critical factors for modulating cardiomyocyte proliferation.

2.3. Epidemiologic studies of populations living at moderate or high altitude

The first articles studying the occurrence of CVDs and their survival rates in populations living at different altitudes (very high: > 3500 m, high: 2500-3500 m and moderate 1500-2500 m altitude) were published in the middle of the 20th century [106]. Living in altitude has physiological consequences on healthy organisms as the partial pressure of oxygen (hypobaric hypoxia) is decreased, which leads to a decrease of oxygen availability, hyperventilation, pulmonary vasoconstriction, increased cardiac contractility and metabolic modifications. Furthermore, increased UV radiations (which stimulates Vitamin D synthesis) and less pollution can also have physiological effects on the organisms [107].

The first epidemiological studies concerning the occurrence of CVDs and their dependent-mortality rate in populations living in altitude were performed in Peru, in Mexico, in the United States or in Yemen and reported controversial results when compared to people living at sea level [106]. For example, the rates of coronary thrombus and MI were decreased in people living at 4540 m in Peru, whereas the people living at 2260 m in Yemen displayed an increase rate of acute coronary syndrome. The mortality rates due to heart diseases including coronary heart failure decreased in the population living over 2135 m in Mexico and in the United States. These discrepancies can be explained by the reduced number of people involved in the study (in Yemen's study only 768 people) and also by other cardiac risk factors such as smoking, alcohol consumption, nutrition, obesity which were not taken account in these first reports.

Recent surveys from Europe provided more consistent results based on a more homogenous population concerning healthcare. One of them, in Switzerland is based on 1.4 million subjects mainly living between 260 and 1500 m [108]. In this study, a marked progressive decrease in CHD-induced mortality in people living in altitude (max 1960 m) was reported when compared to people living at 260 m. Thus, the authors calculated that the mortality rate induced by CHD decreased by 22% per 1000 m increased altitude. However, the incidence of altitude on the mortality rate is different between male and female.

It should however be noted that all these epidemiological studies were performed on population involving healthy and sick people and living “permanently” in altitude since birth (chronic hypoxia). For patients suffering from heart diseases, the results obtained from several clinical studies led to clinical recommendations [109]. Indeed, the effect of altitude could have a different impact on patients suffering from CVDs, depending on the nature and severity of the pre-existing diseases, the type of “hypoxia” exposure (acute, intermittent or chronic exposure) and the level of altitude. For example, high altitude (> 2500 m) could represent a risk for patients with coronary artery diseases or systemic hypertension, whereas no detrimental effect was detected for patients suffering from heart failure [110]. Other clinical studies on Peruvian patients with coronary heart failure revealed that “intermittent hypoxia” (14 weeks at 4200 m) improves cardiac perfusion [106].

Altogether, epidemiological and clinical studies suggest that living at moderate or high altitude is rather beneficial than detrimental for patients suffering from CVDs [111]. Therefore, strategies based on reducing oxygen supply after CVDs in order to stimulate heart regeneration and CM proliferation emerge. For example, “intermittent hypoxia training (IHT)” was developed to treat patients with CVDs and demonstrated improved cardiac metabolism, enhanced tolerance of myocardium to ischemia/reperfusion injury by reducing free radical damages [110]. IHT hypobaric or normobaric chambers can be adapted to treat patients suffering from CVDs. However, the effectiveness of this new approach depends on the individual reactivity to hypoxia (time of exposure, severity and frequency) and on the type and stage of the disease. More research is need before using “intermittent hypoxia” as a non-pharmacological therapy for CVDs in the future.

2.4. Our own research

The fact that oxygen concentration could modulate cardiomyocyte proliferation has to be taken account in the in vitro experiments. Indeed, cardiomyocyte cell cultures which represent a powerful tool to study the morphological, biochemical, molecular, and electrophysiological characteristics of the isolated cells, are mainly performed

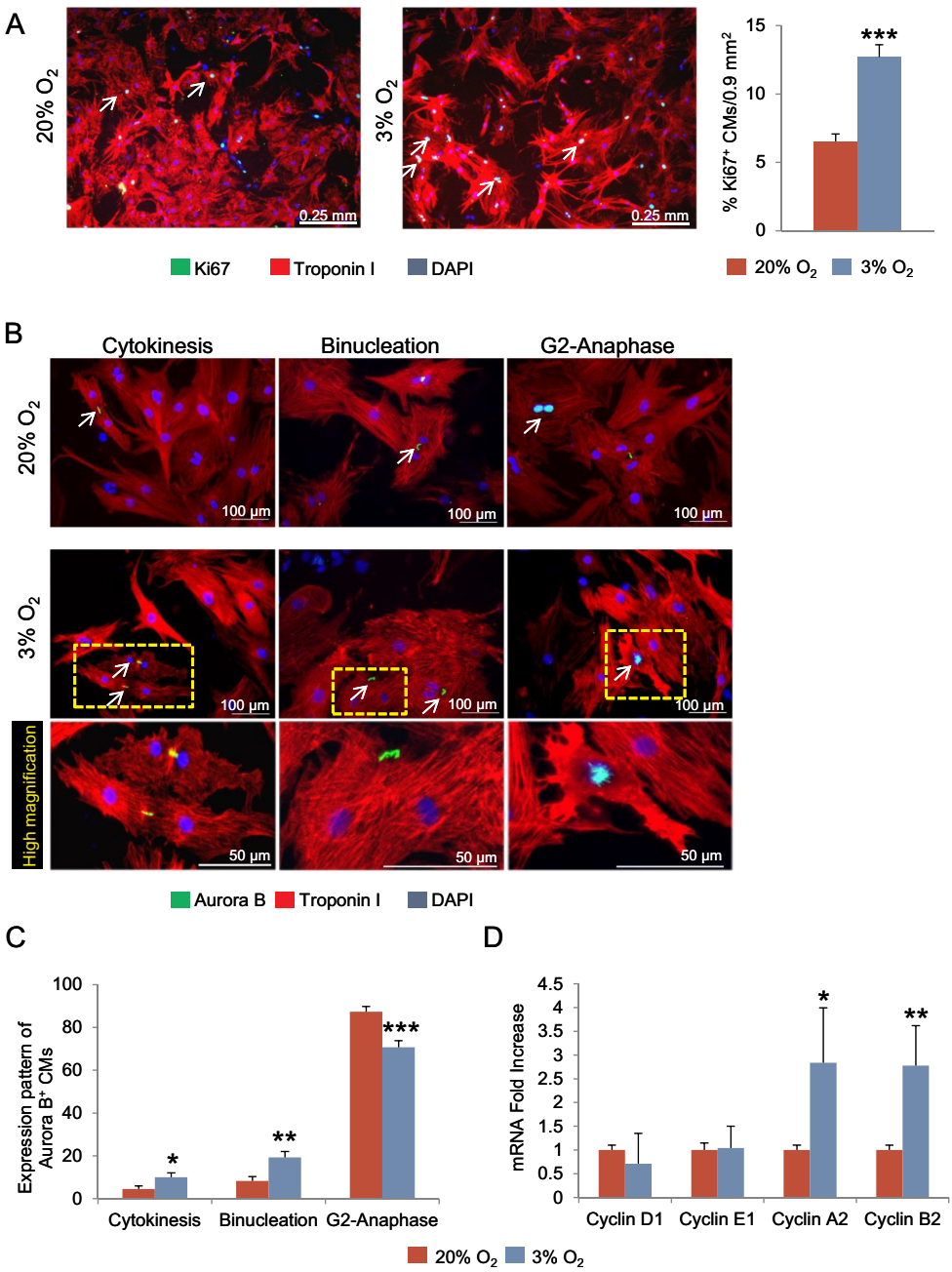

Fig. 1. 3% oxygen promotes cardiomyocyte proliferation.
A: Representative immunostainings against cardiac Troponin I (red) and Ki67 (in green) in neonatal cardiomyocyte cell cultures performed at 20 or 3% O_2 after 14 days of culture. White arrows correspond to proliferating cardiomyocytes (i.e. $Ki67^+$ Troponin I^+ cardiomyocytes). The graph depicts the percentage of $Ki67^+$ CMs, calculated as the number of $Ki67^+$ CMs related to the total number of CMs per pictures (0.9 mm^2) at 3 and 20% O_2. Results are from 3 independent cell cultures, and at least 3895 CMs and 338 $Ki67^+$ CMs were counted per group. **B**: Representative immunostainings against cTroponin I (red) and Aurora B (green) in neonatal cardiomyocyte cultures at 3 and 20% O_2 after 14 days of culture. Cells in the three phases of the cell cycle are represented: cytokinesis, binucleation and G2-Anaphase [114]. **C**: The percentage of the cardiomyocytes in the different phases of the cell cycle is obtained by relating the numbers of Aurora B^+ CMs in different phases of the cell cycle to the total number of Aurora B^+ CMs. Results are from 4 independent experiments, and at least 217 Aurora B^+ CMs were counted per group. For all results, data are mean ± SEM, $*p < 0.05$ **, $p < 0.01$ ***$p < 0.001$ related to 20% O_2. **D**: mRNA fold increase of genes coding for Cyclin D1, E1, A2 or B2 in 14 days old cardiomyocyte cell cultures at 3 and 20% O_2, $n = 5$. For all results, data are mean ± SEM, $*p < 0.05$, $**p = 0.01$ related to 20% O_2.

in “hyperoxic” conditions (in 20% oxygen). Previously, physiological studies estimated that the pO_2 in adult heart in situ is <21 mmHg, corresponding approximatively to 3% O_2 [112]. Thus, the oxygen conditions of the cardiomyocyte cell culture could blunt some of physiological processes occurring in vivo and invalidate the extrapolation of the results obtained “in vitro” to the “in vivo” conditions. That is why the aim of our study was to evaluate whether the rate of proliferation of neonatal cardiomyocytes in culture differs depending on oxygen concentration. Cardiomyocytes isolated from neonatal mouse hearts (1–2 days old) were cultured up to 2 weeks either in 20% oxygen (which is “supra-physiological” but which is the normal condition for cell cultures) or in 3% oxygen (which is the normoxic condition).

For the material and methods, please refer to the supplementary data.

Neonatal cardiomyocytes were cultured the first week with cytosine-β-D arabinofuranoside (AraC, 20 μM) to block non-myocyte cell proliferation. Then AraC was removed and cardiomyocyte cell proliferation was assessed 7 days after. As depicted in Fig. 1A, the number of cardiomyocytes expressing the proliferating marker Ki67 was increased (+94%) in the cultures performed at 3% oxygen compared to those performed at 20% oxygen. Furthermore, among cardiomyocytes expressing Aurora B, higher percentages of CMs undergoing cytokinesis (+124%) and binucleation (+134%) were detected in 3% versus 20% oxygen cell cultures (Fig. 1B–C). Our results demonstrate that more cardiomyocytes proliferate in 3% oxygen than in 20%, which is confirmed by the increase expression of mRNAs coding for cyclin A2 (+183%) and B2 (+177%) (Fig. 1D).

We thus investigated by which mechanism oxygen triggers cardiomyocyte cell proliferation in vitro. As explained above, some published results claimed that cardiomyocytes have to “de-differentiate” before to be able to proliferate [47–50]. Interestingly, in our cell cultures performed in 3 or 20% of oxygen, the Ki67 and Aurora B proteins are expressed by differentiated cardiomyocytes (i.e. with a Troponin I structurally well organized, see Fig. 1A and B) but also by de-differentiated cells (i.e. with disorganized Troponin I protein) (Fig. 2A). In 3% oxygen after 7 and 14 days of culture, the number of Troponin I^+ cells (i.e. structurally well organized) was decreased (−22%; −54%, respectively) compared to the cell cultures performed in 20% oxygen (Fig. 2B). Accordingly, the number of disorganized Troponin I expressing cardiomyocytes (Troponin $I^{+/-}$ cells) and of Troponin I negative cells were increased in 3% oxygen (+584%; +359% respectively 14 days after the onset of cell culture) (Fig. 2B).

Troponin I negative cells are either completely disorganized cardiomyocytes or non-myocyte cells. To determine the origin of the Troponin negative cells, neonatal cardiomyocytes were isolated from heterozygous Myh6 MerCreMer/Tomato-EGFP mice. These neonatal mice were injected with Tamoxifen 1 day before sacrifice to induce EGFP protein expression in the cardiomyocytes. Thus, after 1 week in culture, staining against Troponin I was performed and demonstrated that some Troponin I negative cells expressed the EGFP protein (Fig. 3A and B). The number of GFP^+ Troponin $I^{+/-}$ and GFP^+ Troponin I^- cells was quantified in both oxygen conditions and related to the total number of GFP^+ cardiomyocytes (Fig. 3B). Thus, 35% of the cardiomyocytes are de-differentiated in 3% oxygen compared to 24% in cell cultures performed in 20% oxygen.

The CM de-differentiation process in 3% oxygen was confirmed by the upregulation of genes coding for α-SKA (x 6.1 fold), Runx1 (x 4.7 fold) and β-MHC (x 13 fold) between 7 and 14 days (Fig. 4A). None of these genes was upregulated at 20% oxygen, demonstrating that more de-differentiation occurred in 3% oxygen after 14 days of culture (Fig. 4B). Furthermore, cardiomyocyte specific genes were increased only in 3% oxygen cell culture between 7 and 14 days (Fig. 4C): Nkx2.5 (x 2.4 fold), Gata-4 (x 2.7 fold), Mlc-2v (x 1.7 fold), cTroponin T (x 3.5 fold), α-MHC (x 2.7 fold). The CM area were smaller as well as the expression of the mRNA coding for the atrial natriuretic peptide which was lower, in 3% oxygen compared to 20% oxygen (Fig. 4D and E).

Altogether, these results suggest higher cardiomyocyte proliferation and higher CM de-differentiation in cultures performed in 3% oxygen compared to those performed in 20% oxygen. These results are very important in the context of cell cultures as they demonstrate that the “more physiological” conditions for the culture of neonatal cardiomyocytes is 3% oxygen and that some cellular mechanisms can be highlighted only in specific oxygen concentration. This is the case for neonatal cardiomyocyte proliferation.

Furthermore, these results demonstrated also that proliferation of neonatal cardiomyocytes is not necessary preceded by a step of de-differentiation, as suggested by others [38,47–51]. Indeed, as shown in the different figures, structurally well-organized cardiomyocytes express proliferation markers, suggesting that they are able to undergo cytokinesis. Our assumption is based mainly on the expression of Aurora B and could be completed with live imaging experiments. In the works published by other groups [38,47–51], no experiment was performed in vitro with neonatal mouse cardiomyocytes: some of the works were performed using adult rodent cardiomyocytes [47,48] and other using zebrafish cells [50]. Thus, the proliferation of mature cardiomyocytes without de-differentiation in vitro could be a characteristic of neonatal cardiomyocytes. Porrello and his group showed in neonatal mouse hearts, proliferation of neonatal cardiomyocytes using phosphohistone H3 and Troponin stainings and increased cardiomyocyte dedifferentiation. However, no direct link between these both mechanisms was established by this group in vivo [38].

This is also a limitation of our study. Indeed, we cannot prove with the results presented here that de-differentiated cardiomyocytes undergo cytokinesis. Further experiments using cardiomyocytes isolated from heterozygous Myh6 MerCreMer/Tomato-EGFP mice and expressing the EGFP protein have to be performed for 2 weeks. The cytokinesis (thanks to AuroraB stainings) will be evaluated in GFP^+ Troponin $I^{+/-}$ and Troponin I^- cells.

3. Conclusions

Increasing cardiomyocyte proliferation in injured hearts is the endpoint of new therapeutic strategies aimed to replace the dying cells and to restore heart function after CVDs. These experimental treatments are based on interesting but controversial results concerning the role of oxygen, which is currently considered as “a friend” or “a foe” for heart regeneration. Indeed, high oxygen concentration could not be such beneficial for the hearts as expected.

Increased oxygen supply at birth leads to increased heart contractility thanks to metabolism adaptation but also to ROS generation. Furthermore, this situation coincides with the cardiomyocyte proliferation arrest, without any direct correlation has been until now proved. Interestingly, we present in this review, results demonstrating that the proliferation of neonatal cardiomyocytes in vitro can be increased by reducing the oxygen concentration from a “conventional” (i.e. 20%) to a “physiological” (i.e. 3%) level. Our data highlighted thus, the “inhibitory” role of high oxygen concentration on cardiomyocyte proliferation at least in vitro. The same conclusion can be drawn from the experiments of the group of Sadek who showed in mice after MI, that reducing the oxygen supply after MI can increase CM proliferation [113].

Finally, before to generating new hope for patients suffering from CVDs, the term of “hypoxia” has also to be better defined. The need of oxygen varies according to the cell nature, age, function or environment. Thus, it is very important to define for each clinical situation, the optimal oxygen concentration inducing maximal heart regeneration and minimal apoptosis.

Transparency document

The Transparency document associated with this article can be found, in online version.

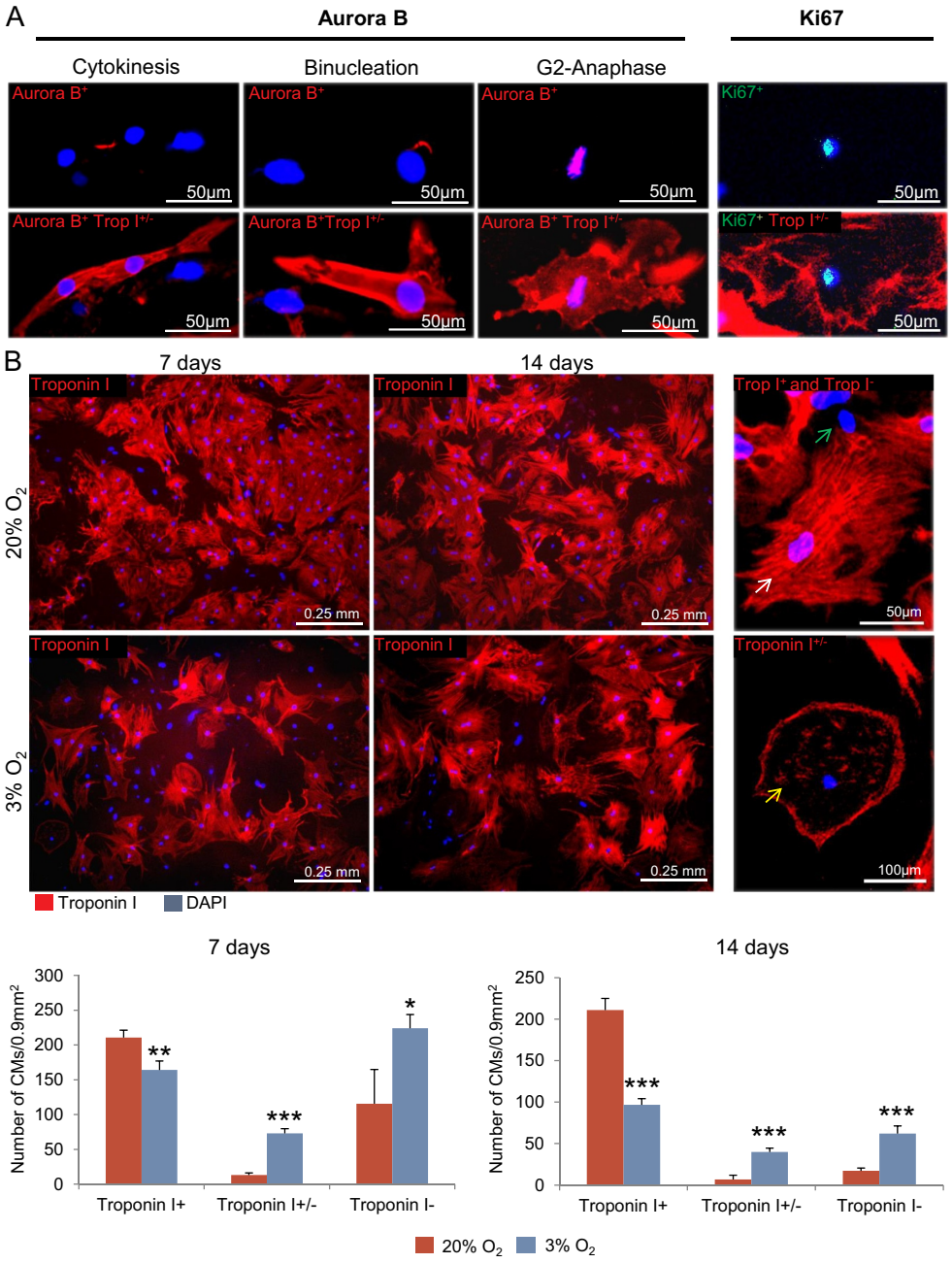

Fig. 2. 3% oxygen increases the number of disorganized Troponin I^+ cells as well as the number of Troponin I^- cells.
A: Neonatal cardiomyocytes cultured in 3% oxygen are stained with cTroponin I (red) associated either with Aurora B (dark red) or Ki67 (green) to detect proliferating cardiomyocytes at different stages of the cell cycle. Representative pictures of disorganized cardiomyocytes (Troponin $I^{+/-}$) expressing Aurora B or Ki67. **B:** Representative pictures of cardiomyocytes stained against cardiac Troponin I (red), 7 days and 14 days after the onset of culture at 3 or 20% O_2. Pictures on the right represent a magnification of a mature differentiated (white arrow), of de-differentiated (yellow arrow) cardiomyocytes, and of a Troponin I^- cell (green arrow). The number of cells expressing organized (i.e. Troponin I^+) or disorganized Troponin I (i.e. Troponin $I^{+/-}$) as well as cells Troponin I^- were counted per pictures. At least 4162 $cTnI^+$, 349 $cTnI^{+/-}$ and 882 $cTnI^-$ cells were counted per group from at least 3 different independent experiments. For all results, data are mean ± SEM; $*p < 0.05$, $**p < 0.01$, $***p < 0.001$ related to 20% O_2.

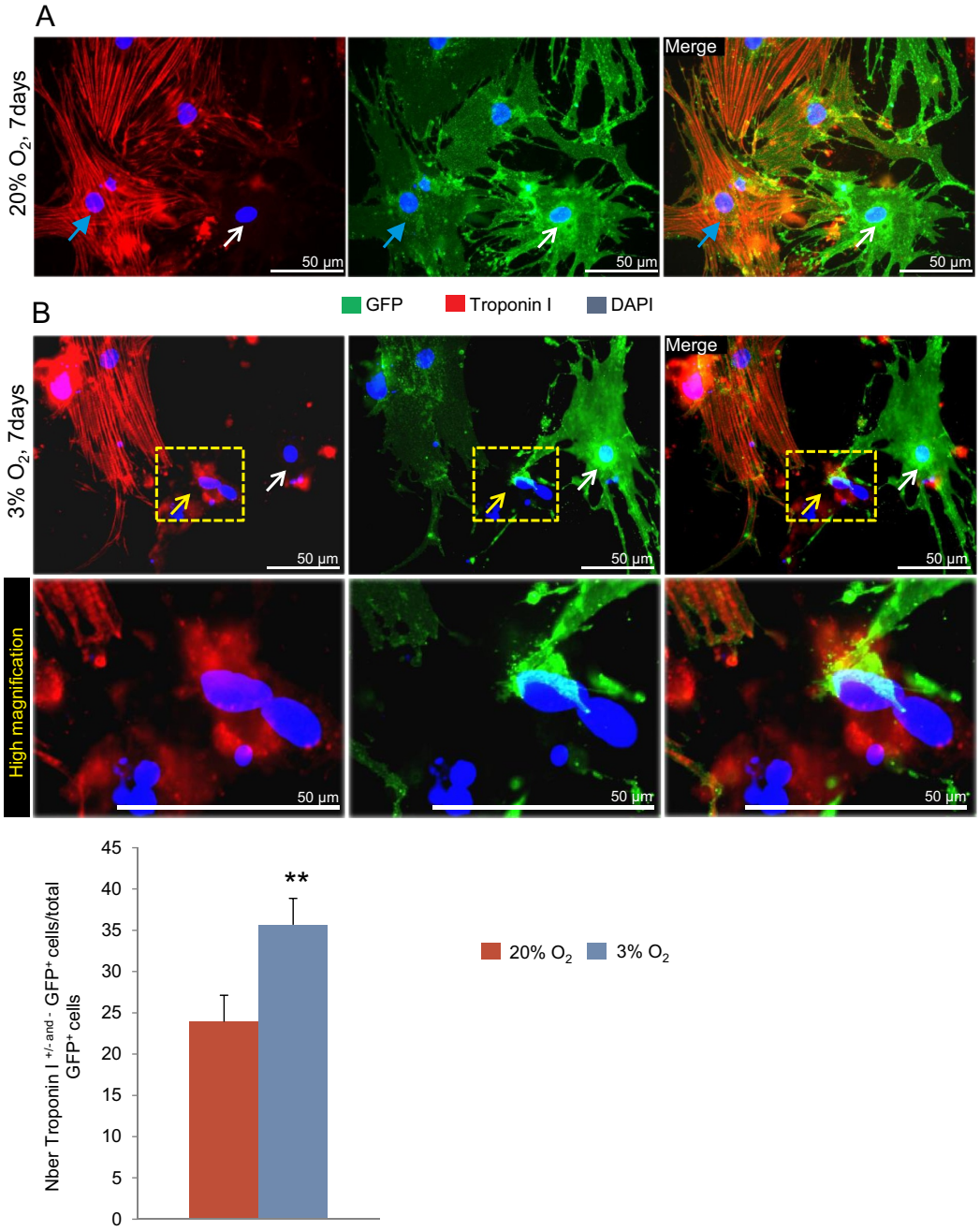

Fig. 3. 3% oxygen stimulates neonatal cardiomyocyte de-differentiation.
A-B: Representative pictures of neonatal cardiomyocytes isolated from Myh6 MerCreMer/Tomato-EGFP hearts and cultured during 7 days in 3 or 20% oxygen and stained with cardiac Troponin I antibody. As neonatal mice were treated with one dose of tamoxifen (1 mg/pup) 1 day before sacrifice, cardiomyocytes express the EGFP protein. **A-B**: Pre-existing GFP^+ cardiomyocytes express a well-organized (blue arrow), or disorganized (yellow arrow) Troponin I protein or no expression of this protein anymore (white arrow) in both oxygen conditions. **C**: The percentages of de-differentiated cardiomyocytes in both cell culture conditions are obtained by relating the number of Troponin $I^{+/-}$ and Troponin I^- GFP^+ cells to the total number of GFP^+ cells. Results are obtained from 3 independent experiments and at least 257 GFP^+ CMs were counted per group. Data are mean ± SEM; $^{**}p < 0.01$ related to 20% O_2.

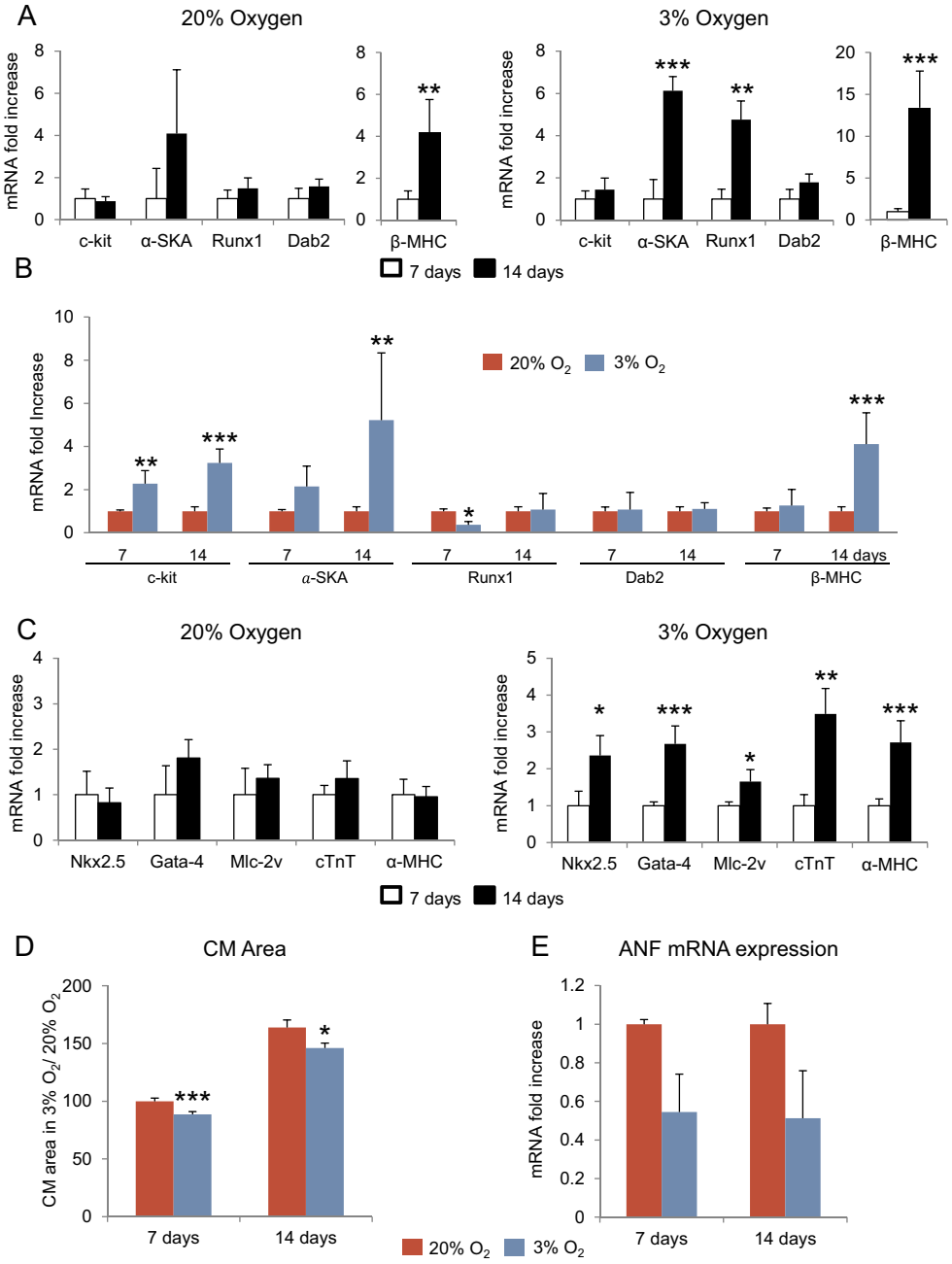

Fig. 4. Cardiomyocyte gene modulation and decreased cell size confirm increased cell de-differentiation at 3% oxygen.
A: Quantitative relative expression of mRNAs coding for genes specific for cardiomyocyte de-differentiation (c-kit, alpha skeletal actin (α-SKA), runt-related transcription factor 1 (Runx1), Dab2 and beta myosin heavy chain (β-MHC)) in neonatal cardiomyocytes cultured for 7 and 14 days in 20 or 3% oxygen. All results obtained after 14 days of culture were related to the levels of the cells cultured in the same oxygen condition at 7 days. **B**: The results at 3% oxygen were compared to the results obtained at 20% oxygen after 7 and 14 days of culture. **C:** Modulation of cardiomyocyte specific genes (Nkx2.5, Gata-4, ventricular Myosin light chain 2 (Mlc-2v), Troponin T, and alpha Myosin Heavy Chain (α-MHC)) in 20 or 3% oxygen cell cultures. The results after 14 days were related to those obtained after 7 days of culture. **A-C**: $n = 3$–9 different experiments per group. Results are mean ± SEM, $^{*}p < 0.05$, $^{**}p \leq 0.01$. $^{***}p \leq 0.001$ **D**: The cardiomyocyte cell area was measured after Troponin I stainings using Image J software. The area of the cardiomyocytes cultured at 3% oxygen is related to those of cardiomyocytes cultured at 20% after 7 days of culture. **E**: mRNA expressions coding for ANF at 7 and 14 days of culture are measured by quantitative RT-PCR. $n \geq 8$ independent experiments. For all results, data are mean ± SEM, $^{*}p < 0.05$, $^{***}p = 0.001$ related to 20% O_2.

Source of funding

This work is supported by a grant from the Swiss National Science Foundation (PMPDB-310030_162985).

Conflict of interest

The authors declare that they have no conflict of interest.

Appendix A. Supplementary data

Supplementary data to this article can be found online at https://doi.org/10.1016/j.bbamcr.2019.03.007.

References

[1] M.A. Laflamme, C.E. Murry, Regenerating the heart, Nat. Biotechnol. 23 (2005) 845–856.
[2] S. Ausoni, S. Sartore, From fish to amphibians to mammals: in search of novel strategies to optimize cardiac regeneration, J. Cell Biol. 184 (2009) 357–364.
[3] O. Bergmann, R.D. Bhardwaj, S. Bernard, S. Zdunek, F. Barnabe-Heider, S. Walsh, J. Zupicich, K. Alkass, B.A. Buchholz, H. Druid, S. Jovinge, J. Frisen, Evidence for cardiomyocyte renewal in humans, Science 324 (2009) 98–102.
[4] N. Rosenblatt-Velin, S. Badoux, L. Liaudet, Pharmacological therapy in the heart as an alternative to cellular therapy: a place for the brain natriuretic peptide? Stem Cells Int. 2016 (2016) 5961342.
[5] P. Menasche, Cell therapy trials for heart regeneration - lessons learned and future directions, Nat. Rev. Cardiol. 15 (2018) 659–671.
[6] T. Eschenhagen, R. Bolli, T. Braun, L.J. Field, B.K. Fleischmann, J. Frisen, M. Giacca, J.M. Hare, S. Houser, R.T. Lee, E. Marban, J.F. Martin, J.D. Molkentin, C.E. Murry, P.R. Riley, P. Ruiz-Lozano, H.A. Sadek, M.A. Sussman, J.A. Hill, Cardiomyocyte regeneration: a consensus statement, Circulation 136 (2017) 680–686.
[7] R.J. Vagnozzi, J.D. Molkentin, S.R. Houser, New myocyte formation in the adult heart: endogenous sources and therapeutic implications, Circ. Res. 123 (2018) 159–176.
[8] C. Gonzales, T. Pedrazzini, Progenitor cell therapy for heart disease, Exp. Cell Res. 315 (2009) 3077–3085.
[9] R.R. Smith, L. Barile, H.C. Cho, M.K. Leppo, J.M. Hare, E. Messina, A. Giacomello, M.R. Abraham, E. Marban, Regenerative potential of cardiosphere-derived cells expanded from percutaneous endomyocardial biopsy specimens, Circulation 115 (2007) 896–908.
[10] G.M. Ellison, C. Vicinanza, A.J. Smith, I. Aquila, A. Leone, C.D. Waring, B.J. Henning, G.G. Stirparo, R. Papait, M. Scarfo, V. Agosti, G. Viglietto, G. Condorelli, C. Indolfi, S. Ottolenghi, D. Torella, B. Nadal-Ginard, Adult c-kit (pos) cardiac stem cells are necessary and sufficient for functional cardiac regeneration and repair, Cell 154 (2013) 827–842.
[11] S. Uchida, P. De Gaspari, S. Kostin, K. Jenniches, A. Kilic, Y. Izumiya, I. Shiojima, K. Grosse Kreymborg, H. Renz, K. Walsh, T. Braun, Sca1-derived cells are a source of myocardial renewal in the murine adult heart, Stem Cell Reports 1 (2013) 397–410.
[12] V. Di Felice, G. Zummo, Stem cell populations in the heart and the role of Isl1 positive cells, European Journal of Histochemistry: EJH 57 (2013) e14.
[13] K.L. Laugwitz, A. Moretti, L. Caron, A. Nakano, K.R. Chien, Islet1 cardiovascular progenitors: a single source for heart lineages? Development 135 (2008) 193–205.
[14] L. Bu, X. Jiang, S. Martin-Puig, L. Caron, S. Zhu, Y. Shao, D.J. Roberts, P.L. Huang, I.J. Domian, K.R. Chien, Human ISL1 heart progenitors generate diverse multipotent cardiovascular cell lineages, Nature 460 (2009) 113–117.
[15] A. Moretti, M. Bellin, C.B. Jung, T.M. Thies, Y. Takashima, A. Bernshausen, M. Schiemann, S. Fischer, S. Moosmang, A.G. Smith, J.T. Lam, K.L. Laugwitz, Mouse and human induced pluripotent stem cells as a source for multipotent Isl1 + cardiovascular progenitors, FASEB J. 24 (2010) 700–711.
[16] N. Rosenblatt-Velin, M.G. Lepore, C. Cartoni, F. Beermann, T. Pedrazzini, FGF-2 controls the differentiation of resident cardiac precursors into functional cardiomyocytes, J. Clin. Invest. 115 (2005) 1724–1733.
[17] N. Smart, S. Bollini, K.N. Dube, J.M. Vieira, B. Zhou, S. Davidson, D. Yellon, J. Riegler, A.N. Price, M.F. Lythgoe, W.T. Pu, P.R. Riley, De novo cardiomyocytes from within the activated adult heart after injury, Nature 474 (2011) 640–644.
[18] P.C. Hsieh, V.F. Segers, M.E. Davis, C. MacGillivray, J. Gannon, J.D. Molkentin, J. Robbins, R.T. Lee, Evidence from a genetic fate-mapping study that stem cells refresh adult mammalian cardiomyocytes after injury, Nat. Med. 13 (2007) 970–974.
[19] H. Oh, S.B. Bradfute, T.D. Gallardo, T. Nakamura, V. Gaussin, Y. Mishina, J. Pocius, L.H. Michael, R.R. Behringer, D.J. Garry, M.L. Entman, M.D. Schneider, Cardiac progenitor cells from adult myocardium: homing, differentiation, and fusion after infarction, Proc. Natl. Acad. Sci. U. S. A. 100 (2003) 12313–12318.
[20] R. Bolli, A.R. Chugh, D. D'Amario, J.H. Loughran, M.F. Stoddard, S. Ikram, G.M. Beache, S.G. Wagner, A. Leri, T. Hosoda, F. Sanada, J.B. Elmore, P. Goichberg, D. Cappetta, N.K. Solankhi, I. Fahsah, D.G. Rokosh, M.S. Slaughter, J. Kajstura, P. Anversa, Cardiac stem cells in patients with ischaemic cardiomyopathy (SCIPIO): initial results of a randomised phase 1 trial, Lancet 378 (2011) 1847–1857.
[21] J.H. van Berlo, O. Kanisicak, M. Maillet, R.J. Vagnozzi, J. Karch, S.C. Lin, R.C. Middleton, E. Marban, J.D. Molkentin, C-kit+ cells minimally contribute cardiomyocytes to the heart, Nature 509 (2014) 337–341.
[22] Q. Liu, R. Yang, X. Huang, H. Zhang, L. He, L. Zhang, X. Tian, Y. Nie, S. Hu, Y. Yan, L. Zhang, Z. Qiao, Q.D. Wang, K.O. Lui, B. Zhou, Genetic lineage tracing identifies in situ Kit-expressing cardiomyocytes, Cell Res. 26 (2016) 119–130.
[23] N. Sultana, L. Zhang, J. Yan, J. Chen, W. Cai, S. Razzaque, D. Jeong, W. Sheng, L. Bu, M. Xu, G.Y. Huang, R.J. Hajjar, B. Zhou, A. Moon, C.L. Cai, Resident c-kit (+) cells in the heart are not cardiac stem cells, Nat. Commun. 6 (2015) 8701.
[24] L. He, Y. Li, Y. Li, W. Pu, X. Huang, X. Tian, Y. Wang, H. Zhang, Q. Liu, L. Zhang, H. Zhao, J. Tang, H. Ji, D. Cai, Z. Han, Z. Han, Y. Nie, S. Hu, Q.D. Wang, R. Sun, J. Fei, F. Wang, T. Chen, Y. Yan, H. Huang, W.T. Pu, B. Zhou, Enhancing the precision of genetic lineage tracing using dual recombinases, Nat. Med. 23 (2017) 1488–1498.
[25] Y. Li, L. He, X. Huang, S. Issa Bhaloo, H. Zhao, S. Zhang, W. Pu, X. Tian, Y. Li, Q. Liu, W. Yu, L. Zhang, X. Liu, K. Liu, J. Tang, H. Zhang, D. Cai, R.H. Adams, Q. Xu, K.O. Lui, B. Zhou, Genetic lineage tracing of non-myocyte population by dual recombinases, Circulation 138 (23) (2018) 793–805.
[26] X. Wang, Q. Hu, Y. Nakamura, J. Lee, G. Zhang, A.H. From, J. Zhang, The role of the sca-1 +/CD31- cardiac progenitor cell population in postinfarction left ventricular remodeling, Stem Cells 24 (2006) 1779–1788.
[27] L. Zhang, N. Sultana, J. Yan, F. Yang, F. Chen, E. Chepurko, F.C. Yang, Q. Du, L. Zangi, M. Xu, L. Bu, C.L. Cai, Cardiac Sca-1(+) cells are not intrinsic stem cells for myocardial development, renewal, and repair, Circulation 138 (2018) 2919–2930.
[28] R.T. Lee, Adult cardiac stem cell concept and the process of science, Circulation 138 (2018) 2940–2942.
[29] L.E. Neidig, F. Weinberger, N.J. Palpant, J. Mignone, A.M. Martinson, D.W. Sorensen, I. Bender, N. Nemoto, H. Reinecke, L. Pabon, J.D. Molkentin, C.E. Murry, J.H. van Berlo, Evidence for minimal cardiogenic potential of stem cell antigen 1-positive cells in the adult mouse heart, Circulation 138 (2018) 2960–2962.
[30] R.J. Vagnozzi, M.A. Sargent, S.J. Lin, N.J. Palpant, C.E. Murry, J.D. Molkentin, Genetic lineage tracing of Sca-1(+) cells reveals endothelial but not myogenic contribution to the murine heart, Circulation 138 (2018) 2931–2939.
[31] J. Tang, H. Zhang, L. He, X. Huang, Y. Li, W. Pu, W. Yu, L. Zhang, D. Cai, K.O. Lui, B. Zhou, Genetic fate mapping defines the vascular potential of endocardial cells in the adult heart, Circ. Res. 122 (2018) 984–993.
[32] M.H. Soonpaa, P.J. Lafontant, S. Reuter, J.A. Scherschel, E.F. Srour, M.M. Zaruba, M. Rubart-von der Lohe, L.J. Field, Absence of cardiomyocyte differentiation following transplantation of adult cardiac-resident Sca-1(+) cells into infarcted mouse hearts, Circulation 138 (2018) 2963–2966.
[33] A. Moretti, L. Caron, A. Nakano, J.T. Lam, A. Bernshausen, Y. Chen, Y. Qyang, L. Bu, M. Sasaki, S. Martin-Puig, Y. Sun, S.M. Evans, K.L. Laugwitz, K.R. Chien, Multipotent embryonic isl1 + progenitor cells lead to cardiac, smooth muscle, and endothelial cell diversification, Cell 127 (2006) 1151–1165.
[34] F. Weinberger, D. Mehrkens, F.W. Friedrich, M. Stubbendorff, X. Hua, J.C. Muller, S. Schrepfer, S.M. Evans, L. Carrier, T. Eschenhagen, Localization of Islet-1-positive cells in the healthy and infarcted adult murine heart, Circ. Res. 110 (2012) 1303–1310.
[35] K.D. Poss, L.G. Wilson, M.T. Keating, Heart regeneration in zebrafish, Science 298 (2002) 2188–2190.
[36] F.X. Galdos, Y. Guo, S.L. Paige, N.J. VanDusen, S.M. Wu, W.T. Pu, Cardiac regeneration: lessons from development, Circ. Res. 120 (2017) 941–959.
[37] A.C. Sturzu, K. Rajarajan, D. Passer, K. Plonowska, A. Riley, T.C. Tan, A. Sharma, A.F. Xu, M.C. Engels, R. Feistritzer, G. Li, M.K. Selig, R. Geissler, K.D. Robertson, M. Scherrer-Crosbie, I.J. Domian, S.M. Wu, Fetal mammalian heart generates a robust compensatory response to cell loss, Circulation 132 (2015) 109–121.
[38] E.R. Porrello, A.I. Mahmoud, E. Simpson, J.A. Hill, J.A. Richardson, E.N. Olson, H.A. Sadek, Transient regenerative potential of the neonatal mouse heart, Science 331 (2011) 1078–1080.
[39] W. Zhu, E. Zhang, M. Zhao, Z. Chong, C. Fan, Y. Tang, J.D. Hunter, A.V. Borovjagin, G.P. Walcott, J.Y. Chen, G. Qin, J. Zhang, Regenerative potential of neonatal porcine hearts, Circulation 138 (24) (2018) 2809–2816.
[40] B.J. Haubner, J. Schneider, U. Schweigmann, T. Schuetz, W. Dichtl, C. Velik-Salchner, J.I. Stein, J.M. Penninger, Functional recovery of a human neonatal heart after severe myocardial infarction, Circ. Res. 118 (2016) 216–221.
[41] Y. Nakagama, R. Inuzuka, K. Ichimura, M. Hinata, H. Takehara, N. Takeda, S. Kakiuchi, K. Shiraga, H. Asakai, T. Shindo, Y. Hirata, M. Saitoh, A. Oka, Accelerated cardiomyocyte proliferation in the heart of a neonate with LEOPARD syndrome-associated fatal cardiomyopathy, Circ Heart Fail 11 (2018) e004660.
[42] K.M. Farooqi, N. Sutton, S. Weinstein, M. Menegus, H. Spindola-Franco, R.H. Pass, Neonatal myocardial infarction: case report and review of the literature, Congenit. Heart Dis. 7 (2012) E97–102.
[43] S.E. Senyo, M.L. Steinhauser, C.L. Pizzimenti, V.K. Yang, L. Cai, M. Wang, T.D. Wu, J.L. Guerquin-Kern, C.P. Lechene, R.T. Lee, Mammalian heart renewal by pre-existing cardiomyocytes, Nature 493 (2013) 433–436.
[44] S.R. Ali, S. Hippenmeyer, L.V. Saadat, L. Luo, I.L. Weissman, R. Ardehali, Existing cardiomyocytes generate cardiomyocytes at a low rate after birth in mice, Proc. Natl. Acad. Sci. U. S. A. 111 (2014) 8850–8855.
[45] J. Piquereau, R. Ventura-Clapier, Maturation of cardiac energy metabolism during perinatal development, Front. Physiol. 9 (2018) 959.
[46] G.A. Porter Jr., J. Hom, D. Hoffman, R. Quintanilla, K. de Mesy Bentley, S.S. Sheu, Bioenergetics, mitochondria, and cardiac myocyte differentiation, Prog. Pediatr. Cardiol. 31 (2011) 75–81.

[47] Y. Zhang, T.S. Li, S.T. Lee, K.A. Wawrowsky, K. Cheng, G. Galang, K. Malliaras, M.R. Abraham, C. Wang, E. Marban, Dedifferentiation and proliferation of mammalian cardiomyocytes, PLoS One 5 (2010) e12559.
[48] W.E. Wang, L. Li, X. Xia, W. Fu, Q. Liao, C. Lan, D. Yang, H. Chen, R. Yue, C. Zeng, L. Zhou, B. Zhou, D.D. Duan, X. Chen, S.R. Houser, C. Zeng, Dedifferentiation, proliferation, and redifferentiation of adult mammalian cardiomyocytes after ischemic injury, Circulation 136 (2017) 834–848.
[49] G.D. Dispersyn, L. Mesotten, B. Meuris, A. Maes, L. Mortelmans, W. Flameng, F. Ramaekers, M. Borgers, Dissociation of cardiomyocyte apoptosis and dedifferentiation in infarct border zones, Eur. Heart J. 23 (2002) 849–857.
[50] C. Jopling, E. Sleep, M. Raya, M. Marti, A. Raya, J.C. Izpisua Belmonte, Zebrafish heart regeneration occurs by cardiomyocyte dedifferentiation and proliferation, Nature 464 (2010) 606–609.
[51] T. Kubin, J. Poling, S. Kostin, P. Gajawada, S. Hein, W. Rees, A. Wietelmann, M. Tanaka, H. Lorchner, S. Schimanski, M. Szibor, H. Warnecke, T. Braun, Oncostatin M is a major mediator of cardiomyocyte dedifferentiation and remodeling, Cell Stem Cell 9 (2011) 420–432.
[52] R.B. Driesen, F.K. Verheyen, W. Debie, E. Blaauw, F.A. Babiker, R.N. Cornelussen, J. Ausma, M.H. Lenders, M. Borgers, C. Chaponnier, F.C. Ramaekers, Re-expression of alpha skeletal actin as a marker for dedifferentiation in cardiac pathologies, J. Cell. Mol. Med. 13 (2009) 896–908.
[53] C. Rucker-Martin, F. Pecker, D. Godreau, S.N. Hatem, Dedifferentiation of atrial myocytes during atrial fibrillation: role of fibroblast proliferation in vitro, Cardiovasc. Res. 55 (2002) 38–52.
[54] J. Poling, P. Gajawada, H. Lorchner, V. Polyakova, M. Szibor, T. Bottger, H. Warnecke, T. Kubin, T. Braun, The Janus face of OSM-mediated cardiomyocyte dedifferentiation during cardiac repair and disease, Cell Cycle 11 (2012) 439–445.
[55] J. Poling, P. Gajawada, M. Richter, H. Lorchner, V. Polyakova, S. Kostin, J. Shin, T. Boettger, T. Walther, W. Rees, A. Wietelmann, H. Warnecke, T. Kubin, T. Braun, Therapeutic targeting of the oncostatin M receptor-beta prevents inflammatory heart failure, Basic Res. Cardiol. 109 (2014) 396.
[56] B.N. Puente, W. Kimura, S.A. Muralidhar, J. Moon, J.F. Amatruda, K.L. Phelps, D. Grinsfelder, B.A. Rothermel, R. Chen, J.A. Garcia, C.X. Santos, S. Thet, E. Mori, M.T. Kinter, P.M. Rindler, S. Zacchigna, S. Mukherjee, D.J. Chen, A.I. Mahmoud, M. Giacca, P.S. Rabinovitch, A. Aroumougame, A.M. Shah, L.I. Szweda, H.A. Sadek, The oxygen-rich postnatal environment induces cardiomyocyte cell-cycle arrest through DNA damage response, Cell 157 (2014) 565–579.
[57] K. Bersell, S. Arab, B. Haring, B. Kuhn, Neuregulin1/ErbB4 signaling induces cardiomyocyte proliferation and repair of heart injury, Cell 138 (2009) 257–270.
[58] M. Mollova, K. Bersell, S. Walsh, J. Savla, L.T. Das, S.Y. Park, L.E. Silberstein, C.G. Dos Remedios, D. Graham, S. Colan, B. Kuhn, Cardiomyocyte proliferation contributes to heart growth in young humans, Proc. Natl. Acad. Sci. U. S. A. 110 (2013) 1446–1451.
[59] A.I. Mahmoud, F. Kocabas, S.A. Muralidhar, W. Kimura, A.S. Koura, S. Thet, E.R. Porrello, H.A. Sadek, Meis1 regulates postnatal cardiomyocyte cell cycle arrest, Nature 497 (2013) 249–253.
[60] M. Patterson, L. Barske, B. Van Handel, C.D. Rau, P. Gan, A. Sharma, S. Parikh, M. Denholtz, Y. Huang, Y. Yamaguchi, H. Shen, H. Allayee, J.G. Crump, T.I. Force, C.L. Lien, T. Makita, A.J. Lusis, S.R. Kumar, H.M. Sucov, Frequency of mononuclear diploid cardiomyocytes underlies natural variation in heart regeneration, Nat. Genet. 49 (2017) 1346–1353.
[61] J. Wang, S. Liu, T. Heallen, J.F. Martin, The Hippo pathway in the heart: pivotal roles in development, disease, and regeneration, Nat Rev Cardiol (2018).
[62] Z. Lin, P. Zhou, A. von Gise, F. Gu, Q. Ma, J. Chen, H. Guo, P.R. van Gorp, D.Z. Wang, W.T. Pu, Pi3kcb links hippo-YAP and PI3K-AKT signaling pathways to promote cardiomyocyte proliferation and survival, Circ. Res. 116 (2015) 35–45.
[63] S. Chakraborty, A. Sengupta, K.E. Yutzey, Tbx20 promotes cardiomyocyte proliferation and persistence of fetal characteristics in adult mouse hearts, J. Mol. Cell. Cardiol. 62 (2013) 203–213.
[64] S. Maddika, S.R. Ande, E. Wiechec, L.L. Hansen, S. Wesselborg, M. Los, Akt-mediated phosphorylation of CDK2 regulates its dual role in cell cycle progression and apoptosis, J. Cell Sci. 121 (2008) 979–988.
[65] Q. Liang, O.F. Bueno, B.J. Wilkins, C.Y. Kuan, Y. Xia, J.D. Molkentin, c-Jun N-terminal kinases (JNK) antagonize cardiac growth through cross-talk with calcineurin-NFAT signaling, EMBO J. 22 (2003) 5079–5089.
[66] F.B. Engel, M. Schebesta, M.T. Duong, G. Lu, S. Ren, J.B. Madwed, H. Jiang, Y. Wang, M.T. Keating, p38 MAP kinase inhibition enables proliferation of adult mammalian cardiomyocytes, Genes Dev. 19 (2005) 1175–1187.
[67] Q. Liang, J.D. Molkentin, Redefining the roles of p38 and JNK signaling in cardiac hypertrophy: dichotomy between cultured myocytes and animal models, J. Mol. Cell. Cardiol. 35 (2003) 1385–1394.
[68] F.B. Engel, P.C. Hsieh, R.T. Lee, M.T. Keating, FGF1/p38 MAP kinase inhibitor therapy induces cardiomyocyte mitosis, reduces scarring, and rescues function after myocardial infarction, Proc. Natl. Acad. Sci. U. S. A. 103 (2006) 15546–15551.
[69] K.B. Pasumarthi, H. Nakajima, H.O. Nakajima, M.H. Soonpaa, L.J. Field, Targeted expression of cyclin D2 results in cardiomyocyte DNA synthesis and infarct regression in transgenic mice, Circ. Res. 96 (2005) 110–118.
[70] T.M.A. Mohamed, Y.S. Ang, E. Radzinsky, P. Zhou, Y. Huang, A. Elfenbein, A. Foley, S. Magnitsky, D. Srivastava, Regulation of cell cycle to stimulate adult cardiomyocyte proliferation and cardiac regeneration, Cell 173 (2018) 104–116 (e112).
[71] T. Braun, S. Dimmeler, Breaking the silence: stimulating proliferation of adult cardiomyocytes, Dev. Cell 17 (2009) 151–153.
[72] B. Kuhn, F. del Monte, R.J. Hajjar, Y.S. Chang, D. Lebeche, S. Arab, M.T. Keating, Periostin induces proliferation of differentiated cardiomyocytes and promotes cardiac repair, Nat. Med. 13 (2007) 962–969.
[73] F. Rochais, R. Sturny, C.M. Chao, K. Mesbah, M. Bennett, T.J. Mohun, S. Bellusci, R.G. Kelly, FGF10 promotes regional foetal cardiomyocyte proliferation and adult cardiomyocyte cell-cycle re-entry, Cardiovasc. Res. 104 (2014) 432–442.
[74] A. Magadum, Y. Ding, L. He, T. Kim, M.D. Vasudevarao, Q. Long, K. Yang, N. Wickramasinghe, H.V. Renikunta, N. Dubois, G. Weidinger, Q. Yang, F.B. Engel, Live cell screening platform identifies PPARdelta as a regulator of cardiomyocyte proliferation and cardiac repair, Cell Res. 27 (2017) 1002–1019.
[75] K.F. Lee, H. Simon, H. Chen, B. Bates, M.C. Hung, C. Hauser, Requirement for neuregulin receptor erbB2 in neural and cardiac development, Nature 378 (1995) 394–398.
[76] G. D'Uva, A. Aharonov, M. Lauriola, D. Kain, Y. Yahalom-Ronen, S. Carvalho, K. Weisinger, E. Bassat, D. Rajchman, O. Yifa, M. Lysenko, T. Konfino, J. Hegesh, O. Brenner, M. Neeman, Y. Yarden, J. Leor, R. Sarig, R.P. Harvey, E. Tzahor, ERBB2 triggers mammalian heart regeneration by promoting cardiomyocyte dedifferentiation and proliferation, Nat. Cell Biol. 17 (2015) 627–638.
[77] B.D. Polizzotti, B. Ganapathy, S. Walsh, S. Choudhury, N. Ammanamanchi, D.G. Bennett, C.G. dos Remedios, B.J. Haubner, J.M. Penninger, B. Kuhn, Neuregulin stimulation of cardiomyocyte regeneration in mice and human myocardium reveals a therapeutic window, Sci Transl Med, 7 (2015) 281ra245.
[78] W.X. Schulze, L. Deng, M. Mann, Phosphotyrosine interactome of the ErbB-receptor kinase family, Mol. Syst. Biol. 1 (2005) (2005) 0008.
[79] R. Gao, J. Zhang, L. Cheng, X. Wu, W. Dong, X. Yang, T. Li, X. Liu, Y. Xu, X. Li, M. Zhou, A phase II, randomized, double-blind, multicenter, based on standard therapy, placebo-controlled study of the efficacy and safety of recombinant human neuregulin-1 in patients with chronic heart failure, J. Am. Coll. Cardiol. 55 (2010) 1907–1914.
[80] A. Waldenstrom, G. Ronquist, Role of exosomes in myocardial remodeling, Circ. Res. 114 (2014) 315–324.
[81] R.R. Makkar, R.R. Smith, K. Cheng, K. Malliaras, L.E. Thomson, D. Berman, L.S. Czer, L. Marban, A. Mendizabal, P.V. Johnston, S.D. Russell, K.H. Schuleri, A.C. Lardo, G. Gerstenblith, E. Marban, Intracoronary cardiosphere-derived cells for heart regeneration after myocardial infarction (CADUCEUS): a prospective, randomised phase 1 trial, Lancet 379 (2012) 895–904.
[82] R. Gallet, J. Dawkins, J. Valle, E. Simsolo, G. de Couto, R. Middleton, E. Tseliou, D. Luthringer, M. Kreke, R.R. Smith, L. Marban, B. Ghaleb, E. Marban, Exosomes secreted by cardiosphere-derived cells reduce scarring, attenuate adverse remodelling, and improve function in acute and chronic porcine myocardial infarction, Eur. Heart J. 38 (2017) 201–211.
[83] J.K. Lang, R.F. Young, H. Ashraf, J.M. Canty Jr., Inhibiting extracellular vesicle release from human cardiosphere derived cells with lentiviral knockdown of nSMase2 differentially effects proliferation and apoptosis in cardiomyocytes, fibroblasts and endothelial cells in vitro, PLoS One 11 (2016) e0165926.
[84] M. Khan, E. Nickoloff, T. Abramova, J. Johnson, S.K. Verma, P. Krishnamurthy, A.R. Mackie, E. Vaughan, V.N. Garikipati, C. Benedict, V. Ramirez, E. Lambers, A. Ito, E. Gao, S. Misener, T. Luongo, J. Elrod, G. Qin, S.R. Houser, W.J. Koch, R. Kishore, Embryonic stem cell-derived exosomes promote endogenous repair mechanisms and enhance cardiac function following myocardial infarction, Circ. Res. 117 (2015) 52–64.
[85] W. Huang, Y. Feng, J. Liang, H. Yu, C. Wang, B. Wang, M. Wang, L. Jiang, W. Meng, W. Cai, M. Medvedovic, J. Chen, C. Paul, W.S. Davidson, S. Sadayappan, P.J. Stambrook, X.Y. Yu, Y. Wang, Loss of microRNA-128 promotes cardiomyocyte proliferation and heart regeneration, Nat. Commun. 9 (2018) 700.
[86] S. Qu, C. Zeng, W.E. Wang, Noncoding RNA and cardiomyocyte proliferation, Stem Cells Int. 2017 (2017) 6825427.
[87] A. Vujic, C. Lerchenmuller, T.D. Wu, C. Guillermier, C.P. Rabolli, E. Gonzalez, S.E. Senyo, X. Liu, J.L. Guerquin-Kern, M.L. Steinhauser, R.T. Lee, A. Rosenzweig, Exercise induces new cardiomyocyte generation in the adult mammalian heart, Nat. Commun. 9 (2018) 1659.
[88] O.K. Choong, D.S. Lee, C.Y. Chen, P.C.H. Hsieh, The roles of non-coding RNAs in cardiac regenerative medicine, Noncoding RNA Res 2 (2017) 100–110.
[89] J. Wang, Z. Geng, J. Weng, L. Shen, M. Li, X. Cai, C. Sun, M. Chu, Microarray analysis reveals a potential role of LncRNAs expression in cardiac cell proliferation, BMC Dev. Biol. 16 (2016) 41.
[90] G. Chen, H. Li, X. Li, B. Li, L. Zhong, S. Huang, H. Zheng, M. Li, G. Jin, W. Liao, Y. Liao, Y. Chen, J. Bin, Loss of long non-coding RNA CRRL promotes cardiomyocyte regeneration and improves cardiac repair by functioning as a competing endogenous RNA, J. Mol. Cell. Cardiol. 122 (2018) 152–164.
[91] B. Cai, W. Ma, F. Ding, L. Zhang, Q. Huang, X. Wang, B. Hua, J. Xu, J. Li, C. Bi, S. Guo, F. Yang, Z. Han, Y. Li, G. Yan, Y. Yu, Z. Bao, M. Yu, F. Li, Y. Tian, Z. Pan, B. Yang, The long noncoding RNA CAREL controls cardiac regeneration, J. Am. Coll. Cardiol. 72 (2018) 534–550.
[92] G.D. Lopaschuk, M.A. Spafford, D.R. Marsh, Glycolysis is predominant source of myocardial ATP production immediately after birth, Am. J. Phys. 261 (1991) H1698–H1705.
[93] G.D. Lopaschuk, J.R. Ussher, C.D. Folmes, J.S. Jaswal, W.C. Stanley, Myocardial fatty acid metabolism in health and disease, Physiol. Rev. 90 (2010) 207–258.
[94] J.S. Jaswal, W. Keung, W. Wang, J.R. Ussher, G.D. Lopaschuk, Targeting fatty acid and carbohydrate oxidation–a novel therapeutic intervention in the ischemic and failing heart, Biochim. Biophys. Acta 1813 (2011) 1333–1350.
[95] J.R. Hom, R.A. Quintanilla, D.L. Hoffman, K.L. de Mesy Bentley, J.D. Molkentin, S.S. Sheu, G.A. Porter Jr., The permeability transition pore controls cardiac mitochondrial maturation and myocyte differentiation, Dev. Cell 21 (2011) 469–478.
[96] L. Liaudet, G. Vassalli, P. Pacher, Role of peroxynitrite in the redox regulation of cell signal transduction pathways, Front. Biosci. 14 (2009) 4809–4814.
[97] R. Sarangarajan, S. Meera, R. Rukkumani, P. Sankar, G. Anuradha, Antioxidants:

friend or foe? Asian Pac J Trop Med 10 (2017) 1111–1116.
[98] G. Tao, P.C. Kahr, Y. Morikawa, M. Zhang, M. Rahmani, T.R. Heallen, L. Li, Z. Sun, E.N. Olson, B.A. Amendt, J.F. Martin, Pitx2 promotes heart repair by activating the antioxidant response after cardiac injury, Nature 534 (2016) 119–123.
[99] H. Hara, N. Takeda, M. Kondo, M. Kubota, T. Saito, J. Maruyama, T. Fujiwara, S. Maemura, M. Ito, A.T. Naito, M. Harada, H. Toko, S. Nomura, H. Kumagai, Y. Ikeda, H. Ueno, E. Takimoto, H. Akazawa, H. Morita, H. Aburatani, Y. Hata, M. Uchiyama, I. Komuro, Discovery of a small molecule to increase cardiomyocytes and protect the heart after ischemic injury, JACC Basic Transl Sci 3 (2018) 639–653.
[100] A. de Carvalho, V. Bassaneze, M.F. Forni, A.A. Keusseyan, A.J. Kowaltowski, J.E. Krieger, Early postnatal cardiomyocyte proliferation requires high oxidative energy metabolism, Sci. Rep. 7 (2017) 15434.
[101] M.D.L. Sousa Fialho, A.H. Abd Jamil, G.A. Stannard, L.C. Heather, Hypoxia-inducible factor 1 signalling, metabolism and its therapeutic potential in cardiovascular disease, Biochim Biophys Acta Mol Basis Dis (2018).
[102] W. Kimura, F. Xiao, D.C. Canseco, S. Muralidhar, S. Thet, H.M. Zhang, Y. Abderrahman, R. Chen, J.A. Garcia, J.M. Shelton, J.A. Richardson, A.M. Ashour, A. Asaithamby, H. Liang, C. Xing, Z. Lu, C.C. Zhang, H.A. Sadek, Hypoxia fate mapping identifies cycling cardiomyocytes in the adult heart, Nature 523 (2015) 226–230.
[103] Y. Nakada, D.C. Canseco, S. Thet, S. Abdisalaam, A. Asaithamby, C.X. Santos, A.M. Shah, H. Zhang, J.E. Faber, M.T. Kinter, L.I. Szweda, C. Xing, Z. Hu, R.J. Deberardinis, G. Schiattarella, J.A. Hill, O. Oz, Z. Lu, C.C. Zhang, W. Kimura, H.A. Sadek, Hypoxia induces heart regeneration in adult mice, Nature 541 (2017) 222–227.
[104] W. Tong, F. Xiong, Y. Li, L. Zhang, Hypoxia inhibits cardiomyocyte proliferation in fetal rat hearts via upregulating TIMP-4, Am J Physiol Regul Integr Comp Physiol 304 (2013) R613–R620.
[105] W. Tong, Q. Xue, Y. Li, L. Zhang, Maternal hypoxia alters matrix metalloproteinase expression patterns and causes cardiac remodeling in fetal and neonatal rats, Am. J. Physiol. Heart Circ. Physiol. 301 (2011) H2113–H2121.
[106] J.D. Anderson, B. Honigman, The effect of altitude-induced hypoxia on heart disease: do acute, intermittent, and chronic exposures provide cardioprotection? High Alt. Med. Biol. 12 (2011) 45–55.
[107] M. Burtscher, Effects of living at higher altitudes on mortality: a narrative review, Aging Dis. 5 (2014) 274–280.
[108] D. Faeh, F. Gutzwiller, M. Bopp, G. Swiss National Cohort Study, Lower mortality from coronary heart disease and stroke at higher altitudes in Switzerland, Circulation, 120 (2009) 495–501.
[109] G. Parati, P. Agostoni, B. Basnyat, G. Bilo, H. Brugger, A. Coca, L. Festi, G. Giardini, A. Lironcurti, A.M. Luks, M. Maggiorini, P.A. Modesti, E.R. Swenson, B. Williams, P. Bartsch, C. Torlasco, Clinical recommendations for high altitude exposure of individuals with pre-existing cardiovascular conditions: A joint statement by the European Society of Cardiology, the Council on Hypertension of the European Society of Cardiology, the European Society of Hypertension, the International Society of Mountain Medicine, the Italian Society of Hypertension and the Italian Society of Mountain Medicine, Eur Heart J, 39 (2018) 1546–1554.
[110] T.V. Serebrovskaya, L. Xi, Intermittent hypoxia training as non-pharmacologic therapy for cardiovascular diseases: practical analysis on methods and equipment, Exp Biol Med (Maywood) 241 (2016) 1708–1723.
[111] J.J. Savla, B.D. Levine, H.A. Sadek, The effect of hypoxia on cardiovascular disease: friend or foe? High Alt. Med. Biol. 19 (2018) 124–130.
[112] B. Losse, S. Schuchhardt, N. Niederle, The oxygen pressure histogram in the left ventricular myocardium of the dog, Pflugers Arch. 356 (1975) 121–132.
[113] W. Kimura, Y. Nakada, H.A. Sadek, Hypoxia-induced myocardial regeneration, J. Appl. Physiol. 123 (2017) (1985) 1676–1681.
[114] F.B. Engel, M. Schebesta, M.T. Keating, Anillin localization defect in cardiomyocyte binucleation, J. Mol. Cell. Cardiol. 41 (2006) 601–612.

ONLINE SUPPLEMENTARY DATA

Mice

All animal procedures were performed conform the guidelines from Directive 2010/63/EU of the European Parliament on the protection of animals used for research and are also in accordance with the recommendations of the U.S. National Institutes of Health Guide for the Care and Use of Laboratory Animals (National Institutes of Health publication 86-23, 2011). All our experiments were approved by the Swiss animal welfare authorities (authorizations VD3096 and VD3211). C57BL/6 mice (Wild Type mice, WT) were bred in our animal facility. Myh6 MerCreMer mice (JAK-5657) and Tomato-EGFP mice (JAK-7576) were purchased from the Jackson Laboratory (Bar Harbor, Main, US). Heterozygous Myh6 MerCreMer/Tomato-EGFP adult mice are bred in our animal facility. Prior cell isolation, Myh6 MerCreMer/Tomato-EGFP pups were injected intraperitoneally with tamoxifen (1mg / 2g) 1 day after birth. Neonatal mice (0-2 days after birth) were used.

Primary culture of neonatal mouse cardiomyocytes

Cardiomyocytes were isolated from neonatal C57BL/6 and heterozygous Myh6 MerCreMer/Tomato-EGFP mice as previously described (227).

Cardiomyocyte cultures were performed in two different oxygen conditions: at 20% O_2 in a standard incubator or in a hypoxia chamber (ref: 29829, Billups-Rothenberg hypoxic chamber, Stem Cell Technologies, Basel, Switzerland) flushed with 3% O_2/ 5% CO_2/ 92% N_2 (Carbagas, Lausanne, Switzerland). The oxygen concentration was controlled with an oxymeter (Stem Cell Technologies, Basel, Switzerland). The chamber was placed in a standard incubator at 37°C. Medium was replaced 2 times/week. Cytosine-β-D-arabinofuranoside (AraC, C1768 Sigma) was added during the first 7 days of culture (20 μM) to inhibit cell proliferation. After 7 days of culture, AraC was removed. Cardiomyocytes were cultivated in a 3:1 mixture of DMEM and Medium 199 (Invitrogen Corp, San Diego, CA, USA) supplemented with 10% horse serum (Oxoid), 5% fetal bovine serum (FBS) (Invitrogen), 10 mM Hepes, 100 U/ml penicillin G, and 100 microg/ml streptomycin. For each experiment, 5 x 10^5 cardiomyocytes were plated per well (1.9 cm^2). Immunohistochemistry as well as quantitative RT-qPCR were performed after 7 and 14 days of culture to compare the CM gene expression and structure in both oxygen conditions.

Immunohistochemistry

Cells were washed in PBS 1X and fixed in paraformaldehyde (2%) for 10 min at room temperature (RT). After permeabilization (0.3% Triton x-100 in PBS for 10min at RT) and blocking with 15% donkey serum (Vector Laboratories, Burlingame, CA) cells were stained with primary antibodies overnight at 4°C (**Supplemental Table 1**). The second day, cells were washed and coupled with secondary antibodies

were captured with fluorescent microscope (Nikon Eclipse TS100 and 90i). Images were processed with Adobe Photoshop CC2015.

Supplementary Table 1: Antibodies used for Immunohistochemistry.

Primary antibodies		
rabbit anti-Aurora B	1/1000	Abcam
rat anti-Ki67	1/1000	eBioscience
goat anti-Troponin I	1/100	Santa Cruz Biotechnology
Secondary antibodies		
donkey anti-rabbit Alexa 488	1/1000	Molecular Probes
donkey anti-rat Alexa 488	1/1000	Molecular Probes
donkey anti-goat Alexa 594	1/1000	Molecular Probes

Assessment of Cardiomyocyte size

CM cell area were measured after cardiac Troponin I stainings with the imageJ software.

Quantitative RT-PCR

Total RNA was isolated from CM cell cultures using the Trizol reagent (Invitrogen Corp, San Diego, CA, USA). cDNA was synthesized from RNA using PrimeScript RT with gDNA eraser reagent kit (Takara Bio Inc). Polymerase chain reactions (PCR) were performed using the SYBR Premix Ex Taq polymerase (Takara Bio Inc) with the ViiATM7 Instrument (Applied Biosystems). The primers used are listed in Supplementary Table 2. Results were obtained after 40 cycles of a thermal step protocol consisting of an initial denaturation 95°C (1s), followed by 60°C (20s) of elongation (α-skeletal actin has an elongation time of 30s at 60°C). All results were normalized with the 18S housekeeping gene (ΔCT values). Means of ΔΔCT (ΔCT 3%O_2 - ΔCT 20%O_2) values were calculated and results were represented as $2^{-\Delta\Delta CT}$. Statistics were performed on ΔΔCT individual values. SEM fold increase was calculated using $2^{-\Delta\Delta CT\ high\ values}$ - $2^{-\Delta\Delta CT}$ (226).

Supplementary Table 2: List of primers.

Gene	Forward primer	Reverse primer	Product size (bp)
ANF	ACAGGATTGGAGCCCAGAGC	GTCCATGGTGCTGAAGTTTATTC	337
c-kit	ATCTGCTCTGCGTCCTGTTG	CTGATTGTGCTGGATGGATG	108
Cyclin A2	ATGTCAACCCCGAAAAACTG	GCAGTGACATGCTCATCGTT	157
Cyclin B2	AGCTCCCAAGGATCGTCCTC	TGTCCTCGTTATCTATGTCCTCG	116
Cyclin E1	GAAAGAAGAAGGTGGCTCCGAC	GTTAGGGGTGGGGATGAAAGAG	190
Cyclin D1	TGAGAACAAGCAGACCATCC	TGAACTTCACATCTGTGGCA	71
Dab2	TGCTCGTGATGTGACAGACA	AGGGTCATTAGGGCCTCACT	225
Gata-4	CTGTCATCTCACTATGGGCA	CCAAGTCCGAGCAGGAATTT	259
α-MHC	AACCAGAGTTTGAGTGACAGAATG	ACTCCGTGCGGATGTCAA	130
β-MHC	ATGAGACGGTGGTGGGTTT	CTTTCTTTGCCTTGCCTTTG	117
Mlc-2v	GACCCAGATCCAGGAGTTCA	AATTGGACCTGGAGCCTCTT	163
Nkx2.5	CAAGTGCTCTCCTGCTTTCC	GTCCAGCTCCACTGCCTTCT	130
Runx1	GATGGCACTCTGGTCACCG	GCCGCTCGGAAAAGGACA	298
α -SKA	TGGACTTCGAGAATGAGATGG	TCGTCCTGAGGAGAGAGAGC	509
Troponin T	GCGGAAGAGTGGGAAGAGACA	CCACAGCTCCTTGGCCTTCT	127
18S	ACTTTTGGGGCCTTCGTGTC	GCCCAGAGACTCATTTCTTCTTG	96

Statistical analysis

All results were presented as means ± SEM. Statistical analyses were performed using the unpaired Student T test. The alpha level was 0.05.

References

1. Khalil H, Rosenblatt N, Liaudet L, and Widmann C. The role of endogenous and exogenous RasGAP-derived fragment N in protecting cardiomyocytes from peroxynitrite-induced apoptosis. *Free Radic Biol Med*. 2012;53(4):926-35.

2. Livak KJ, and Schmittgen TD. Analysis of relative gene expression data using real-time quantitative PCR and the 2(-Delta Delta C(T)) Method. *Methods*. 2001;25(4):402-8.

4.2. Brain Natriuretic Peptide (BNP) treatment on cardiomyocyte fate

4.2.1. Intraperitoneal BNP injections trigger cellular responses in CMs

Myocardial infarction (MI) was induced in 8 weeks-old adult mice by left anterior descending coronary artery (LAD) ligation. Intraventricular as well as intraperitoneal (i.p.) injections of BNP or NaCl were performed. Mice were sacrificed 1, 3 or 10 days after MI. The biological active form of BNP can bind on three receptors: NPR-A, NPR-B and NPR-C (171). The fixation on NPR-A and NPR-B leads to increased cGMP level and the activation of cGMP-dependent protein kinase (PKG) (171). Intracellular cGMP level could be decreased either by cGMP hydrolysis via phosphodiesterases (PDEs) or by the export of cGMP into the extracellular space via multidrug resistance proteins (i.e. MRP4 or MRP5) (176, 177). Thus, cGMP concentration was measured in the plasma of treated mice and the activation of the PKG was assessed by the determination of the phosphorylation of the phospholamban (PLB) protein.

In unmanipulated adult mice, cGMP concentration markedly increased one hour after BNP injection compared to saline mice (+725%, p=0.05) (Fig. 18A). One day after MI, BNP treatment led to an increased plasmatic concentration of cGMP (+636%, p=0.05) (Fig. 18A). Thus, the increased plasmatic cGMP level observed after BNP treatment can induce a response from many organs including the heart.

To confirm that BNP acts directly on heart and cardiac cells, the pPLB/PLB ratio was evaluated on proteins isolated from heart tissue. The pPLB/PLB ratio was increased in adult unmanipulated BNP-treated hearts compared to NaCl-treated hearts (+112%, p=0.04) (Fig. 18B). Furthermore, increased expression of the pPLB/PLB ratio was detected after BNP stimulation in infarcted hearts 10 days after surgery in ZI+BZ (+400%, p=0.008), but not in the RZ (Fig. 18B), demonstrating that i.p. BNP injection stimulates cardiac cells. In order to determine if BNP directly stimulates CMs, the ratio pPLB/PLB was assessed on CMs isolated from different areas of the injured hearts, 10 days after LAD ligation. After BNP injections, the pPLB/PLB ratio was increased in CMs isolated from the ZI+BZ (+230%, p=0.003) and decreased in CMs from the RZ (-66%, p=0.001) (Fig. 18C). These data suggest that BNP binds on NPR-A and/or NPR-B receptors and increases cGMP level, which stimulates PKG activity in CMs.

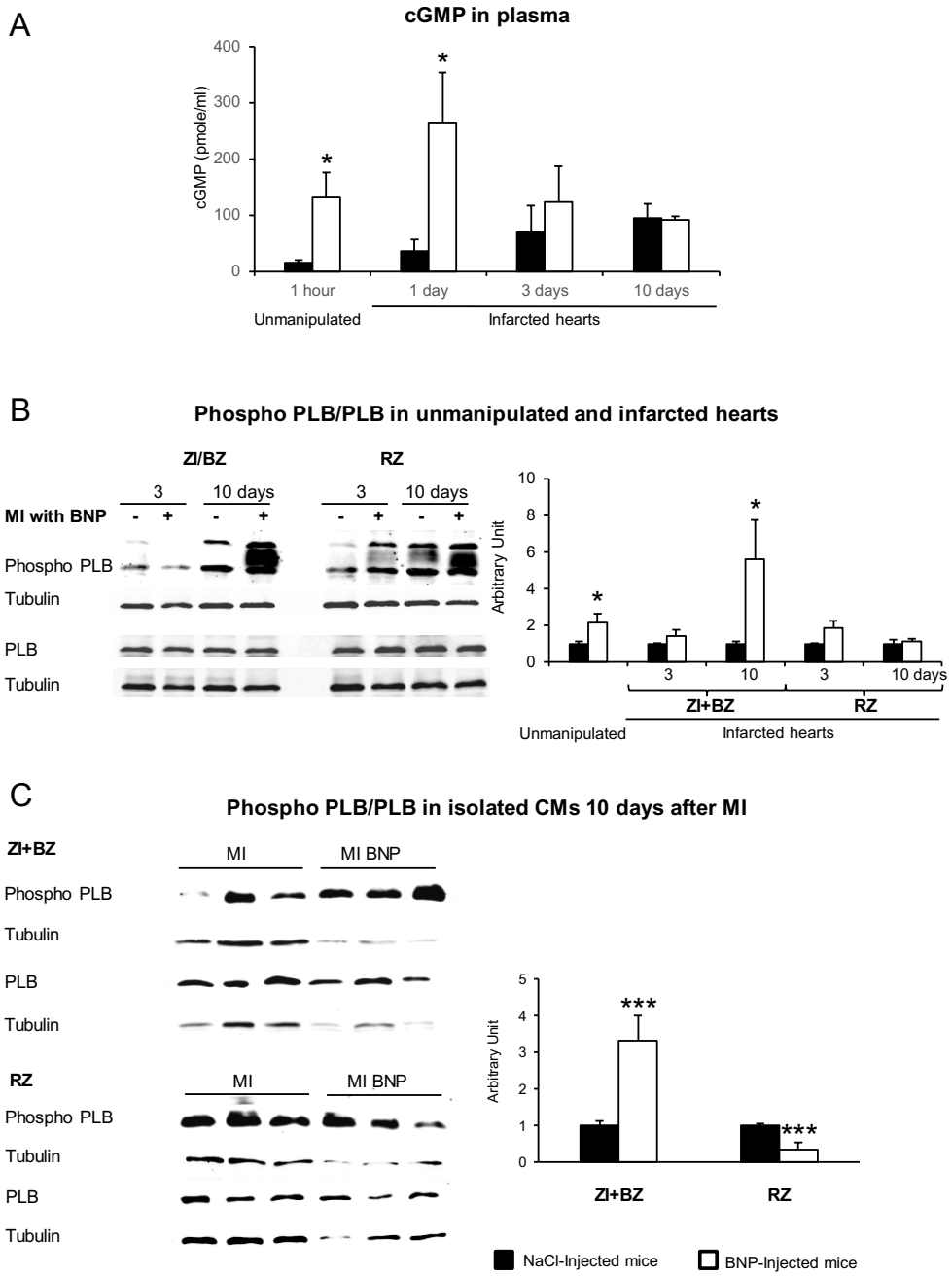

Figure 18: *BNP signaling is activated after BNP treatment in CMs after MI.* **A:** cGMP levels were measured in the plasma of adult mice treated with BNP or NaCl in unmanipulated and in injured hearts (1, 3 and 10 days after MI). n=4 mice per group. **B:** Representative western blots of unmanipulated and injured hearts 3 and 10 days after MI. Hearts were stimulated with BNP or NaCl. Graph on the right represents the quantification of the data issue from western blot analysis. Protein expression in BNP-treated hearts are related to the average of saline-treated hearts. n=5-8 mice per group. **C**: Representative western blots of isolated CMs 10 days after MI, stimulated with BNP or NaCl. Graph on the right represents the quantification of the data issue from western blot analysis. Protein expression in BNP-treated hearts are related to the NaCl-treated hearts of the same experiment. n=5 mice per group. **B-C:** Blots on the left were stained with antibodies against phospho phospholamban (pPLB), phospholamban (PLB) and Tubulin (used as loading control). Only the bands at the adequate molecular weight were represented here: pPLB between 21 and 26 kDa and PLB 25 kDa, Tubulin 55 kDa. For all results, data are mean ±SEM, *p≤0.05, ***p≤0.005.

To confirm the expression of the BNP receptors on CMs, immunohistofluorescence stainings (IHF) were performed on heart sections. Both receptors were expressed in adult CMs (Fig. 19A). Furthermore, FACS analysis on neonatal isolated CMs revealed that 28% of neonatal CMs expressed NPR-A and 21% expressed NPR-B (Fig. 19B-C).

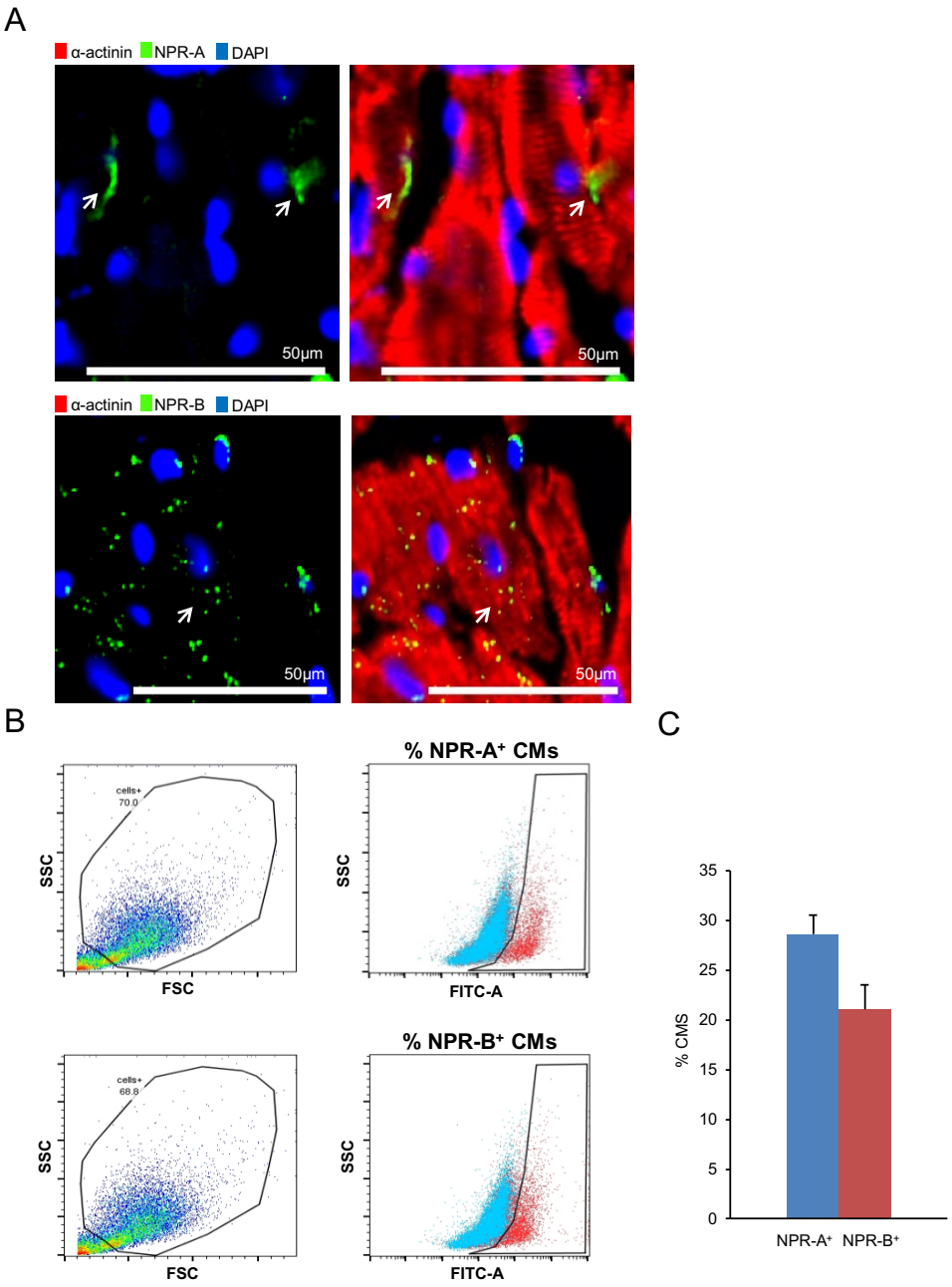

Figure 19: *Cardiomyocytes express the two natriuretic peptide receptors, NPR-A and NPR-B.* **A:** Representative pictures of the adult hearts stained with NPR-A or NPR-B (green) and α-actinin (red). White arrows represent NPR-A$^+$ or NPR-B$^+$ CMs. Each picture covered an area of 0.035mm^2. **B:** Representative flow cytometry dot plot graphs of isolated CMs from C57BL/6 neonatal hearts. **C:** Graph indicates the percentage of NPR-A$^+$ and NPR-B$^+$ CMs in neonatal CMs obtained from 6 different cell isolations.

4.2.2. BNP treatment leads to increased number of CMs after MI

To determine the role of BNP on CMs in pathological conditions, C57BL/6 mice were submitted to permanent LAD ligation and were sacrificed 1, 3, or 10 days after MI. One day after MI, the heart to body weight-ratio (i.e. cardiac mass) remained unchanged between BNP-treated mice and saline-injected mice (Fig. 20A). However, 3 and 10 days after MI, this ratio was significantly decreased in BNP-treated mice (-21% p=0.02; -20% p=0.007 respectively), demonstrating that BNP prevents the increase of the cardiac mass induced by MI (Fig. 20A).

As MI induced CM hypertrophy, we evaluated the BNP effect on CM hypertrophy. CM area as well as ANF mRNA level were evaluated 10 days after MI. After BNP treatment, cross-sectional CM area and the level of mRNA coding for ANF remained unchanged in all zones of the heart compared to saline-injected mice (Fig. 20B). Thus, BNP treatment has no effect on CM hypertrophy 10 days after MI.

In addition, mRNA levels coding for other cardiac genes were measured. In presence of BNP, the levels of mRNAs coding for GATA4 and cTnT increased significantly 10 days after MI in ZI (+70%, p=0.03 for both) (Fig. 20C). In BZ and RZ, no change was observed in hearts from BNP- and saline-treated mice 10 days after MI (data not shown). These results suggest that either BNP increased CM number or increased CM hypertrophy. Nevertheless, as no change in hypertrophy was detected, the next experiment aimed to quantify the number of CMs.

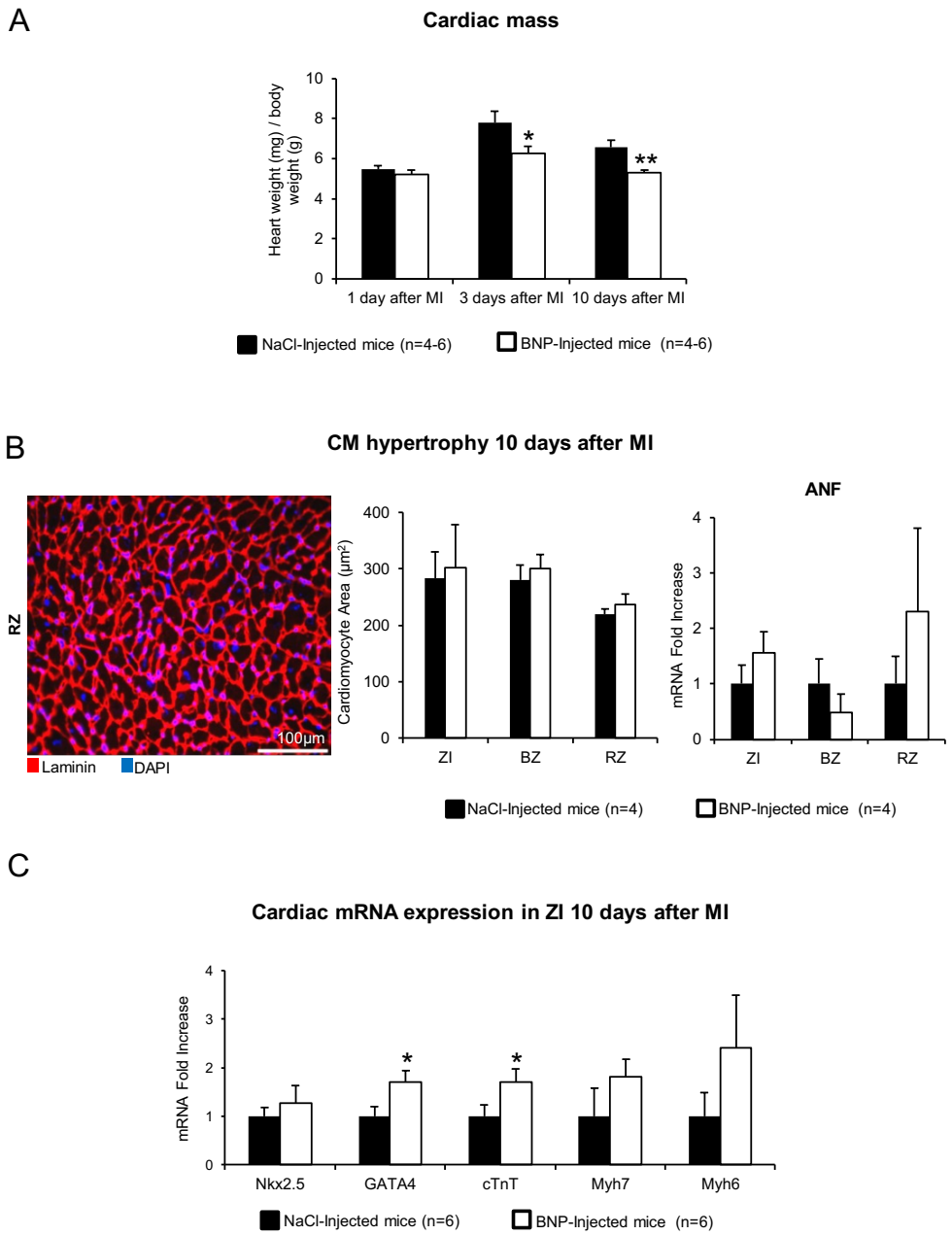

Figure 20: *BNP treatment prevents the increase of the cardiac mass induced by MI.* **A:** Graph represents the cardiac mass (heart/body weight ratio) 1, 3 and 10 days after MI of BNP-treated mice and saline-injected mice. **B:** Representative picture of RZ from injured heart stained with laminin (red) 10 days after MI. Picture covered a range of 0.016mm^2. Graph represents cross sectional area of CMs evaluated on heart sections in the three zones of injured heart (ZI, BZ, RZ) in BNP-treated mice and saline mice. Only CMs with circularity >0.5 are considered. At least 212 CMs in RZ, 219 CMs in BZ and 131 in ZI are counted. Graph on the right represents mRNA level coding for ANF 10 days after MI in BNP- and NaCl-treated mice. **C:** Graph represents mRNA levels coding for cardiac genes, 10 days after MI in the infarction zone of BNP- and NaCl-treated hearts. Results expressed as fold increase above the levels of saline-injected mice. For all results, data are mean ±SEM, *p≤0.05, p**≤0.01.

Therefore, CMs were isolated 10 days after MI from RZ, BZ and ZI by enzymatic digestion using a Langendorff-Free method (229) (Fig. 21A). The number of CMs and the expression of genes coding for the different cyclins and for cardiac genes were evaluated. Interestingly, ZI displayed an increase of the total number of CMs/heart in BNP-treated hearts related to saline-treated hearts (+156%, p=0.01), whereas in BZ and RZ, no change was observed regarding the number of CMs (Fig. 21B). The levels of mRNA coding for Myh7 and Myh6 were modulated in CMs isolated from the ZI+BZ (+90% p=0.05; -37% p=0.05 respectively) after BNP treatment (Fig. 21C). Furthermore, cyclin D2 mRNA expression slightly increased in BNP-treated CMs isolated from the same zone (+20%, p=0.06) (Fig. 21C). mRNA expression coding for cardiac and cell cycle genes remained unchanged in RZ after BNP treatment (Fig. 21D). As we provide evidence that BNP treatment increased CM number in ZI, the next step aimed to determine which mechanism triggers this effect: **CM cell death protection (4.2.2.1)** or **stimulation of CM regeneration (4.2.2.2)**.

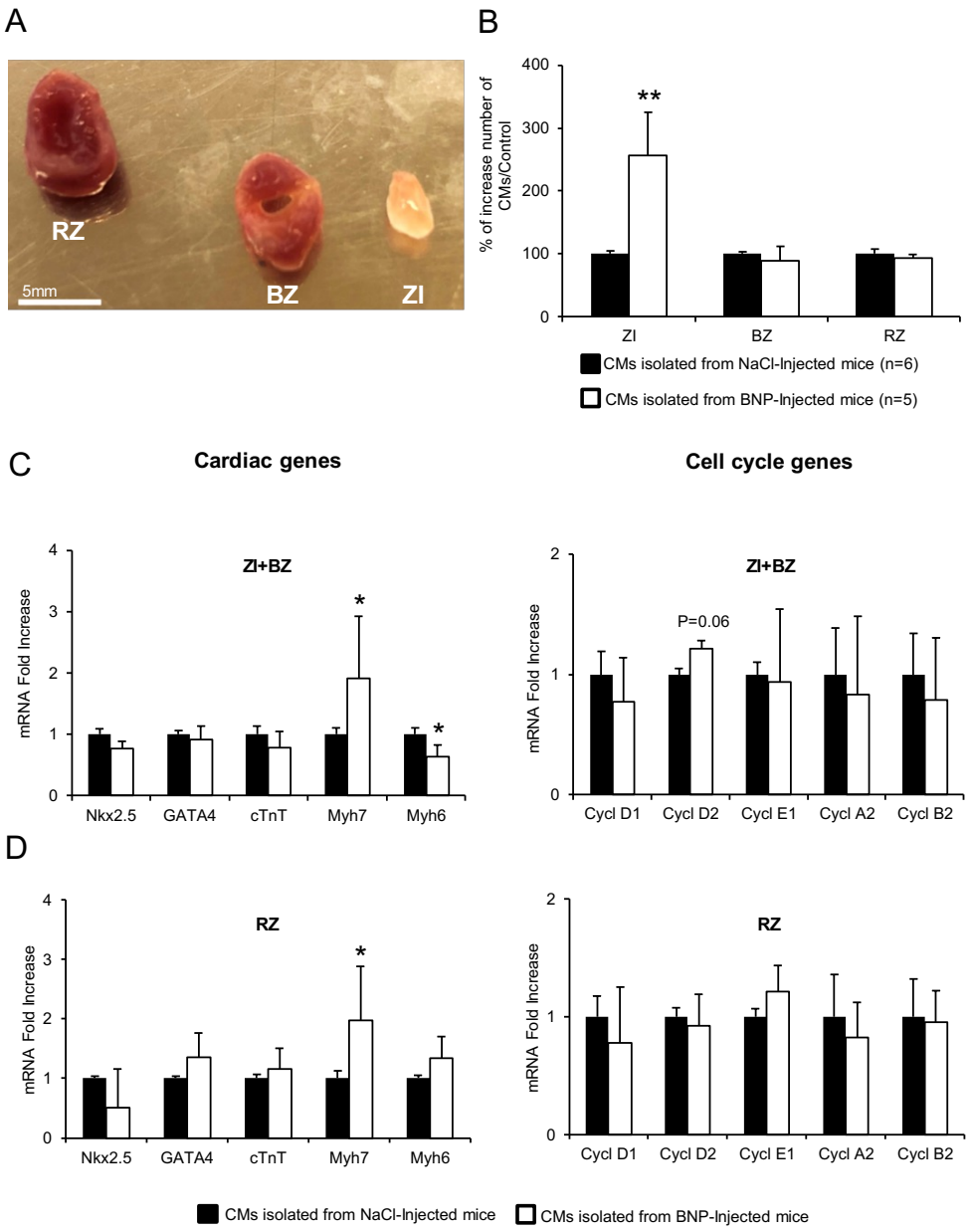

Figure 21: *The number of CMs increases in response to BNP stimulation after MI in the infarction zone.* **A**: Representative picture of the RZ, BZ and ZI zones of BNP-treated heart during CM isolation, 10 days after MI. Scale bar 5mm. **B:** The graph represents the total number of isolated CMs/area (ZI, BZ, RZ) 10 days after MI in BNP-treated mice related to saline mice. **C:** (Left) quantitative relative expression of mRNAs coding for cardiac genes and (right) cell cycle genes in CMs isolated from the ZI+BZ of infarcted hearts, 10 days after MI. **D:** (Left) quantitative relative expression of mRNAs coding for cardiac genes and (right) cell cycle genes in CMs isolated from RZ of infarcted hearts, 10 days after MI. **C-D:** Results expressed as fold increase above the levels in saline-injected mice. n=10 for saline-injected mice and n=7 for BNP-treated mice. For all results, data are mean ±SEM, *p≤0.05, **p≤0.01.

4.2.2.1. BNP promotes CM survival after MI

After myocardial infarction, cardiac cells, including CMs, undergo rapidly cell death (in the first 24 hours after MI) (3). CM cell death leads to the release of Troponin protein into the plasma.

BNP effect on CM cell death was studied 1 and 3 days after MI. Therefore, quantification of the cardiac Troponin concentration in the plasma of mice was performed to evaluate the level of CM cell death after MI. One day after MI, Troponin plasma level was reduced in the plasma of BNP-treated mice compared to the level measured in saline-injected mice (-67%, p=0.04) (Fig. 22A). The reduction of plasmatic Troponin level was preserved until 3 days after MI (-58%, p=0.1), suggesting that BNP protects CMs from cell death. The next experiment aimed to define whether the protection of BNP on CM cell death is mediated by an inhibition of apoptosis.

Western blots analysis were performed 1 day after MI on proteins isolated from the ZI, to measure the protein levels of cleaved-caspase 8 and caspase 3 as well as the ratio Bax/Bcl-2 (Fig. 22B). Interestingly, the protein level of cleaved-caspase 3 is decreased in BNP-treated hearts compared to saline-treated hearts in ZI (-33%, p=0.07), whereas the cleaved-caspase 8 and the ratio Bax/Bcl-2 remained unchanged (Fig. 22B). By contrast, the number of cleaved-caspase 3^+ CMs (determined by IHF) remained unchanged in hearts of BNP- and NaCl-treated mice in ZI (Fig. 22C). Considering all these results together, BNP protects CMs against cell death, likely by decreasing apoptosis. Nevertheless, we could not exclude that BNP protects also CMs from necrosis, necroptosis and/or autophagy.

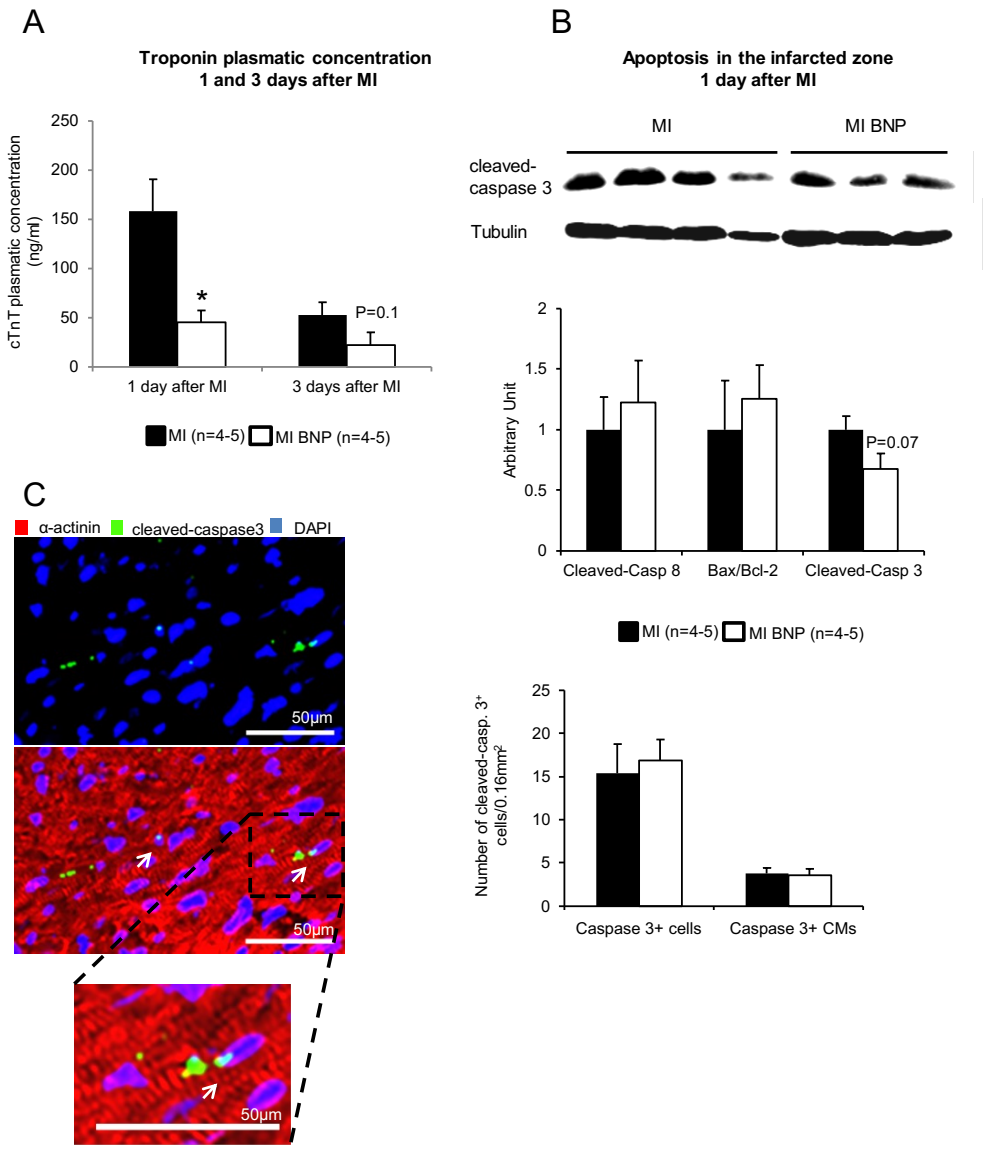

Figure 22: *BNP treatment protects CM from cell death 1 day after MI.* **A:** Graph represents the concentration of cardiac Troponin I in the plasma of BNP- and saline-treated hearts, 1 and 3 days after MI. **B:** Representative western blot of the infarction zone of BNP- and saline-treated hearts, 1 day after MI. Blot was stained with antibody against the cleaved-caspase 3. Only the bands at the adequate molecular weight were represented here: cleaved-caspase 3 12 kDa and Tubulin 55 kDa (used as loading control). Graph on the bottom represents the quantification of western blot analysis for the cleaved-caspase 8, the ratio Bax/Bcl-2 and the cleaved-caspase 3, in BNP-treated hearts related to saline hearts. **C:** Representative pictures of the heart stained with cleaved-caspase 3 (green) and α-actinin (red). White arrows represent cleaved-caspase 3^+ CMs. Graph on the right represents the total number of cardiac cells expressing cleaved-caspase 3 as well as the number of CMs expressing cleaved-caspase 3 in the infarction zone, one day after MI in BNP and saline mice. Picture covered a range of $0.016mm^2$. Positive cells are counted from at least 57 different pictures/group. Scale bars are 50µm. For all results, data are mean ±SEM, *p≤0.05.

4.2.2.2. BNP promotes CM re-entry into the cell cycle after MI

There are two main strategies to replace dying CMs: 1) the stimulation of CPC differentiation into CMs and 2) the stimulation of CM proliferation. In our study, both mechanisms were investigated in BNP-treated hearts. Mice were sacrificed 10 days after MI and we focused only on the infarction zone where the number of CMs increased after BNP treatment (Fig. 21B).

BNP stimulation on CPC differentiation was analyzed by using heterozygous Myh6-MerCreMer/Tomato-EGFP transgenic mouse model. 2 weeks after injection of one single dose of Tamoxifen, mice were submitted to LAD ligation and treated or not with BNP. BrdU was added to drinking water. Mice were sacrificed 10 days after surgery. IHFs against GFP and α-actinin on heart sections revealed three different CM cell populations: 1) GFP^+ $\alpha\text{-act}^+$ CMs represent pre-existing well-organized CMs 2) GFP^+ $\alpha\text{-act}^{+/-}$ CMs represent pre-existing dedifferentiated CMs and 3) GFP^- $\alpha\text{-act}^+$ CMs represent CMs originating from CPC differentiation and/or from a lack of recombination after Tamoxifen injection (Fig. 23A).

The number of GFP^+ $\alpha\text{-act}^{+/-}$ CMs and GFP^+ $\alpha\text{-act}^+$ CMs remained unchanged after BNP treatment compared to the number detected in saline-injected mice (Fig. 23B). By contrast, the number of GFP^- $\alpha\text{-act}^+$ CMs decreased significantly in BNP-treated hearts compared to saline mice (-57%, $p=0.02$) (Fig. 23B). This result suggests that either BNP decreases the capacity of CPCs to differentiate into CMs or that the recombination after Tamoxifen injection is lower in BNP-treated mice compared to saline mice. Furthermore, no increased number of CMs was observed after CM quantification on heart sections. This technic is clearly different from CM quantification after CM isolation. Indeed, by quantifying CMs after isolation, it was possible to determine the total number of CMs per heart, which is not the case with IHFs on heart sections.

To evaluate cell cycle activity, stainings against BrdU were performed on heart sections isolated from mice treated or not with BNP. The percentage of pre-existing GFP^+ CMs expressing BrdU (including GFP^+ $\alpha\text{-act}^{+/-}$ CMs and GFP^+ $\alpha\text{-act}^+$ CMs) increased significantly between BNP- and NaCl-treated mice (+17%, $p=0.03$) (Fig. 23C). Finally, BNP did not change the percentage of GFP^- $\alpha\text{-act}^+$ CMs expressing BrdU (Fig. 23D).

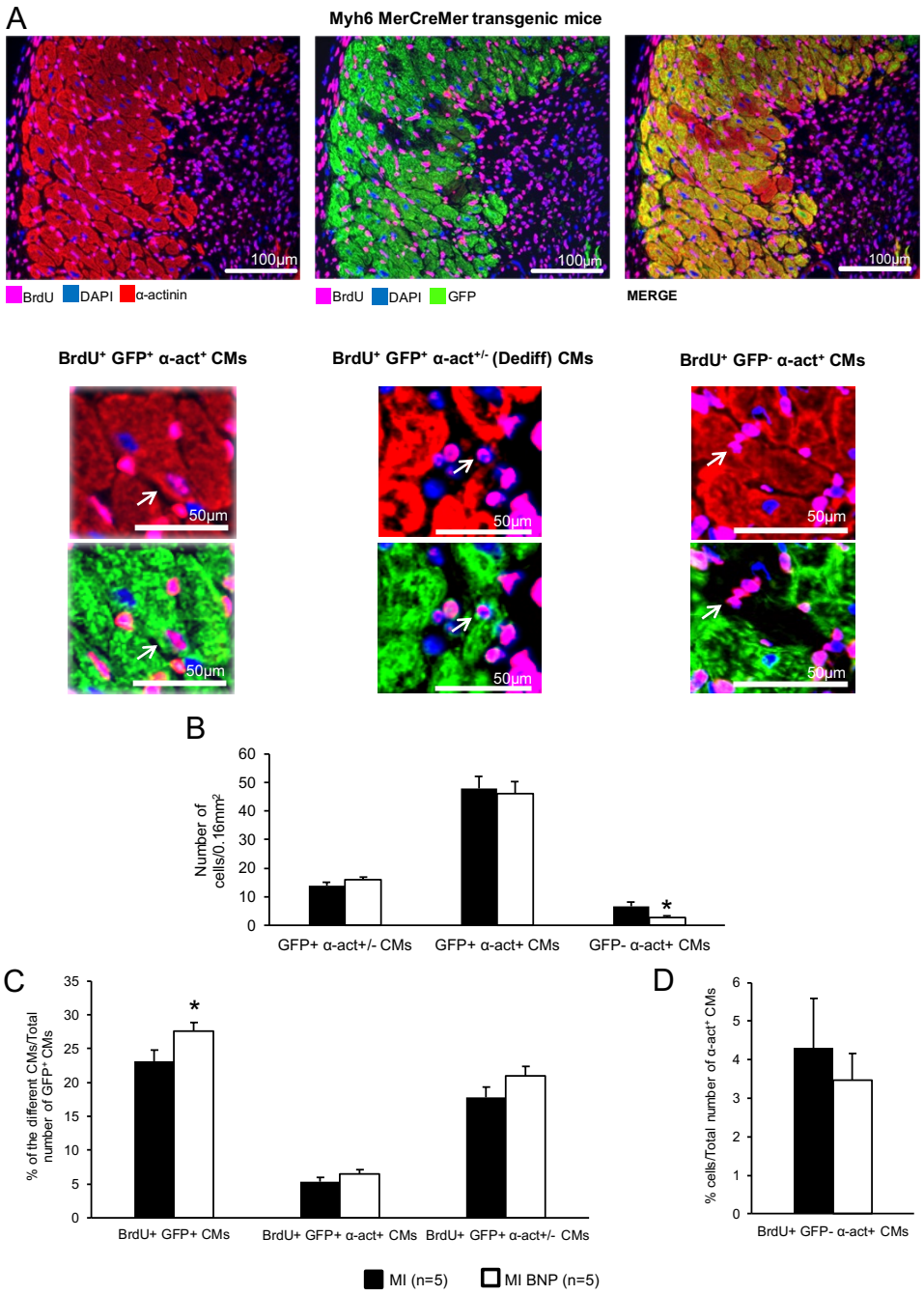

Figure 23: *BNP treatment increases the percentage of pre-existing BrdU⁺ CMs 10 days after MI, in the infarction zone.* **A:** Representative pictures of Myh6-MerCreMer transgenic heart sections of the infarction zone, 10 days after MI. Hearts were stained with α-actinin (red), GFP (green) and BrdU (dark red). Three different CM populations were observed: 1) GFP$^+$ α-act$^+$ CMs (representing pre-existing well-organized CMs), 2) GFP$^+$ α-act$^{+/-}$ CMs (representing pre-existing dedifferentiated CMs) and 3) GFP$^-$ α-act$^+$ CMs (representing CMs issue from CPC differentiation and/or from a lack of recombination). Pictures at the bottom represent the three CM populations expressing BrdU. White arrows depict CMs from each group. Scale bars represent 100 µm and for magnification 50 µm. **B:** Graph represents the number of GFP$^+$ α-act$^{+/-}$ CMs, GFP$^+$ α-act$^+$ CMs and GFP$^-$ α-act$^+$ CMs counted per heart sections, in BNP-treated mice and saline mice. **C:** Graph represents the percentage of CMs expressing BrdU in the three different CM groups related to the total number of GFP$^+$ CMs in BNP- and saline-treated mice. BrdU$^+$ GFP$^+$ CMs include well-organized CMs (α-act$^+$ CMs) and dedifferentiated CMs (α-act$^{+/-}$ CMs). **D:** Graph represents the percentage of CMs expressing BrdU originated from CPC differentiation (GFP$^-$ α-act$^+$ CMs) and/or from a lack of recombination. The number of cells is related to the total number of α-act$^+$ CMs. At least 2730 GFP$^+$ CMs and 2160 α-actinin$^+$ CMs are counted. For all results, data are mean ±SEM, *p≤0.05.

Thus, we demonstrated that BNP treatment did not increase the number of CMs originating from CPC differentiation 10 days after MI in ZI. However, BNP increased the percentage of pre-existing CMs expressing BrdU, suggesting that BNP stimulates pre-existing CM re-entry into the cell cycle after MI. Therefore, the next step is to determine whether BNP stimulates CM proliferation.

To study the role of BNP on CM proliferation, LAD ligations were performed on C57BL/6 hearts. Mice were sacrificed 3 and 10 days after MI. To investigate CM cell cycle activity, double immunostainings on heart sections against BrdU, Aurkb and α-actinin were conducted 3 and 10 days after MI. In the infarction zone, the number of CMs expressing BrdU and Aurkb increased significantly 3 and 10 days after MI in BNP-treated mice compared to the saline mice: 3 days after MI: BrdU +163% $p \leq 0.001$, Aurkb +66% $p=0.01$; 10 days after MI: BrdU +101% $p=0.001$, Aurkb +127% $p=0.008$ (Fig. 24).

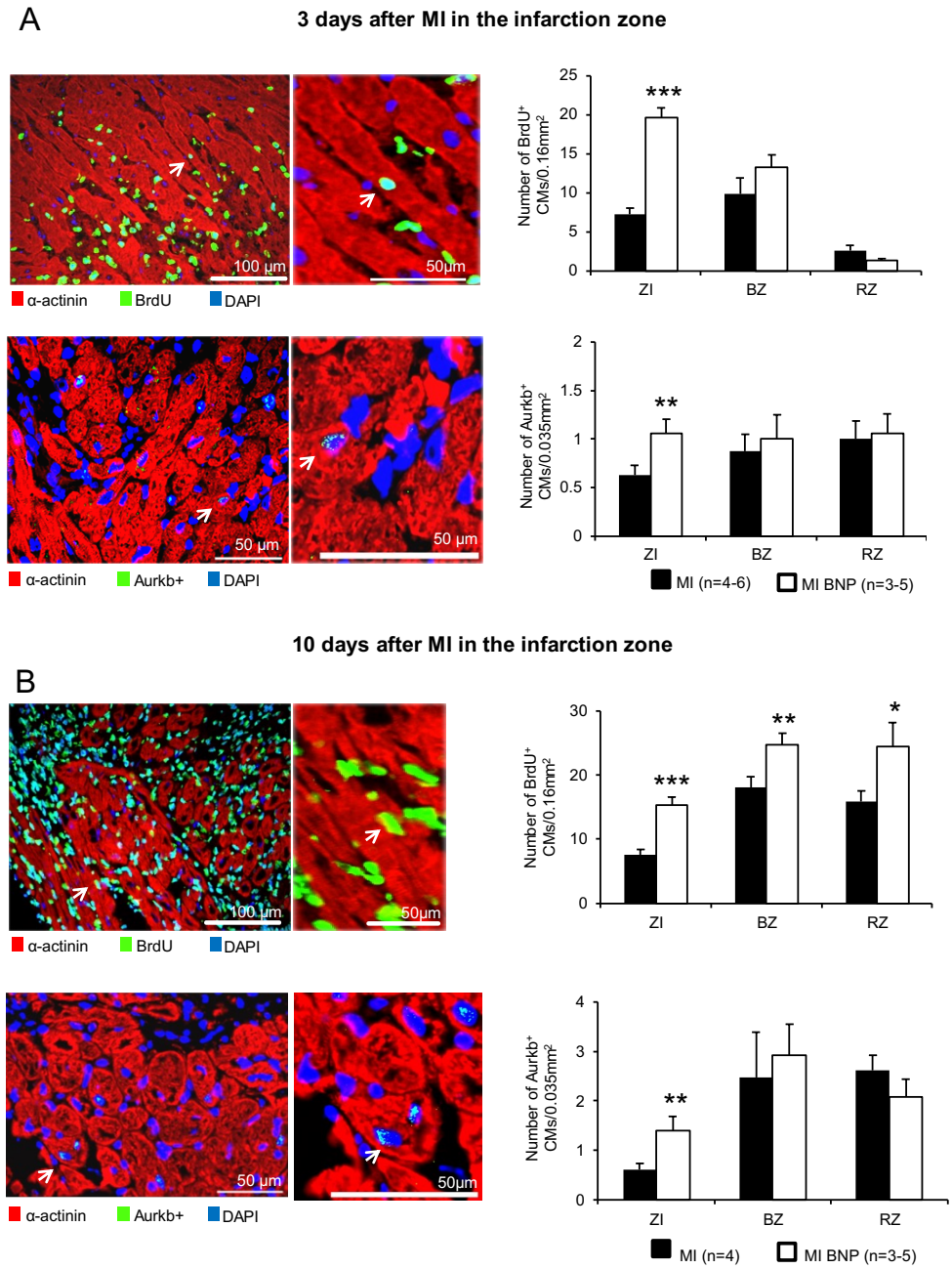

Figure 24: *BNP treatment increases the number of CMs expressing proliferative markers 3 and 10 days after MI in the infarction zone.* **A:** Representative pictures of C57BL/6 of heart sections 3 days after MI. **B:** Representative pictures of C57BL/6 of heart sections 10 days after MI. **A-B:** Heart sections are stained with BrdU (upper panel) or Aurkb (lower panel) in green and combined with α-actinin in red. White arrows show CMs expressing BrdU (at the top) or Aurkb (at the bottom). Graphs on the right represent the number of CMs expressing either BrdU or Aurkb, counted per heart sections at 3 and 10 days in BNP- and saline-treated mice. Scale bars for BrdU and α-actinin stainings are 100 µm and 50 µm for magnification. Scale bars for Aurkb and α-actinin stainings are 50 µm. Positive cells are counted 3 days after MI on at least 54 pictures for ZI, 20 pictures for BZ and 19 pictures for RZ. 10 days after MI, positive cells are counted on at least 50 pictures for ZI, 28 pictures for BZ and 27 for RZ. For all results, data are mean ±SEM, *p≤0.05 and, **p≤0.01, ***p≤0.005.

The increased number of CMs expressing proliferative markers in BNP-treated heart might be the consequence of cell death inhibition (increasing number of CMs) rather than CM proliferation. Thus, the numbers of CMs expressing proliferative markers were related to the total number of CMs, 10 days after MI. BNP treatment increased the percentage of CMs expressing BrdU, pH3 and Aurkb compared to saline mice in ZI (+90% p=0.01; +62% p=0.04; +400% p=0.03 respectively) (Fig. 25A-C). These results strongly suggest that BNP triggers CM proliferation after MI.

In order to distinguish between a real cell division from a binucleation, we focused in the next step on cytokinesis by using stainings against Aurkb. Only CMs expressing Aurkb were targeted in BNP- and NaCl-treated hearts. Interestingly, BNP treatment increased the percentage of CMs undergoing cytokinesis (+29%, p=0.05), whereas it tended to decrease the percentage of CMs undergoing binucleation (-50%, p>0.05) (Fig. 25D). Finally, the percentage of CMs undergoing the G2 phase (Aurkb localization into the nucleus) remained unchanged (Fig. 25D).

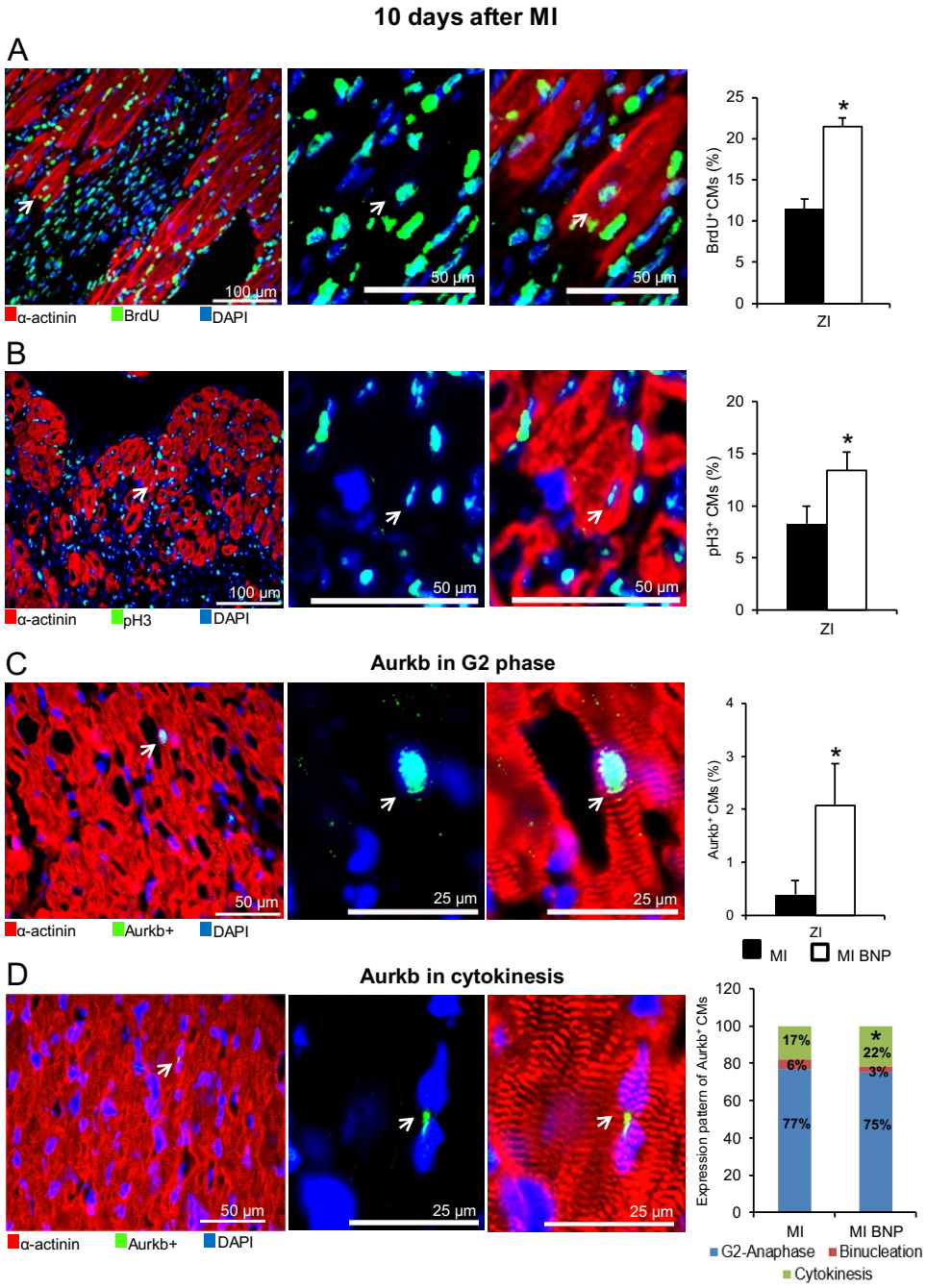

Figure 25: *BNP treatment increases the percentage of CMs expressing proliferative markers 10 days after MI in the infarction zone.* **A-D:** (Left) representative pictures of C57BL/6 of heart sections, 10 days after MI. Heart sections are stained with BrdU, pH3 and Aurkb (in green) and combined with α-actinin (in red). White arrows show CMs expressing BrdU, pH3 and Aurkb in G2 phase (C) or in cytokinesis (D). **A-C**: Graphs on the right represent the percentage of CMs expressing BrdU, pH3 or Aurkb (including G2 phase and cytokinesis) in BNP- and saline-treated mice. **D:** Graph on the right represents the percentage of CMs in the different phases of the cell cycle calculated by relating the number of CMs in cytokinesis, binucleation and G2 phase to the total number of CMs expressing Aurkb in BNP- and NaCl-treated hearts. At least 3650 CMs for BrdU, 3525 CMs for pH3 and 1072 CMs for Aurkb are counted for each group. MI and MI BNP n=5-6 mice per group. Scale bars are 100 µm, 50 µm or 25 µm. For all results, data are mean ±SEM, *p≤0.05.

These results confirm that in the infarction zone, BNP stimulates CM re-entry after MI. In addition, the cyclin D2 mRNA level increased (Fig. 21C), suggesting that BNP drives CMs to re-enter the cell cycle in the G1/S phase.

Finally, the process of CM cell cycle re-entry was not linked with CM dedifferentiation. In fact, the number of dedifferentiated CMs observed in BNP- and NaCl-treated Myh6-MerCreMer transgenic mice (Fig. 23B) remained unchanged. In addition, the levels of mRNAs coding for dedifferentiated genes (Nkx2.5, cTnT, Myh6, Myh7, Runx1, Dab2 and α-SKA) were stable between BNP-treated mice and saline-injected mice (data not shown).

In the next section, in order to investigate whether BNP stimulates the proliferation of CMs, we tested BNP on neonatal hearts which exhibit full potential of regeneration until 7 days after birth thanks to the natural capacity of neonatal CMs to proliferate (60).

4.2.3. BNP treatment leads to increased number of CMs in neonatal mice

Neonatal mice, 3 days after birth, were i.p. injected every 2 days with BNP or NaCl. BrdU was also i.p. injected on days 5 and 9 after birth. Mice were sacrificed 11 days after birth and CMs were isolated by enzymatic digestion using the Langendorff-Free method (229).

No variation of the cardiac mass was detected between BNP- and saline-treated mice (Fig. 26A). However, the total number of CMs/heart increased by 25% in BNP-treated mice ($p=0.005$) (Fig. 26B). Interestingly, the expressions of mRNA coding for cyclin E1 (+100%, $p=0.01$), A2 (+126% $p=0.002$) and B2 (+70%, $p=0.04$) were increased in CMs isolated from BNP-treated mice (Fig. 26C). Finally, the percentage of mononucleated CMs increased (+11%, $p=0.01$), whereas the percentage of binucleated CMs decreased (-8%, $p=0.01$) in BNP-treated hearts compared to NaCl-treated hearts (Fig. 26D).

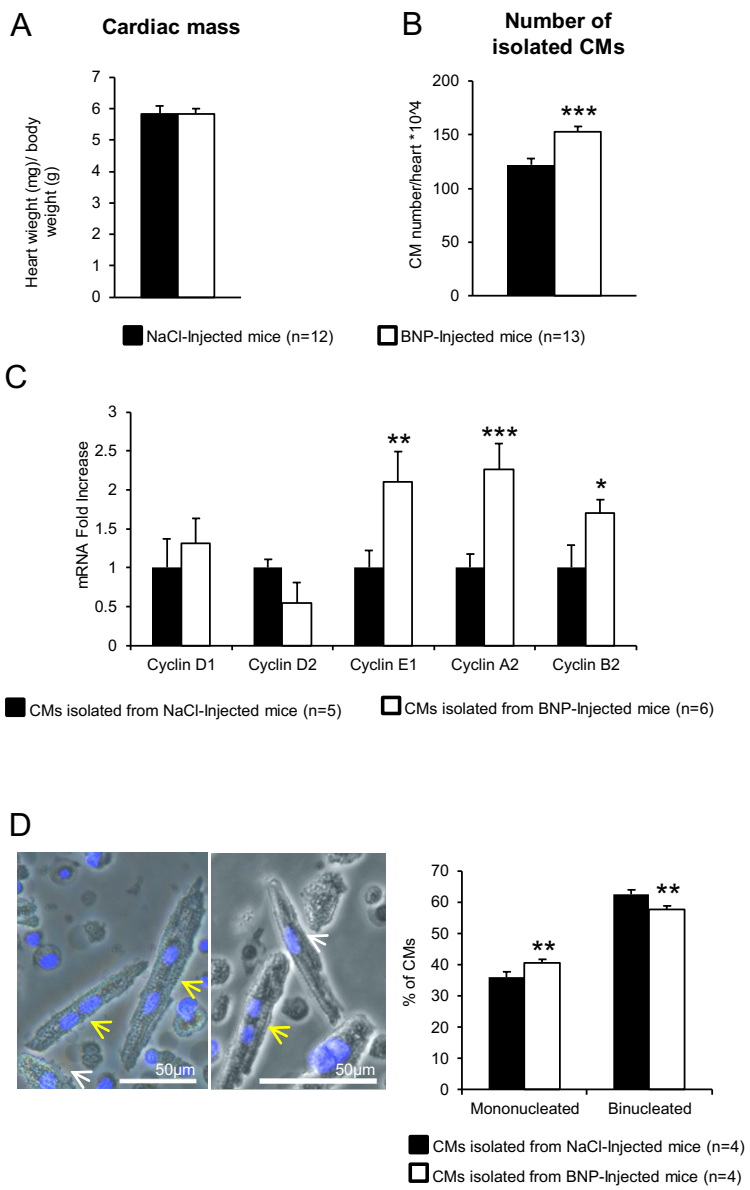

Figure 26: *BNP treatment leads to increased CM number in neonatal mice.* **A:** Cardiac mass (heart/body weight ratio) of BNP- and saline-injected mice. **B:** Total number of CMs/heart isolated from BNP- and NaCl-treated mice. **C:** mRNA expression coding for cyclins D1, D2, E1, A2 and B2 genes in isolated CMs. Results expressed as fold increase above the levels in CMs isolated from saline mice. **D:** Representative pictures of isolated CMs stained with DAPI. White arrows highlight mononucleated CMs and yellow arrows binucleated CMs. Graph on the right demonstrates the percentage of mono- and binucleated CMs in BNP- and saline-treated mice. At least, 1407 CMs are counted for both groups. For all results, data are mean ±SEM, *p≤0.05 and, **p≤0.01, ***p≤0.005.

4.2.3.1. BNP stimulates CM proliferation in neonatal hearts

To investigate whether BNP stimulates neonatal CM proliferation, IHF stainings against proliferative markers were performed on neonatal mouse heart sections. BNP treatment increased the number of CMs expressing BrdU (+21%, p=0.04), pH3 (+30%, p=0.04) and Aurkb (+47%, p=0.001) compared to saline-treated mice (Fig. 27A and C; Fig. 28B respectively). By contrast, the number of CMs expressing Ki67 remained unchanged (Fig. 27B).

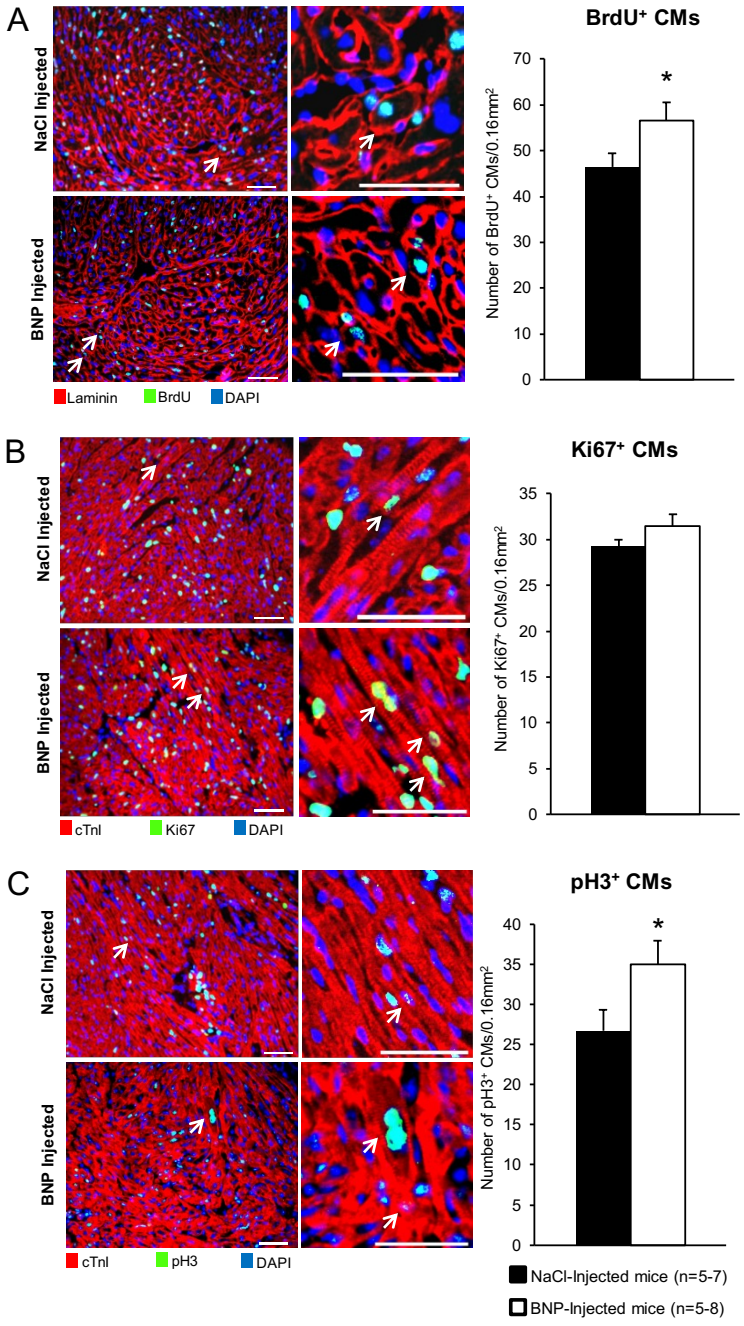

Figure 27: *BNP treatment increases the number of CMs expressing proliferative markers in neonatal hearts.* **A-C:** Representative pictures of neonatal hearts isolated from mice injected with BNP or saline and stained with BrdU, Ki67 or pH3 (green) combined with laminin for BrdU and cTnI for Ki67 or pH3 (red). White arrows and magnification on the left represent BrdU⁺, Ki67⁺ and pH3⁺ CMs. Graphs on the right represent the number of BrdU⁺, Ki67⁺ and pH3⁺ CMs counted per heart sections in BNP-treated mice and NaCl-injected mice. Each picture covers a range of 0.16mm² and the scale bar corresponds to 50µm. Positive cells are counted on at least 44 different pictures/group. For all results, data are mean ±SEM, *p≤0.05.

To distinguish between cytokinesis and binucleation, Aurkb and cTnI stainings were performed and only CMs expressing Aurkb were targeted in BNP- and NaCl-treated hearts. BNP-treated mice increased the percentage of CMs undergoing cytokinesis (+23%, $p>0.05$), while the percentage of CMs undergoing binucleation tended to decrease (-31%, $p>0.05$) (Fig. 28C). The percentage of CMs undergoing G2/M phase remained unchanged between BNP- and saline-treated mice (Fig. 28C). We also observed CMs where both nuclei (mother and daughter nuclei) are less than 5µm from each other and which express Ki67, signal of a real CM proliferation (Fig. 28A) (155).

Thus, all these results suggest that BNP stimulates CM proliferation in neonatal mice. Next, we analyzed whether dedifferentiation is required for CM proliferation. RT-qPCR analysis revealed no variation of the levels of mRNAs coding for dedifferentiated genes in CMs isolated from BNP and saline-injected mice (Fig. 28D). However, some CMs expressing proliferative markers might be dedifferentiated as shown in Figure 28D, suggesting that CMs during the cell cycle could naturally dedifferentiate in neonatal hearts.

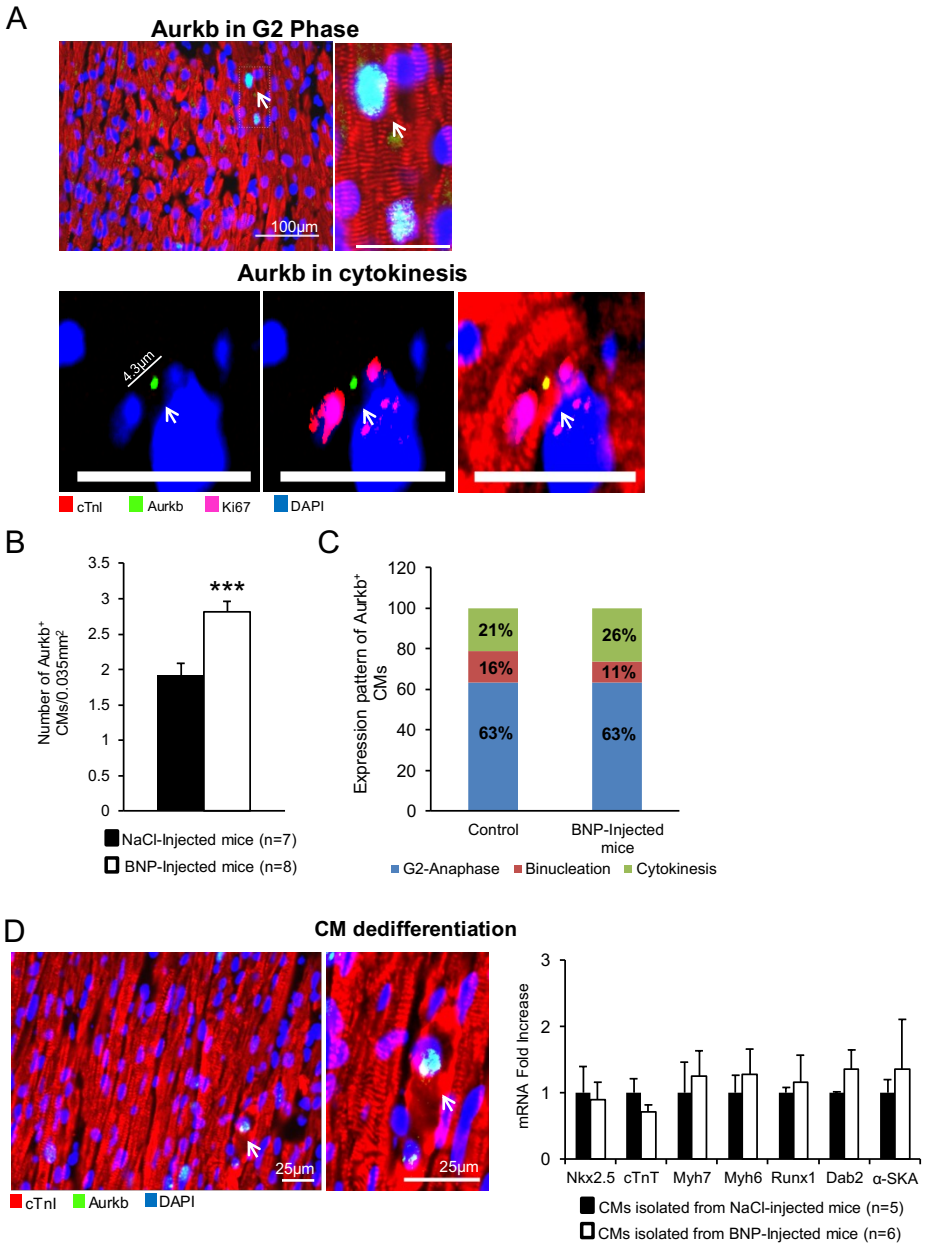

Figure 28: *BNP treatment stimulates CM proliferation in neonatal hearts.* **A:** Representative pictures of neonatal hearts stained with Aurkb (green) and cTnI (red). (Upper panel)-pictures and white arrows correspond to Aurkb$^+$ CMs in G2 phase. (Bottom panel)-pictures and white arrows represent CMs expressing Aurkb and Ki67 in cytokinesis in BNP-treated heart. The distance between both nuclei is less than 5µm, corresponding to a real CM cell division. Scale bar at the top indicates 50µm for magnification and on the bottom indicates 25µm. **B:** Number of Aurkb$^+$ CMs (including G2 phase, cytokinesis and binucleation) in BNP- and NaCl-treated mice. **C:** The percentage of CMs in the different phases of the cell cycle is obtained by relating the number of CMs in cytokinesis, binucleation and G2 phase to the total number of CMs expressing Aurkb in BNP- and NaCl-treated hearts. Each picture covered a range of 0.035mm^2. For all results, positive cells were counted from at least 123 different pictures/group. At least 300 Aurkb$^+$ CMs are evaluated to determine the expression pattern in each group. **D:** Representative pictures of double staining against Aurkb (in green) and cTnI (in red). White arrow represents dedifferentiated CM expressing Aurkb. Graph on the right represents the level of mRNA expression coding for genes involved in dedifferentiation in isolated CMs. Results expressed as fold increase above the levels in CMs isolated from saline mice. Data are mean ±SEM ***p≤0.005.

4.2.3.2. BNP stimulates also neonatal CM proliferation *in vitro*

To validate the direct effect of BNP on CM proliferation, CMs were isolated from neonatal mouse hearts (1-2 days old), cultured for 14 days (7 days with AraC and 7 days without AraC) and treated with BNP or NaCl.

We have previously demonstrated that 3% O_2 environment stimulates CM proliferation, CM dedifferentiation as well as an increase of the number of dedifferentiated CMs (see section 4.1). To determine whether BNP treatment can be studied at 3% O_2, we evaluated the expression of BNP receptors on CMs. Therefore, the expressions of mRNAs coding for NPR-A or NPR-B were compared in CMs cultured at 3% or 20% O_2. After 7 days of culture, no variation of NPR-A and NPR-B mRNA expression was observed between both oxygen conditions, whereas after 14 days, the level of NPR-B mRNA was significantly increased at 3% O_2 (+127%, p=0.03) (Fig. 29). Since 3% O_2 did not decrease the expression of NPR-A and NPR-B, all experiments aimed to establish BNP effect on CMs *in vitro,* were performed at 3% O_2.

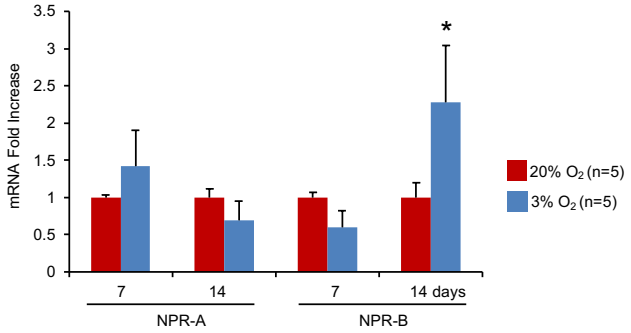

Figure 29: *NPR-A and NPR-B mRNA expression at 3 and 20% O_2.* Graph represents mRNA level coding for NPR-A and NPR-B receptors in cultured neonatal CMs after 7 and 14 days of culture in 20 % and 3% oxygen. Results in 3% oxygen expressed as fold increase compared to the receptors levels in 20% oxygen. For all results, data are mean ±SEM, *p≤0.05.

Three different BNP concentrations were tested to determine whether BNP is able to induce CM proliferation *in vitro*. A study from Becker demonstrated the importance of the natriuretic peptide concentration *in vitro* (195). Indeed, the potential of ANP to induce CM proliferation was dependent on its concentration: High level of ANP (1000nM) decreased CM proliferation, while a low level of ANP (10nM) stimulated CM proliferation (195). Therefore, we tested three different concentrations of BNP: 10, 100 and 1000nM.

After 14 days of culture, low concentration of BNP (10nM) increased the number of CMs compared to untreated cells (+21%, p=0.03) (Fig. 30B). CM size decreased (with 10 and 100nM of BNP) when compared to untreated cells (-10% p=0.03 and

-14% p=0.002, respectively) (Fig. 30C). Regarding the expression of mRNAs coding for cyclins D1 and D2, both increased after BNP treatment (+31%, p=0.04; +25%, p=0.05 respectively) (Fig. 30D), suggesting that BNP stimulates cyclin D1 and D2 expression and drives CMs to re-enter the cell cycle in the G1/S phase. Finally, the number of binucleated CMs decreased with BNP treatment at 10nM (-32%, p=0.01) (Fig. 30E).

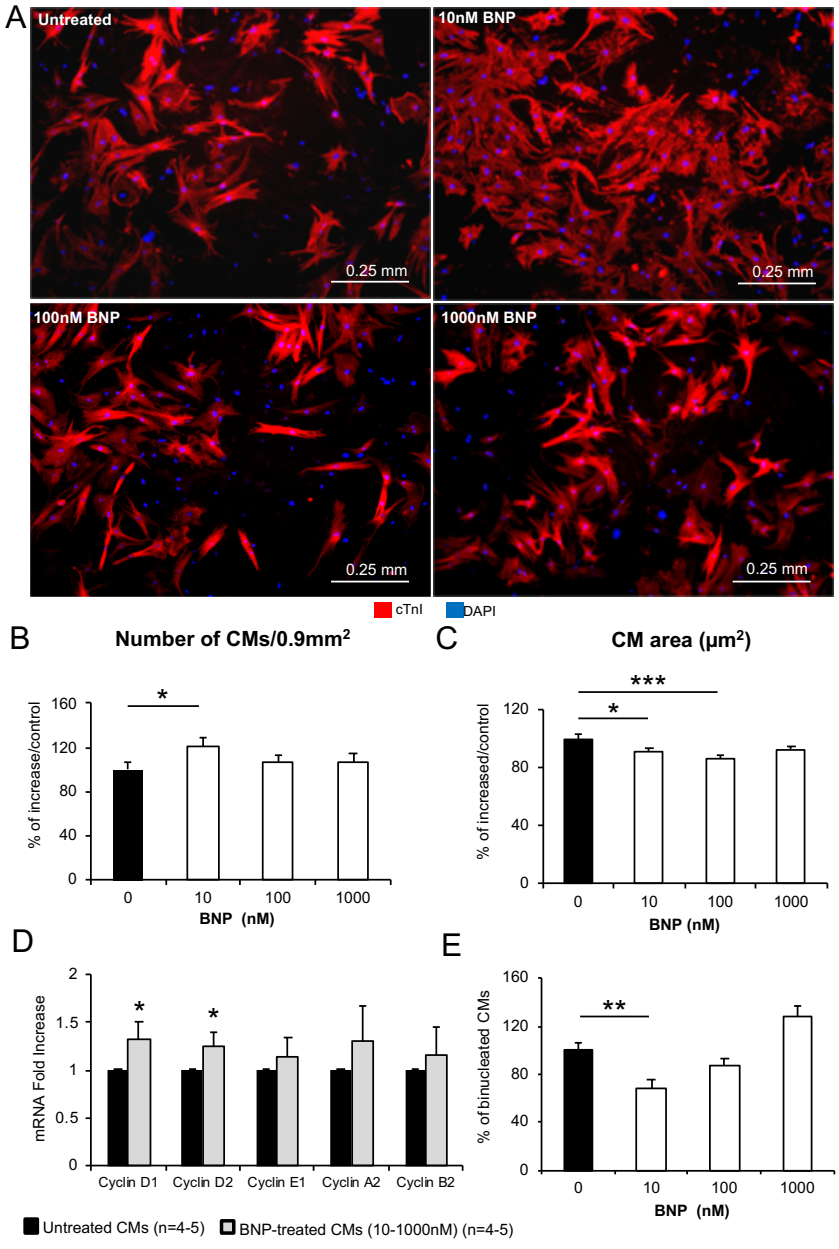

Figure 30: *14 days after the onset of culture, low concentration of BNP increases the number of neonatal CMs.* **A:** Representative pictures of 14 days old CM cell culture with or without BNP treatment (10, 100 and 1000nM). Cells were stained with antibody against cTnI (red). **B:** Total number of CMs/0.9mm² treated with 10, 100 and 1000nM BNP and related to the number of CMs in untreated cells. **C:** CM cell area in BNP-treated CM cell cultures and related to untreated CMs. **D:** mRNA expression coding for genes of cyclin D1, D2, E1, A2 and B2. Results expressed as fold increase above the levels in untreated CMs. **E:** Panel shows the percentage of binucleated CMs obtained by relating the number of binucleated CMs to the total number of CMs. At least, 2718 CMs are counted. For all results, data are mean ±SEM, *p≤0.05, **p≤0.01, ***p≤0.005.

To assess for CM proliferation, double immunostainings against Ki67, pH3, Aurkb and cTnI were performed. BNP treatment at low concentrations (10 and 100nM) increased the percentage of Ki67^{+}, pH3^{+} and Aurkb^{+} CMs compared to untreated CMs (Ki67: +19% p=0.03; pH3: +75% p=0.04, Aurkb: +59% p=0.01) (Fig. 31A-C). Furthermore, in the Aurkb^{+} CM cell population, the percentage of CMs undergoing cytokinesis increased (+80%, p=0.04) in presence of BNP, whereas the percentage of CMs undergoing binucleation tended to decrease (-25%, p>0.05) (Fig. 31D). Finally, the percentage of CMs undergoing G2 phase remained unchanged (Fig. 31D). All these results confirm that BNP stimulates CM proliferation in *in vitro* studies.

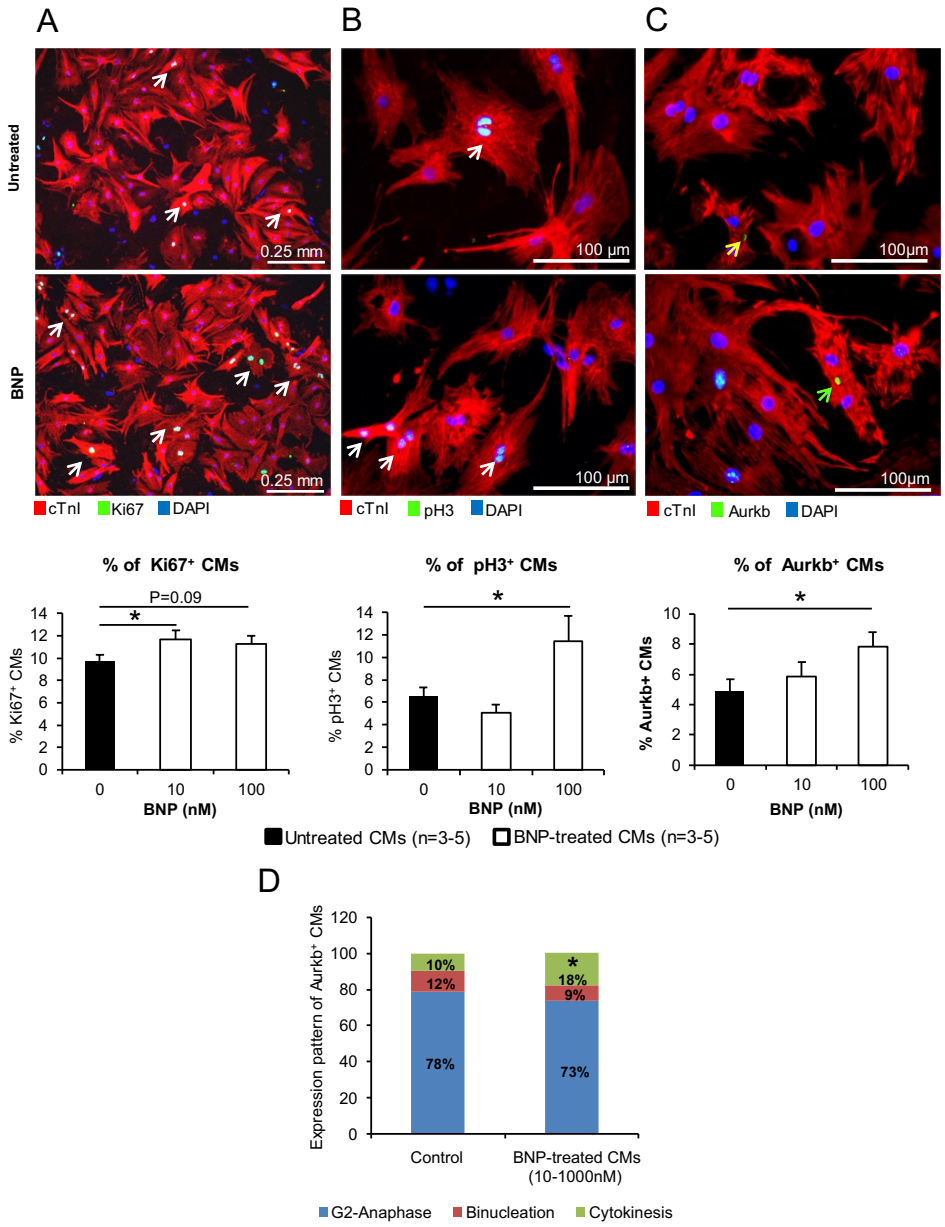

Figure 31: *BNP treatment at low concentration stimulates neonatal CM proliferation in vitro.* **A-C:** Representative pictures of immunostainings against Ki67, pH3 and Aurkb (in green) and cTnI (in red) in BNP-treated CMs (10 and 100 nM) and untreated CMs. On the panel A and B, white arrows correspond to the $Ki67^+$ or $pH3^+$ CMs. On the panel C, yellow arrow indicates binucleation and green arrow cytokinesis. Graphs below represent the percentage of $Ki67^+$, $pH3^+$ and $Aurkb^+$ CMs related to the total number of CMs (2350, 520, 809 CMs are counted respectively in both groups). **D:** The percentage of CMs in the different phases of the cell cycle is obtained by relating the number of CMs in cytokinesis, binucleation and G2 phase to the total number of CMs expressing Aurkb in BNP- and NaCl-treated cells. At least, 124 $Aurkb^+$ CMs are counted for each group. For all results, data are mean ±SEM *p≤0.05.

An association between BNP treatment and CM dedifferentiation was not clearly established *in vitro*. In fact, after 7 days of culture, mRNA expression coding for Runx1, Dab2 and Nkx2.5 were upregulated (+60%, p=0.04; +75%, p=0.1; +48%, p=0.03 respectively) in BNP-treated CMs compared to untreated CMs (Fig. 32A). However, no change in the expression of mRNAs coding for structural CM genes was observed (Fig. 32A). After 14 days of culture, the expression of mRNAs coding for dedifferentiated and structural CM markers as well as the percentage of dedifferentiated ($cTnI^{+/-}$) CMs remained unchanged in BNP-treated cells (Fig. 32).

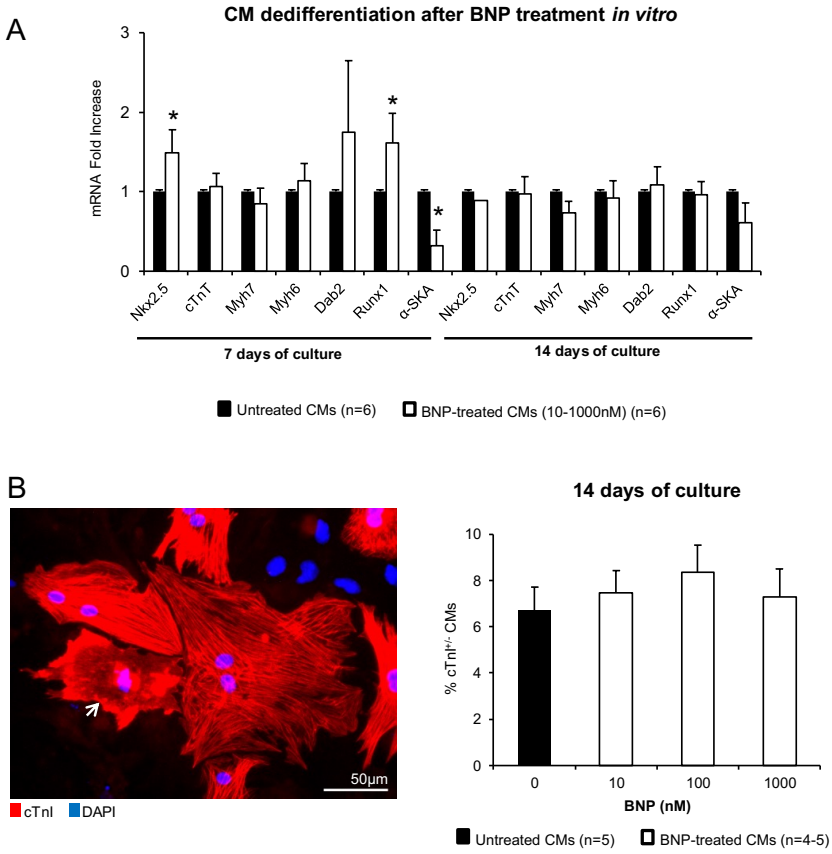

Figure 32: *BNP treatment has low impact on neonatal CM dedifferentiation.* **A:** Graph represents mRNA levels of genes coding for dedifferentiated markers in neonatal CMs after 7 and 14 days, treated with (10-1000nM) or without BNP. Results expressed as fold increase above the levels of untreated CMs. **B:** Representative picture of CM cell culture stained with cTnI (red) after 14 days of culture. White arrow represents a dedifferentiated CM ($cTnI^{+/-}$ CMs). Panel on the right indicates the percentage of dedifferentiated CMs, 14 days after the onset of culture. Scale bar represents 50µm. At least 819 CMs are counted. For all results, data are mean ±SEM, *p≤0.05.

To conclude, *in vitro* studies showed that neonatal CMs can dedifferentiate naturally (Fig. 32B, picture on the left). BNP treatment might stimulate CM dedifferentiation after 7 days of culture by re-expressing CM dedifferentiated genes, whereas after 14 days of culture no increased level of dedifferentiation was observed.

4.2.4. BNP treatment leads to increased number of CMs in unmanipulated adult mice

BNP stimulates neonatal CM proliferation *in vivo* and *in vitro*. We tested therefore the BNP effect on adult CMs, which exhibit a lower proliferative capacity than neonatal CMs. To determine if BNP treatment is able to stimulate CM proliferation in adult unmanipulated hearts, Myh6-MerCreMer transgenic mice were used. Mice were injected with Tamoxifen two weeks prior the first BNP injection. BNP was injected i.p. every 2 days during 14 days. Two weeks after the first BNP injection, mice were sacrificed and CMs were isolated by enzymatic digestion using the Langendorff-Free method, in order to determine the total number of CMs in BNP- and NaCl-treated hearts (Fig. 33A).

Cardiac mass remained unchanged between BNP- and saline-treated hearts (Fig. 33B). By contrast, BNP injection led to significant increase of the total number of CMs/heart compared to saline-injected mice (+25%, p=0.03) (Fig. 33C). mRNA expressions of cardiac genes, such as GATA4 (+55%, p=0.06), Myh6 (+77%, p=0.05) and ANF (69%, p=0.05), were upregulated in isolated adult CMs after BNP treatment (Fig. 33E). mRNA expression coding for the cyclin E1 (+32%, p=0.02) was also upregulated (Fig. 33F). The percentage of $BrdU^+$ CMs was increased (+40%, p=0.03) in BNP-treated mice compared to saline mice (Fig. 33F). Furthermore, the percentage of binucleated CMs slightly increased in BNP-treated mice (+14%, p>0.5) (Fig. 33D).

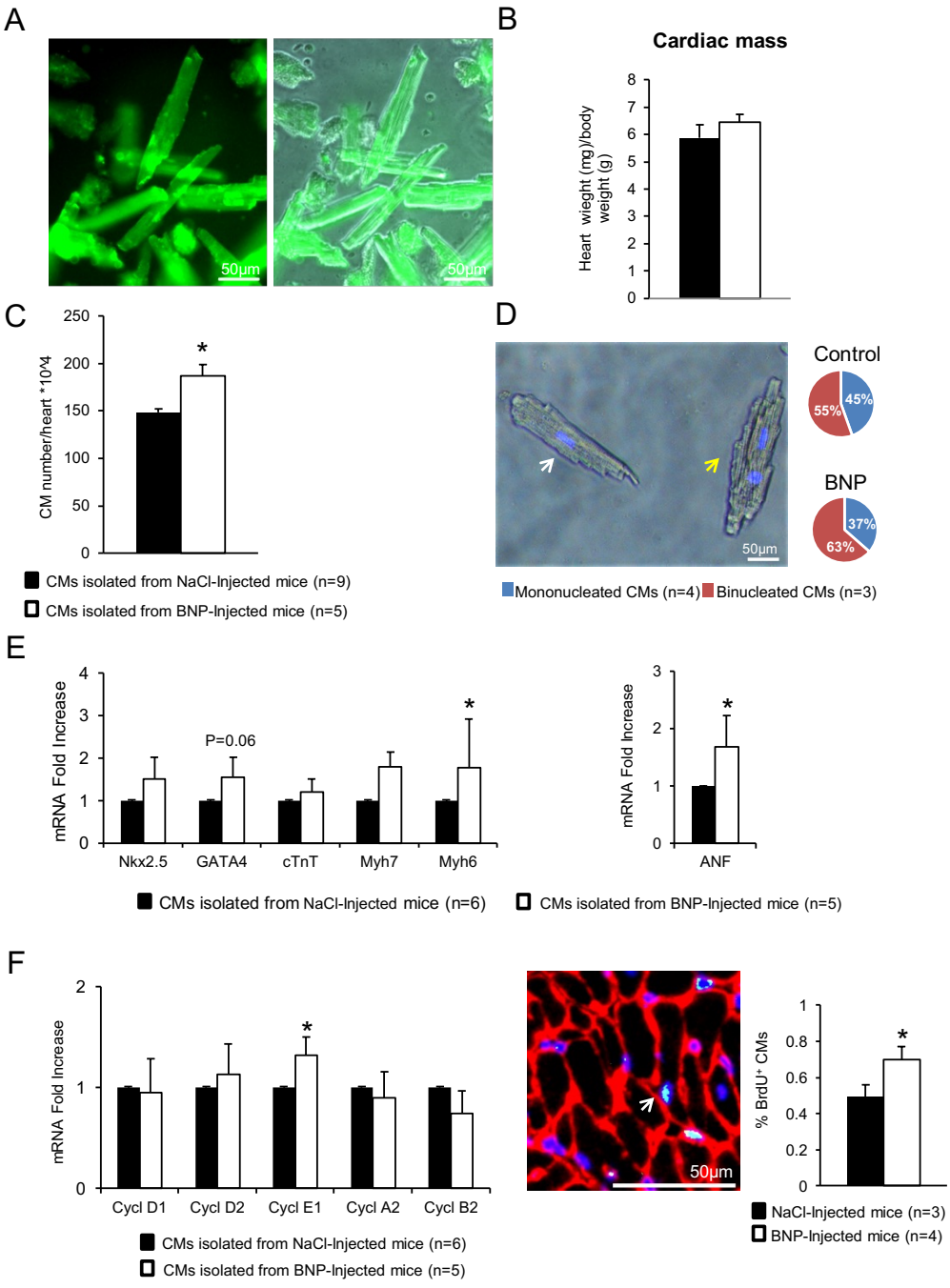

Figure 33: *BNP treatment leads to increased CM number in adult mice.* **A:** Representative pictures of freshly isolated CMs from Myh6-MerCreMer mice. CMs express GFP as a consequence of Tamoxifen injection 2 weeks before BNP- or NaCl-treatment. **B:** Heart/body weight ratio of BNP-treated mice and saline-treated mice. **C:** Total number of CMs/heart isolated from BNP- and NaCl-treated mice. **D:** Representative picture of CMs stained with DAPI. White arrow depicts mononucleated CMs and yellow arrow binucleated CMs. Pie charts on the right represent the number of mono- or bi-nucleated CMs related to the total number of CMs in BNP- and saline-treated mice. At least, 1407 CMs are counted. **E:** mRNA expression coding for cardiac markers (Nkx2.5, GATA4, cTnT, Myh7, Myh6) and ANF in CMs isolated from BNP- and saline-treated hearts. Results expressed as fold increase above the levels of saline hearts. **F:** Graph on the left represents mRNA level of genes coding for cyclins (D1, D2, E1, A2 and B2) in CMs isolated from BNP- and NaCl-treated hearts. On the right, picture represents heart sections stained with BrdU (green) and laminin (red). White arrow shows $BrdU^+$ CMs. Graph exhibits the percentage of $BrdU^+$ CMs in BNP- and NaCl-treated mice. At least 1360 CMs are counted. For all results, data are mean ±SEM, *p≤0.05.

In order to determine by which mechanism BNP increased the number of CMs (i.e. CPC differentiation and/or pre-existing CM proliferation), we performed flow cytometry (FACS) analysis (Fig. 34). Three different CM populations were observed after staining with antibody against cTnT: 1) GFP^+ $cTnT^+$ CMs corresponding to well-organized pre-existing CMs, 2) GFP^+ $cTnT^-$ CMs corresponding to dedifferentiated pre-existing CMs and 3) GFP^- $cTnT^+$ CMs originating from CPC differentiation or from a lack of recombination. Interestingly, BNP-treated mice exhibited an increased number of GFP^+ $cTnT^+$ cells/heart compared to the saline mice (+27%, p=0.01) (Fig. 34E). By contrast, BNP treatment did not change the number of GFP^+ $cTnT^-$ cells/heart or GFP^- $cTnT^+$ cells/heart, when compared to saline-injected mice (Fig. 34E-F).

To summarize, BNP increases the number of CMs by stimulating the proliferation of pre-existing CMs. Furthermore, in adult unmanipulated hearts, BNP had no effect on CM dedifferentiation.

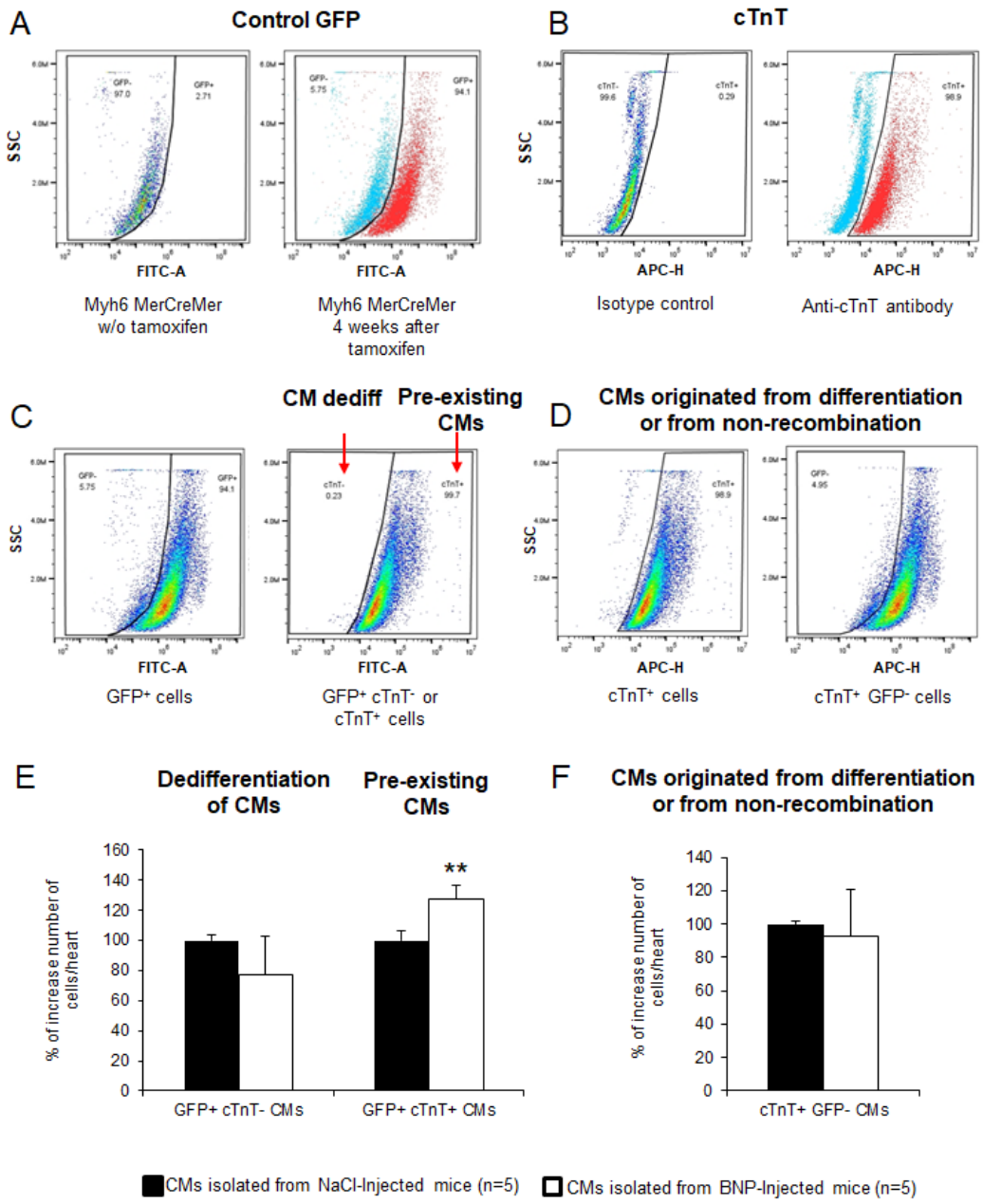

Figure 34: *BNP treatment stimulates pre-existing CM proliferation in adult hearts.* **A-D:** Representative flow cytometry dot plot graphs of CMs isolated from Myh6-MerCreMer adult hearts and stained with antibody against cTnT. **A:** Dot plot graphs represent the CM isolated from Myh6-MerCreMer hearts without Tamoxifen injection (on the left) and 4 weeks after Tamoxifen injection (on the right). 94% of the CMs express GFP protein. **B:** Dot plot graphs show that 99% of the isolated CMs express the cTnT protein. **C:** GFP^+ cells are studied for the expression of cTnT. The GFP^+ $cTnT^-$ CMs represent pre-existing dedifferentiated CMs and the GFP^+ $cTnT^+$ CMs represent pre-existing well-organized CMs. **D:** $cTnT^+$ cells are studied for the expression of GFP. The $cTnT^+$ GFP^- CMs represent cells originating from CPC differentiation or from non-recombination after Tamoxifen injection. **E:** Graph represents the percentage increase of the number of dedifferentiatied CMs (GFP^+ $cTnT^-$ CMs) and the number of pre-existing well-organized CMs (GFP^+ $cTnT^+$ CMs) in BNP related to NaCl-treated hearts. **F:** Graph represents the percentage increase of the number of CMs originating from CPC differentiation and/or from a lack of recombination in BNP related to saline hearts. **E-F:** For all results, the percentage of cells obtained by FACS analysis are related to the total number of CMs/heart. Data are mean ±SEM, **p≤0.01.

4.2.5. BNP signaling activates ERK in isolated CMs from injured, neonatal and adult hearts

Our results demonstrated that BNP modulates CM proliferation in pathological and physiological conditions. We thus determined by which signaling pathways BNP modulates CM proliferation. Three main signaling pathways were investigated: PI3K/AKT, p38 MAPK, MAPK/ERK (137, 142, 231). The activation of PI3K/AKT, p38 MAPK and MAPK/ERK pathways were assessed by measuring the phosphorylation of AKT, p38 and ERK proteins related to the total amount of protein. Western blots were performed on CMs isolated from adult infarcted and unmanipulated hearts as well as on CMs isolated from neonatal hearts, treated or not with BNP. In addition, we measured the mRNA expression coding for Pi3kcb (142). This gene is linked to the activation of Hippo signaling pathway. Once, YAP translocates into the nucleus, it upregulates the transcription of Pi3kcb, leading to PI3K/AKT activation (see section 1.2.2.5). Thus, the upregulation of Pi3kcb gene expression combined with the activation of PI3K/AKT pathway are markers of the activation of the Hippo signaling pathway.

10 days after MI, BNP treatment increased the phosphorylation of ERK in ZI+BZ (+52%, p=0.14) and decreased its phosphorylation in RZ (-60%, p=0.01) (Fig. 35A). The two other pathways (PI3K/AKT and p38 MAPK) remained unchanged in ZI+BZ after BNP treatment, whereas in RZ the phosphorylation of AKT (+140%, p=0.1) and p38 (+56%, p>0.05) tended to increase (Fig. 35A). ERK activation (+160%, p=0.008) was also observed in neonatal isolated CMs after BNP treatment (Fig. 35B). In addition, BNP increased the phosphorylation of AKT (+90%, p=0.1) in these cells (Fig. 35B). ERK was also activated in CMs isolated from unmanipulated adult hearts after BNP treatment (+66%, p=0.05) (Fig. 35C). Furthermore, no variation was observed on PI3K/AKT and p38 MAPK signaling pathways.

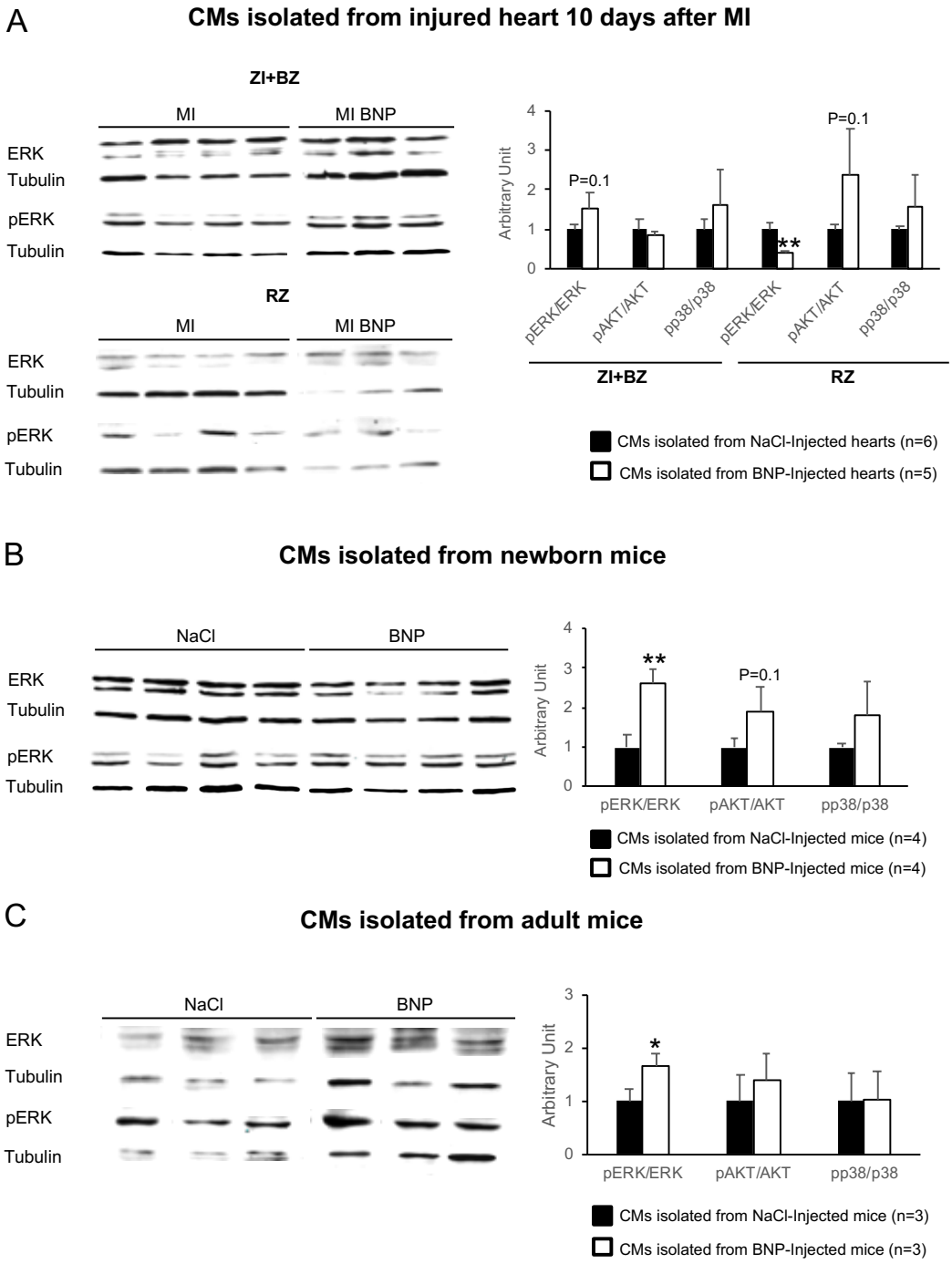

Figure 35: *MAPK/ERK signaling pathway is one of the main pathways activated in CMs after BNP treatment.* **A:** Representative western blots of CMs isolated from the ZI+BZ and RZ of saline and BNP-treated hearts, 10 days after MI. **B:** Representative western blots of CMs isolated from neonatal hearts of mice treated or not with BNP. **C:** Representative western blots of CMs isolated from unmanipulated adult hearts of BNP- and saline-treated mice. **A-C:** Graphs on the right represent the quantification of the data issue from western blot analysis. Results from BNP-treated hearts are related to these saline-treated hearts. Blots on the left were stained with antibodies against ERK, pERK and Tubulin (used as loading control). Only the bands at the adequate molecular weight are represented here: ERK and pERK 42-44 kDa, Tubulin 55 kDa. For all results, data are mean ±SEM, *p≤0.05; **p≤0.01.

Finally, BNP treatment showed no significant change of Pi3kcb gene expression in CMs isolated from adult infarcted and unmanipulated hearts as well as neonatal hearts, suggesting that BNP did not modulate CM proliferation via Hippo signaling pathway (Fig. 36).

To conclude, BNP activates in adult and neonatal treated hearts the MAPK/ERK signaling pathway in physiological and pathological conditions.

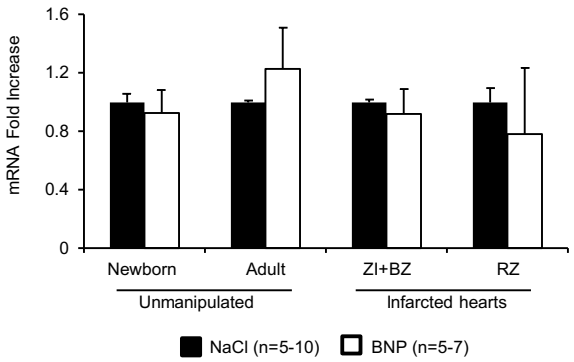

Figure 36: *BNP has no effect on Pi3kcb gene expression in CMs isolated from BNP- and NaCl-treated hearts.* mRNA expression coding for Pi3kcb in CMs isolated from BNP- and saline-treated hearts in newborn, adult unmanipulated and infarcted hearts (ZI+BZ+RZ). Results expressed as fold increase above the levels of saline hearts.

5. Discussion

In my PhD thesis, I describe for the first time a new function for BNP on CM survival and proliferation. For this purpose, BNP was injected in: 1) injured adult mice, 2) unmanipulated adult mice, which exhibit a low potential of CM proliferation and 3) unmanipulated neonatal mice, which exhibit a high potential of CM proliferation.

Interestingly, in all these mice, we showed that BNP modulates the fate of CMs, and BNP treatment resulted in increased number of CMs in treated hearts. In pathological conditions, 10 days after MI, BNP treatment increases CM number by protecting them against cell death and maybe also by stimulating their proliferation as we demonstrated that BNP stimulates the re-entry of CMs into the cell cycle. In healthy neonatal and adult mice, we clearly established that BNP stimulates CM proliferation. We observed that BNP activates the MAP/ERK signaling pathway in CMs isolated from these three animal models, suggesting that BNP could trigger CM proliferation via the activation of this pathway.

The fact that natriuretic peptides (NPs) modulate CM fate was already reported. Indeed, NPs regulate CM fate during embryogenesis and postnatal cardiac growth (191-193, 195, 196). Under mechanical stretch, induced by volume or pressure overload, cardiac cells secrete high BNP levels. However, secreted BNP is to a large extent biologically inactive, suggesting that heart failure progression could be the consequence of a deficit of the biological active form of BNP (204). As CMs express BNP receptors NPR-A and NPR-B, I investigated during my PhD work whether addition of BNP, in its biological active form, could modulate CM fate in pathological and in physiological conditions.

The results obtained during my thesis clearly demonstrate that BNP treatment increases the number of CMs in pathological and physiological conditions (Fig. 21B, 26B, 33C). In adult mice after MI as well as in unmanipulated adult mice, BNP treatment increases plasmatic cGMP level. In isolated CMs from injured heart (ZI+BZ), BNP activates phospholamban (PLB), which proves that i.p. BNP injections act directly on CMs, at least in the ZI+BZ area (Fig. 18C).

Three BNP receptors exist: NPR-A and NPR-B which possess a transmembrane guanylyl cyclase, and NPR-C, a non-guanylyl cyclase receptor. Contrarily to NPR-A and NPR-B, whose binding to BNP increases intracellular cGMP level, the activation of NPR-C leads to the intracellular inhibition of cAMP (see section 1.3.2) (232). Thus, our results suggest that BNP binds on NPR-A and/or NPR-B to

modulate CM cell fate. However, a study from Becker and his group demonstrated that ANP is able to stimulate neonatal CM proliferation via the activation of NPR-C *in vitro* (195). In my work, we cannot totally exclude that BNP does not act on CMs via the receptor NPR-C, since cAMP level was not measured. However, the decreased activity of PLB, observed in adult infarcted heart in RZ after BNP treatment (Fig. 18C), could be the consequence of BNP binding affinity to NPR-C. Indeed, a decrease in cAMP level could lead to a decrease of PKA and PLB activity (233). Thus, further experiments have to be performed, which consist in evaluating the level of cAMP in order to determine the role of NPR-C after BNP treatment. Nevertheless, we clearly demonstrated in this study that BNP treatment stimulates a biological response from CMs in adult infarcted hearts by activating the NPR-A and/or NPR-B receptors, cGMP signaling and PLB.

Thus, BNP stimulations 10 days after MI led to increased number of CMs in ZI area (+156%, p=0.01), but not in RZ (Fig. 21B). In parallel, BNP induced a phosphorylation of PLB in isolated CMs from ZI+BZ, whereas it decreased the pPLB/PLB ratio in isolated CMs from RZ. There might be two main reasons explaining why the biological activity of BNP is different between ZI+BZ and RZ: 1) BNP bioavailability in the heart can depend on the vascularization and 2) CM regulatory mechanisms, such as cGMP compartmentation and differential expression of NP receptors, can be major determinants. All these mechanisms and factors influencing the biological activity of BNP in CMs will be discussed in the next part.

BNP distribution in the heart is gradual, meaning that BNP treatment can be distributed progressively over time through the areas of injury. During the first few days after MI, BNP is mainly distributed in RZ, where the vascularization is more or less intact, but less in ZI+BZ, where the vascularization is impaired. Indeed, 3 days after MI, our group demonstrated that the neovascularization is higher 3 days after MI in RZ and increases progressively in ZI+BZ 10 days after MI (Li Na et al., 2020; article under submission). Thus, BNP could induce a response from CMs in RZ with a delay shorter than 10 days after MI. To test this hypothesis further experiments could be performed, for example, 3 days after MI. At this time, the expression of pPLB and pERK could be assessed in CMs to determine if BNP is able to stimulate them.

In infarcted heart, the vascularization modulates the level of oxygen in cardiac tissue, which in turn will differ from one heart area to the other. Indeed, in ZI+BZ, the oxygen level is lower (hypoxic conditions) compared to RZ (normoxic conditions) (234). Based on literature, a decrease in oxygen level after ischemia in ZI+BZ could induce three different modifications in CMs: 1) a switch in the regulation of gene expression, 2) a switch of CM architecture and 3) a metabolic switch from fatty acid to a "fetal–like" metabolism based on glycolysis (82, 88).

A hypoxic environment can induce a change in gene expression (i.e. via HIF-1α), resulting in a different response of CMs in ZI+BZ compared to those in RZ. Interestingly, in neonatal CMs cultured at 3% O_2, mRNA coding for NPR-B is increased (+127%; p=0.03) when compared to the level in CMs cultured at 20% O_2 (Fig. 29). By contrast, the mRNA expression coding for HIF-1α remained unchanged between both oxygen conditions (data not shown). In isolated CMs from injured heart, NPR-B mRNA expression increases in RZ when compared to ZI area (+74%; p=0.018) (data not shown). This is related to a decreased mRNA expression of HIF-1α in RZ area (-40%; p<0.001) (data not shown). These results suggest that the expression of NP receptors is sensitive to oxygen concentration and probably also to HIF-1α. Thus, the expression of NP receptors is a factor which can affect the biological activity of BNP.

Furthermore, when CMs are submitted to hypoxic condition, their architecture switches from a well-organized to a dedifferentiated one. Indeed, we demonstrated that hypoxia (3% O_2), compared to hyperoxic environment (20% O_2), triggers neonatal CM dedifferentiation *in vitro* (see section 4.1). Furthermore, CMs isolated from ZI area display an increased mRNA expression coding for Dab2 (+210%; p=0.008) and Runx1 (+850%; p=0.001) compared to RZ area (data not shown). Several studies also described *in vivo* that ZI+BZ are mainly composed of dedifferentiated CMs (106, 113, 115, 117, 235). Thus, BNP could affect in a different manner dedifferentiated CMs in ZI+BZ compared to mature structurally differentiated CMs in RZ.

Dedifferentiated CMs have a different intracellular compartmentation of cGMP than differentiated CMs. cGMP compartmentation involves the regulation of cGMP signaling, which is temporally and spatially regulated by the phosphodiesterases (PDEs). PDEs are localized at different loci in the cells and are responsible for cGMP degradation (187, 236). PDE3 was shown to be associated with T-Tubule microdomains and with internally-organized sarcoplasmic reticulum structures,

whereas PDE4 is localized within the sarcolemma of CMs (Fig. 37, in green) (237). In addition, PDE2 is mainly localized in T-Tubular membrane (Fig. 37, in red) (190).

Since dedifferentiated CMs are devoid of T-Tubule and thus of PDE3, we could suggest that BNP signaling may be sensitive to PED3 degradation in the RZ and avoid its activity in ZI+BZ, where CMs are dedifferentiated and PDE3 absent (237). Thus, cGMP concentration and bioavailability could be increased in ZI+BZ when compared to RZ.

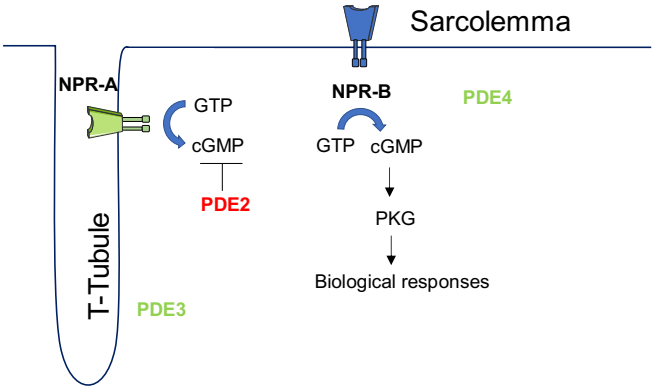

Figure 37: *PDEs localization into CMs.*

The localization of NP receptors is also a factor influencing the biological activity of BNP (190). Indeed, NPR-A is linked to T-Tubular membrane, whereas NPR-B is linked to sarcolemma membrane in CMs (Fig. 37) (190). As PDE2 is mainly localized in T-Tubular membrane, cGMP produced by NPR-A will be degraded by PDE2 (Fig. 37, in red). By contrast, cGMP produced by NPR-B is not under the control of PDE2, leading to high cGMP concentration in sarcolemma (Fig. 37) (190). To conclude, the biological activity of BNP (intensity and duration) in CMs from different areas of the heart may depend on the cGMP compartmentation by PDEs.

In summary, all these mechanisms could explain why the biological activity of BNP is different between ZI+BZ and RZ. Interestingly, in a natural environment, CM dedifferentiation, low oxygen concentration and glycolysis-based metabolism promote CM proliferation (18, 77, 89-91, 106, 112, 113). Therefore, we suppose that all these mechanisms in ZI+BZ might facilitate the biological activity of BNP to induce faster CM re-entry in the cell cycle and proliferation.

One essential question of this study is also to understand by which mechanisms BNP treatment leads to an increased CM number.

First, we evaluated if the increased CM number could be due to an experimental artefact during enzymatic digestion of hearts. In this context, Leone and his group described that isolation of CMs by enzymatic digestion could lead to cell death (65). Therefore, we hypothesized that enzymatic digestion may induce CM cell death during isolation, which could be prevented by BNP treatment. To evaluate this hypothesis, the percentage of $DAPI^+$ CMs was quantified by FACS analysis after CM isolations from BNP- and NaCl-treated hearts. The percentage of $DAPI^+$ CMs between BNP- and NaCl-treated hearts remained unchanged (12.9% and 11.4% respectively) (data not shown). Therefore, we concluded that in our conditions, the increased number of CMs obtained after CM isolation from BNP-treated hearts is not due to the isolation procedure, but rather to a modulation of CM cell fate.

Therefore, the essential question remains to understand by which mechanism(s) BNP treatment leads to increased number of CMs: 1) a protection of CM against cell death, 2) a stimulation of CPC differentiation into CMs and/or 3) a stimulation of pre-existing CM proliferation.

CM cell death is a process which takes place during the first 6-24 hours after ischemia (11). Several cardiac cell death mechanisms were described, such as necrosis, apoptosis, autophagy and necroptosis (see section 1.1) (3, 5, 238). However, the two main mechanisms responsible for cell death after a permanent occlusion or in the ischemia/reperfusion model (I/R) remain apoptosis and necrosis (3). To determine, whether BNP treatment can protect CMs from cell death, we investigated CM cell death on infarcted hearts 1 day after LAD permanent ligature. First, we highlighted a reduced cTnT plasma level in BNP-treated mice (-67%, $p=0.04$), suggesting that less CMs die in these animals (Fig. 22A). In addition, we compared the levels of proteins involved in apoptosis in the hearts of BNP- and NaCl-treated mice 24h after MI. We observed that BNP treatment decreases the activity of the caspase 3 (-33%, $p=0.07$), which is a result in favor of a protection mediated by BNP on CMs from infarcted hearts (Fig. 22B). However, immunohistochemistry stainings revealed that the number of CM expressing the cleaved-caspase 3 remains unchanged in the hearts of BNP- and NaCl-treated mice (Fig. 22C).

The apoptotic level measured in heart failure is less than 1% (80–250 myocytes/10^5 nuclei) (239). As the level of apoptosis is low, the method of detection used here (i.e. IHF) may not be sufficient to detect a difference in the number of CMs undergoing apoptosis between BNP- and saline-treated mice. Therefore, other technics could be used to evaluate the number of apoptotic CMs (i.e. Annexin V staining combined with phosphatidylethanolamine (PE) staining and followed by the quantification of CMs undergoing apoptosis and necrosis by FACS analysis) (3).

Several studies evaluated already the role of BNP on apoptosis with contrasted results (240-242). In the rabbit heart, BNP treatment protects cardiac cells from apoptosis after ischemia/reperfusion (200, 241). Furthermore, neonatal rat CMs in culture are protected against apoptosis by BNP treatment after I/R (240). But it seems also that BNP triggers apoptosis. Zhang and his group determined that BNP stimulates the increased expression of lncRNA LSINCT5 in human myocardial CMs (*in vitro*), leading to CM apoptosis (242).

In our case, BNP protects CM from cell death via decreased apoptosis. However, we cannot exclude that other cell death mechanisms, such as necrosis, necroptosis and/or autophagy could also be modulated by BNP treatment. To elucidate the exact mechanism of CM protection after BNP treatment, further experiments have to be performed. However, we clearly demonstrated in this study a new role for BNP to protect CMs in infarcted hearts and this is likely responsible for a part of its cardioprotective effect.

If the increased number of CMs in BNP-treated hearts originates from BNP protection against cell death, other mechanisms can also participate at this cell increase. We thus used adult Myh6-MerCreMer transgenic mice to determine the origin of the CMs 10 days after MI in infarcted hearts and in unmanipulated hearts. In injured hearts, the origin of the CMs was determined by immunohistochemistry and GFP^- α-act^+ and GFP^+ α-act^+ CMs were quantified. In unmanipulated hearts, FACS analysis on isolated CMs were performed and GFP^- $cTnT^+$ and GFP^+ $cTnT^+$ CMs were quantified. We demonstrated that BNP treatment does not increase the number of CMs originating from CPC differentiation (i.e. GFP^- α-act^+ or $cTnT^+$ CMs), neither in ZI of infarcted hearts, nor in adult hearts in physiological conditions (Fig. 23 and 34). These results confirm those already published. Indeed, it was reported that the differentiation of CPCs into CMs takes place during heart development, and not really in adult hearts in physiological and pathological conditions (40, 117).

Thus, new adult CMs in adult hearts originate from the proliferation of pre-existing CMs rather than from CPC differentiation.

Therefore, in the next step, we would like to determine the role of BNP on the proliferation of pre-existing CMs in pathological and physiological conditions.

In the hearts of adult infarcted mice (ZI), healthy adult mice and healthy neonatal mice, we showed that BNP treatment increases the number of CMs expressing proliferative markers, such as Ki67, BrdU, pH3 and Aurkb, suggesting that BNP treatment stimulates the re-entry of CMs into the cell cycle. However, the key challenge in the field of CM regeneration is to confirm a real cell division (i.e. cytokinesis) and not only the re-entry of CMs into the cell cycle. Indeed, CMs can enter the cell cycle without going to karyokinesis or cytokinesis, leading to the formation of polyploid and/or binucleated CMs (see section 1.2.2.3). In our study, quantification of binucleated CMs and analysis of the localization of the Aurkb protein were used to determine whether BNP treatment triggers a real CM proliferation. The staining against Aurkb allows visualizing the mitotic spindle orientation, which is symmetric during cytokinesis and asymmetric during binucleation (154).

In adult infarcted hearts, BNP treatment increases the percentage of CMs undergoing cytokinesis in ZI, 10 days after injury (+29%, p=0.05) (Fig. 25D). Recent publications mentioned that Aurkb alone is not sufficient to easily distinguish a real cell division from a binucleation (156, 243). However, in our study, we not only observed an increase of cytokinesis, but we also demonstrated that BNP treatment increases the percentage of CMs expressing BrdU (+90% p=0.01), pH3 (+62% p=0.04) and Aurkb (+400% p=0.03) (Fig. 25A-C), decreases the percentage of binucleation (-50%, p>0.05) (Fig. 25D) and upregulates the cyclin D2 in ZI (+20%, p=0.06) (Fig. 21C). All these results suggest that BNP treatment stimulates CM proliferation in injured hearts, in addition to protecting CMs from cell death.

In adult unmanipulated mice, which display a low potential of CM proliferation, BNP treatment increases by 25% (p=0.03) the number of CMs (Fig. 33C). This result was confirmed by FACS analysis, where BNP-treated hearts increased by 27% (p=0.01) the number of CMs compared to NaCl-treated hearts (Fig 34E). Furthermore, we observed that BNP treatment upregulates the cyclin E1 (+32%, p=0.02) and increases the percentage of CMs expressing BrdU (+40%, p=0.03)

(Fig. 33F). However, BNP did not decrease the percentage of binucleated CMs (+14%, p>0.5) (Fig. 33D). In adult unmanipulated hearts, no or only very few CMs undergo cell death (3). Thus, increased number of CMs in these hearts is unlikely the consequence of protection against cell death, but results rather from BNP stimulation on CM proliferation.

To determine, if BNP can induce CM proliferation in optimal conditions, we focused on unmanipulated neonatal mice, which exhibit a high potential of CM proliferation. We demonstrated that BNP treatment in neonatal mice leads to 25% (p=0.005) increase of the number of CMs (Fig. 26B). Furthermore, the percentage of binucleated CMs is decreased (-8%; p=0.01) and the mRNA expressions of two cyclins, required at the end of the cell cycle progression, are upregulated (cyclin A2: +126% p=0.002; cyclin B2: +70% p=0.04) (Fig. 26C-D). In addition, neonatal CMs in cell culture treated with low concentration of BNP, displayed a decreased percentage of binucleated CMs (-32%, p=0.01) (Fig. 30E), which is linked to an increased number of CMs undergoing cytokinesis (+80%, p=0.04) (Fig. 31D).

To summarize, BNP treatment in adult and neonatal unmanipulated hearts increases 1) the number of CMs, 2) the percentage of CMs expressing markers related to cell cycle progression (BrdU, Ki67, pH3 and Aurkb), 3) the expression of some cyclins (cyclin E1, A2 and B2). Furthermore, in neonatal hearts, we detected an increased cytokinesis and an increased percentage of mononucleated CMs. Therefore, taken all these results together, we conclude that BNP treatment stimulates CM proliferation in unmanipulated adult and neonatal hearts. In injured heart, BNP treatment protects CMs from cell death. Evidences also suggest that increased proliferation exists in the ZI after BNP treatment. Indeed, BNP treatment in ZI increases the percentage of CM expressing proliferative markers, increases cytokinesis and decreases binucleation. In this situation, we could hypothesize that, if there is no CM proliferation, the process of binucleation should be increased, which could also participate in the protection of hearts in ischemic conditions (see section 1.2.2.3)

During my thesis, I also assessed the signaling pathway activated by BNP in CMs. The three signaling pathways which have been already described to play a role in the fate of CMs were studied: MAPK/ERK, PI3K/AKT and p38 MAPK (95, 136, 137).

Interestingly, we highlighted the activation of the same signaling pathway after BNP treatment in physiological (neonatal and adult hearts) and pathological (ZI+BZ) hearts. Indeed, BNP modulates the fate of CMs by activating the MAPK/ERK signaling pathway (Fig. 35).

The MAPK/ERK pathway plays a central role in cardiac physiology by modulating cell proliferation, cell growth and hypertrophy (244-246). After phosphorylation of ERK, it translocates into the nucleus and upregulated the transcription of cyclin D1 and D2 and thus the transition from G1 to S phase (130, 131). Interestingly, in our study isolated CMs, 10 days after MI, exhibit an increased expression of the cyclin D2 in ZI+BZ after BNP treatment. In addition, cell culture of neonatal CMs in presence of low concentration of BNP also displays an increased expression of the cyclin D1 and D2 (Fig. 30D). Thus, BNP could activate the MAPK/ERK signaling pathway and the cyclin D1 and D2 in order to push CMs to re-enter the cell cycle in the S phase. This hypothesis is in correlation with the literature. In fact, the MAP/ERK pathway was described to modulate CM proliferation alone or in synergy with PI3K/AKT (245-249).

Furthermore, BNP treatment slightly modulates PI3K/AKT (+140%, $p>0.5$) in CMs isolated from RZ and in CMs isolated from neonatal hearts (+90%, $p>0.5$). In addition, p38 MAPK is also modulated by BNP in CMs isolated from neonatal hearts (+80%, $p>0.5$) (Fig. 35B). By contrast, no variation occurs in unmanipulated adult hearts (Fig. 35C). These results suggest that in our conditions, BNP does not directly modulate these signaling pathways. However, we could hypothesize that some factors (i.e. environmental factors) counterbalance the BNP effect on the regulation of these signaling pathways.

Finally, the Hippo signaling pathway and the effector YAP are also key regulators of CM proliferation (250-252). Once YAP is translocated into the nucleus, it activates the transcription of several genes, such as Pi3kcb gene (142). In this study, we evaluated the effect of BNP on the expression of Pi3kcb gene. In the three different models of this study, isolated CMs after BNP treatment display no variation of the Pi3kcb gene expression (Fig 36).

Taken all these findings together, our results strongly suggest that BNP stimulates CM proliferation through the activation of the MAK/ERK signaling pathway. To confirm this hypothesis, the next experiment is to inhibit the phosphorylation of ERK by using drugs such as PD0325901 (253). If the MAPK/ERK signaling pathway is linked to BNP modulation of CM's fate, less CMs in adult BNP-treated unmanipulated hearts should be observed. Furthermore, by modulating the use of ERK inhibitor and the time after MI, we could dissociate BNP effect on cell death from its effect on CM proliferation. Indeed, if the increased CM number, observed 10 days after MI, is due to a protection against cell death, the use of ERK inhibitor one day after MI should induce no difference in the number of CMs. By contrast, if the increased CM number is due to a stimulation of CM proliferation, the use of ERK inhibitor will decrease CM number 10 days after MI.

Identifying the role and the mechanism of action of the biologically active form of BNP in injured heart is essential for cardiac rehabilitation. Several clinical studies already exist and focus on increasing BNP concentration in the injured heart. The recombinant human natriuretic peptide BNP (nesiritide) was used, but showed conflicting outcomes depending on its concentration and its way of administration (254).

In 2014, a promising therapeutic treatment for patients with heart failure, the LCZ696, was developed. Its beneficial effects on the structure and function of the heart have been demonstrated (see section 1.3.6) (255). However, it remains unclear, whether the treatment has a direct effect on cardiac cells. Therefore, our group was interested to study the role of LCZ696 on adult mice 10 days after MI (see chapter 8, supplementary data). For this experiment, two concentrations of LCZ696 were tested: 6 and 60 mg/kg/day (Supplementary Fig. 1A).

LCZ696 treatment (60mg/kg/day) increases fractional shortening (+100%; p=0.09) as well as ejection fraction (+83%; p=0.1) and decreases heart remodeling during systole (-70%; p=0.07) (Supplementary Fig. 1C). Furthermore, the heart to body weight-ratio remains unchanged (Supplementary Fig. 1B).

Preliminary results highlight also a direct role of LCZ696 on CMs. Indeed, LCZ696 treatment (6 and 60mg/kg/day) reduces CM cross-sectional area in all zones of the heart compared to untreated mice, suggesting that LCZ696 decreases CM hypertrophy induced by MI (Supplementary Fig. 2C). In addition, LCZ696

(60mg/kg/day) increases the number of CMs in RZ (+40%, P<0.5), whereas in ZI+BZ, CM number remains unchanged (Supplementary Fig. 2B).

Regarding CM proliferation, LCZ696 treatment increases the number of CMs expressing BrdU in all zones of the hearts and increases the percentage of CMs expressing Ki67 in RZ (LCZ696 6mg/kg/day for Ki67 in RZ: +125%, P<0.5) (Supplementary Fig. 3). Furthermore, MAPK/ERK signaling pathway is activated in RZ after LCZ696 treatment (6mg/kg/day) (+150%, P<0.5), whereas it remains unchanged in ZI+BZ (Supplementary Fig. 4A).

Finally, LCZ696 treatment (60mg/kg/day) also increases cGMP plasma level by 3-fold (44.5 for untreated mice vs 138 for LCZ696-treated mice; data not shown), suggesting that the treatment could increase concentrations of NPs as already demonstrated by others in mice and rats (256, 257). In patients with heart failure, a decreased NEP activity after LCZ696 treatment is also correlated with an increased concentration of proBNP and ANP (224). Since it is complicated to determine which NPs (ANP, BNP or CNP) are involved in the cardioprotective role of LCZ696 treatment, there is a real interest in targeting every NP separately (i.e. BNP) and to study its direct role on CMs.

Taken all these results together, we demonstrated that LCZ696 treatment increases the number of CMs after MI in RZ, which could be one reason of its cardioprotective role. By contrast, in ZI+BZ no increased number of CMs is observed after LCZ696 treatment. In addition, MAPK/ERK signaling pathway is activated in RZ, whereas it remains unchanged in ZI+BZ.

Therefore, LCZ696 treatment acts on CMs in a different area of injured hearts than BNP treatment. Indeed, 10 days after MI, BNP increases the number of CMs in ZI, whereas LCZ696 treatment increases the number of CMs in RZ.

Regarding these results, the following question raises: why BNP increased number of CMs 10 days after MI in ZI, but not LCZ696. Three hypotheses are put forward: 1) LCZ696 stimulates CM proliferation in this zone, however this process takes more than 10 days. Thus, an increased CM number could be detected by using an extended experimental protocol (i.e. study of CM cell fate 14 days after MI). 2) Contrarily to BNP protocol, mice from LCZ696 protocol were not treated with LCZ696 directly after MI but only one day after injury. As cardiac cell death occurs in the first 24 hours after injury, LCZ696 cannot protect CMs from cell death with this protocol. Thus, the increased number of CMs detected in the ZI+BZ of BNP-

treated hearts could be due to protection against cell death and a limited number of CMs must be present to detect CM proliferation. 3) NEP activity could be dependent on the area of injury. This hypothesis suggests that NEP could be inactive in ZI after MI as a consequence of the environment, whereas its activity could remain high in RZ. In this case, LCZ696 treatment should have no effect on CM cell fate in ZI, by contrast to RZ, where the level of NPs should be increased due to NEP inhibition.

Furthermore, the second question is to understand why LCZ696 increases the number of CMs in RZ, while BNP treatment has no effect on CM number in the same zone (Fig. 38). The main difference between LCZ696 and BNP treatment is that LCZ696 increases the concentration of the three NPs (ANP, BNP, CNP) by inhibiting NEP activity. These NPs have a specific affinity for NP receptors (see section 1.3.2). In addition, ANP and CNP have been shown to be more sensitive to NEP degradation than BNP, suggesting that ANP and CNP levels after LCZ696 treatment are expected to be strongly increased compared to BNP (258).

Thus, increased number of CMs in the RZ after LCZ696 treatment could be due to ANP and/or CNP increase, and not due to BNP increase. This could be the consequence of activation of different receptors than those activated by BNP treatment (NPR-A or NPR-C for example versus NPR-B) (Fig. 38).

Finally, regarding MAPK/ERK signaling pathway, the increased CM number in RZ after LCZ696 treatment and the activation of MAPK/ERK pathway observed in the same area strongly suggests that ERK signaling is linked to CM proliferation rather than a protection against CM cell death.

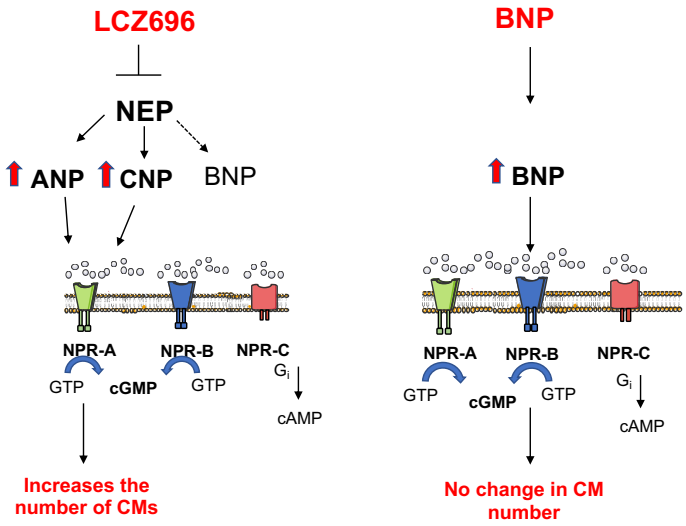

Figure 38: *LCZ696 and BNP treatment model on CM cell fate in remote zone.* On the left: LCZ696 treatment in RZ increases number of CMs. On the right: BNP treatment in RZ has no effect on CM number.

6. Conclusions and Perspectives

Increasing CM replacement in injured hearts is the goal of new therapeutic strategies aimed to restore heart function after CVDs. That is why during my thesis I focused on determining the role of oxygen and of brain natriuretic peptide (BNP) on cardiomyocyte (CM) cell fate.

The results presented in my thesis demonstrate that low (or physiologically normoxic) oxygen concentration (i.e 3% O_2) compared to atmospheric oxygen concentration (20% O_2) favors CM dedifferentiation and proliferation *in vitro* in neonatal CM cell culture. These results are crucial for cardiac research as they demonstrate that cultivated neonatal CMs at low oxygen concentration highlight some cellular physiological mechanisms occurring in CMs which can be blind in 20% oxygen. Nevertheless, in our study, one limitation is that neonatal CMs were cultivated in a hypoxia chamber which was opened three times during the 14 days of culture, in order to change the medium. Thus, cells were submitted several times to increased oxygen concentration (20% O_2) that could generate the release of ROS and cell damage. Therefore, we tested the use of an antioxidant, the N-acetylcysteine, in order to regulate ROS scavenging. The use of this antioxidant increases the number of surviving CMs (+200%; n=2) after 14 days of culture compared to untreated cells, suggesting that this approach could limit the harmful effects of ROS production.

Interestingly, strategies based on reducing oxygen supply in order to treat CVDs emerge, such as intermittent hypoxia therapy (IHT). This strategy is defined as recurrent episodes of hypoxia interspersed with episodes of normoxia after heart injury.

In various animal models (mice, rats and dogs) it was shown that animals, conditioned to intermittent hypoxia prior to MI, present less damage in the heart after I/R injury. Indeed, intermittent hypoxia conditioning (IHC; performed prior heart injury) on animal models enhances cardiac function, reduces infarct size and has a cardioprotective effect by reducing necrosis and increasing antioxidant enzymatic capacity (259-264). This cardioprotective role observed after IHC may be also associated with a stimulation of cardiac regeneration. Thus, IHC may be a potential therapeutically approach to treat CVDs. Clinical trials on patients with ischemic heart diseases and indication for coronary artery bypass graft were

already performed. Indeed, IHT showed promising results by decreasing the level of plasmatic Troponin I and serum lactate after I/R (265). An increased level of plasmatic Troponin I is related to CM cell death, and an increase of lactate concentration is related to a deficiency of oxygen supply to the tissues. Thus, these results demonstrate the cardioprotective role of IHT therapy on patients suffering from ischemia (265). The benefit of IHT depends however on the patients and on the severity of hypoxia (level of hypoxia, the number as well as the duration of hypoxic episodes) (266). Indeed, high number of prolonged hypoxia per day leads to detrimental outcomes, whereas a small number of short hypoxia per day leads to beneficial outcomes (267).

Therefore, our protocol used on neonatal CM cell culture (low oxygen concentration and reoxygenation) could be adapted to a model in order to study IHT therapy and its role on CM cell fate.

Regarding the role of BNP on CM cell fate in physiological and pathological conditions, I clearly demonstrated in my thesis that BNP protects CMs from cell death, increases the number of CMs and stimulates the re-entry of CMs into the cell cycle in the infarction zone (ZI) of adult mice 10 days after MI. Thus, a part of the "BNP cardioprotective effect" in ischemic conditions is due to a protection of CMs against cell death and maybe also due to a stimulation of CM proliferation. By targeting unmanipulated adult and neonatal mice, we provide evidences that BNP increases the number of CMs by stimulating their proliferation. Interestingly, BNP treatment activates the MAPK/ERK signaling pathway in CMs isolated from the three models, suggesting a possible correlation between BNP treatment, MAPK/ERK pathway and CM proliferation.

In infarcted hearts, BNP effects on CMs are dependent on the area of the heart, suggesting that probably different mechanisms regulate the biological activity of BNP in the ZI+BZ and RZ (Fig. 39).

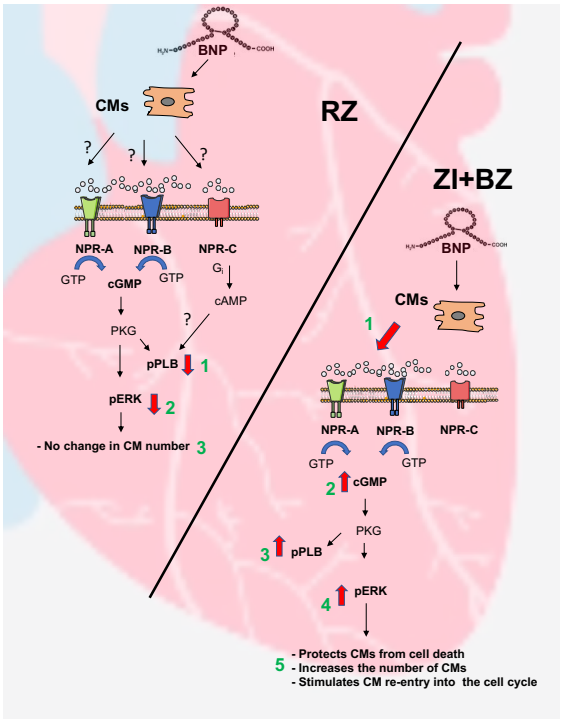

Figure 39: *BNP effects on CMs after ischemia in RZ and ZI+BZ.* On the left, in RZ, BNP treatment decreases the activity of PLB (1) and ERK (2). No increased CM number was observed (3). The activated-NP receptors are unknown. On the right, in ZI, BNP treatment increases cGMP level (2) via NPR-A and/or NPR-B activation (1). This leads to increased PLB (3) and ERK (4) activity. BNP treatment in ZI protects CMs from cell death, increases the number of CMs and stimulates CM re-entry into the cell cycle (5).

Thus, in order to maximize the biological activity of BNP on patients suffering from CVDs, it is essential to determine in the future, by which mechanism BNP acts in the different areas of infarcted hearts. We will thus focus on the regulation of NP receptor expression (NPR-A, NPR-B and NPR-C) and the cGMP compartmentation.

Therefore, further experiments have to be done in order to characterize, which NP receptor is activated during BNP treatment. First, we could take advantage of transgenic mouse models, of NPR-A, NPR-B or NPR-C transgenes linked with a fluorescent marker and under the activity of the α-MHC promoter. The main advantage of these mice compared to immunostainings will be to facilitate the follow up of expression and localization of NP receptors in CMs. For example, intracellular NP trafficking (see section 1.3.2) could be followed by time lapse imaging on adult and neonatal CM cell culture after BNP treatment. Also, the localization and expression of NP receptors in CMs could be assessed in different areas of injured infarcted heart treated or not with BNP. In a second time, to determine which NP receptor is associated with BNP effects on CMs, NPR-A, NPR-B and NPR-C, transgenic knockout (KO) mice could be used. To overcome the issue encountered with our systemic NPR-A and NPR-B knockout (KO) mice (low survival

rate during embryogenesis for NPR-A KO mice and rapid death after birth for NPR-B KO mice), we could generate transgenic mice with an inducible CM-specific excision of the NPR-A, NPR-B or NPR-C gene (Fig. 40A). Using Cre recombinase expression, driven by the α-MHC, NPR-A, B or C can be deleted. Thanks to these mice, NP receptors expression could be silenced only in CMs and at a specific time after Tamoxifen injection.

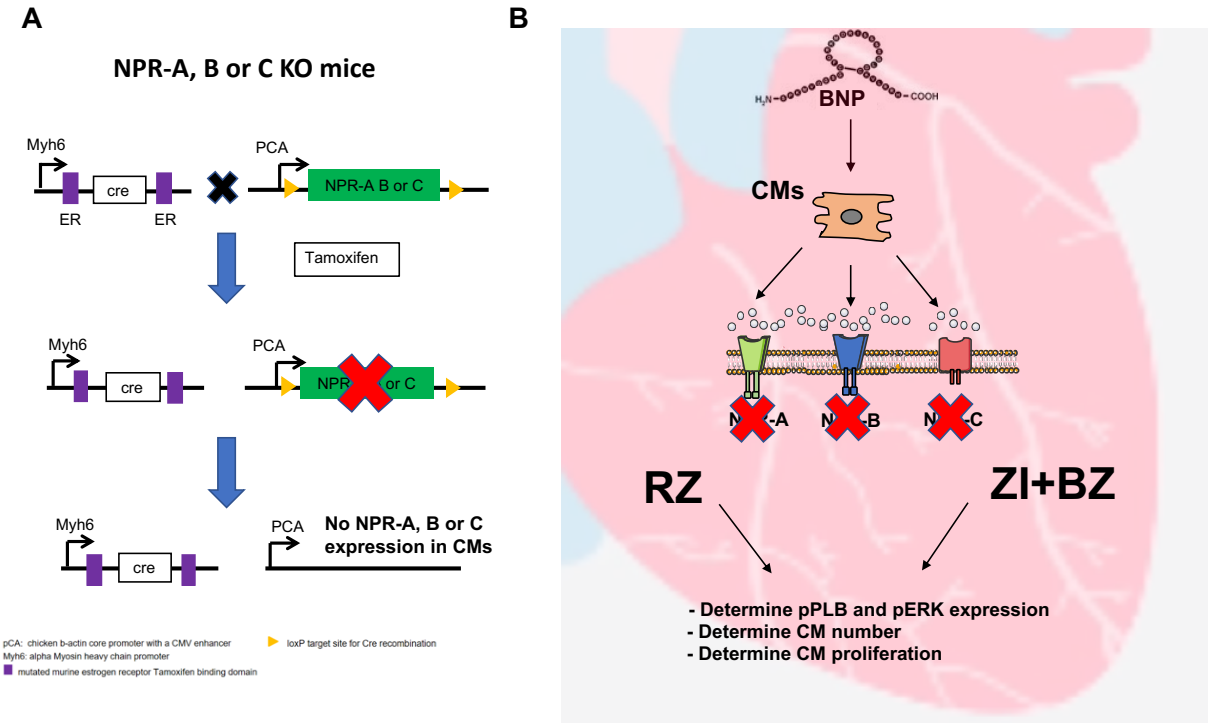

Figure 40: *Which NP receptor is involved in CM responses after BNP treatment?* **A:** The NPR-A, B or C-KO mice could be used. Thanks to the Cre recombinase expression driven by α-MHC promoter (Myh6), the NPR-A, B or C genes flanked by loxP sites (yellow arrows) can be deleted. Thus, after Tamoxifen injection, the NPR-A, B or C expression is silenced only in CMs. **B:** In RZ, by using the KO mice, the aim is to define which NP receptor is related to the decreased expression of pPLB and pERK and showing no change in CM number. In ZI, the aim is to define which NP receptor is related to PLB and ERK activation and to an increased CM number.

Furthermore, cGMP compartmentation is a key mechanism, which depends on NP receptors and phosphodiesterases (PDEs) localization. This mechanism regulates the intracellular level of cGMP and thus the biological activity of BNP. Because PDEs hydrolyze intracellular cGMP, the perspective is to determine, whether BNP signaling is associated to some PDEs. Therefore, it would be interesting to test the effect of a PDE inhibitor in combination with BNP treatment after MI and observe the response from CMs (Fig. 41). In RZ, where BNP treatment induces no change of CM number compared to ZI, the use of PDE inhibitors can suppress PDE activity and then stimulates CM responses after BNP treatment. In ZI, the use of PDE

inhibitors can delay over time cGMP activity and induces a stronger response from CMs compared to BNP treatment. Furthermore, delayed cGMP signal over time can also stimulate additional signaling pathways and/or promote longer CM cell cycle activity.

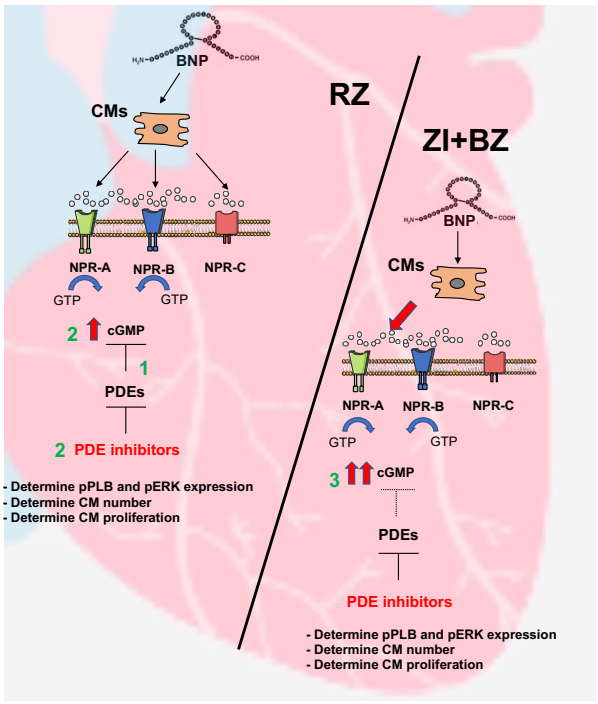

Figure 41: *Do PDE inhibitors increase the biological activity of BNP treatment?* On the left, in RZ, the first question is (1) to determine if some PDEs decrease cGMP level after BNP treatment. This could explain why pPLB and pERK expression decreases after BNP treatment. The second question is (2) to determine if, by using PDE inhibitors combined with BNP, the cGMP level increases. In this case, pPLB and pERK expression will increase and maybe also CM proliferation and the number of CMs. On the right, in ZI, the question is to determine if the use of PDE inhibitors combined with BNP treatment can increase over time the level of cGMP (3). With this approach, CM response after BNP treatment could be stronger compared to BNP treatment alone.

Interestingly, some PDE (i.e. PDE1, 3) inhibitors already exist, which are used to treat cardiac failure and then could be easily combined with BNP treatment. Indeed, PDE1 or PDE4 inhibitors on mice and rats were shown to promote cardiac function and cardioprotection by decreasing, for PDE1, CM cell death (268, 269).

In patients suffering from heart failure, PDE3 inhibitor was already used and increases heart rate and cardiac contractility (270). Besides the promising positive effects of PDE3 inhibitor, negative effects such as arrhythmias and sudden death have also been observed during chronic treatment over time (271). Furthermore, a clinical trial already combined low dose of BNP (nesiritide) with a PDE5 inhibitor (sildenafil) in order to improve the renal function on patients with chronic heart failure (272). Thus, if biological activity of BNP is regulated by PDEs across areas

of injured hearts, the perspective will be to associate BNP treatment with PDE inhibitors in order to delay cGMP activity over time and increase CM responses after ischemia.

An alternative to increase the signaling pathway(s) mediated by BNP could be to decrease the natural degradation of BNP by neprilysin. That is, why we also evaluated the role of LCZ696 on CM cell fate after MI in mice. Interestingly, we determined that LCZ696 treatment increases the cardiac function and attenuates cardiac remodeling 10 days after MI. In addition, preliminary results showed that LCZ696 increases the number of CMs and stimulates CM re-entry into the cell cycle in the remote zone (Fig. 42).

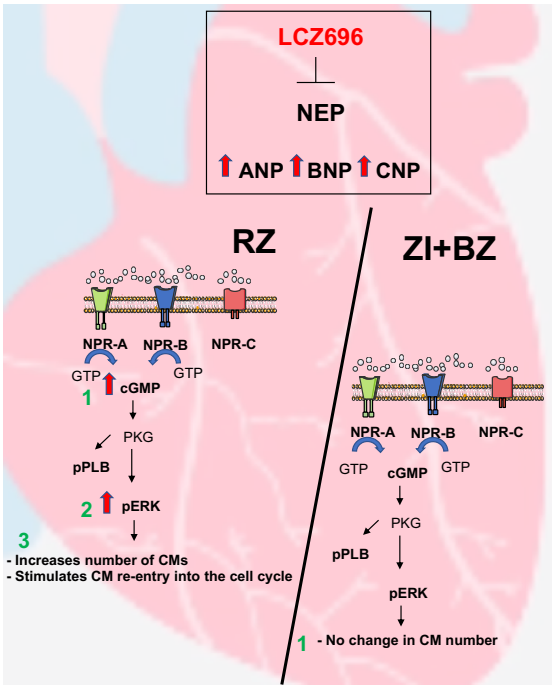

Figure 42: *LCZ696 effects on CM cell fate after ischemia in RZ and ZI+BZ.* The box represents the mechanism of action of LCZ696. LCZ696 inhibits neprilysin (NEP), leading to an increased concentration and activity of ANP, BNP and CNP. On the left, in RZ, LCZ696 treatment increases cGMP level (1) and ERK activity (2). In addition, LCZ696 increases the number of CMs and stimulates CM re-entry into the cell cycle (3). On the right, in ZI, LCZ696 treatment has no effect on pERK expression and induces no change in CM number (1).

These results are clearly relevant, because for the first time we demonstrated that a part of the cardioprotective role of LCZ696 could be associated with CM cell fate regulation.

Interestingly, LCZ696 and BNP treatments showed similar benefits on the heart function and on CM cell fate, suggesting that LCZ696 may increase the biological

activity of BNP after MI. Nevertheless, one limitation of this study is that the relation between LCZ696 and BNP remains to be established. Therefore, it seems relevant to determine whether the beneficial effects of LCZ696 on CMs are the consequence of an increased activity of BNP. To answer this question, BNP-KO mice could be used (Fig. 43). These mice are viable throughout adulthood and both sexes were fertile. They develop no signs of hypertension and ventricular hypertrophy (199). In addition, the systolic blood pressure and the heart to body weight ratio do not differ between BNP-KO and WT mice in physiological conditions. However, they develop fibrotic lesions in the ventricle and CMs could be disorganized with supercontracted sarcomeres in the same conditions as mentioned above (199). By using these mice treated with LCZ696 and comparing them with WT mice treated with LCZ696 after MI, we will be able to determine if the beneficial effects of LCZ696 observed in CMs is due to the biological activity of BNP or whether other NPs, such as ANP and CNP, also participate (Fig. 43).

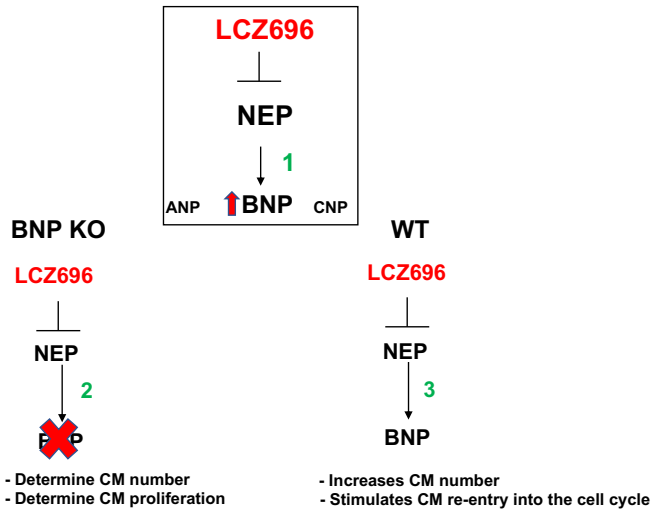

Figure 43: *Is the LCZ696 effect on CM cell fate due to an increased activity of BNP?* The aim will be to determine if LCZ696 benefits, observed on CM cell fate after ischemia, are due to an increase of BNP activity (1). To answer this question, the transgenic BNP-KO mice can be used and compared to WT mice, both treated with LCZ696. If LCZ696 treatment increases BNP activity, BNP-KO mice could display no increased CM number and no stimulation of CM re-entry into the cell cycle (2), contrarily to WT mice (3).

Furthermore, preliminary results have shown that LCZ696 treatment does not increase the number of CMs in ZI+BZ. In this experiment, the first dose of LCZ696 administered to mice was performed one day after MI. Thus, with this protocol, it seems unlikely that LCZ696 protects CMs from cell death. Therefore, in order to determine the role of LCZ696 treatment on CM cell death protection, further experiments consist in treating mice with LCZ696 directly after surgery and

sacrifice animals 24 hours and 10 days after MI. With this approach, the measure of plasmatic Troponin I concentration could be assessed 24 hours after MI in LCZ696-treated mice and compared with untreated mice. In addition, 10 days after MI, the number of CMs could be assessed. In the case of a CM protection from cell death, we expect to observe in LCZ696-treated mice a decrease of Troponin I plasma level 24 hours after MI and an increased number of CMs 10 days after MI.

Finally, why LCZ696 increases the number of CMs in the RZ and not BNP, remains an opened question. LCZ696 increases the level of NPs (ANP, BNP and CNP), suggesting that ANP and CNP, rather than BNP, can trigger a response from CM in RZ. Furthermore, the route of administration between LCZ696 (oral gavage) and BNP (intraperitoneal injection) is not the same. Thus, both treatments could be metabolized differently, leading to activation of others mechanisms. The dosage of treatment could be also a key factor influencing the response from CMs. Indeed, we and others already demonstrated that BNP concentration influences the response from CMs (195). Therefore, we could suggest that the concentration of BNP in ZI and LCZ696 in RZ promotes CM response, whereas the dose after diffusion into the heart is no longer adequate to observe a beneficial response on CMs.

To conclude, low oxygen concentration, BNP and LCZ696 are three factors able to modulate CM cell fate in infarcted hearts. LCZ696 is already used in clinic to treat patients suffering from HF, whereas for BNP and low oxygen concentration, trials are still ongoing. Therefore, based on the results presented in this thesis, it appears clearly that improving knowledge regarding their role on cardiac regeneration will help to identify them as new options to treat patients suffering from CVDs.

7. Bibliography

1. Levy D, Kenchaiah S, Larson MG, Benjamin EJ, Kupka MJ, Ho KK, et al. Long-term trends in the incidence of and survival with heart failure. N Engl J Med. 2002;347(18):1397-402.
2. Yan AT, Yan RT, Liu PP. Narrative review: pharmacotherapy for chronic heart failure: evidence from recent clinical trials. Ann Intern Med. 2005;142(2):132-45.
3. Mishra PK, Adameova A, Hill JA, Baines CP, Kang PM, Downey JM, et al. Guidelines for evaluating myocardial cell death. Am J Physiol Heart Circ Physiol. 2019;317(5):H891-H922.
4. Huang S, Chen HH, Yuan H, Dai G, Schuhle DT, Mekkaoui C, et al. Molecular MRI of acute necrosis with a novel DNA-binding gadolinium chelate: kinetics of cell death and clearance in infarcted myocardium. Circ Cardiovasc Imaging. 2011;4(6):729-37.
5. Schlüter K-D. Cardiomyocytes - Active players in cardiac disease: Springer; 2016.
6. Wesley T. O'Neal WFG, Susan D. Kent and Jitka A. I. Virag. Cellular Pathways of Death and Survival in Acute Myocardial Infarction. Clinical & Experimental Cardiology. 2012.
7. Kanduc D, Mittelman A, Serpico R, Sinigaglia E, Sinha AA, Natale C, et al. Cell death: apoptosis versus necrosis (review). Int J Oncol. 2002;21(1):165-70.
8. Decker RS, Wildenthal K. Lysosomal alterations in hypoxic and reoxygenated hearts. I. Ultrastructural and cytochemical changes. Am J Pathol. 1980;98(2):425-44.
9. Orogo AM, Gustafsson AB. Therapeutic targeting of autophagy: potential and concerns in treating cardiovascular disease. Circ Res. 2015;116(3):489-503.
10. Corsetti G, Chen-Scarabelli C, Romano C, Pasini E, Dioguardi FS, Onorati F, et al. Autophagy and Oncosis/Necroptosis Are Enhanced in Cardiomyocytes from Heart Failure Patients. Med Sci Monit Basic Res. 2019;25:33-44.
11. Konstantinidis K, Whelan RS, Kitsis RN. Mechanisms of cell death in heart disease. Arterioscler Thromb Vasc Biol. 2012;32(7):1552-62.
12. Adameova A, Goncalvesova E, Szobi A, Dhalla NS. Necroptotic cell death in failing heart: relevance and proposed mechanisms. Heart Fail Rev. 2016;21(2):213-21.
13. Nikoletopoulou V, Markaki M, Palikaras K, Tavernarakis N. Crosstalk between apoptosis, necrosis and autophagy. Biochim Biophys Acta. 2013;1833(12):3448-59.
14. Nishida K, Kyoi S, Yamaguchi O, Sadoshima J, Otsu K. The role of autophagy in the heart. Cell Death Differ. 2009;16(1):31-8.
15. Nishida K, Yamaguchi O, Otsu K. Crosstalk between autophagy and apoptosis in heart disease. Circ Res. 2008;103(4):343-51.
16. Teringova E, Tousek P. Apoptosis in ischemic heart disease. J Transl Med. 2017;15(1):87.

17. Sabbah HN. Apoptotic cell death in heart failure. Cardiovasc Res. 2000;45(3):704-12.

18. Jopling C, Sleep E, Raya M, Marti M, Raya A, Izpisua Belmonte JC. Zebrafish heart regeneration occurs by cardiomyocyte dedifferentiation and proliferation. Nature. 2010;464(7288):606-9.

19. Bergmann O, Bhardwaj RD, Bernard S, Zdunek S, Barnabe-Heider F, Walsh S, et al. Evidence for cardiomyocyte renewal in humans. Science. 2009;324(5923):98-102.

20. Eschenhagen T, Bolli R, Braun T, Field LJ, Fleischmann BK, Frisen J, et al. Cardiomyocyte Regeneration: A Consensus Statement. Circulation. 2017;136(7):680-6.

21. Ghiroldi A, Piccoli M, Cirillo F, Monasky MM, Ciconte G, Pappone C, et al. Cell-Based Therapies for Cardiac Regeneration: A Comprehensive Review of Past and Ongoing Strategies. Int J Mol Sci. 2018;19(10).

22. Hastings CL, Roche ET, Ruiz-Hernandez E, Schenke-Layland K, Walsh CJ, Duffy GP. Drug and cell delivery for cardiac regeneration. Adv Drug Deliv Rev. 2015;84:85-106.

23. Menasche P. Cell therapy trials for heart regeneration - lessons learned and future directions. Nat Rev Cardiol. 2018;15(11):659-71.

24. Emmert MY. Cell-based cardiac regeneration. Eur Heart J. 2017;38(15):1095-8.

25. Cambria E, Pasqualini FS, Wolint P, Gunter J, Steiger J, Bopp A, et al. Translational cardiac stem cell therapy: advancing from first-generation to next-generation cell types. NPJ Regen Med. 2017;2:17.

26. Gonzales C, Pedrazzini T. Progenitor cell therapy for heart disease. Exp Cell Res. 2009;315(18):3077-85.

27. Barreto S, Hamel L, Schiatti T, Yang Y, George V. Cardiac Progenitor Cells from Stem Cells: Learning from Genetics and Biomaterials. Cells. 2019;8(12).

28. Bu L, Jiang X, Martin-Puig S, Caron L, Zhu S, Shao Y, et al. Human ISL1 heart progenitors generate diverse multipotent cardiovascular cell lineages. Nature. 2009;460(7251):113-7.

29. Laugwitz KL, Moretti A, Caron L, Nakano A, Chien KR. Islet1 cardiovascular progenitors: a single source for heart lineages? Development. 2008;135(2):193-205.

30. Di Felice V, Zummo G. Stem cell populations in the heart and the role of Isl1 positive cells. Eur J Histochem. 2013;57(2):e14.

31. Bolli R, Chugh AR, D'Amario D, Loughran JH, Stoddard MF, Ikram S, et al. Cardiac stem cells in patients with ischaemic cardiomyopathy (SCIPIO): initial results of a randomised phase 1 trial. Lancet. 2011;378(9806):1847-57.

32. Makkar RR, Smith RR, Cheng K, Malliaras K, Thomson LE, Berman D, et al. Intracoronary cardiosphere-derived cells for heart regeneration after myocardial infarction (CADUCEUS): a prospective, randomised phase 1 trial. Lancet. 2012;379(9819):895-904.

33. Rosenblatt-Velin N, Lepore MG, Cartoni C, Beermann F, Pedrazzini T. FGF-2 controls the differentiation of resident cardiac precursors into functional cardiomyocytes. J Clin Invest. 2005;115(7):1724-33.

34. Smart N, Bollini S, Dube KN, Vieira JM, Zhou B, Davidson S, et al. De novo cardiomyocytes from within the activated adult heart after injury. Nature. 2011;474(7353):640-4.

35. Plaisance I, Perruchoud S, Fernandez-Tenorio M, Gonzales C, Ounzain S, Ruchat P, et al. Cardiomyocyte Lineage Specification in Adult Human Cardiac Precursor Cells Via Modulation of Enhancer-Associated Long Noncoding RNA Expression. JACC Basic Transl Sci. 2016;1(6):472-93.

36. van Berlo JH, Kanisicak O, Maillet M, Vagnozzi RJ, Karch J, Lin SC, et al. c-kit+ cells minimally contribute cardiomyocytes to the heart. Nature. 2014;509(7500):337-41.

37. Liu Q, Yang R, Huang X, Zhang H, He L, Zhang L, et al. Genetic lineage tracing identifies in situ Kit-expressing cardiomyocytes. Cell Res. 2016;26(1):119-30.

38. Sultana N, Zhang L, Yan J, Chen J, Cai W, Razzaque S, et al. Resident c-kit(+) cells in the heart are not cardiac stem cells. Nat Commun. 2015;6:8701.

39. He L, Li Y, Li Y, Pu W, Huang X, Tian X, et al. Enhancing the precision of genetic lineage tracing using dual recombinases. Nat Med. 2017;23(12):1488-98.

40. Li Y, He L, Huang X, Bhaloo SI, Zhao H, Zhang S, et al. Genetic Lineage Tracing of Nonmyocyte Population by Dual Recombinases. Circulation. 2018;138(8):793-805.

41. Yang L, Soonpaa MH, Adler ED, Roepke TK, Kattman SJ, Kennedy M, et al. Human cardiovascular progenitor cells develop from a KDR+ embryonic-stem-cell-derived population. Nature. 2008;453(7194):524-8.

42. Menasche P, Vanneaux V, Hagege A, Bel A, Cholley B, Parouchev A, et al. Transplantation of Human Embryonic Stem Cell-Derived Cardiovascular Progenitors for Severe Ischemic Left Ventricular Dysfunction. J Am Coll Cardiol. 2018;71(4):429-38.

43. Caspi O, Huber I, Kehat I, Habib M, Arbel G, Gepstein A, et al. Transplantation of human embryonic stem cell-derived cardiomyocytes improves myocardial performance in infarcted rat hearts. J Am Coll Cardiol. 2007;50(19):1884-93.

44. van Laake LW, Passier R, Monshouwer-Kloots J, Verkleij AJ, Lips DJ, Freund C, et al. Human embryonic stem cell-derived cardiomyocytes survive and mature in the mouse heart and transiently improve function after myocardial infarction. Stem Cell Res. 2007;1(1):9-24.

45. Kolossov E, Bostani T, Roell W, Breitbach M, Pillekamp F, Nygren JM, et al. Engraftment of engineered ES cell-derived cardiomyocytes but not BM cells restores contractile function to the infarcted myocardium. J Exp Med. 2006;203(10):2315-27.

46. Laflamme MA, Chen KY, Naumova AV, Muskheli V, Fugate JA, Dupras SK, et al. Cardiomyocytes derived from human embryonic stem cells in pro-

survival factors enhance function of infarcted rat hearts. Nat Biotechnol. 2007;25(9):1015-24.

47. Duelen R, Sampaolesi M. Stem Cell Technology in Cardiac Regeneration: A Pluripotent Stem Cell Promise. EBioMedicine. 2017;16:30-40.

48. Kawamura M, Miyagawa S, Fukushima S, Saito A, Miki K, Funakoshi S, et al. Enhanced Therapeutic Effects of Human iPS Cell Derived-Cardiomyocyte by Combined Cell-Sheets with Omental Flap Technique in Porcine Ischemic Cardiomyopathy Model. Sci Rep. 2017;7(1):8824.

49. Shiba Y, Gomibuchi T, Seto T, Wada Y, Ichimura H, Tanaka Y, et al. Allogeneic transplantation of iPS cell-derived cardiomyocytes regenerates primate hearts. Nature. 2016;538(7625):388-91.

50. Ieda M, Fu JD, Delgado-Olguin P, Vedantham V, Hayashi Y, Bruneau BG, et al. Direct reprogramming of fibroblasts into functional cardiomyocytes by defined factors. Cell. 2010;142(3):375-86.

51. Song K, Nam YJ, Luo X, Qi X, Tan W, Huang GN, et al. Heart repair by reprogramming non-myocytes with cardiac transcription factors. Nature. 2012;485(7400):599-604.

52. Jayawardena TM, Finch EA, Zhang L, Zhang H, Hodgkinson CP, Pratt RE, et al. MicroRNA induced cardiac reprogramming in vivo: evidence for mature cardiac myocytes and improved cardiac function. Circ Res. 2015;116(3):418-24.

53. Inagawa K, Miyamoto K, Yamakawa H, Muraoka N, Sadahiro T, Umei T, et al. Induction of cardiomyocyte-like cells in infarct hearts by gene transfer of Gata4, Mef2c, and Tbx5. Circ Res. 2012;111(9):1147-56.

54. Senyo SE, Steinhauser ML, Pizzimenti CL, Yang VK, Cai L, Wang M, et al. Mammalian heart renewal by pre-existing cardiomyocytes. Nature. 2013;493(7432):433-6.

55. Porrello ER, Mahmoud AI, Simpson E, Johnson BA, Grinsfelder D, Canseco D, et al. Regulation of neonatal and adult mammalian heart regeneration by the miR-15 family. Proc Natl Acad Sci U S A. 2013;110(1):187-92.

56. Malliaras K, Terrovitis J. Cardiomyocyte proliferation vs progenitor cells in myocardial regeneration: The debate continues. Glob Cardiol Sci Pract. 2013;2013(3):303-15.

57. Sturzu AC, Rajarajan K, Passer D, Plonowska K, Riley A, Tan TC, et al. Fetal Mammalian Heart Generates a Robust Compensatory Response to Cell Loss. Circulation. 2015;132(2):109-21.

58. Vagnozzi RJ, Molkentin JD, Houser SR. New Myocyte Formation in the Adult Heart: Endogenous Sources and Therapeutic Implications. Circ Res. 2018;123(2):159-76.

59. Soonpaa MH, Kim KK, Pajak L, Franklin M, Field LJ. Cardiomyocyte DNA synthesis and binucleation during murine development. Am J Physiol. 1996;271(5 Pt 2):H2183-9.

60. Porrello ER, Mahmoud AI, Simpson E, Hill JA, Richardson JA, Olson EN, et al. Transient regenerative potential of the neonatal mouse heart. Science. 2011;331(6020):1078-80.

61. Zhu W, Zhang E, Zhao M, Chong Z, Fan C, Tang Y, et al. Regenerative Potential of Neonatal Porcine Hearts. Circulation. 2018;138(24):2809-16.

62. Nakagama Y, Inuzuka R, Ichimura K, Hinata M, Takehara H, Takeda N, et al. Accelerated Cardiomyocyte Proliferation in the Heart of a Neonate With LEOPARD Syndrome-Associated Fatal Cardiomyopathy. Circ Heart Fail. 2018;11(4):e004660.

63. Haubner BJ, Schneider J, Schweigmann U, Schuetz T, Dichtl W, Velik-Salchner C, et al. Functional Recovery of a Human Neonatal Heart After Severe Myocardial Infarction. Circ Res. 2016;118(2):216-21.

64. Farooqi KM, Sutton N, Weinstein S, Menegus M, Spindola-Franco H, Pass RH. Neonatal myocardial infarction: case report and review of the literature. Congenit Heart Dis. 2012;7(6):E97-102.

65. Leone M, Engel FB. Advances in heart regeneration based on cardiomyocyte proliferation and regenerative potential of binucleated cardiomyocytes and polyploidization. Clin Sci (Lond). 2019;133(11):1229-53.

66. Roesner A, Hankeln T, Burmester T. Hypoxia induces a complex response of globin expression in zebrafish (Danio rerio). J Exp Biol. 2006;209(Pt 11):2129-37.

67. Dawes GS, Mott JC, Widdicombe JG. The foetal circulation in the lamb. J Physiol. 1954;126(3):563-87.

68. Turrens JF. Mitochondrial formation of reactive oxygen species. J Physiol. 2003;552(Pt 2):335-44.

69. Hoeijmakers JH. DNA damage, aging, and cancer. N Engl J Med. 2009;361(15):1475-85.

70. Marnett LJ, Riggins JN, West JD. Endogenous generation of reactive oxidants and electrophiles and their reactions with DNA and protein. J Clin Invest. 2003;111(5):583-93.

71. Puente BN, Kimura W, Muralidhar SA, Moon J, Amatruda JF, Phelps KL, et al. The oxygen-rich postnatal environment induces cardiomyocyte cell-cycle arrest through DNA damage response. Cell. 2014;157(3):565-79.

72. Webster KA, Discher DJ, Kaiser S, Hernandez O, Sato B, Bishopric NH. Hypoxia-activated apoptosis of cardiac myocytes requires reoxygenation or a pH shift and is independent of p53. J Clin Invest. 1999;104(3):239-52.

73. Sousa Fialho MDL, Abd Jamil AH, Stannard GA, Heather LC. Hypoxia-inducible factor 1 signalling, metabolism and its therapeutic potential in cardiovascular disease. Biochim Biophys Acta Mol Basis Dis. 2019;1865(4):831-43.

74. Wang JZ, Zhang YH, Du WT, Liu G, Zhang XY, Cheng SZ, et al. A post-surgical adjunctive hypoxic therapy for myocardial infarction: Initiate endogenous cardiomyocyte proliferation in adults. Med Hypotheses. 2019;125:16-20.

75. Sun Y, Jiang C, Hong H, Liu J, Qiu L, Huang Y, et al. Effects of hypoxia on cardiomyocyte proliferation and association with stage of development. Biomed Pharmacother. 2019;118:109391.

76. Jiang YH, Wang HL, Peng J, Zhu Y, Zhang HG, Tang FQ, et al. Multinucleated polyploid cardiomyocytes undergo an enhanced adaptability to hypoxia via mitophagy. J Mol Cell Cardiol. 2020;138:115-35.

77. Kimura W, Xiao F, Canseco DC, Muralidhar S, Thet S, Zhang HM, et al. Hypoxia fate mapping identifies cycling cardiomyocytes in the adult heart. Nature. 2015;523(7559):226-30.

78. Nakada Y, Canseco DC, Thet S, Abdisalaam S, Asaithamby A, Santos CX, et al. Hypoxia induces heart regeneration in adult mice. Nature. 2017;541(7636):222-7.

79. Vujic A, Lerchenmuller C, Wu TD, Guillermier C, Rabolli CP, Gonzalez E, et al. Exercise induces new cardiomyocyte generation in the adult mammalian heart. Nat Commun. 2018;9(1):1659.

80. Tong W, Xiong F, Li Y, Zhang L. Hypoxia inhibits cardiomyocyte proliferation in fetal rat hearts via upregulating TIMP-4. Am J Physiol Regul Integr Comp Physiol. 2013;304(8):R613-20.

81. Tong W, Xue Q, Li Y, Zhang L. Maternal hypoxia alters matrix metalloproteinase expression patterns and causes cardiac remodeling in fetal and neonatal rats. Am J Physiol Heart Circ Physiol. 2011;301(5):H2113-21.

82. Lopaschuk GD, Spafford MA, Marsh DR. Glycolysis is predominant source of myocardial ATP production immediately after birth. Am J Physiol. 1991;261(6 Pt 2):H1698-705.

83. Lopaschuk GD, Ussher JR, Folmes CD, Jaswal JS, Stanley WC. Myocardial fatty acid metabolism in health and disease. Physiol Rev. 2010;90(1):207-58.

84. Hom JR, Quintanilla RA, Hoffman DL, de Mesy Bentley KL, Molkentin JD, Sheu SS, et al. The permeability transition pore controls cardiac mitochondrial maturation and myocyte differentiation. Dev Cell. 2011;21(3):469-78.

85. Liaudet L, Vassalli G, Pacher P. Role of peroxynitrite in the redox regulation of cell signal transduction pathways. Front Biosci (Landmark Ed). 2009;14:4809-14.

86. Sarangarajan R, Meera S, Rukkumani R, Sankar P, Anuradha G. Antioxidants: Friend or foe? Asian Pac J Trop Med. 2017;10(12):1111-6.

87. Moris D, Spartalis M, Spartalis E, Karachaliou GS, Karaolanis GI, Tsourouflis G, et al. The role of reactive oxygen species in the pathophysiology of cardiovascular diseases and the clinical significance of myocardial redox. Ann Transl Med. 2017;5(16):326.

88. Neely JR, Morgan HE. Relationship between carbohydrate and lipid metabolism and the energy balance of heart muscle. Annu Rev Physiol. 1974;36:413-59.

89. Lim GB. Inhibiting fatty acid oxidation promotes cardiomyocyte proliferation. Nat Rev Cardiol. 2020.

90. Honkoop H, de Bakker DE, Aharonov A, Kruse F, Shakked A, Nguyen PD, et al. Single-cell analysis uncovers that metabolic reprogramming by ErbB2 signaling is essential for cardiomyocyte proliferation in the regenerating heart. Elife. 2019;8.

91. Magadum A, Singh N, Kurian AA, Munir I, Mehmood T, Brown K, et al. Pkm2 Regulates Cardiomyocyte Cell Cycle and Promotes Cardiac Regeneration. Circulation. 2020;141(15):1249-65.

92. Cao T, Liccardo D, LaCanna R, Zhang X, Lu R, Finck BN, et al. Fatty Acid Oxidation Promotes Cardiomyocyte Proliferation Rate but Does Not Change Cardiomyocyte Number in Infant Mice. Front Cell Dev Biol. 2019;7:42.

93. de Carvalho A, Bassaneze V, Forni MF, Keusseyan AA, Kowaltowski AJ, Krieger JE. Early Postnatal Cardiomyocyte Proliferation Requires High Oxidative Energy Metabolism. Sci Rep. 2017;7(1):15434.

94. Mollova M, Bersell K, Walsh S, Savla J, Das LT, Park SY, et al. Cardiomyocyte proliferation contributes to heart growth in young humans. Proc Natl Acad Sci U S A. 2013;110(4):1446-51.

95. D'Uva G, Aharonov A, Lauriola M, Kain D, Yahalom-Ronen Y, Carvalho S, et al. ERBB2 triggers mammalian heart regeneration by promoting cardiomyocyte dedifferentiation and proliferation. Nat Cell Biol. 2015;17(5):627-38.

96. Bersell K, Arab S, Haring B, Kuhn B. Neuregulin1/ErbB4 signaling induces cardiomyocyte proliferation and repair of heart injury. Cell. 2009;138(2):257-70.

97. Mohamed TMA, Ang YS, Radzinsky E, Zhou P, Huang Y, Elfenbein A, et al. Regulation of Cell Cycle to Stimulate Adult Cardiomyocyte Proliferation and Cardiac Regeneration. Cell. 2018;173(1):104-16 e12.

98. Adler CP, Friedburg H, Herget GW, Neuburger M, Schwalb H. Variability of cardiomyocyte DNA content, ploidy level and nuclear number in mammalian hearts. Virchows Arch. 1996;429(2-3):159-64.

99. Derks W, Bergmann O. Polyploidy in Cardiomyocytes: Roadblock to Heart Regeneration? Circ Res. 2020;126(4):552-65.

100. Gonzalez-Rosa JM, Sharpe M, Field D, Soonpaa MH, Field LJ, Burns CE, et al. Myocardial Polyploidization Creates a Barrier to Heart Regeneration in Zebrafish. Dev Cell. 2018;44(4):433-46 e7.

101. Hirose K, Payumo AY, Cutie S, Hoang A, Zhang H, Guyot R, et al. Evidence for hormonal control of heart regenerative capacity during endothermy acquisition. Science. 2019;364(6436):184-8.

102. Anatskaya OV, Vinogradov AE. Paradoxical relationship between protein content and nucleolar activity in mammalian cardiomyocytes. Genome. 2004;47(3):565-78.

103. Bensley JG, De Matteo R, Harding R, Black MJ. Three-dimensional direct measurement of cardiomyocyte volume, nuclearity, and ploidy in thick histological sections. Sci Rep. 2016;6:23756.

104. Patterson M, Barske L, Van Handel B, Rau CD, Gan P, Sharma A, et al. Frequency of mononuclear diploid cardiomyocytes underlies natural variation in heart regeneration. Nat Genet. 2017;49(9):1346-53.

105. Jiang YH, Zhu Y, Chen S, Wang HL, Zhou Y, Tang FQ, et al. Re-enforcing hypoxia-induced polyploid cardiomyocytes enter cytokinesis through activation of beta-catenin. Sci Rep. 2019;9(1):17865.

106. Wang WE, Li L, Xia X, Fu W, Liao Q, Lan C, et al. Dedifferentiation, Proliferation, and Redifferentiation of Adult Mammalian Cardiomyocytes After Ischemic Injury. Circulation. 2017;136(9):834-48.

107. Cao J, Wang J, Jackman CP, Cox AH, Trembley MA, Balowski JJ, et al. Tension Creates an Endoreplication Wavefront that Leads Regeneration of Epicardial Tissue. Dev Cell. 2017;42(6):600-15 e4.

108. Cao J, Poss KD. The epicardium as a hub for heart regeneration. Nat Rev Cardiol. 2018;15(10):631-47.

109. Galdos FX, Guo Y, Paige SL, VanDusen NJ, Wu SM, Pu WT. Cardiac Regeneration: Lessons From Development. Circ Res. 2017;120(6):941-59.

110. Piquereau J, Ventura-Clapier R. Maturation of Cardiac Energy Metabolism During Perinatal Development. Front Physiol. 2018;9:959.

111. Porter GA, Jr., Hom J, Hoffman D, Quintanilla R, de Mesy Bentley K, Sheu SS. Bioenergetics, mitochondria, and cardiac myocyte differentiation. Prog Pediatr Cardiol. 2011;31(2):75-81.

112. Zhang Y, Li TS, Lee ST, Wawrowsky KA, Cheng K, Galang G, et al. Dedifferentiation and proliferation of mammalian cardiomyocytes. PLoS One. 2010;5(9):e12559.

113. Dispersyn GD, Mesotten L, Meuris B, Maes A, Mortelmans L, Flameng W, et al. Dissociation of cardiomyocyte apoptosis and dedifferentiation in infarct border zones. Eur Heart J. 2002;23(11):849-57.

114. Bon-Mathier AC, Rignault-Clerc S, Bielmann C, Rosenblatt-Velin N. Oxygen as a key regulator of cardiomyocyte proliferation: New results about cell culture conditions! Biochim Biophys Acta Mol Cell Res. 2019.

115. Kubin T, Poling J, Kostin S, Gajawada P, Hein S, Rees W, et al. Oncostatin M is a major mediator of cardiomyocyte dedifferentiation and remodeling. Cell Stem Cell. 2011;9(5):420-32.

116. Driesen RB, Verheyen FK, Debie W, Blaauw E, Babiker FA, Cornelussen RN, et al. Re-expression of alpha skeletal actin as a marker for dedifferentiation in cardiac pathologies. J Cell Mol Med. 2009;13(5):896-908.

117. Zhang Y, Gago-Lopez N, Li N, Zhang Z, Alver N, Liu Y, et al. Single-cell imaging and transcriptomic analyses of endogenous cardiomyocyte dedifferentiation and cycling. Cell Discov. 2019;5:30.

118. Rucker-Martin C, Pecker F, Godreau D, Hatem SN. Dedifferentiation of atrial myocytes during atrial fibrillation: role of fibroblast proliferation in vitro. Cardiovasc Res. 2002;55(1):38-52.

119. Poling J, Gajawada P, Lorchner H, Polyakova V, Szibor M, Bottger T, et al. The Janus face of OSM-mediated cardiomyocyte dedifferentiation during cardiac repair and disease. Cell Cycle. 2012;11(3):439-45.

120. Poling J, Gajawada P, Richter M, Lorchner H, Polyakova V, Kostin S, et al. Therapeutic targeting of the oncostatin M receptor-beta prevents inflammatory heart failure. Basic Res Cardiol. 2014;109(1):396.

121. Liao Y, Li H, Pi Y, Li Z, Jin S. Cardioprotective effect of IGF-1 against myocardial ischemia/reperfusion injury through activation of PI3K/Akt pathway in rats in vivo. J Int Med Res. 2019;47(8):3886-97.

122. Lee KF, Simon H, Chen H, Bates B, Hung MC, Hauser C. Requirement for neuregulin receptor erbB2 in neural and cardiac development. Nature. 1995;378(6555):394-8.

123. Schulze WX, Deng L, Mann M. Phosphotyrosine interactome of the ErbB-receptor kinase family. Mol Syst Biol. 2005;1:2005 0008.

124. D'Uva G, Tzahor E. The key roles of ERBB2 in cardiac regeneration. Cell Cycle. 2015;14(15):2383-4.

125. Rochais F, Sturny R, Chao CM, Mesbah K, Bennett M, Mohun TJ, et al. FGF10 promotes regional foetal cardiomyocyte proliferation and adult cardiomyocyte cell-cycle re-entry. Cardiovasc Res. 2014;104(3):432-42.

126. McDevitt TC, Laflamme MA, Murry CE. Proliferation of cardiomyocytes derived from human embryonic stem cells is mediated via the IGF/PI 3-kinase/Akt signaling pathway. J Mol Cell Cardiol. 2005;39(6):865-73.

127. Hashmi S, Ahmad HR. Molecular switch model for cardiomyocyte proliferation. Cell Regen (Lond). 2019;8(1):12-20.

128. Maddika S, Wiechec E, Ande SR, Poon IK, Fischer U, Wesselborg S, et al. Interaction with PI3-kinase contributes to the cytotoxic activity of apoptin. Oncogene. 2008;27(21):3060-5.

129. Mutlak M, Kehat I. Extracellular signal-regulated kinases 1/2 as regulators of cardiac hypertrophy. Front Pharmacol. 2015;6:149.

130. Chambard JC, Lefloch R, Pouyssegur J, Lenormand P. ERK implication in cell cycle regulation. Biochim Biophys Acta. 2007;1773(8):1299-310.

131. Murray TV, Smyrnias I, Schnelle M, Mistry RK, Zhang M, Beretta M, et al. Redox regulation of cardiomyocyte cell cycling via an ERK1/2 and c-Myc-dependent activation of cyclin D2 transcription. J Mol Cell Cardiol. 2015;79:54-68.

132. Wellbrock C, Karasarides M, Marais R. The RAF proteins take centre stage. Nat Rev Mol Cell Biol. 2004;5(11):875-85.

133. Bassat E, Mutlak YE, Genzelinakh A, Shadrin IY, Baruch Umansky K, Yifa O, et al. The extracellular matrix protein agrin promotes heart regeneration in mice. Nature. 2017;547(7662):179-84.

134. Liang Q, Bueno OF, Wilkins BJ, Kuan CY, Xia Y, Molkentin JD. c-Jun N-terminal kinases (JNK) antagonize cardiac growth through cross-talk with calcineurin-NFAT signaling. EMBO J. 2003;22(19):5079-89.

135. Liang Q, Molkentin JD. Redefining the roles of p38 and JNK signaling in cardiac hypertrophy: dichotomy between cultured myocytes and animal models. J Mol Cell Cardiol. 2003;35(12):1385-94.

136. Engel FB, Schebesta M, Duong MT, Lu G, Ren S, Madwed JB, et al. p38 MAP kinase inhibition enables proliferation of adult mammalian cardiomyocytes. Genes Dev. 2005;19(10):1175-87.

137. Engel FB, Hsieh PC, Lee RT, Keating MT. FGF1/p38 MAP kinase inhibitor therapy induces cardiomyocyte mitosis, reduces scarring, and rescues function after myocardial infarction. Proc Natl Acad Sci U S A. 2006;103(42):15546-51.

138. Wang J, Liu S, Heallen T, Martin JF. The Hippo pathway in the heart: pivotal roles in development, disease, and regeneration. Nat Rev Cardiol. 2018;15(11):672-84.

139. Ikeda S, Mizushima W, Sciarretta S, Abdellatif M, Zhai P, Mukai R, et al. Hippo Deficiency Leads to Cardiac Dysfunction Accompanied by Cardiomyocyte Dedifferentiation During Pressure Overload. Circ Res. 2019;124(2):292-305.

140. Odashima M, Usui S, Takagi H, Hong C, Liu J, Yokota M, et al. Inhibition of endogenous Mst1 prevents apoptosis and cardiac dysfunction without affecting cardiac hypertrophy after myocardial infarction. Circ Res. 2007;100(9):1344-52.

141. Heallen T, Zhang M, Wang J, Bonilla-Claudio M, Klysik E, Johnson RL, et al. Hippo pathway inhibits Wnt signaling to restrain cardiomyocyte proliferation and heart size. Science. 2011;332(6028):458-61.

142. Lin Z, Zhou P, von Gise A, Gu F, Ma Q, Chen J, et al. Pi3kcb links Hippo-YAP and PI3K-AKT signaling pathways to promote cardiomyocyte proliferation and survival. Circ Res. 2015;116(1):35-45.

143. Wang X, Ha T, Liu L, Hu Y, Kao R, Kalbfleisch J, et al. TLR3 Mediates Repair and Regeneration of Damaged Neonatal Heart through Glycolysis Dependent YAP1 Regulated miR-152 Expression. Cell Death Differ. 2018;25(5):966-82.

144. Shah SP. Evaluation of the E ects of Walnut Extract on the Cell Division G2/M Cyclin-Cyclin B1 in Breast Cancer Cells. San José: San José State University; 2016.

145. Pasumarthi KB, Nakajima H, Nakajima HO, Soonpaa MH, Field LJ. Targeted expression of cyclin D2 results in cardiomyocyte DNA synthesis and infarct regression in transgenic mice. Circ Res. 2005;96(1):110-8.

146. Tane S, Kubota M, Okayama H, Ikenishi A, Yoshitome S, Iwamoto N, et al. Repression of cyclin D1 expression is necessary for the maintenance of cell cycle exit in adult mammalian cardiomyocytes. J Biol Chem. 2014;289(26):18033-44.

147. Woo YJ, Panlilio CM, Cheng RK, Liao GP, Atluri P, Hsu VM, et al. Therapeutic delivery of cyclin A2 induces myocardial regeneration and enhances cardiac function in ischemic heart failure. Circulation. 2006;114(1 Suppl):I206-13.

148. Chaudhry HW, Dashoush NH, Tang H, Zhang L, Wang X, Wu EX, et al. Cyclin A2 mediates cardiomyocyte mitosis in the postmitotic myocardium. J Biol Chem. 2004;279(34):35858-66.

149. Shapiro SD, Ranjan AK, Kawase Y, Cheng RK, Kara RJ, Bhattacharya R, et al. Cyclin A2 induces cardiac regeneration after myocardial infarction through cytokinesis of adult cardiomyocytes. Sci Transl Med. 2014;6(224):224ra27.

150. Ebelt H, Liu Z, Muller-Werdan U, Werdan K, Braun T. Making omelets without breaking eggs: E2F-mediated induction of cardiomyoycte cell proliferation without stimulation of apoptosis. Cell Cycle. 2006;5(21):2436-9.

151. Malek Mohammadi M, Kattih B, Grund A, Froese N, Korf-Klingebiel M, Gigina A, et al. The transcription factor GATA4 promotes myocardial regeneration in neonatal mice. EMBO Mol Med. 2017;9(2):265-79.

152. Chakraborty S, Sengupta A, Yutzey KE. Tbx20 promotes cardiomyocyte proliferation and persistence of fetal characteristics in adult mouse hearts. J Mol Cell Cardiol. 2013;62:203-13.

153. Mahmoud AI, Kocabas F, Muralidhar SA, Kimura W, Koura AS, Thet S, et al. Meis1 regulates postnatal cardiomyocyte cell cycle arrest. Nature. 2013;497(7448):249-53.

154. Leone M, Magadum A, Engel FB. Cardiomyocyte proliferation in cardiac development and regeneration: a guide to methodologies and interpretations. Am J Physiol Heart Circ Physiol. 2015;309(8):H1237-50.

155. Hesse M, Doengi M, Becker A, Kimura K, Voeltz N, Stein V, et al. Midbody Positioning and Distance Between Daughter Nuclei Enable Unequivocal Identification of Cardiomyocyte Cell Division in Mice. Circ Res. 2018;123(9):1039-52.

156. Leone M, Musa G, Engel FB. Cardiomyocyte binucleation is associated with aberrant mitotic microtubule distribution, mislocalization of RhoA and IQGAP3, as well as defective actomyosin ring anchorage and cleavage furrow ingression. Cardiovasc Res. 2018;114(8):1115-31.

157. Zong H, Espinosa JS, Su HH, Muzumdar MD, Luo L. Mosaic analysis with double markers in mice. Cell. 2005;121(3):479-92.

158. Ali SR, Hippenmeyer S, Saadat LV, Luo L, Weissman IL, Ardehali R. Existing cardiomyocytes generate cardiomyocytes at a low rate after birth in mice. Proc Natl Acad Sci U S A. 2014;111(24):8850-5.

159. Raulf A, Horder H, Tarnawski L, Geisen C, Ottersbach A, Roll W, et al. Transgenic systems for unequivocal identification of cardiac myocyte nuclei and analysis of cardiomyocyte cell cycle status. Basic Res Cardiol. 2015;110(3):33.

160. Mechali M, Lutzmann M. The cell cycle: now live and in color. Cell. 2008;132(3):341-3.

161. Newman RH, Zhang J. Fucci: street lights on the road to mitosis. Chem Biol. 2008;15(2):97-8.

162. Nishitani H, Lygerou Z, Nishimoto T. Proteolysis of DNA replication licensing factor Cdt1 in S-phase is performed independently of geminin through its N-terminal region. J Biol Chem. 2004;279(29):30807-16.

163. Nishikimi T, Kuwahara K, Nakao K. Current biochemistry, molecular biology, and clinical relevance of natriuretic peptides. J Cardiol. 2011;57(2):131-40.

164. de Bold AJ, Bruneau BG, Kuroski de Bold ML. Mechanical and neuroendocrine regulation of the endocrine heart. Cardiovasc Res. 1996;31(1):7-18.

165. Lugnier C, Meyer A, Charloux A, Andres E, Geny B, Talha S. The Endocrine Function of the Heart: Physiology and Involvements of Natriuretic Peptides and Cyclic Nucleotide Phosphodiesterases in Heart Failure. J Clin Med. 2019;8(10).

166. Bielmann C, Rignault-Clerc S, Liaudet L, Li F, Kunieda T, Sogawa C, et al. Brain natriuretic peptide is able to stimulate cardiac progenitor cell proliferation and differentiation in murine hearts after birth. Basic Res Cardiol. 2015;110(1):455.

167. Sudoh T, Kangawa K, Minamino N, Matsuo H. A new natriuretic peptide in porcine brain. Nature. 1988;332(6159):78-81.

168. Nakagawa Y, Nishikimi T, Kuwahara K. Atrial and brain natriuretic peptides: Hormones secreted from the heart. Peptides. 2019;111:18-25.

169. Weber M, Mitrovic V, Hamm C. B-type natriuretic peptide and N-terminal pro-B-type natriuretic peptide - Diagnostic role in stable coronary artery disease. Exp Clin Cardiol. 2006;11(2):99-101.

170. Ichiki T, Schirger JA, Huntley BK, Brozovich FV, Maleszewski JJ, Sandberg SM, et al. Cardiac fibrosis in end-stage human heart failure and the cardiac natriuretic peptide guanylyl cyclase system: regulation and therapeutic implications. J Mol Cell Cardiol. 2014;75:199-205.

171. Potter LR, Yoder AR, Flora DR, Antos LK, Dickey DM. Natriuretic peptides: their structures, receptors, physiologic functions and therapeutic applications. Handb Exp Pharmacol. 2009(191):341-66.

172. Takimoto E. Cyclic GMP-dependent signaling in cardiac myocytes. Circ J. 2012;76(8):1819-25.

173. Colyer J. Phosphorylation states of phospholamban. Ann N Y Acad Sci. 1998;853:79-91.

174. Kerkela R, Ulvila J, Magga J. Natriuretic Peptides in the Regulation of Cardiovascular Physiology and Metabolic Events. J Am Heart Assoc. 2015;4(10):e002423.

175. Boerrigter G, Lapp H, Burnett JC. Modulation of cGMP in heart failure: a new therapeutic paradigm. Handb Exp Pharmacol. 2009(191):485-506.

176. Dazert P, Meissner K, Vogelgesang S, Heydrich B, Eckel L, Bohm M, et al. Expression and localization of the multidrug resistance protein 5 (MRP5/ABCC5), a cellular export pump for cyclic nucleotides, in human heart. Am J Pathol. 2003;163(4):1567-77.

177. Kruh GD, Belinsky MG. The MRP family of drug efflux pumps. Oncogene. 2003;22(47):7537-52.

178. Rose RA, Lomax AE, Giles WR. Inhibition of L-type Ca2+ current by C-type natriuretic peptide in bullfrog atrial myocytes: an NPR-C-mediated effect. Am J Physiol Heart Circ Physiol. 2003;285(6):H2454-62.

179. Cohen D, Koh GY, Nikonova LN, Porter JG, Maack T. Molecular determinants of the clearance function of type C receptors of natriuretic peptides. J Biol Chem. 1996;271(16):9863-9.

180. Moyes AJ, Chu SM, Aubdool AA, Dukinfield MS, Margulies KB, Bedi KC, et al. C-type natriuretic peptide co-ordinates cardiac structure and function. Eur Heart J. 2019.

181. Holtwick R, van Eickels M, Skryabin BV, Baba HA, Bubikat A, Begrow F, et al. Pressure-independent cardiac hypertrophy in mice with cardiomyocyte-restricted inactivation of the atrial natriuretic peptide receptor guanylyl cyclase-A. J Clin Invest. 2003;111(9):1399-407.

182. Pandey KN. Internalization and trafficking of guanylyl cyclase/natriuretic peptide receptor-A. Peptides. 2005;26(6):985-1000.

183. Brackmann M, Schuchmann S, Anand R, Braunewell KH. Neuronal Ca2+ sensor protein VILIP-1 affects cGMP signalling of guanylyl cyclase B by

regulating clathrin-dependent receptor recycling in hippocampal neurons. J Cell Sci. 2005;118(Pt 11):2495-505.

184. Fan D, Bryan PM, Antos LK, Potthast RJ, Potter LR. Down-regulation does not mediate natriuretic peptide-dependent desensitization of natriuretic peptide receptor (NPR)-A or NPR-B: guanylyl cyclase-linked natriuretic peptide receptors do not internalize. Mol Pharmacol. 2005;67(1):174-83.

185. Pandey KN. Endocytosis and Trafficking of Natriuretic Peptide Receptor-A: Potential Role of Short Sequence Motifs. Membranes (Basel). 2015;5(3):253-87.

186. Mani I, Garg R, Tripathi S, Pandey KN. Subcellular trafficking of guanylyl cyclase/natriuretic peptide receptor-A with concurrent generation of intracellular cGMP. Biosci Rep. 2015;35(5).

187. Bork NI, Nikolaev VO. cGMP Signaling in the Cardiovascular System-The Role of Compartmentation and Its Live Cell Imaging. Int J Mol Sci. 2018;19(3).

188. Mongillo M, Tocchetti CG, Terrin A, Lissandron V, Cheung YF, Dostmann WR, et al. Compartmentalized phosphodiesterase-2 activity blunts beta-adrenergic cardiac inotropy via an NO/cGMP-dependent pathway. Circ Res. 2006;98(2):226-34.

189. Preedy MEJ. Cardiac Cyclic Nucleotide Phosphodiesterases: Roles and Therapeutic Potential in Heart Failure. Cardiovasc Drugs Ther. 2020.

190. Subramanian H, Froese A, Jonsson P, Schmidt H, Gorelik J, Nikolaev VO. Distinct submembrane localisation compartmentalises cardiac NPR1 and NPR2 signalling to cGMP. Nat Commun. 2018;9(1):2446.

191. Rosenblatt-Velin N, Badoux S, Liaudet L. Pharmacological Therapy in the Heart as an Alternative to Cellular Therapy: A Place for the Brain Natriuretic Peptide? Stem Cells Int. 2016;2016:5961342.

192. Cameron VA, Ellmers LJ. Minireview: natriuretic peptides during development of the fetal heart and circulation. Endocrinology. 2003;144(6):2191-4.

193. Schwachtgen L, Herrmann M, Georg T, Schwarz P, Marx N, Lindinger A. Reference values of NT-proBNP serum concentrations in the umbilical cord blood and in healthy neonates and children. Z Kardiol. 2005;94(6):399-404.

194. Abdelalim EM, Tooyama I. BNP signaling is crucial for embryonic stem cell proliferation. PLoS One. 2009;4(4):e5341.

195. Becker JR, Chatterjee S, Robinson TY, Bennett JS, Panakova D, Galindo CL, et al. Differential activation of natriuretic peptide receptors modulates cardiomyocyte proliferation during development. Development. 2014;141(2):335-45.

196. Koide M, Akins RE, Harayama H, Yasui K, Yokota M, Tuan RS. Atrial natriuretic peptide accelerates proliferation of chick embryonic cardiomyocytes in vitro. Differentiation. 1996;61(1):1-11.

197. Rignault-Clerc S, Bielmann C, Liaudet L, Waeber B, Feihl F, Rosenblatt-Velin N. Natriuretic Peptide Receptor B modulates the proliferation of the cardiac cells expressing the Stem Cell Antigen-1. Sci Rep. 2017;7:41936.

198. Forte M, Madonna M, Schiavon S, Valenti V, Versaci F, Zoccai GB, et al. Cardiovascular Pleiotropic Effects of Natriuretic Peptides. Int J Mol Sci. 2019;20(16).

199. Tamura N, Ogawa Y, Chusho H, Nakamura K, Nakao K, Suda M, et al. Cardiac fibrosis in mice lacking brain natriuretic peptide. Proc Natl Acad Sci U S A. 2000;97(8):4239-44.

200. Wu B, Jiang H, Lin R, Cui B, Wen H, Lu Z. Pretreatment with B-type natriuretic peptide protects the heart from ischemia-reperfusion injury by inhibiting myocardial apoptosis. Tohoku J Exp Med. 2009;219(2):107-14.

201. Ren B, Shen Y, Shao H, Qian J, Wu H, Jing H. Brain natriuretic peptide limits myocardial infarct size dependent of nitric oxide synthase in rats. Clin Chim Acta. 2007;377(1-2):83-7.

202. Kapoun AM, Liang F, O'Young G, Damm DL, Quon D, White RT, et al. B-type natriuretic peptide exerts broad functional opposition to transforming growth factor-beta in primary human cardiac fibroblasts: fibrosis, myofibroblast conversion, proliferation, and inflammation. Circ Res. 2004;94(4):453-61.

203. Li X, Peng H, Wu J, Xu Y. Brain Natriuretic Peptide-Regulated Expression of Inflammatory Cytokines in Lipopolysaccharide (LPS)-Activated Macrophages via NF-kappaB and Mitogen Activated Protein Kinase (MAPK) Pathways. Med Sci Monit. 2018;24:3119-26.

204. Chen HH. Heart failure: a state of brain natriuretic peptide deficiency or resistance or both! J Am Coll Cardiol. 2007;49(10):1089-91.

205. Rorth R, Jhund PS, Yilmaz MB, Kristensen SL, Welsh P, Desai AS, et al. Comparison of BNP and NT-proBNP in Patients With Heart Failure and Reduced Ejection Fraction. Circ Heart Fail. 2020;13(2):e006541.

206. Semenov AG, Postnikov AB, Tamm NN, Seferian KR, Karpova NS, Bloshchitsyna MN, et al. Processing of pro-brain natriuretic peptide is suppressed by O-glycosylation in the region close to the cleavage site. Clin Chem. 2009;55(3):489-98.

207. Miyazaki J, Nishizawa H, Kambayashi A, Ito M, Noda Y, Terasawa S, et al. Increased levels of soluble corin in pre-eclampsia and fetal growth restriction. Placenta. 2016;48:20-5.

208. Ralat LA, Guo Q, Ren M, Funke T, Dickey DM, Potter LR, et al. Insulin-degrading enzyme modulates the natriuretic peptide-mediated signaling response. J Biol Chem. 2011;286(6):4670-9.

209. Clerico A, Recchia FA, Passino C, Emdin M. Cardiac endocrine function is an essential component of the homeostatic regulation network: physiological and clinical implications. Am J Physiol Heart Circ Physiol. 2006;290(1):H17-29.

210. Ahmad T, Felker GM. Subcutaneous B-type natriuretic peptide for treatment of heart failure: a dying therapy reborn? J Am Coll Cardiol. 2012;60(22):2313-5.

211. Gottlieb SS, Stebbins A, Voors AA, Hasselblad V, Ezekowitz JA, Califf RM, et al. Effects of Nesiritide and Predictors of Urine Output in Acute Decompensated Heart Failure: Results From ASCEND-HF (Acute Study of

Clinical Effectiveness of Nesiritide and Decompensated Heart Failure). J Am Coll Cardiol. 2013;62(13):1177-83.

212. O'Connor CM, Starling RC, Hernandez AF, Armstrong PW, Dickstein K, Hasselblad V, et al. Effect of nesiritide in patients with acute decompensated heart failure. N Engl J Med. 2011;365(1):32-43.

213. Chen HH, Martin FL, Gibbons RJ, Schirger JA, Wright RS, Schears RM, et al. Low-dose nesiritide in human anterior myocardial infarction suppresses aldosterone and preserves ventricular function and structure: a proof of concept study. Heart. 2009;95(16):1315-9.

214. Chen HH, Glockner JF, Schirger JA, Cataliotti A, Redfield MM, Burnett JC, Jr. Novel protein therapeutics for systolic heart failure: chronic subcutaneous B-type natriuretic peptide. J Am Coll Cardiol. 2012;60(22):2305-12.

215. Lyu T, Zhao Y, Zhang T, Zhou W, Yang F, Ge H, et al. Natriuretic peptides as an adjunctive treatment for acute myocardial infarction: insights from the meta-analysis of 1,389 patients from 20 trials. International heart journal. 2014;55(1):8-16.

216. Sangaralingham SJ, Burnett JC, Jr., McKie PM, Schirger JA, Chen HH. Rationale and design of a randomized, double-blind, placebo-controlled clinical trial to evaluate the efficacy of B-type natriuretic peptide for the preservation of left ventricular function after anterior myocardial infarction. J Card Fail. 2013;19(8):533-9.

217. Schiering N, D'Arcy A, Villard F, Ramage P, Logel C, Cumin F, et al. Structure of neprilysin in complex with the active metabolite of sacubitril. Sci Rep. 2016;6:27909.

218. Richards AM, Wittert GA, Espiner EA, Yandle TG, Ikram H, Frampton C. Effect of inhibition of endopeptidase 24.11 on responses to angiotensin II in human volunteers. Circ Res. 1992;71(6):1501-7.

219. McMurray JJ, Packer M, Desai AS, Gong J, Lefkowitz MP, Rizkala AR, et al. Angiotensin-neprilysin inhibition versus enalapril in heart failure. N Engl J Med. 2014;371(11):993-1004.

220. Xia Y, Chen Z, Chen A, Fu M, Dong Z, Hu K, et al. LCZ696 improves cardiac function via alleviating Drp1-mediated mitochondrial dysfunction in mice with doxorubicin-induced dilated cardiomyopathy. J Mol Cell Cardiol. 2017;108:138-48.

221. Kompa AR, Lu J, Weller TJ, Kelly DJ, Krum H, von Lueder TG, et al. Angiotensin receptor neprilysin inhibition provides superior cardioprotection compared to angiotensin converting enzyme inhibition after experimental myocardial infarction. Int J Cardiol. 2018;258:192-8.

222. von Lueder TG, Wang BH, Kompa AR, Huang L, Webb R, Jordaan P, et al. Angiotensin receptor neprilysin inhibitor LCZ696 attenuates cardiac remodeling and dysfunction after myocardial infarction by reducing cardiac fibrosis and hypertrophy. Circ Heart Fail. 2015;8(1):71-8.

223. Gu J, Noe A, Chandra P, Al-Fayoumi S, Ligueros-Saylan M, Sarangapani R, et al. Pharmacokinetics and pharmacodynamics of LCZ696, a novel dual-acting angiotensin receptor-neprilysin inhibitor (ARNi). J Clin Pharmacol. 2010;50(4):401-14.

224. Nougue H, Pezel T, Picard F, Sadoune M, Arrigo M, Beauvais F, et al. Effects of sacubitril/valsartan on neprilysin targets and the metabolism of natriuretic peptides in chronic heart failure: a mechanistic clinical study. Eur J Heart Fail. 2019;21(5):598-605.

225. Dizaye K, Ali RH. Effects of neprilysin-renin inhibition in comparison with neprilysin-angiotensin inhibition on the neurohumoral changes in rats with heart failure. BMC Pharmacol Toxicol. 2019;20(1):23.

226. Losse B, Schuchhardt S, Niederle N. The oxygen pressure histogram in the left ventricular myocardium of the dog. Pflugers Arch. 1975;356(2):121-32.

227. Clerico A, Vittorini S, Passino C. Circulating forms of the b-type natriuretic peptide prohormone: pathophysiologic and clinical considerations. Adv Clin Chem. 2012;58:31-44.

228. Suematsu Y, Miura S, Goto M, Matsuo Y, Arimura T, Kuwano T, et al. LCZ696, an angiotensin receptor-neprilysin inhibitor, improves cardiac function with the attenuation of fibrosis in heart failure with reduced ejection fraction in streptozotocin-induced diabetic mice. Eur J Heart Fail. 2016;18(4):386-93.

229. Ackers-Johnson M, Li PY, Holmes AP, O'Brien SM, Pavlovic D, Foo RS. A Simplified, Langendorff-Free Method for Concomitant Isolation of Viable Cardiac Myocytes and Nonmyocytes From the Adult Mouse Heart. Circ Res. 2016;119(8):909-20.

230. Livak KJ, Schmittgen TD. Analysis of relative gene expression data using real-time quantitative PCR and the 2(-Delta Delta C(T)) Method. Methods. 2001;25(4):402-8.

231. Liu P, Zhong TP. MAPK/ERK signalling is required for zebrafish cardiac regeneration. Biotechnol Lett. 2017;39(7):1069-77.

232. Egom EE. Pulmonary Arterial Hypertension Due to NPR-C Mutation: A Novel Paradigm for Normal and Pathologic Remodeling? Int J Mol Sci. 2019;20(12).

233. Mika D, Richter W, Conti M. A CaMKII/PDE4D negative feedback regulates cAMP signaling. Proc Natl Acad Sci U S A. 2015;112(7):2023-8.

234. Davis BH, Morimoto Y, Sample C, Olbrich K, Leddy HA, Guilak F, et al. Effects of myocardial infarction on the distribution and transport of nutrients and oxygen in porcine myocardium. J Biomech Eng. 2012;134(10):101005.

235. Driesen RB, Verheyen FK, Dijkstra P, Thone F, Cleutjens JP, Lenders MH, et al. Structural remodelling of cardiomyocytes in the border zone of infarcted rabbit heart. Mol Cell Biochem. 2007;302(1-2):225-32.

236. Arora K, Sinha C, Zhang W, Ren A, Moon CS, Yarlagadda S, et al. Compartmentalization of cyclic nucleotide signaling: a question of when, where, and why? Pflugers Arch. 2013;465(10):1397-407.

237. Bhogal NK, Hasan A, Gorelik J. The Development of Compartmentation of cAMP Signaling in Cardiomyocytes: The Role of T-Tubules and Caveolae Microdomains. J Cardiovasc Dev Dis. 2018;5(2).

238. Chiong M, Wang ZV, Pedrozo Z, Cao DJ, Troncoso R, Ibacache M, et al. Cardiomyocyte death: mechanisms and translational implications. Cell Death Dis. 2011;2:e244.

239. van Empel VP, Bertrand AT, Hofstra L, Crijns HJ, Doevendans PA, De Windt LJ. Myocyte apoptosis in heart failure. Cardiovasc Res. 2005;67(1):21-9.

240. Sun Y, Deng T, Lu N, Yan M, Zheng X. B-type natriuretic peptide protects cardiomyocytes at reperfusion via mitochondrial calcium uniporter. Biomed Pharmacother. 2010;64(3):170-6.

241. Deng YJ, Tan N, Zeng HK, Fu YH, Dong XL. [Effects of BNP preconditioning on myocardial cell apoptosis and expressions of bcl-2 and Bax during myocardial ischemia-reperfusion injury in rats]. Zhonghua Yi Xue Za Zhi. 2010;90(48):3431-4.

242. Zhang X, Sha M, Yao Y, Da J, Jing D. Increased B-type-natriuretic peptide promotes myocardial cell apoptosis via the B-type-natriuretic peptide/long non-coding RNA LSINCT5/caspase-1/interleukin 1beta signaling pathway. Mol Med Rep. 2015;12(5):6761-7.

243. Engel FB, Schebesta M, Keating MT. Anillin localization defect in cardiomyocyte binucleation. J Mol Cell Cardiol. 2006;41(4):601-12.

244. Gallo S, Vitacolonna A, Bonzano A, Comoglio P, Crepaldi T. ERK: A Key Player in the Pathophysiology of Cardiac Hypertrophy. Int J Mol Sci. 2019;20(9).

245. Kehat I, Molkentin JD. Extracellular signal-regulated kinase 1/2 (ERK1/2) signaling in cardiac hypertrophy. Ann N Y Acad Sci. 2010;1188:96-102.

246. Wang Y. Mitogen-activated protein kinases in heart development and diseases. Circulation. 2007;116(12):1413-23.

247. Ramos JW. The regulation of extracellular signal-regulated kinase (ERK) in mammalian cells. Int J Biochem Cell Biol. 2008;40(12):2707-19.

248. Stork PJ, Schmitt JM. Crosstalk between cAMP and MAP kinase signaling in the regulation of cell proliferation. Trends Cell Biol. 2002;12(6):258-66.

249. Chattergoon NN, Louey S, Stork PJ, Giraud GD, Thornburg KL. Unexpected maturation of PI3K and MAPK-ERK signaling in fetal ovine cardiomyocytes. Am J Physiol Heart Circ Physiol. 2014;307(8):H1216-25.

250. von Gise A, Lin Z, Schlegelmilch K, Honor LB, Pan GM, Buck JN, et al. YAP1, the nuclear target of Hippo signaling, stimulates heart growth through cardiomyocyte proliferation but not hypertrophy. Proc Natl Acad Sci U S A. 2012;109(7):2394-9.

251. Heallen T, Morikawa Y, Leach J, Tao G, Willerson JT, Johnson RL, et al. Hippo signaling impedes adult heart regeneration. Development. 2013;140(23):4683-90.

252. Xin M, Kim Y, Sutherland LB, Murakami M, Qi X, McAnally J, et al. Hippo pathway effector Yap promotes cardiac regeneration. Proc Natl Acad Sci U S A. 2013;110(34):13839-44.

253. Siddappa D, Beaulieu E, Gevry N, Roux PP, Bordignon V, Duggavathi R. Effect of the transient pharmacological inhibition of Mapk3/1 pathway on ovulation in mice. PLoS One. 2015;10(3):e0119387.

254. de Lemos JA, McGuire DK, Drazner MH. B-type natriuretic peptide in cardiovascular disease. Lancet. 2003;362(9380):316-22.

255. Almufleh A, Marbach J, Chih S, Stadnick E, Davies R, Liu P, et al. Ejection fraction improvement and reverse remodeling achieved with

Sacubitril/Valsartan in heart failure with reduced ejection fraction patients. Am J Cardiovasc Dis. 2017;7(6):108-13.

256. Ushijima K, Ando H, Arakawa Y, Aizawa K, Suzuki C, Shimada K, et al. Prevention against renal damage in rats with subtotal nephrectomy by sacubitril/valsartan (LCZ696), a dual-acting angiotensin receptor-neprilysin inhibitor. Pharmacol Res Perspect. 2017;5(4).

257. Ishii M, Kaikita K, Sato K, Sueta D, Fujisue K, Arima Y, et al. Cardioprotective Effects of LCZ696 (Sacubitril/Valsartan) After Experimental Acute Myocardial Infarction. JACC Basic Transl Sci. 2017;2(6):655-68.

258. Pankow K, Schwiebs A, Becker M, Siems WE, Krause G, Walther T. Structural substrate conditions required for neutral endopeptidase-mediated natriuretic Peptide degradation. J Mol Biol. 2009;393(2):496-503.

259. Zong P, Setty S, Sun W, Martinez R, Tune JD, Ehrenburg IV, et al. Intermittent hypoxic training protects canine myocardium from infarction. Exp Biol Med (Maywood). 2004;229(8):806-12.

260. Cai Z, Manalo DJ, Wei G, Rodriguez ER, Fox-Talbot K, Lu H, et al. Hearts from rodents exposed to intermittent hypoxia or erythropoietin are protected against ischemia-reperfusion injury. Circulation. 2003;108(1):79-85.

261. Xie Y, Zhu Y, Zhu WZ, Chen L, Zhou ZN, Yuan WJ, et al. Role of dual-site phospholamban phosphorylation in intermittent hypoxia-induced cardioprotection against ischemia-reperfusion injury. Am J Physiol Heart Circ Physiol. 2005;288(6):H2594-602.

262. Zhu WZ, Dong JW, Ding HL, Yang HT, Zhou ZN. Postnatal development in intermittent hypoxia enhances resistance to myocardial ischemia/reperfusion in male rats. Eur J Appl Physiol. 2004;91(5-6):716-22.

263. Chen L, Lu XY, Li J, Fu JD, Zhou ZN, Yang HT. Intermittent hypoxia protects cardiomyocytes against ischemia-reperfusion injury-induced alterations in Ca2+ homeostasis and contraction via the sarcoplasmic reticulum and Na+/Ca2+ exchange mechanisms. Am J Physiol Cell Physiol. 2006;290(4):C1221-9.

264. Aguilar M, Gonzalez-Candia A, Rodriguez J, Carrasco-Pozo C, Canas D, Garcia-Herrera C, et al. Mechanisms of Cardiovascular Protection Associated with Intermittent Hypobaric Hypoxia Exposure in a Rat Model: Role of Oxidative Stress. Int J Mol Sci. 2018;19(2).

265. Tuter DS, Kopylov PY, Syrkin AL, Glazachev OS, Komarov RN, Katkov AI, et al. Intermittent systemic hypoxic-hyperoxic training for myocardial protection in patients undergoing coronary artery bypass surgery: first results from a single-centre, randomised controlled trial. Open Heart. 2018;5(2):e000891.

266. Navarrete-Opazo A, Mitchell GS. Therapeutic potential of intermittent hypoxia: a matter of dose. Am J Physiol Regul Integr Comp Physiol. 2014;307(10):R1181-97.

267. Mateika JH, El-Chami M, Shaheen D, Ivers B. Intermittent hypoxia: a low-risk research tool with therapeutic value in humans. J Appl Physiol (1985). 2015;118(5):520-32.

268. Zhang Y, Knight W, Chen S, Mohan A, Yan C. Multiprotein Complex With TRPC (Transient Receptor Potential-Canonical) Channel, PDE1C (Phosphodiesterase 1C), and A2R (Adenosine A2 Receptor) Plays a Critical Role in Regulating Cardiomyocyte cAMP and Survival. Circulation. 2018;138(18):1988-2002.

269. Huang H, Xie M, Gao L, Zhang W, Zhu X, Wang Y, et al. Rolipram, a PDE4 Inhibitor, Enhances the Inotropic Effect of Rat Heart by Activating SERCA2a. Front Pharmacol. 2019;10:221.

270. Jaski BE, Fifer MA, Wright RF, Braunwald E, Colucci WS. Positive inotropic and vasodilator actions of milrinone in patients with severe congestive heart failure. Dose-response relationships and comparison to nitroprusside. J Clin Invest. 1985;75(2):643-9.

271. Packer M. Effect of phosphodiesterase inhibitors on survival of patients with chronic congestive heart failure. Am J Cardiol. 1989;63(2):41A-5A.

272. Chen DHH. Study of Low Dose Nesiritide With or Without Sildenafil in Congestive Heart Failure Patients With Renal Dysfunction (BNP+PDEVI). 2010.

8. Supplementary Data

The LCZ696 experiments were performed by our master student, Alexia Carboni. I had the opportunity to supervise Alexia.

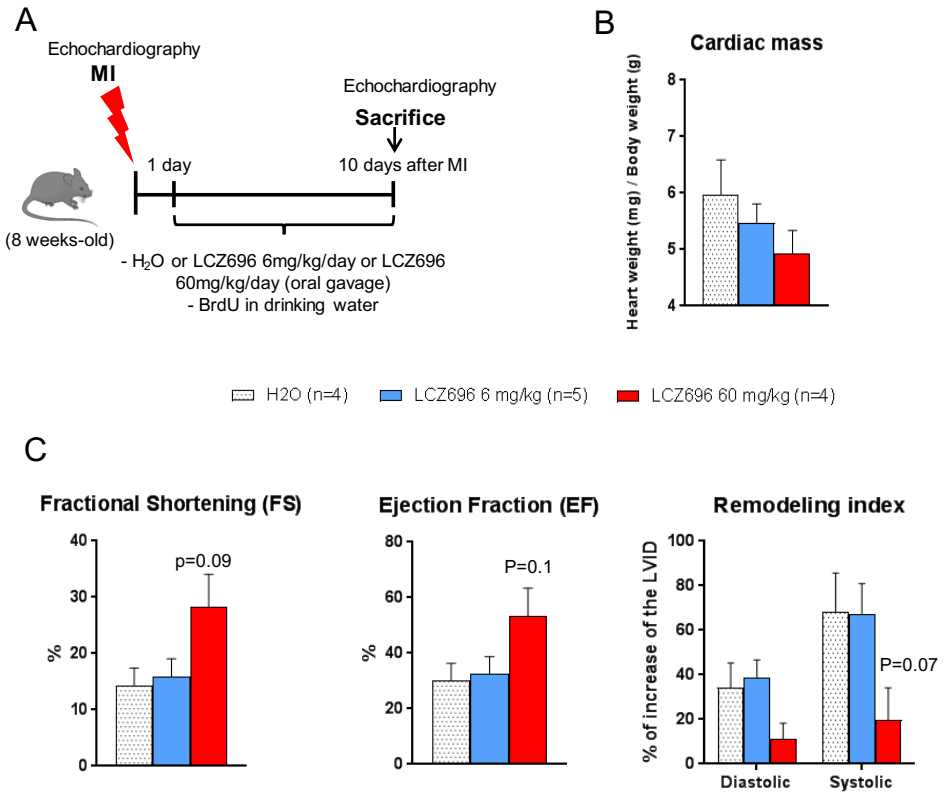

Supplementary Figure 1: *High dose of LCZ696 (60 mg/kg) improves cardiac function.* **A:** Experimental protocol as described in details in Materials and Methods. **B:** Cardiac mass (Heart/body weight ratio) of infarcted mice 10 days after MI. **C:** Cardiac function and remodeling index measured by echocardiography 10 days after MI.

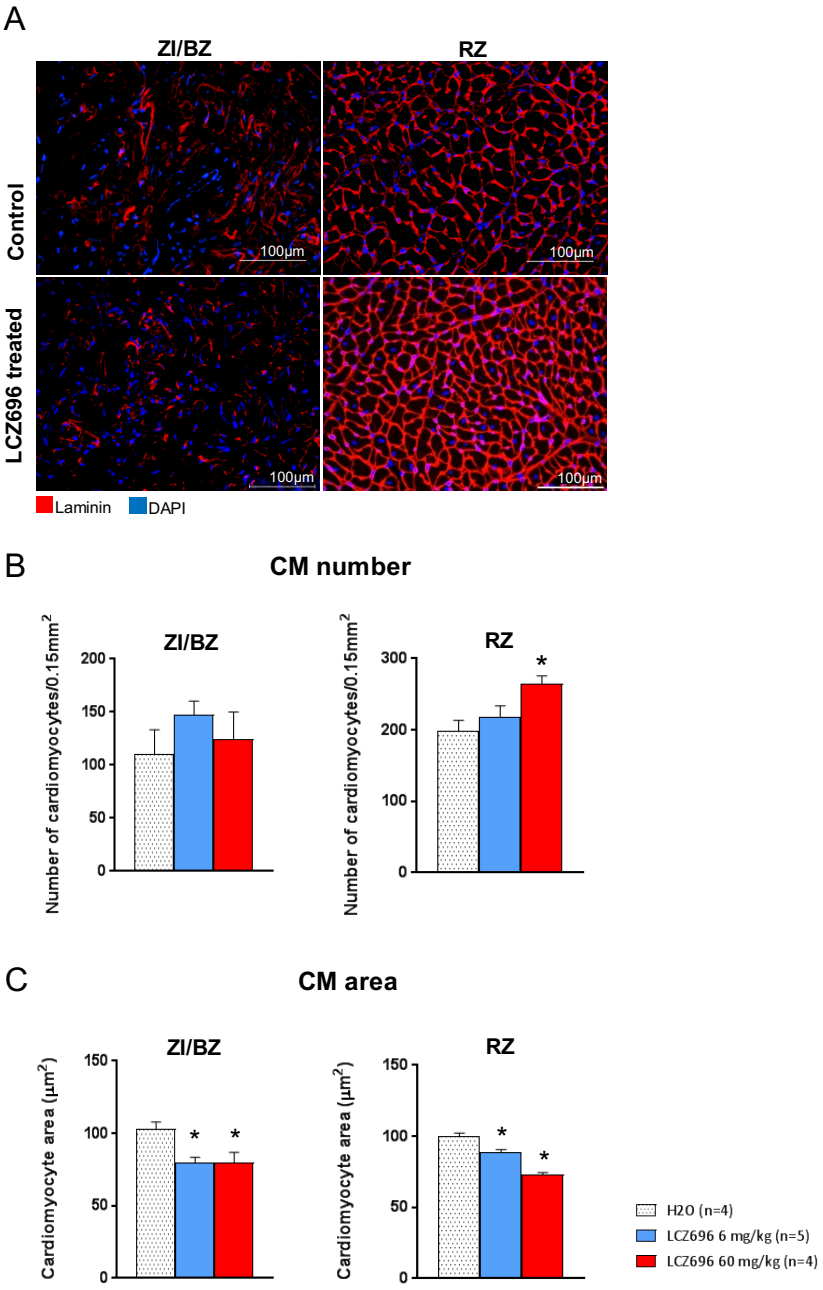

Supplementary Figure 2: *The number of CMs increases in response to high dose of LCZ696 (60 mg/kg) 10 days after MI in RZ.* **A:** Representative pictures of injured heart stained with laminin (red) 10 days after MI. Pictures covered a range of 0.015mm2. **B:** Graphs represent the number of CMs counted per heart sections in ZI+BZ and RZ. **C:** Graphs represent cross sectional area of CMs evaluated on heart sections in ZI+BZ and RZ. Only CMs with circularity >0.5 are considered. Data are mean ±SEM, *p≤0.05.

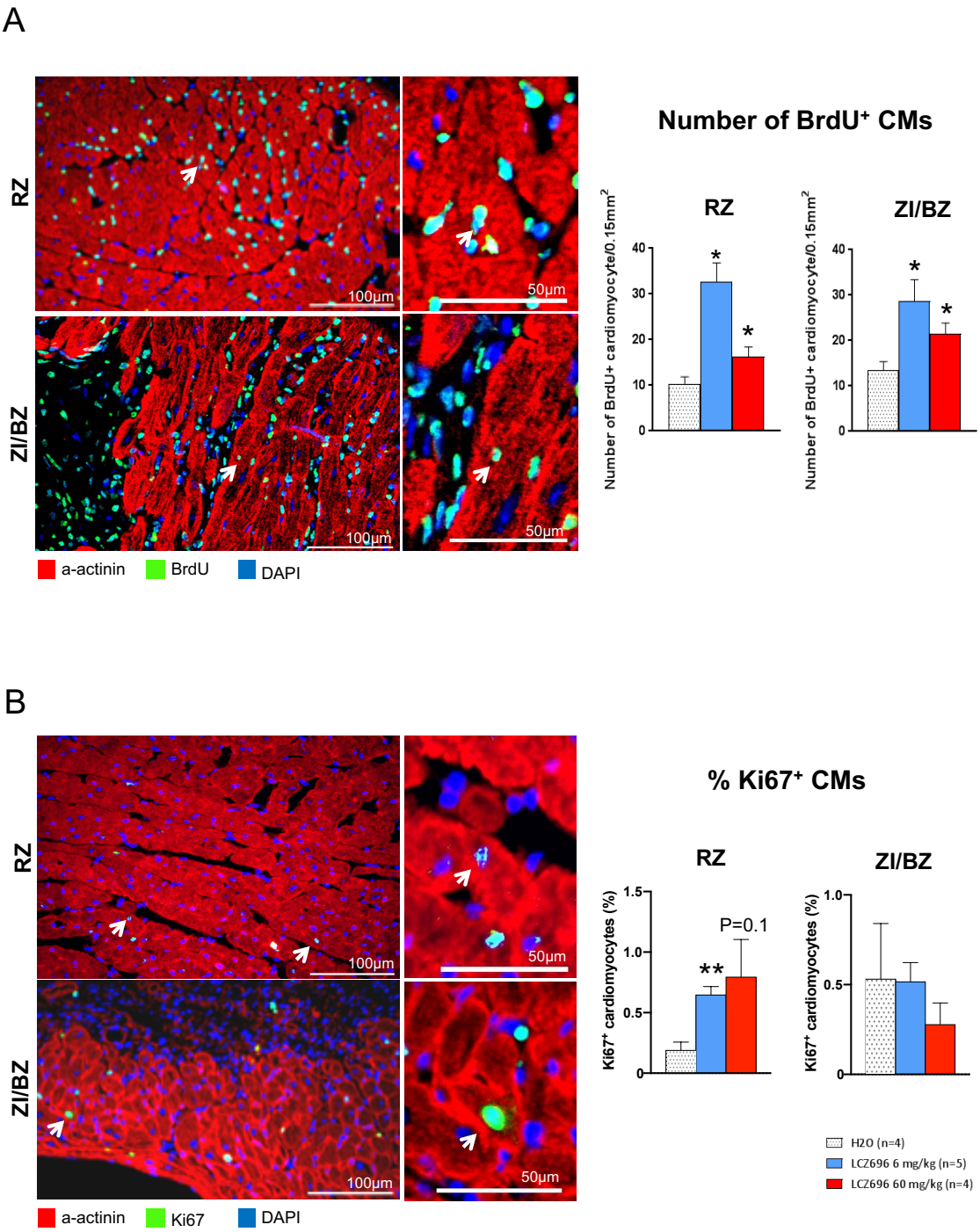

Supplementary Figure 3: *LCZ696 treatment stimulates the re-entry of CMs into the cell cycle 10 days after MI.* **A-B:** Representative pictures of injured heart (RZ and ZI+BZ) 10 days after MI stained with BrdU (upper panel) or Ki67 (lower panel) in green and combined with α-actinin in red. Pictures covered a range of 0.015mm^2. White arrows show CMs expressing BrdU (upper panel) or Ki67 (lower panel). **A:** Graphs on the right represent the number of CMs expressing BrdU counted per heart section in RZ and ZI+BZ. **B:** Graphs on the right represent the percentage of Ki67$^+$ CMs in RZ and ZI+BZ. Scale bars are 100µm and 50µm for magnification. For all results, data are mean ±SEM, *p≤0.05 and, **p≤0.01.

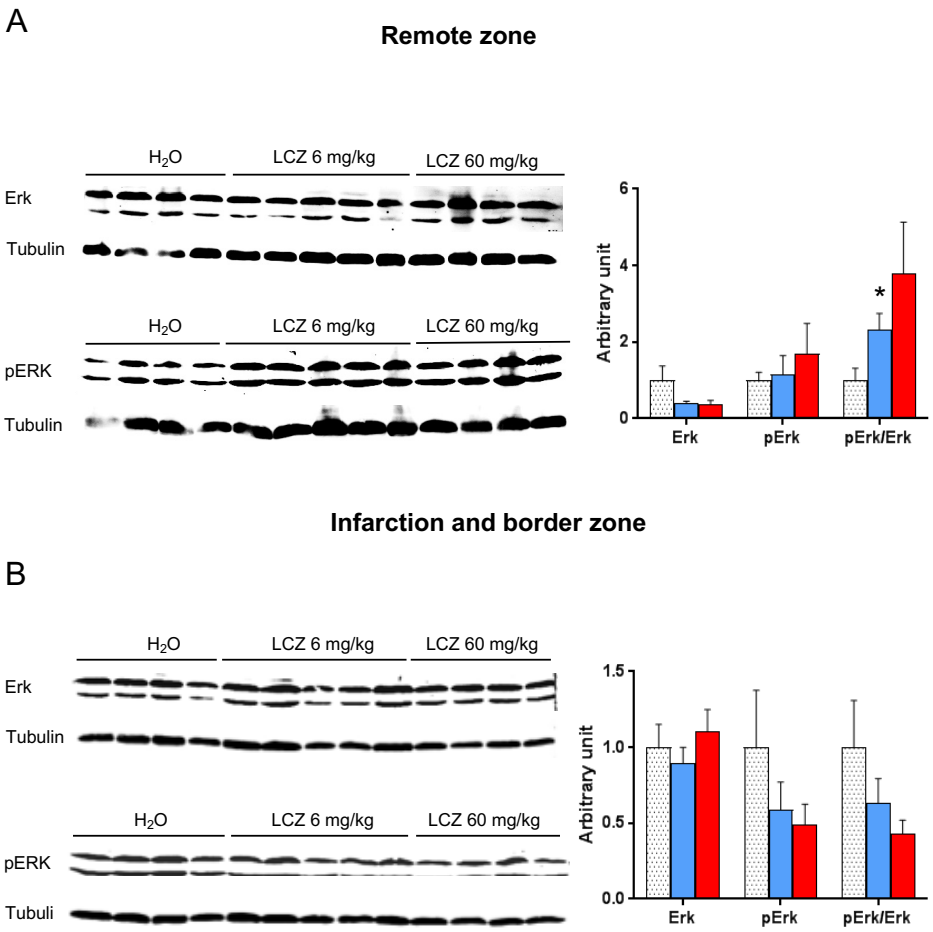

Supplementary Figure 4: *MAPK/ERK signaling pathway is activated after LCZ696 treatment, 10 days after MI in RZ*. **A-B:** Representative western blots of untreated and LCZ696-treated hearts 10 days after MI. Blots on the left were stained with antibodies against ERK, pERK and Tubulin (used as loading control) in RZ **(A)** and ZI+BZ **(B)**. Only the bands at the adequate molecular weight are represented here: ERK and pERK 42-44 kDa, Tubulin 55 kDa. Graphs on the right represent the quantification of the data issue from western blot analysis. Protein expression in LCZ696-treated hearts are related to the average of untreated-hearts. For all results, data are mean ±SEM, *p≤0.05.

Primary antibodies	Species	Dilution	Reference	Usage
a-actinin	mouse	1/50	sigma A7811	Immunohistology
Aurkb	rabbit	1/1000	Abcam ab139188	Immunohistology
BrdU	rat	1/100	Abcam ab6326	Immunohistology
cleaved caspase 3	rabbit	1/400	Cell Signaling 9661	Immunohistology
GFP	rabbit	1/1000	Abcam ab290	Immunohistology
Histone H3 (phospho s10)	rabbit	1/100	Millipore 06-570	Immunohistology
ki67	rat	1/1000	ebioscience 14-5698-80	Immunohistology
Laminin	rabbit	1/200	Sigma L9393	Immunohistology
NPR-A	rabbit	1/50	Abcam ab70848	Immunohistology
NPR-B	rabbit	1/100	Abcam ab139188	Immunohistology
Troponine I	goat	1/100	Santa Cruz Biotechnology SC-8118	Immunohistology
Akt	rabbit	1/1000	Cell Signaling	Western Blot
Phospho-Akt	rabbit	1/500	Cell Signaling	Western Blot
Bax	rabbit	1/1000	Cell Signaling	Western Blot
Bcl-2	rabbit	1/1000	Cell Signaling	Western Blot
cleaved caspase 8	rabbit	1/1000	Cell Signaling	Western Blot
cleaved caspase 3	rabbit	1/1000	Cell Signaling	Western Blot
Erk	rabbit	1/3000	Cell Signaling	Western Blot
NPR-B	goat	1/20	Santa Cruz SC-34421	Flow cytometry
NPR-A	rabbit	1/50	Abcam ab70848	Flow cytometry
Phospho-Erk	rabbit	1/2000	Cell Signaling	Western Blot
p38	rabbit	1/1000	Cell Signaling	Western Blot
Phospho-p38	rabbit	1/500	Cell Signaling	Western Blot
phospholamban	mouse	1/1000	Abcam	Western Blot
Phospho-phospholamban	rabbit	1/500	Millipore	Western Blot
Troponine T	goat	1/50	Abcam ab56357	Flow cytometry
Tubulin	mouse	1/10000	Sigma T5168	Western Blot
Secondary antibodies				
Anti-rabbit Alexa 488	donkey	1/1000	Molecular Probes A21206	Immunohistology
Anti-rabbit Alexa 594	donkey	1/1000	Molecular Probes A21207	immunohistology
Anti-goat Alexa 594	donkey	1/1000	Molecular Probes A11058	Immunohistology
Anti-mouse Alexa 647	goat	1/1000	Molecular Probes A21240	Immunohistology
Anti-rat 647	donkey	1/500	Jackson Immuno 712-605-150	Immunohistology
Anti-rat Alexa 488	donkey	1/1000	Molecular Probes A21208	Immunohistology
Anti-rat biotinylated	goat	1/200	Vector BA-9400	Immunohistology
Steptavidine Alexa 594		1/1000	Molecular Probes S11227	Immunohistology
anti-rabbit Alexa 680	goat	1/5000	Molecular Probes A21109	Western Blot
Anti-mouse IRDye 800	goat	1/10000	Rockland Immunochemicals 610-132-121	Western Blot
Anti-goat APC-conjugated	chicken	1/10	R&D systems F0108	Flow cytometry

Supplementary Table 1: *Antibodies used in flow cytometry analysis, immunohistology and western blot analysis.*

Gene	Forward primer	Reverse primer	Product size (bp)
ANF	ACAGGATTGGAGCCCAGAGC	GTCCATGGTGCTGAAGTTTATTC	337
Cyclin D1	TGAGAACAAGCAGACCATCC	TGAACTTCACATCTGTGGCA	71
Cyclin D2	GGATGATGAAGTGAACACACTCAC	GGATCTTCCACAGACTTGGATCC	180
Cyclin E1	GAAAGAAGAAGGTGGCTCCGAC	GTTAGGGGTGGGGATGAAAGAG	190
Cyclin A2	ATGTCAACCCCGAAAAACTG	GCAGTGACATGCTCATCGTT	157
Cyclin B2	AGCTCCCAAGGATCGTCCTC	TGTCCTCGTTATCTATGTCCTCG	116
Dab2	TGCTCGTGATGTGACAGACA	AGGGTCATTAGGGCCTCACT	225
GATA4	CTGTCATCTCACTATGGGCA	CCAAGTCCGAGCAGGAATTT	259
Nkx2.5	CAAGTGCTCTCCTGCTTTCC	GTCCAGCTCCACTGCCTTCT	130
Troponin T	GCGGAAGAGTGGGAAGAGACA	CCACAGCTCCTTGGCCTTCT	127
α-MHC	AACCAGAGTTTGAGTGACAGAATG	ACTCCGTGCGGATGTCAA	130
β-MHC	ATGAGACGGTGGTGGGTTT	CTTTCTTTGCCTTGCCTTTG	117
Runx1	GATGGCACTCTGGTCACCG	GCCGCTCGGAAAAGGACA	298
α-SKA	TGGACTTCGAGAATGAGATGG	TCGTCCTGAGGAGAGAGAGC	509
NPR-A	CCAATTATGGCTCCCTGCTA	CGGTACAAGCTCCCACAAAT	198
NPR-B	TCATGACAGCCCATGGGAAA	GGTGACAATGCAGATGTTGG	209
18S	ACTTTTGGGGCCTTCGTGTC	GCCCAGAGACTCATTTCTTCTTG	96

Supplementary Table 2: *Sequences of primers used in quantitative RT-qPCR.*